AFCRL-TR-75-0414

SIO Ref. 75-24

AIRBORNE MEASUREMENTS OF OPTICAL ATMOSPHERIC PROPERTIES IN WESTERN WASHINGTON

by

Seibert Q. Duntley, Richard W. Johnson, Jacqueline I. Gordon

Visibility Laboratory
University of California, San Diego
Scripps Institution of Oceanography
San Diego, California 92152

Approved:

Seibert Q. Duntley, Director
Visibility Laboratory

Approved:

William A. Nierenberg, Director
Scripps Institution of Oceanography

CONTRACT NO. F19628-73-C-0013
Project No. 7621
Task No. 762104
Work Unit No. 76210401

Scientific Report No. 5
July 1975

Contract Monitor: Major Robert W. Endlich, Optical Physics Laboratory

Approved for public release; distribution unlimited.

Prepared for

AIR FORCE CAMBRIDGE RESEARCH LABORATORIES
AIR FORCE SYSTEMS COMMAND
UNITED STATES AIR FORCE
HANSCOM AFB, MASSACHUSETTS 01730

UNCLASSIFIED

SECURITY CLASSIFICATION OF THIS PAGE (When Data Entered)

REPORT DOCUMENTATION PAGE

READ INSTRUCTIONS BEFORE COMPLETING FORM

1. REPORT NUMBER: AFCRL-TR-75-0414	2. GOVT ACCESSION NO.
3. RECIPIENT'S CATALOG NUMBER	
4. TITLE (and Subtitle): AIRBORNE MEASUREMENTS OF OPTICAL ATMOSPHERIC PROPERTIES IN WESTERN WASHINGTON	5. TYPE OF REPORT & PERIOD COVERED: Scientific – Interim; Scientific Report No. 5
	6. PERFORMING ORG. REPORT NUMBER: SIO Ref. 75-24
7. AUTHOR(s): Seibert Q. Duntley; Richard W. Johnson; Jacqueline I. Gordon	8. CONTRACT OR GRANT NUMBER(s): F19628-73-C-0013
9. PERFORMING ORGANIZATION NAME AND ADDRESS: University of California, San Diego; Visibility Laboratory; San Diego, California 92152	10. PROGRAM ELEMENT, PROJECT, TASK AREA & WORK UNIT NUMBERS: DoD Element 62101F; Project, Task, Work Unit No. 7621-04-01
11. CONTROLLING OFFICE NAME AND ADDRESS: Air Force Cambridge Research Laboratories; Hanscom AFB, Massachusetts 01731; Contract Monitor: Major Endlich/OPA	12. REPORT DATE: August 1975
	13. NUMBER OF PAGES: 266
14. MONITORING AGENCY NAME & ADDRESS (if different from Controlling Office)	15. SECURITY CLASS. (of this report): Unclassified
	15a. DECLASSIFICATION/DOWNGRADING SCHEDULE

16. DISTRIBUTION STATEMENT (of this Report)

Approved for public release; distribution unlimited.

17. DISTRIBUTION STATEMENT (of the abstract entered in Block 20, if different from Report)

18. SUPPLEMENTARY NOTES

19. KEY WORDS (Continue on reverse side if necessary and identify by block number)

Albedos
Atmospheric Optical Properties
Atmospheric Scattering Coefficient
Atmospheric Beam Transmittance
Atmospheric Contrast Transmittance
Atmospheric Path Radiance
Atmospheric Directional Path Reflectance
Natural Daytime Irradiance
Terrain Reflectance

20. ABSTRACT (Continue on reverse side if necessary and identify by block number)

This report presents daytime atmospheric optical data collected chiefly with airborne instruments during a field expedition to western Washington in the summer of 1974. Results from seven flights are presented. The data include the natural irradiance upon horizontal plane surfaces, scalar irradiances, total volume scattering coefficients, atmospheric beam transmittances, path radiances, directional path reflectances, and directional terrain reflectances. Data for daytime conditions ranging from clear skies to completely overcast were derived for downward-looking paths of sight inclined at six zenith angles

DD FORM 1 JAN 73 1473 EDITION OF 1 NOV 65 IS OBSOLETE
S/N 0102-014-6601

UNCLASSIFIED

SECURITY CLASSIFICATION OF THIS PAGE (When Data Entered)

20. ABSTRACT continued:

(95, 100, 105, 120, 150, and 180 degrees) from altitudes of 1200 meters above ground level and lower. All data were measured with a broad band sensitivity representing pseudo-photopic spectral response with a mean wavelength of 557 nanometers.

SUMMARY

This report, which describes the Visibility Laboratory's Project SEEKVAL* effort, was prepared under AFCRL Contract F19628-73-C-0013. The principal project task was to take daytime atmospheric optical measurements in western Washington and, from these measurements, to determine optical properties for various downward-inclined paths of sight. These properties include the natural irradiance upon horizontal plane surfaces, scalar irradiances, total volume scattering coefficients, atmospheric beam transmittances, path radiances, directional path reflectances, and directional terrain reflectances.

The field trip was made to Washington in July 1974. All data were recorded on similar flight tracks centered over Weir Prairie, near Rainier, Washington. The prairie terrain was flat, covered with long dry grass and surrounded by dark evergreen woods. Typical daytime flight conditions ranged from clear skies to overcast with light rain.

The airborne radiometric instrumentation, developed at the Visibility Laboratory and mounted in Air Force C-130A aircraft No. 50022, consisted of a total scattering meter (or integrating nephelometer) for determining the total scattering coefficient, two sky scanning radiometers for measuring upper and lower hemisphere (sky and terrain) radiances, a dual irradiometer for measuring alternately the downwelling and upwelling irradiances, an equilibrium radiance telephotometer, and a variable direction path function meter. The meteorological instrumentation included an absolute pressure transducer, a dewpoint hygrometer, and an AN/AMQ-17 aerograph for measuring ambient temperature and pressure.

A Visibility Laboratory ground-based data station was located immediately below the flight track. It contained duplicate radiometric instrumentation for obtaining ground-level measurements of total scattering coefficient, upper hemisphere (sky) radiances, and downwelling irradiance. Additionally, the ground station was equipped with a contrast reduction meter for determining earth-to-space beam transmittance.

All optical measurements were made within the visible spectrum, using a pseudo-photopic spectral response with a mean wavelength of 557 nanometers.

All primary data were recorded on magnetic tapes which were returned to the Visibility Laboratory for processing at the computer facilities of the University of California, San Diego.

---

* The project title SEEKVAL has been assigned to this activity for procedural identification only and is not necessarily utilized or recognized by agencies or organizations outside the Visibility Laboratory. The relationship between this activity and other similar activities conducted by the Visibility Laboratory is well-illustrated in AFCRL-72-0593, Duntley, *et al.* (1972c).

TABLE OF CONTENTS

LIST OF ILLUSTRATIONS

RELATED CONTRACTS AND PUBLICATIONS

Related Contracts: None

Publications:

Duntley, S. Q., R. W. Johnson, and J. I. Gordon (July 1972), "Airborne Measurements of Optical Atmospheric Properties in Southern Germany," AFCRL-72-0255, SIO Ref. 72-64.

Duntley, S. Q., R. W. Johnson, and J. I. Gordon (September 1972), "Airborne and Ground-Based Measurements of Optical Atmospheric Properties in Central New Mexico," AFCRL-72-0461, SIO Ref. 72-71.

Duntley, S. Q., R. W. Johnson, and J. I. Gordon (November 1972), "Airborne Measurements of Optical Atmospheric Properties, Summary and Review," AFCRL-72-0593, SIO Ref. 72-82.

Gordon, J. I., J. L. Harris, Sr., and S. Q. Duntley (1973), "Measuring Earth-to-Space Contrast Transmittance from Ground Stations," Appl. Opt. **12**, 1317 – 1324.

Duntley, S. Q., R. W. Johnson, and J. I. Gordon (July 1973), "Airborne Measurements of Optical Atmospheric Properties in Southern Illinois," AFCRL-TR-73-0422, SIO Ref. 73-24.

Gordon, J. I., C. F. Edgerton, and S. Q. Duntley (1975), "Signal-Light, Nomogram," J. Opt. Soc. Am. **65**, 111 – 118.

Duntley, S. Q., R. W. Johnson, and J. I. Gordon (June 1974), "Airborne and Ground-Based Measurements of Optical Atmospheric Properties in Southern Illinois," AFCRL-TR-74-0298, SIO Ref. 74-25.

GLOSSARY AND NOTATION

The notation used in reports and journal articles produced by the Visibility Laboratory staff follows, in general, the rules set forth in pages 499 and 500, Duntley *et al* (1957). These rules are:

Each optical property is indicated by a basic (parent) symbol.

A presubscript may be used with the parent symbol as an identifier, e.g., b indicates background while t denotes an object.

A postsubscript may be used to indicate the length of a path of sight, e.g., r denotes an *apparent* property as measured at the end of a path of sight of length r, while o denotes an *inherent* property based on the hypothetical concept of a photometer located at zero distance from an object.

A postsuperscript*, or a postsubscript$_*$, is employed as a mnemonic symbol signifying that the radiometric quantity has been generated by the scattering of ambient light reaching the path from all directions.

The parenthetical attachments to the parent symbol denote altitude and direction. The letter z indicates altitude in general; z_t is used to specify the altitude of an object. The direction of a path of sight is specified by the zenith angle θ and the azimuth ϕ. In the case of irradiances, the downwelling irradiance is designated by d, the upwelling by u.

The glossary for meteorological symbols is presented in Section 6.

A(z) — Albedo at altitude z, defined by the equation $A(z) \equiv H(z,u)/H(z,d)$.

${}_sA(z)$ — Scalar albedo at altitude z, defined by the equation ${}_sA(z) \equiv h(z,u)/h(z,d)$.

AGL — Above ground level.

$C_o(z_t,\theta,\phi)$ — Inherent universal contrast determined for a path of sight of zero length at altitude of the object z_t in the direction of zenith angle θ and azimuth ϕ. This property is defined by the equation

$$C_o(z_t,\theta,\phi) \equiv \frac{{}_tN_o(z_t,\theta,\phi) - {}_bN_o(z_t,\theta,\phi)}{{}_bN_o(z_t,\theta,\phi)} .$$

$C_r(z,\theta,\phi)$	Apparent universal contrast as determined at altitude z from the end of path of sight of length r in the direction of the zenith angle θ and azimuth ϕ. This property is defined by the equation $$C_r(z,\theta,\phi) \equiv \frac{{}_tN_r(z,\theta,\phi) - {}_bN_r(z,\theta,\phi)}{{}_bN_r(z,\theta,\phi)} .$$
g	Acceleration of gravity.
H(z)	Scale height at altitude z, the height of a homogeneous atmosphere having the density of the layer at altitude z.
H(z,d)	Irradiance produced by downwelling flux as determined on a horizontal flat plate at altitude z. In this report d is used in place of the minus sign in the notation $H(z_t,-)$ which appears in Duntley (1969). This property may be defined by the equation $$H(z,d) \equiv \int_{2\pi} N(z,\theta',\phi') \cos\theta' \, d\Omega .$$
H(z,u)	Irradiance produced by upwelling flux as determined on a horizontal flat plate at altitude z. Here u is substituted for the plus sign formerly used in the notation $H(z,+)$.
h(z)	Scalar irradiance. This may be defined as the radiant flux arriving at a point, from all directions about that point, at altitude z (Tyler and Preisendorfer, 1962): $$h(z) \equiv h(z,d) + h(z,u) .$$
h(z,d)	Scalar irradiance produced by downwelling flux. This may be defined as the radiant flux from the upper hemisphere arriving at a point at altitude z.
${}_kh(z,d)$	Scalar irradiance defined as the radiant flux from the upper hemisphere sky (flux from the sun is not included) arriving at a point at altitude z.
${}_sh(z)$	Scalar irradiance defined as the radiant flux from the sun arriving at a point at altitude z.
h(z,u)	Scalar irradiance produced by upwelling flux. This may be defined as the radiant flux from the lower hemisphere arriving at a point at altitude z.

$L(z)$ — Attenuation length at altitude z. This property is the reciprocal of the attenuation coefficient, that is,

$$L(z) \equiv \alpha(z)^{-1} \ .$$

$\bar{L}(z)$ — Equivalent attenuation length is defined as

$$\bar{L}(z) = \frac{-z}{\ln T_z(0,0)} \ .$$

$m_\infty(z,\theta)/m_\infty(z,0)$ — Relative optical airmass.

$N(z,\theta,\phi)$ — Radiance as determined from altitude z in the direction specified by zenith angle θ and azimuth ϕ.

${}_bN_o(z_t,\theta,\phi)$ — Inherent background radiance as determined at altitude of the photometer z_t at zenith angle θ and azimuth ϕ.

${}_bN_r(z,\theta,\phi)$ — Apparent background radiance as determined at altitude z from the end of a path of sight of length r at zenith angle θ and azimuth ϕ. This property may be defined by the equation

$${}_bN_r(z,\theta,\phi) \equiv {}_bN_o(z_t,\theta,\phi)\, T_r(z,\theta) + N_r^*(z,\theta,\phi) \ .$$

${}_sN_\infty(0,\theta_s,0°)$ — Apparent radiance of the center of the solar disk as determined at ground-level altitude from the end of path of sight of length ∞ from out of the atmosphere to ground at zenith angle of the sun θ_s.

${}_tN_o(z_t,\theta,\phi)$ — Inherent radiance of an object as determined at altitude of the photometer z_t at zenith angle θ and azimuth ϕ.

${}_tN_r(z,\theta,\phi)$ — Apparent radiance of an object as determined at altitude z from the end of a path of sight of length r at zenith angle θ and azimuth ϕ. This property may be defined by the equation

$${}_tN_r(z,\theta,\phi) \equiv {}_tN_o(z_t,\theta,\phi)\, T_r(z,\theta) + N_r^*(z,\theta,\phi) \ .$$

$N_q(z,\theta,\phi)$ — Equilibrium radiance at altitude z with the direction of the path of sight specified by zenith angle θ and azimuth ϕ. This property is a point function of position and direction.

$\bar{N}_q(z,\theta,\phi)$ — Effective equilibrium radiance for a path of sight from out of the atmosphere to altitude z in the direction specified by zenith angle θ and azimuth ϕ. This property may be defined by the equation

$$\bar{N}_q(z,\theta,\phi) \equiv N^*_\infty(z,\theta,\phi)/[1 - T_\infty(z,\theta)] \ .$$

This property may also be denoted as a function of angle from light source (sun or moon) β, i.e., $\bar{N}_q(z,\beta)$.

$N_*(z,\theta,\phi)$ — Path function at altitude z with the direction of the path of sight specified by zenith angle θ and azimuth ϕ. This property is defined by the equation

$$N_*(z,\theta,\phi) \equiv \int_{4\pi} \sigma(z,\beta')\, N(z,\theta',\phi')\, d\Omega \ .$$

This property also is a point function of position and direction.

$N^*_r(z,\theta,\phi)$ — Path radiance as determined at altitude z at the end of a path of sight of length r in the direction specified by zenith angle θ and azimuth ϕ.

$N^*_\infty(0,\gamma_s,180°)$ — Sky radiance at a scattering angle of 90° from the sun. Also the path radiance for the path of sight of length ∞ from out of the atmosphere to ground-level altitude at a zenith angle equal to the solar elevation angle γ_s.

$n(z)$ — Index of refraction at altitude z.

$P(z)$ — Pressure at altitude z.

psia — Pressure, absolute, pounds per square inch.

psid — Pressure, differential, pounds per square inch.

${}_bR_o(z_t,\theta,\phi)$ — Inherent background reflectance as determined at the altitude of an object z_t and viewed at zenith angle θ and azimuth ϕ.

$R_q(z,\theta,\phi)$ — Equilibrium reflectance is defined as $R_q(z,\theta,\phi) \equiv N_q(z,\theta,\phi)\, \pi/H(z,d)$.

$R_r^*(z,\theta,\phi)$ Directional path reflectance as determined at altitude z at the end of a path of sight of length r in the direction specified by zenith angle θ and azimuth ϕ.

R/M(0) Universal gas constant.

$\overline{S_\lambda T_\lambda}$ Standardized relative spectral response of filter/cathode combination where S_λ is spectral sensitivity of the multiplier phototube cathode and T_λ is spectral transmittance of optical filter.

s(z) Total volume scattering coefficient as determined at altitude z. This property may be defined by the equation

$$s(z) \equiv \int_{4\pi} \sigma(z,\beta)\, d\Omega \ .$$

In the absence of atmospheric absorption, the total volume scattering coefficient is numerically equal to the attenuation coefficient.

${}_M s(z)$ Total volume scattering coefficient for Mie scattering at altitude z.

${}_R s(z)$ Total volume scattering coefficient for Rayleigh scattering at altitude z.

T(z) Temperature in degrees Kelvin at altitude z.

$T_r(z,\theta)$ Beam transmittance as determined at altitude z for a path of sight of length r at zenith angle θ. This property is independent of azimuth in atmospheres having horizontal uniformity. It is always the same for the designated path of sight or its reciprocal.

W_λ Spectral emittance (power/unit of area) of electromagnetic flux from a plane surface.

${}_c W_\lambda$ Spectral emittance of calibration source.

W'_λ Spectral emittance of anticipated field scene.

$\bar{y}$ Symbol for visual efficiency function.

ZSV Zero scale value. The zero point on the linear scale when the radiometric or photometric quantity x is equal to a reference radiometric or photometric quantity x_o as shown in the equation

$$\log[x_o/x] = 0 \ .$$

z Altitude, usually used as above ground level.

z_t — Altitude of an object.

$\alpha(z)$ — Volume attenuation coefficient as determined at altitude z. In the absence of atmospheric absorption, the attenuation coefficient is numerically equal to the volume scattering coefficient.

β — Symbol for scattering angle of flux from a light source. It is equal to the angle between the line from the source to the observer and the path of sight.

β' — Symbol for scattering angle of flux from a discrete part of the sky. It is equal to the angle between the direction specified by θ' and ϕ' and the path of sight.

γ_s — Elevation angle of the sun. The solar elevation angle is the complement of the sun zenith angle, $\gamma_s = 90° - \theta_s$.

Δ — Symbol to indicate incremental quantity and used with r and z to indicate small, discrete increments in path length r and altitude z.

δ_λ — Response area is defined as $\delta_\lambda = \Sigma(\overline{S_\lambda T_\lambda})\, \Delta\lambda$.

ϵ_λ — Spectral emissivity of tungsten filament.

ζ — Symbol for radius of the earth in Eq. 2.13 and 2.15 and Figure 2-2.

θ — Symbol for zenith angle. This symbol is usually used as one of two coordinates to specify the direction of a path of sight.

θ' — Symbol for zenith angle usually used as one of two coordinates to specify the direction of a discrete portion of the sky.

λ — Symbol for wavelength.

$\bar{\lambda}$ — Mean wavelength is defined as $\bar{\lambda} \equiv \Sigma\lambda(\overline{S_\lambda T_\lambda})\, \Delta\lambda / \delta\lambda$.

$\rho(z)$ — Density at altitude z.

σ — Symbol for volume scattering function. Parenthetical symbols may be added; for example, β may be used to designate the scattering angle from a source. In Gordon (1969) the parenthetical symbols are z and β for altitude and scattering angle.

$\sigma(z,\beta)/s(z)$ — Proportional directional volume scattering function. This may be defined by the equation

$$\int_{4\pi} [\sigma(z,\beta) / s(z)] \equiv 1 .$$

$_b\tau_r(z,\theta,\phi)$ Contrast transmittance as determined at altitude z at the end of a path of sight of length r and specified by zenith angle θ and azimuth ϕ. This property is *not* independent of azimuth and is *not* the same for the designated path of sight and its reciprocal.

ϕ Symbol for azimuth. The azimuth is the angle in the horizontal plane of the observer between a fixed point and the path of sight. The fixed point may be, for example, true north, the bearing of the sun, or the bearing of the moon. This symbol is usually used as one of two coordinates to specify the direction of a path of sight.

ϕ' This symbol for azimuth is usually used as one of two coordinates to specify the direction of a discrete portion of the sky.

Ψ Angular solar radius at true earth-to-sun distance.

$\bar{\Psi}$ Angular solar radius at mean solar distance.

Ω Symbol for solid angle. For a hemisphere

$$\Omega = 2\pi \text{ steradians;}$$

for a sphere $\Omega = 4\pi$ steradians.

1. INTRODUCTION

The field measurement program described in this report was organized under the project title SEEKVAL. It was conducted during July 1974 at Weir Prairie, near Rainier, Washington. The overall operation of this project was coordinated as a part of Air Force Cambridge Research Laboratory's Project 7621.

The SEEKVAL deployment was organized to support the SEEKVAL Project ID1 as specified by the SEEKVAL Joint Test Force. The ID1 activity was planned as a limited test to determine suitable instrumentation for recording certain characteristics of the visual scene as it exists and as it appears to observers in aircraft operating within line-of-sight distance, and for measuring atmospheric factors which could influence the transmission of scene characteristics.

The Visibility Laboratory maintains a program of continually improved techniques for predicting, by calculation from physical data, the probabilities with which any object can be visually detected and recognized. The program is multifaceted in that it involves the development of techniques and expertise in several different technical areas, each related to the visual detection and recognition task. Several of the major areas are, for example, measurement and analysis of typical terrain characteristics and scene reflectances, studies in the restoration of atmospherically distorted images, measurement and analysis of the optical properties of the atmosphere, and studies into the perceptual capabilities of the human visual system and its electro-optical counterparts. The joint application of the techniques perfected in each of these specialty areas results in the determination of detection probabilities. Inclusion of allowances for *a priori* information and reasoning processes of the brain enable the probabilities of recognition classification, and identification of real-world objects to be predicted.

The instrumental and computational organization for constant improvement of techniques related to optical atmospheric property documentation is summarized in Fig. 1-1, 1-2, and 1-3. These three figures illustrate the experimental inter-relationships among the various pieces of project hardware, listed in rectangles at the top of each figure and discussed in Section 3, the radiometric measurements made by them, and the subsequent computational chains associated with each of the measured values. The optical properties, listed in the blocks at or near the bottom of each figure, are derived in accordance with the theoretical considerations discussed in Section 2, AFCRL-TR-73-0422, Duntley, *et al.* (1973). Through an examination of these generalized flow charts, one can readily evaluate this portion of the project's flexibility and self-checking redundancies. The capability to generate equivalent optical properties from separate independent data sources, as indicated within these three figures, is the key feature in ensuring advancements in technical expertise and data quality.

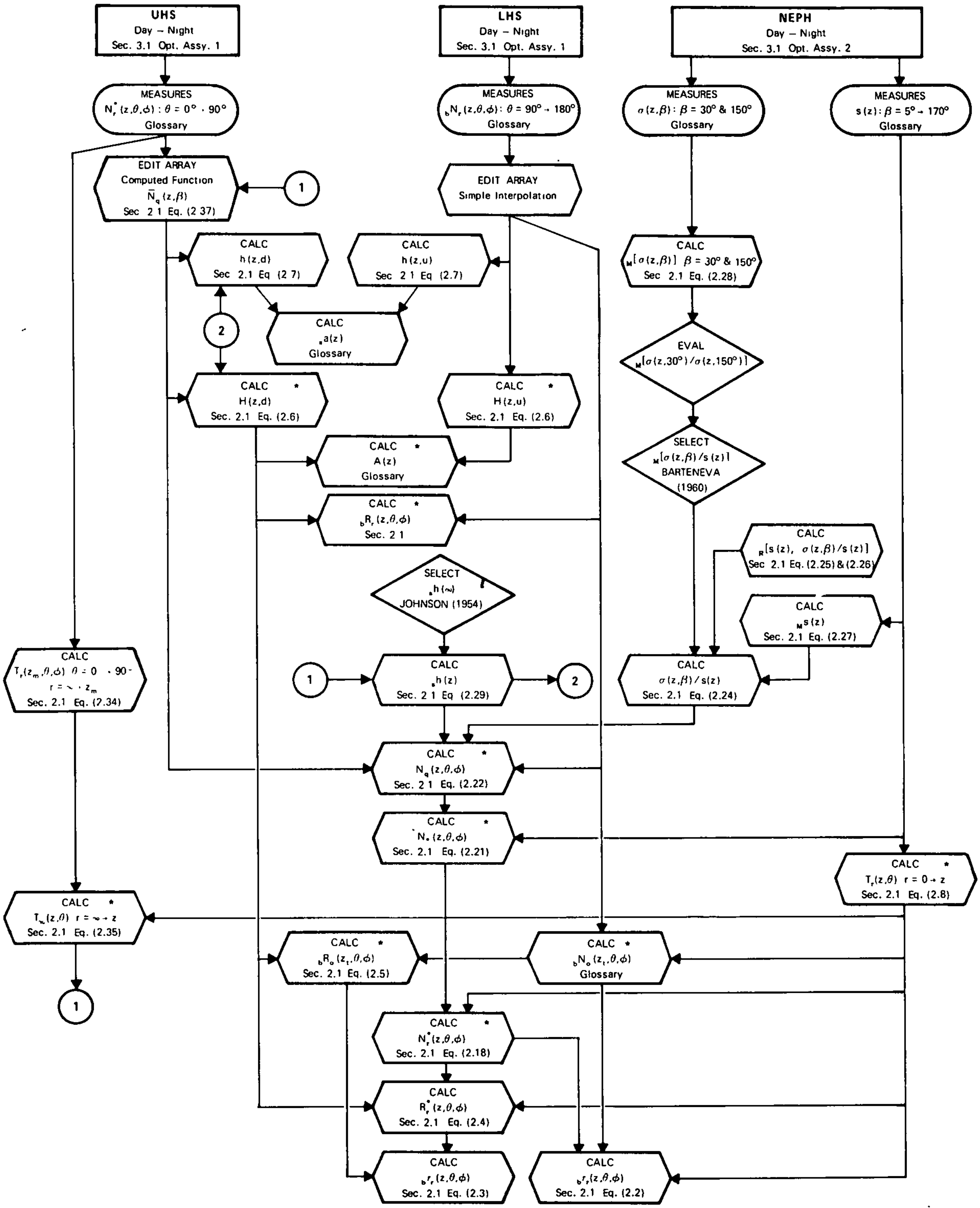

* Indicates Existence of Validation Measurement
in backup data set.

Fig. 1-1. Computations From Basic Airborne Data.

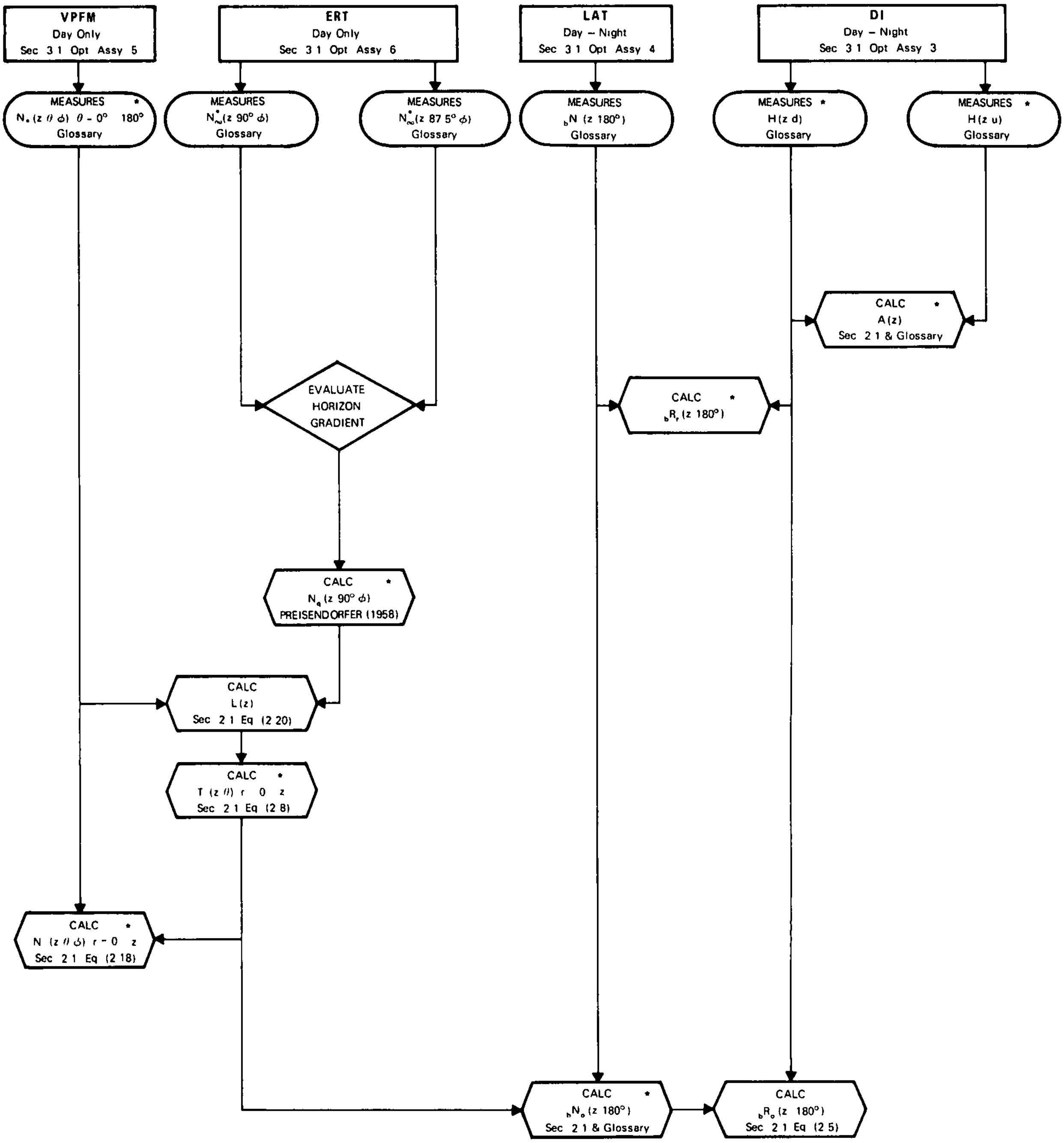

* Indicates utilization as direct validation of computed values.

Fig. 1-2. Computations From Backup Airborne Data.

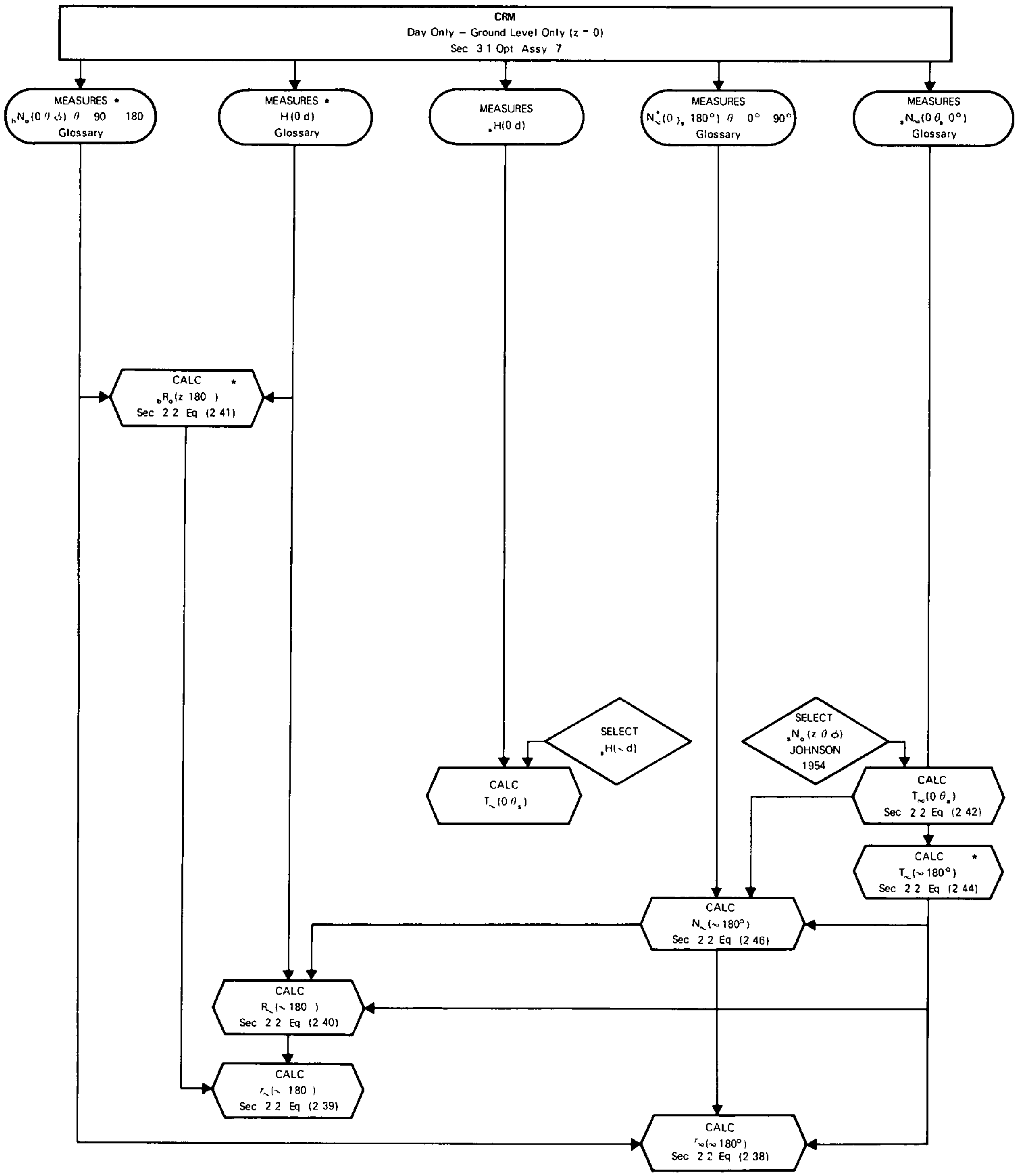

* Indicates utilization as direct validation of computed values.

Fig. 1-3. Computations From Specialized Ground Data.

This report, Scientific Report No. 5, has been prepared under Contract No. F19628-73-C-0013. It contains the optical properties of various downward-inclined paths of sight based upon daytime atmospheric optical measurements. These properties include natural irradiance upon horizontal plane surfaces, scalar irradiance, total volume scattering coefficient, atmospheric beam transmittance, path radiance, directional path reflectance, and directional terrain reflectance. The measurements were made along the flight tracks illustrated in Fig. 1-4.

In addition, this report utilizes, but does not present, selected data from 13 sets of ground-based measurements. These ground-based measurements were made at Weir Prairie during the same general time intervals that the aircraft was in operation along its flight tracks. They are restricted to ground-level scattering coefficient and earth-to-space beam transmittance.

The methods used in the derivation of these optical properties are discussed in Section 2 and are similar to those presented in AFCRL-TR-73-0422, Duntley, *et al.* (1973). The most significant variation from earlier methods is in the derivation of the scattering coefficient profiles. Due to a procedural problem with the airborne integrating nephelometer during this deployment, an alternative computational technique employing data from the sky scanning radiometers and the variable path function meter was used to derive the total scattering coefficient profiles. This alternative technique is discussed in Section 8.

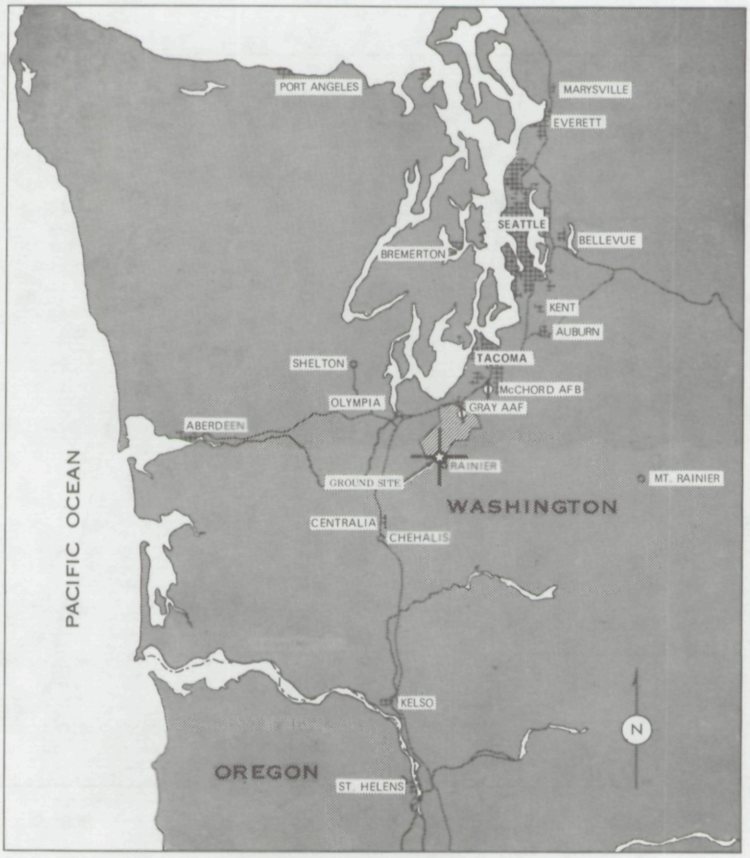

Fig. 1-4. Typical SEEKVAL Flight Tracks.

The instrumentation, developed at the Visibility Laboratory and installed in Air Force C-130A aircraft No. 50022, is reported in detail in AFCRL-70-0137, Duntley, *et al.* (1970), and AFCRL-72-0593, Duntley, *et al.* (1972c). A brief review of the instrumentation as used during the SEEKVAL deployment is presented in Section 3.

The instrumentation used to generate the raw data upon which the reported properties are based consisted of an integrating nephelometer, two sky scanning telephotometers, and a variable path function meter on the aircraft, and an integrating nephelometer on the ground. Reliable data from the airborne integrating nephelometer were available on only two of the seven flights reported. Corroborative data were obtained using a ground-based contrast reduction meter to determine earth-to-space beam transmittances when weather permitted.

The radiometer spectral responses were standardized for the SEEKVAL deployment in the manner illustrated in Fig. 1-5. However, due to the nature of the experimental task, only Filter 4 (pseudo-photopic) was utilized for field measurements.

Data collection methods were similar to those reported in AFCRL-TR-74-0298, Duntley, *et al.* (1974), although all the flight profiles were conducted at relatively low altitudes. The highest straight and level altitude was approximately 1200 meters above ground level (AGL). The basic features of these stylized daytime flight profiles are summarized in Section 4.

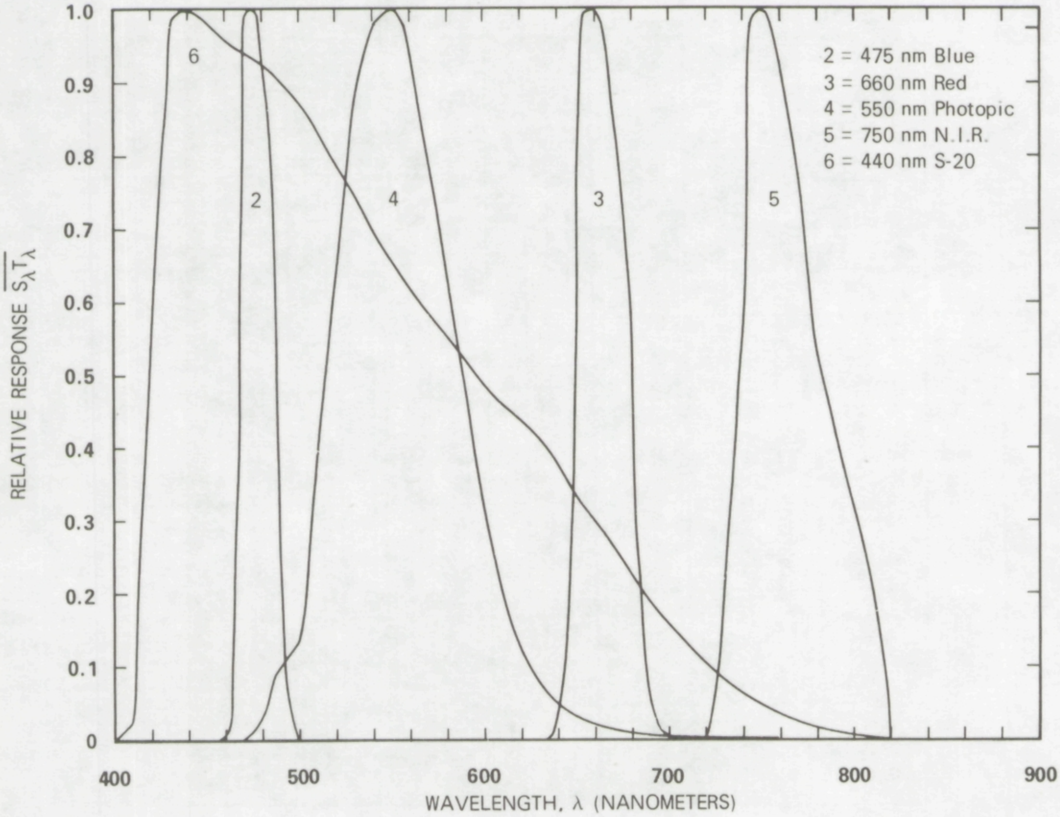

Fig. 1-5. Standard Spectral Responses — Project SEEKVAL.

The computer techniques used for processing the data included in this report are summarized in Section 5. They are, in general, the same as the techniques reported in AFCRL-77-0593, Duntley, *et al.* (1972c).

A general discussion of the weather patterns that predominated in the Rainier area during the data collection interval is presented in Section 6. This section, in conjunction with the flight track photographs shown in Section 7, is intended as an aid to the data user's generalized interpretation and evaluation. The inclusion of the graphical presentations is intended to further facilitate the user's rapid orientation with the overall weather situation.

The radiometric data representing seven separate flights and containing eight double profiles are also presented in Section 7. The presentation format resembles that used in AFCRL-TR-74-0298, Duntley, *et al.* (1974).

Discussion related to the interpretation and evaluation of the data collected is found in Section 8.

2. THEORY

2.1 CONTRAST TRANSMITTANCE IN THE TROPOSPHERE

Contrast transmittance ${}_b\tau_r(z,\theta,\phi)$ is defined as the ratio of the apparent contrast $C_r(z,\theta,\phi)$ to the inherent contrast $C_o(z_t\theta,\phi)$:

$$ {}_b\tau_r(z,\theta,\phi) = C_r(z,\theta,\phi)/C_o(z_t,\theta,\phi) \ . \tag{2.1} $$

The parenthetical modifiers indicate the altitude z of the sensor and the zenith angle θ and azimuth ϕ of the path of sight. In this report, ϕ will always be in terms of azimuth from light source (sun or moon). The path length r in the direction of the path of sight is between the altitude of the target z_t and the sensor altitude z. For the inherent contrast the path length is zero. The presubscript b on the contrast transmittance ${}_b\tau_r(z,\theta,\phi)$ indicates background. The contrast transmittance is a function of the inherent background radiance ${}_bN_o(z_t,\theta,\phi)$, the atmospheric beam transmittance $T_r(z,\theta)$ and the path radiance $N_r^*(z,\theta,\phi)$ of the path of sight as shown in Eq. 2.2 [Duntley (1964) Eq. 2.4]:

$$ {}_b\tau_r(z,\theta,\phi) = [1 + N_r^*(z,\theta,\phi)/{}_bN_o(z_t,\theta,\phi)\ T_r(z,\theta)]^{-1} \ . \tag{2.2} $$

As noted in the glossary, beam transmittance is considered as being independent of azimuth, and thus its notation is typically simplified from the general form by omitting the azimuth designator ϕ.

DIRECTIONAL PATH REFLECTANCE

The concept of directional path reflectance [Duntley (1969) p. 3] is utilized in an alternate form of Eq. 2.2,

$$ {}_b\tau_r(z,\theta,\phi) = [1 + R_r^*(z,\theta,\phi)/{}_bR_o(z_t,\theta,\phi)]^{-1} \ , \tag{2.3} $$

where ${}_bR_o(z_t,\theta,\phi)$ is the directional background reflectance. By definition, the directional path reflectance is

$$R_r^*(z,\theta,\phi) = \pi N_r^*(z,\theta,\phi)/[H(z_t,d)\, T_r(z,\theta)] \ , \quad (2.4)$$

where $H(z_t,d)$ is the downwelling irradiance. We have chosen to present the atmospheric data in the form of directional path reflectance since, in this form, it can be easily utilized with the directional reflectance of a variety of backgrounds smaller in extent but different from the heterogeneous background which contributed to the path radiance and downwelling irradiance. The directional path reflectance is also the most convenient form of presenting the atmospheric data for easy use to obtain contrast transmittance.

BACKGROUND REFLECTANCE

The inherent background reflectance is defined as

$${}_bR_o(z_t,\theta,\phi) = \pi\, {}_bN_o(z_t,\theta,\phi)/H(z_t,d) \ , \quad (2.5)$$

where $H(z_t,d)$ is the downwelling irradiance at the target altitude [Gordon (1964) p. 558 or Boileau and Gordon (1966) p. 805]. The inherent background reflectance may be obtained from either (1) a measurement by a ground-based telephotometer† or (2) measurements by an airborne telephotometer. In this report airborne telephotometer data from the lowest altitude of flight not extrapolated to ground level were used to obtain the terrain reflectances reported here for each flight.

DOWNWELLING AND UPWELLING IRRADIANCE

The downwelling irradiance used to compute the directional path reflectance $R_r^*(z,\theta,\phi)$ and the apparent terrain reflectance is computed from data at the lowest altitude of flight by the equation

$$H(z,d) = {}_sh(z)\cos\theta_s + \int_{2\pi} N(z,\theta',\phi')\cos\theta'\, d\Omega \ , \quad (2.6)$$

where ${}_sh(z)$ is the sun scalar irradiance at altitude z, θ_s is the sun zenith angle, and $N(z,\theta',\phi')$ is the sky radiance at direction θ',ϕ'. When the sky is fully overcast, the first term is essentially zero.

The upwelling irradiance $H(z,u)$ is computed by deleting the first term in Eq. 2.6 and replacing the sky radiances with apparent terrain radiances from the lower hemisphere scanner. The θ' would then be the nadir angle so that $\cos\theta'$ is positive. The albedo $A(z)$ is the ratio of the upwelling to downwelling irradiance $H(z,u)/H(z,d)$.

† Although the measurements are radiometric as opposed to photometric, the instrument used to perform these measurements is referred to herein as a "telephotometer" in lieu of the more precise term "teleradiometer." This is in keeping with the practice established in previous publications.

A second type of irradiance is the scalar or nondirectional irradiance:

$$h(z,d) = {}_s h(z) + \int_{2\pi} N(z,\theta',\phi')\, d\Omega \ . \tag{2.7}$$

The scalar irradiance is not weighted by the cosine. The upwelling irradiance from zenith angles between 90 and 180 degrees is designated by $h(z,u)$ and computed by using Eq. 2.7 without the first term. The total scalar irradiance is the sum of the upwelling and downwelling scalar irradiances, $h(z) = h(z,u) + h(z,d)$. The scalar albedo is defined as the ratio of upwelling to downwelling scalar irradiance, $h(z,u)/h(z,d)$. For a full discussion of scalar irradiances and scalar albedo uses refer to Gordon (1969).

BEAM TRANSMITTANCE

The beam transmittance $T_r(z,\theta)$ is obtained directly from the total scattering coefficient $s(z)$ by means of Eq. 2.8. (Refer also to Boileau (1964) p. 570.) When there is no significant atmospheric absorption in the passbands of the measurements, e.g., from smoke, dust, or smog, the attenuation coefficient $\alpha(z)$ is equivalent to the scattering coefficient $s(z)$. Therefore,

$$T_r(z,\theta) = \exp\left[-\sum_{i=1}^{n} \alpha(z_i)\Delta r\right] = \exp\left[-\sum_{i=1}^{n} s(z_i)\Delta r\right] , \tag{2.8}$$

where Δr is the incremental path length. The measured total scattering coefficient data are extrapolated to ground level when no ground-based measurements are available. The extrapolation assumes that the scattering particles are the same at all altitudes, but decrease or increase according to the density at each altitude $\rho(z)$:

$$s(o) = \frac{s(z)\rho(o)}{\rho(z)} \ . \tag{2.9}$$

Similarly, upward extrapolations are made to the highest reported altitude above ground level when the highest flight altitude is less. Extrapolation in this case is based on the scattering coefficient measured at highest flight altitude. The densities used for the extrapolations are from the U. S. Standard Atmosphere (1962). The density at each altitude is obtained by truncated Chebyshev expansion using the coefficients for the atmosphere between 0 and 80 kilometers [U. S. Standard Atmosphere Supplements (1966), p. 69].

All altitudes reported are between ground level and 6 kilometers. For all paths of sight at zenith angles greater than 95 degrees, Δr equals $\Delta z \sec\theta$ for these altitudes. The Δr is always nonnegative since Δz is defined as $z_1 - z_2$ (the subscripts increase with the flux direction). See Fig. 2-1. The $|\Delta z|$ used is 30 meters (98.4 feet). For zenith angles greater than 95 degrees, the beam transmittance can also be expressed as a function of the vertical beam transmittance $T_r(z,180)$ as follows:

$$T_r(z,\theta) = T_r(z,180)^{|\sec\theta|} \; . \qquad (2.10)$$

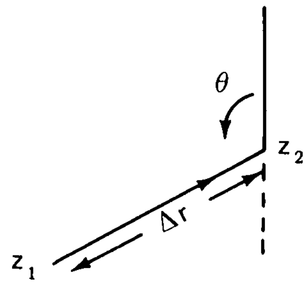

Fig. 2-1. Path Length Geometry for Steeply Inclined Paths of Sight.

ATTENUATION LENGTH

The attenuation length $L(z)$ is defined as the reciprocal of the atmospheric attenuation coefficient $\alpha(z)$. Therefore, when there is no significant absorption, it is also equivalent to the reciprocal of the atmospheric scattering coefficient:

$$L \equiv \frac{1}{\alpha(z)} = \frac{1}{s(z)} \; . \qquad (2.11)$$

The equivalent attenuation length $\bar{L}(z)$ is a pseudo-attenuation length which, when combined with its altitude z, can be used directly in the equation [Boileau (1964), Eq. 6.1]

$$T_r(z,\theta) = \exp\,[-z/\bar{L}(z)]\,|\sec\theta| \; , \qquad (2.12)$$

where $\theta > 95°$.

EARTH CURVATURE AND REFRACTION

For the paths of sight at zenith angles from 90 to 95 degrees, the Δr for $|\Delta z| = 30$ meters (98.4 feet) is significantly longer at ground level than at 6 kilometers due to the curvature of the earth. Therefore, for these paths of sight, the incremental path length Δr_i is computed from

$$\Delta r_i = \left\{ 1 - \left[\frac{n(z)}{n(z_i)} \; \frac{(\zeta + z)}{(\zeta + z_i)} \; \sin\theta \right]^2 \right\}^{-1/2} \Delta z \; . \qquad (2.13)$$

This is the classical equation for computing incremental path length at paths of sight affected by earth curvature and refraction. The n(z) is the refractive index, z is the sensor or observer altitude, ζ is the radius of the earth. Equation 2-13 was derived as follows. The Δr_i due to earth curvature is a function of the angle θ'' which is the angle of the flux path at altitude z_i (see Fig. 2-2 for the relationship of θ and θ'' for the downward path of sight):

$$\Delta r_i = \sec\theta'' \Delta z = (1 - \sin^2\theta'')^{-1/2} \Delta z \ . \tag{2.14}$$

Since $\sin x = \sin(180^\circ - x)$, the law of sines can be used to express Δr as a function of the path of sight θ:

$$\sin\theta'' = \frac{\zeta + z}{\zeta + z_i} \sin\theta \ . \tag{2.15}$$

The refraction effect is added by recourse to Snell's law, thus resulting in Eq. 2.13.

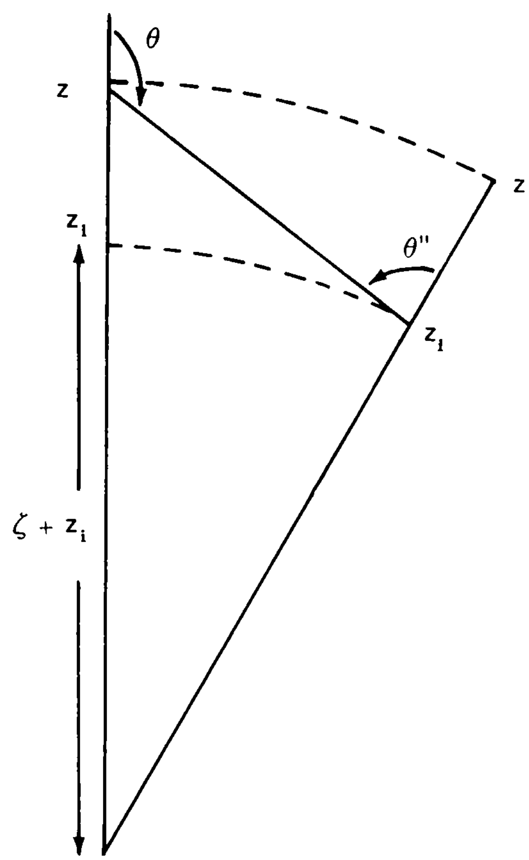

Fig. 2-2. Path Length Geometry for Grazing Paths of Sight in Refractive Spherical Atmospheres.

The square of the refractive index ratio is given in an alternate form by Kasten (1965) as

$$\left[\frac{n(z)}{n(z_i)}\right]^2 = 1 + 2[n(z) - 1]\,[1 - \rho(z_i)/\rho(z)] \ . \qquad (2.16)$$

This can be rewritten in terms of the refractive index at ground level $z = o$ as follows :

$$\left[\frac{n(z)}{n(z_i)}\right]^2 = 1 + 2[n(o) - 1]\left[\frac{\rho(z)}{\rho(o)} - \frac{\rho(z_i)}{\rho(o)}\right] \ . \qquad (2.17)$$

The density values for computing the refraction effect are, as before, based on the U. S. Standard Atmosphere (1962). The refractive index used for ground level was 1.000276, appropriate to a wavelength of 700 nanometers at 15 degrees centigrade. The maximum error in using the Δr based on 700 nanometers for wavelengths of 478 to 770 nanometers is 0.2 percent.

PATH RADIANCE

Path radiance $N_r^*(z,\theta,\phi)$ for the downward-looking path of sight is the integration or summation of the path function $N_*(z,\theta,\phi)$ weighted by the beam transmittance $T_{ri}(z,\theta)$. Path length ri is from the incremental path Δr to the sensor at z :

$$N_r^*(z,\theta,\phi) = \sum_{i=1}^{m} N_*(z_i,\theta,\phi)\, T_{ri}(z,\theta)\, \Delta r \ . \qquad (2.18)$$

Refer to Duntley, *et al.* (1957), Eq. 17 on p. 502.

PATH FUNCTION

Image-forming light is lost by scattering and absorption in each elementary segment of the path of sight, and contrast-reducing path radiance is generated by the scattering of the ambient light which reaches the segment from all directions. The quantitative description of this scattered component of path-segment radiance involves a quantity called the "path function," $N_*(z,\theta,\phi)$. The "path function" depends upon the directional distribution of the lighting on the segment due to its surroundings. It can be operationally defined in terms of the (limiting) ratio of the path radiance associated with a short path to the path length by the relation [Duntley, *et al.* (1957) p. 501]

$$N_*(z,\theta,\phi) = \lim(\Delta r \to 0)\, N_{\Delta r}^*(z,\theta,\phi)/\Delta r \ . \qquad (2.19)$$

In experimental practice, the path length Δr should be sufficiently short so that no change in the ratio can be detected if Δr is made shorter.

In lieu of a direct measurement of path function, it may be derived from related quantities. Path function, attenuation length, and equilibrium radiance are related by [Duntley, *et al.* (1957), Eq. 11]

$$N_q(z,\theta,\phi) = N_*(z,\theta,\phi)\, L(z) \ . \tag{2.20}$$

By substituting Eq. 2.11 into Eq. 2.20 and rearranging, path function is expressed as a function of the total scattering coefficient and the equilibrium radiance :

$$N_*(z_i,\theta,\phi) = N_q(z_i,\theta,\phi)\, s(z_i) \ . \tag{2.21}$$

EQUILIBRIUM RADIANCE

The equilibrium radiance [Duntley, *et al.* (1957), p. 502, and Gordon (1969), p. 15] is first computed from the measurements made at each of the altitudes of level flight and then interpolated and extrapolated to obtain values at each 30-meter (98.4-foot) interval z_i. Equilibrium radiance is interpolated rather than path function since the equilibrium radiance is relatively invariant with altitude, whereas path function is sensitive to changes in aerosol scattering as well as the lighting distribution. To compute the equilibrium radiance the following equation is used (refer to Gordon (1969), Eq. 16* on p. 16):

$$N_q(z,\theta,\phi) = {}_sh(z)\,\frac{\sigma(z,\beta)}{s(z)} + \int_{4\pi} N(z,\theta',\phi')\,\frac{\sigma(z,\beta')}{s(z)}\, d\Omega \ , \tag{2.22}$$

where ${}_sh(z)$ is the scalar irradiance of the sun (or full moon), β is the angle between the sun and the path of sight, and $N(z,\theta',\phi')$ is the apparent radiance of the sky or ground for direction θ' and ϕ'. When the sky is fully overcast, the first term in Eq. 2.22 is essentially zero. The ratio $\sigma(z,\beta')/s(z)$ is the proportional directional scattering coefficient at angle β' and altitude z. The β' is the angle between the path of sight at θ, ϕ, and the radiance θ', ϕ'. It is found by

$$\cos\beta' = \sin\theta\,\sin\phi\,\sin\theta'\,\sin\phi' + \sin\theta\,\cos\phi\,\sin\theta'\,\cos\phi' + \cos\theta\,\cos\theta' \ . \tag{2.23}$$

It is the scalar irradiance which designates the flux that enters into the computations of equilibrium radiance and path function when the directional radiances are not known or used. It is the directionality of that flux combined with the directionality of the volume scattering function which produces the unique equilibrium radiance associated with each path of sight.

---

* Equation 16 applies equally well to real and model atmospheres.

PROPORTIONAL DIRECTIONAL SCATTERING COEFFICIENT

The proportional directional scattering function is found by combining the Rayleigh scattering component and the Mie scattering component:

$$\sigma(z,\beta')/s(z) = \left\{ {}_{R}s(z) \; {}_{R}\!\left[\frac{\sigma(z,\beta')}{s(z)}\right] + {}_{M}s(z) \; {}_{M}\!\left[\frac{\sigma(z,\beta')}{s(z)}\right] \right\} /s(z) \; . \qquad (2.24)$$

The Rayleigh scattering coefficient ${}_{R}s(z)$ for each passband is based upon monochromatic values of Rayleigh volume scattering coefficient computed using the Penndorf (1957) Eq. 14 for 15 degrees centigrade sea level pressure. The Rayleigh scattering coefficient is corrected to ambient temperature and pressure by the ideal gas law equation. Since the Rayleigh scattering is a direct function of density,

$${}_{R}s(z) = {}_{R}s(0)\, P(z)/[T(z)\; 3.516E3] \; , \qquad (2.25)$$

where $P(z)$ is pressure in dynes cm^{-2}, $T(z)$ is temperature in degrees Kelvin, and 3.516E3* has units of dynes $cm^{-2}\,{}^{\circ}K^{-1}$ and is the density at standard sea level pressure and 15 degrees centigrade temperature times the universal gas constant. The proportional directional scattering function for Rayleigh scattering ${}_{R}[\sigma(\beta)/s]$ is not a function of altitude so the parenthetical modifier is not used. It is found by

$${}_{R}[\sigma(\beta)/s] = (1 + \cos^2\beta)\, 3/(16\pi) \; . \qquad (2.26)$$

The Mie scattering coefficient at measurement altitude z is the measured scattering coefficient minus the Rayleigh coefficient computed from Eq. 2.25 above:

$${}_{M}s(z) = s(z) - {}_{R}s(z) \; . \qquad (2.27)$$

The Mie volume scattering function ${}_{M}[\sigma(z,\beta)/s(z)]$ is taken from a catalog of values derived from data on photopic volume scattering functions published by Barteneva (1960) for a range of total scattering coefficients typifying atmospheric conditions from near Rayleigh clarity to hazes which restricted visibilities to less than 4.8 kilometers (3 miles). Barteneva's gradual classes of scattering function are used exclusively since most of the steep classes are encountered only in fog. The classes are based upon the ratio of forward- to backward-scattering coefficients. The ratio of the Mie scattering at 30 and 150 degrees, ${}_{M}[\sigma(30^{\circ})/\sigma(150^{\circ})]$, is directly correlated with the forward- to backward-scattering ratio. The Mie volume scattering functions at 30 and 150 degrees are obtained from the measured volume scattering function at 30 and 150 degrees by subtracting the Rayleigh component, as follows:

---

* The form of 3.516E3 is an alternate format for 3.516×10^3. This computer form is used throughout this report.

$$ {}_{M}\sigma(\beta) = \sigma(\beta) - {}_{R}s(z)\, {}_{R}[\sigma(\beta)/s] \ . \tag{2.28} $$

When valid values for the directional scattering function at 30 and 150 degrees are not available, the selection of the Barteneva function is made on the basis of the photopic scattering coefficient. The ratio of forward- to backward-scattering coefficients is reasonably correlated with the visibility which is defined as three times the reciprocal of the scattering coefficient (when there is no absorption) as illustrated in Fig. 2-3 (taken from Barteneva (1960), Fig. 6. One might note that visibilities below 4.8 kilometers (3 miles) are often less than acceptable conditions for operating aircraft under visual flight rules.

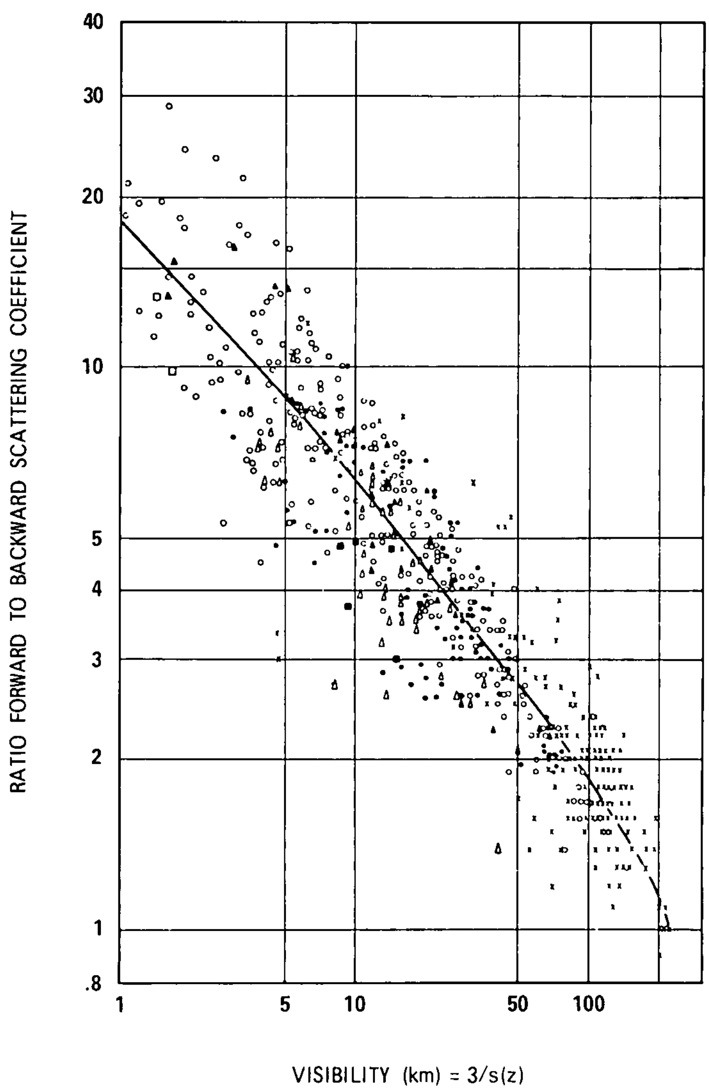

Fig. 2-3. Correlation of Forward- to Backward-Scattering Coefficient ratio with Visibility.

SUN IRRADIANCE

Although the scanner radiance measurements include a measure of the apparent sun radiance, the sun is not always fully in the field of view. Therefore, the sun irradiance used in the computations of the irradiance and the equilibrium radiance is based upon the sun irradiance out of the atmosphere ${}_sh(\infty)$ for the appropriate broadband filter and the beam transmittance from out of the atmosphere to altitude z, $T_\infty(z,\theta_s)$:

$$ {}_sh(z) = {}_sh(\infty)\, T_\infty(z,\theta_s) \ . \tag{2.29} $$

The sun irradiance values for mean solar distance ${}_sh(\bar{\infty})$ are computed from spectral sun irradiance from Johnson (1954). The sun irradiance at true solar distance ${}_sh(\infty)$ is equal to the irradiance at mean distance times the square of the ratio of the angular solar radius Ψ at true solar distance to the radius $\bar{\Psi}$ at mean distance:

$$ {}_sh(\infty) = {}_sh(\bar{\infty}) \left(\frac{\Psi}{\bar{\Psi}} \right)^2 \ . \tag{2.30} $$

The angular solar radius at mean solar distance is 16.016 minutes of arc. The radii at true distance are obtained from the ephemeris for the appropriate date.

When the sky at the highest flight altitude is clear, the transmittance from out of the atmosphere to the highest flight altitude due to scattering is computed from the ratio of sky radiances at equivalent scattering angles from the sun. This method stems from the suggested nomographic method of Kushpil' and Petrova (1971) for obtaining beam transmittance from sky radiance ratios at equivalent scattering angles from the sun. Kushpil' and Petrova do not give equations for the sky radiance ratio as a function of beam transmittance, but such an equation is derived in the following paragraph.

A sky radiance is a path radiance from out of the atmosphere to the altitude of measurement $N^*_\infty(z,\theta,\phi)$. On clear days with no absorption, we have found the sky radiance to be a function of an effective equilibrium radiance $\bar{N}_q$ and the beam transmittance [Gordon, *et al.* (1963), Gordon (1969), and Gordon, *et al.* (1973)]:

$$ N^*_\infty(z,\theta,\phi) = \bar{N}_q(z,\theta,\phi)\,[1 - T_\infty(z,\theta)] \ . \tag{2.31} $$

Thus the ratio of two sky radiances, at angles θ and θ', would be

$$ \frac{N^*_\infty(z,\theta,\phi)}{N^*_\infty(z,\theta',\phi')} = \frac{\bar{N}_q(z,\theta,\phi)\ [1 - T_\infty(z,\theta)]}{\bar{N}_q(z,\theta',\phi')\ [1 - T_\infty(z,\theta')]} \ . \tag{2.32} $$

When the scattering angle from the sun is equivalent for the two paths of sight, the equilibrium radiances are equivalent. Thus Eq. 2.32 simplifies to

$$\frac{N_{\infty}^{*}(z,\theta,\phi)}{N_{\infty}^{*}(z,\theta',\phi')} = \frac{[1 - T_{\infty}(z,\theta)]}{[1 - T_{\infty}(z,\theta')]} \quad . \tag{2.33}$$

Equation 2.33 can be expressed as a function of the vertical transmittance $T(z,0^{\circ})$ and the relative optical airmass $m_{\infty}(z,\theta)/m_{\infty}(z,0^{\circ})$:

$$\frac{N_{\infty}^{*}(z,\theta,\phi)}{N_{\infty}^{*}(z,\theta',\phi')} = \frac{\left[1 - T_{\infty}(z,0^{\circ})^{m_{\infty}(z,\theta)/m_{\infty}(z,0^{\circ})}\right]}{\left[1 - T_{\infty}(z,0^{\circ})^{m_{\infty}(z,\theta')/m_{\infty}(z,0^{\circ})}\right]} \quad . \tag{2.34}$$

Equation 2.34 cannot be directly solved for the vertical transmittance, but by using iterative means, which is a simple task with a computer, a vertical transmittance is obtained which provides a solution to Eq. 2.34 within a tolerance of 0.1 percent.

An error analysis of the transmittance obtained by Eq. 2.34 indicates that the precision error difference of the two radiances is generally multiplied by a factor of between 1 and 2 for many zenith angle combinations. Thus, a series of measurements is used, and the transmittances are averaged to enhance the reliability of the resultant transmittance due to scattering. A validation of the sky radiance ratio method of obtaining beam transmittance was presented in Duntley, *et al.* (1972c), Section 2.1.

Atmospheric absorption acts to reduce the incoming sun irradiance but has no affect on the sky radiance relative distribution. Thus the transmittance based on sky radiance ratios is due to scattering only, and the transmittance losses due to absorption must be added as a separate factor. Tousey and Hulburt (1947) calculated a photopic transmittance of 0.977 due to absorption by ozone at the top of the atmosphere. The photopic transmittance from out of the atmosphere to the highest flight altitude is the product of the transmittance due to scattering and the transmittance due to absorption.

When the sky at the highest altitude is not completely free of clouds, the beam transmittance from space to altitude may be specified on the basis of ground-based contrast reduction meter measurements or other measurements which yield an estimate of space-to-altitude transmittance.

The transmittance for the lower flight altitudes is the product of the transmittance from out of the atmosphere to the highest altitude $T_{\infty}(z_m,0^{\circ})$ and the transmittance between the two flight altitudes $T_r(z,0^{\circ})$:

$$T_{\infty}(z,0^{\circ}) = T_{\infty}(z_m,0^{\circ})\, T_r(z,0^{\circ}) \quad . \tag{2.35}$$

The conversion from vertical transmittance to transmittance at the zenith angle of the sun is made using the relative airmass $m_\infty(z,\theta_s)/m_\infty(z,0°)$:

$$T_\infty(z,\theta_s) = T_\infty(z,0°)^{m_\infty(z,\theta_s)/m_\infty(z,0°)} \quad . \qquad (2.36)$$

The relative airmass equals $\sec\theta$ for $\theta_s \leqq 70°$ to an accuracy of 1 percent. Also, the relative airmass at altitudes up to 6 kilometers equals the relative airmass at sea level, $m_\infty(6,\theta_s)/m_\infty(6,0°) = m_\infty(0,\theta_s)/m_\infty(0,0°)$, to an accuracy of 1 percent for $\theta_s \leqq 86°$. Sea level relative airmass values from Kasten (1965) are used for θ_s 70 → 86°.

The sun zenith angle θ_s changes during the flight interval. In order to reduce this source of variability in the resultant data, an average sun zenith angle for each filter or the total flight is used in Eq. 2.36 as well as in computing the irradiance in Eq. 2.6 and the scattering angle β in Eq. 2.22.

SKY AND TERRAIN RADIANCE

The arrays of sky and terrain radiance measurements have missing values due to the sampling schedule and include values which are questionable due to: possible inclusion of the sun in the field of view; portions of the airplane such as tail or propellers extending into path of sight; values above or below the calibrated range of the sensor; and irregularities in the angular pattern. In order to obtain a basic data array of optimum quality, these well-defined but improper values must be removed and the blank values replaced. To do this, the upper and lower hemisphere data arrays are handled separately, and in the following manner.

Since the terrain radiances have a relatively narrow range, questionable values are simply replaced by interpolations between adjacent valid data points. The same procedure is used for sky radiances under heavy overcast.

For clear skies, in order to evaluate and replace the questionable sky radiance measurements, the effective equilibrium radiance as a function of angle from sun β is established on the basis of the sky radiance measurements $N_\infty^*(z,\theta,\phi)$ of known validity. The effective equilibrium radiance $\bar{N}_q$ is computed by rearranging Eq. 2.31 as follows:

$$\bar{N}_q(z,\beta) = N_\infty^*(z,\theta,\phi)/[1 - T_\infty(z,\theta)] \quad . \qquad (2.37)$$

An average effective equilibrium radiance for each 5 degrees of β is then calculated and the proportional standard deviation from that average function established. The value of the average effective equilibrium radiance at $\beta = 0°$ is determined using Barteneva's method of assuming log $\bar{N}_q(\beta)$ linear with $\cos\beta$ for small values of β. The questionable sky radiance measurements are then replaced using the average equilibrium radiance function and Eq. 2.31.

2.2 GROUND-BASED MEASUREMENTS OF VERTICAL EARTH-TO-SPACE CONTRAST TRANSMITTANCE

The earth-to-space contrast transmittance for the vertical path of sight is found by rewriting Eq. 2.2 in terms of the earth-to-space path length ∞ and the vertical downward path of sight at zenith angle 180°:

$$_b\tau_\infty(\infty,180°) = [1 + N_\infty^*(\infty,180°)/_bN_o(0,180°)\, T_\infty(\infty,180°)]^{-1} \; . \qquad (2.38)$$

The azimuth ϕ has been deleted from the parenthetical modifiers of the path radiance $N_\infty^*(\infty,180°)$ and the inherent background radiance $_bN_o(0,180°)$ since ϕ is undefined when the path of sight is vertically downward.

DIRECTIONAL PATH REFLECTANCE

An alternate form for obtaining contrast transmittance is by use of the vertical path reflectance $R_\infty^*(\infty,180°)$. Thus, Eq. 2.3 is similarly rewritten,

$$_b\tau_\infty(\infty,180°) = [1 + R_\infty^*(\infty,180°)/_bR_o(0,180°)]^{-1} \; . \qquad (2.39)$$

Ground-based data are often presented in the form of vertical path reflectance for convenient use in obtaining contrast transmittance. The path reflectance may be used with the directional reflectance of various backgrounds which are smaller in extent but different from the heterogeneous background which contributes to the path radiance and downwelling irradiance H(0,d). The vertical path reflectance is defined by

$$R_\infty^*(\infty,180°) = \pi N_\infty^*(\infty,180°)/H(0,d)\, T_\infty(\infty,180°) \; . \qquad (2.40)$$

BACKGROUND REFLECTANCE

The inherent vertical background reflectance is defined as

$$_bR_o(0,180°) = \pi\, _bN_o(0,180°)/H(0,d) \; . \qquad (2.41)$$

Terrain radiances $_bN_o(z,\theta,\phi)$ are measured directly by orienting a contrast reduction meter (CRM) telescope toward the ground.

DOWNWELLING IRRADIANCE

Total downwelling irradiance $H(z,d)$ is measured directly by orienting a CRM assembly and its attached cosine collector cap in a horizontal position. In this position, the measurement represents total downwelling irradiance from the full 2π upper hemisphere on a flat plate, cosine-weighted collector.

BEAM TRANSMITTANCE

The beam transmittance for the path of sight from space to earth in the direction of the sun $T_\infty(0,\theta_s)$ is obtained directly from solar transmissometer measurements of the apparent radiance ${}_sN_\infty(0,\theta_s,0°)$ at the center of the solar disk and from the inherent solar radiance† ${}_sN_o(\infty,\theta_s,0°)$ by the following equation:

$$T_\infty(0,\theta_s) = \frac{{}_sN_\infty(0,\theta_s,0°)}{{}_sN_o(\infty,\theta_s,0°)} \quad . \tag{2.42}$$

The vertical earth-to-space beam transmittance is equal to the vertical space-to-earth beam transmittance, and therefore Eq. 2.36 can be rewritten to obtain the vertical downward transmittance from the transmittance at the angle of the sun:

$$T_\infty(\infty,180°) = T_\infty(0,0°) = T_\infty(0,\theta_s)^{m_\infty(0,0°)/m_\infty(0,\theta_s)} \quad . \tag{2.43}$$

For $\theta_s \leqq 70°$, the inverse of the relative airmass $m_\infty(0,0°)/m_\infty(0,\theta_s) = \cos\theta_s$ to an accuracy of 1 percent. Since the solar elevation angle γ_s, which equals $90° - \theta_s$, is read directly off of the ground-based equipment, Eq. 2.43 is rewritten as

$$T_\infty(\infty,180°) = T_\infty(0,\theta_s)^{\sin\gamma_s} \quad . \tag{2.44}$$

This eliminates the need for ephemeris or tabular data in the field in reducing data for $\theta_s \leqq 70°$.

For $\theta_s > 70°$, the sea level relative airmass values $m_\infty(0,\theta_s)/m_\infty(0,0°)$ from Kasten (1965) are used. As noted before, for ground-level altitudes up to 6 kilometers, $m_\infty(6,\theta_s)/m_\infty(6,0°) = m_\infty(0,\theta_s)/m_\infty(0,0°)$ within 1 percent for $\theta_s \leqq 86°$.

† The values for inherent solar radiance at the center of the disk are based upon the solar irradiances out of the atmosphere from Johnson (1954).

PATH RADIANCE

The path radiance for the vertically downward path of sight is derived from an appropriate ground-based measurement of sky radiance and beam transmittance [Gordon, *et al.* (1973), Eq. 8]:

$$N_{\infty}^{*}(\infty,180°) = N_{\infty}^{*}(0,\theta',\phi') \left[\frac{1 - T_{\infty}(\infty,180°)}{1 - T_{\infty}(0,\theta')} \right] , \tag{2.45}$$

where $N_{\infty}^{*}(0,\theta',\phi')$ is the path radiance of an upward-inclined path of sight at zenith angle θ' and azimuth ϕ', which has the same angle β from the sun as does the vertically downward path of sight. This quantity is in fact the apparent sky radiance as measured from the surface of the earth in the direction θ', ϕ'. The $T_{\infty}(0,\theta')$ is the beam transmittance of the upward-inclined path of sight in the direction θ', ϕ'.

The scattering at 90 degrees from the sun is assumed to be reasonably equivalent to the scattering toward the vertically downward path of sight. This assumption simplifies the definition of the equivalent look angle θ' to $90° - \theta_s$, or simply γ_s, and ϕ' becomes 180°. See Fig. 2-4. The CRM illustrated in Fig. 3-2 is built to mechanically insure that the sky radiance is measured at a 90-degree angle from the sun. Equation 2.45 can now be rewritten as

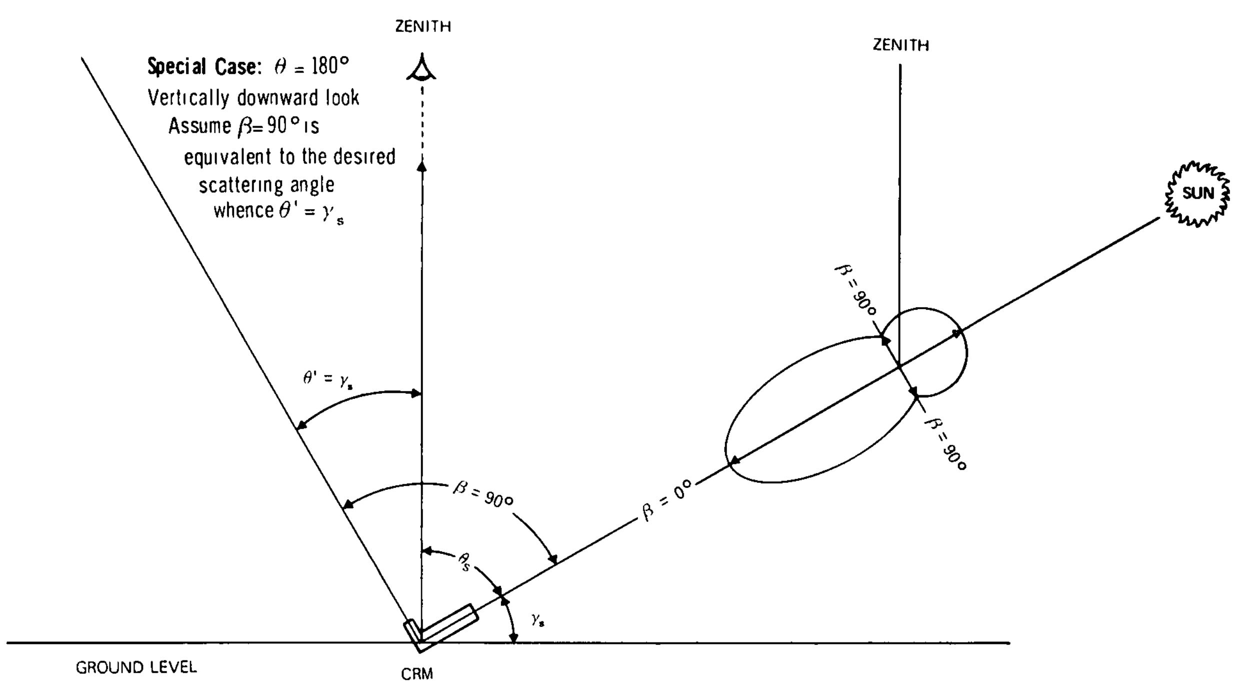

Fig. 2-4. Scattering Angle Relationships for Typical CRM Operations.

$$N^*_\infty(\infty,180°) = N^*_\infty(0,\gamma_s,180°)\left[\frac{1 - T_\infty(\infty,180°)}{1 - T_\infty(0,\gamma_s)}\right] . \quad (2.46)$$

When $\gamma_s \leqq 70°$, the transmittance for the upward inclined path at θ' is

$$T_\infty(0,\gamma_s) = T_\infty(0,0°)^{\sec\gamma_s} . \quad (2.47)$$

For $\gamma_s > 70°$, the relative optical airmass from Kasten (1965) is used instead of $\sec\gamma_s$ in Eq. 2.47.

3. INSTRUMENTATION

The scientific instrumentation utilized for the Project SEEKVAL task was basically the same as that reported in AFCRL-72-0593, Duntley, *et al.* (1972c).

For the convenience of the reader, all significant instrument systems assigned during the Project SEEKVAL exercise are tabulated in Table 3-1 and depicted in Fig. 3-1 and 3-2. The ground-based instrument system illustrated in Fig. 3-2 is in the similar configuration to that utilized on a previous deployment. The SEEKVAL configuration was radiometrically equivalent, but employed a modified upper hemisphere scanner mounting arrangement.

Table 3-1. Project SEEKVAL Instrumentation

I. Radiometric

   A. Multiplier Phototube (MPT) Assembly
   B. Temperature Control Housing Assembly
   C. Optical Filter Assembly
   D. Radiometer Measuring Circuit Assembly
   E. Optical Collector Assembly
      1. Automatic 2π Scanner Assembly
      2. Integrating Nephelometer Mode Selector Head Subassembly
      3. Dual Irradiometer Assembly
      4. Large Aperture Telescope Assembly
      5. Variable Path Function Meter Assembly
      6. Equilibrium Radiance Telephotometer
      7. Contrast Reduction Meter

II. Meteorological

A. Royco Model 220 Particle Counter

B. Cambridge Model 137-C3 Aircraft Hygrometer System

C. AN/AMQ-17 Aerograph Set

D. Bourns Model 430/530 Absolute Pressure Transducer

E. Bourns Model 509 Differential Pressure Transducer

F. Bendix Model 566 Aspirated Hygrometer

G. Science Associates Windspeed and Direction Set

H. Taylor Model SMT-5-51 Aneroid Barometer

III. Control and Communication

A. 2π Scanner Control Console

B. Photometer Temperature Control Panel

C. Optical Filter Control Panel

D. Ten Slide Photometer Module

E. Camera Control Panel

F. Flight Dynamics Display Panel

G. 42 Channel Data Logger

H. 20 Channel Data Logger

IV. Photographic

A. Airborne Automax G-1 Camera System

B. Ground-Based Soligor System

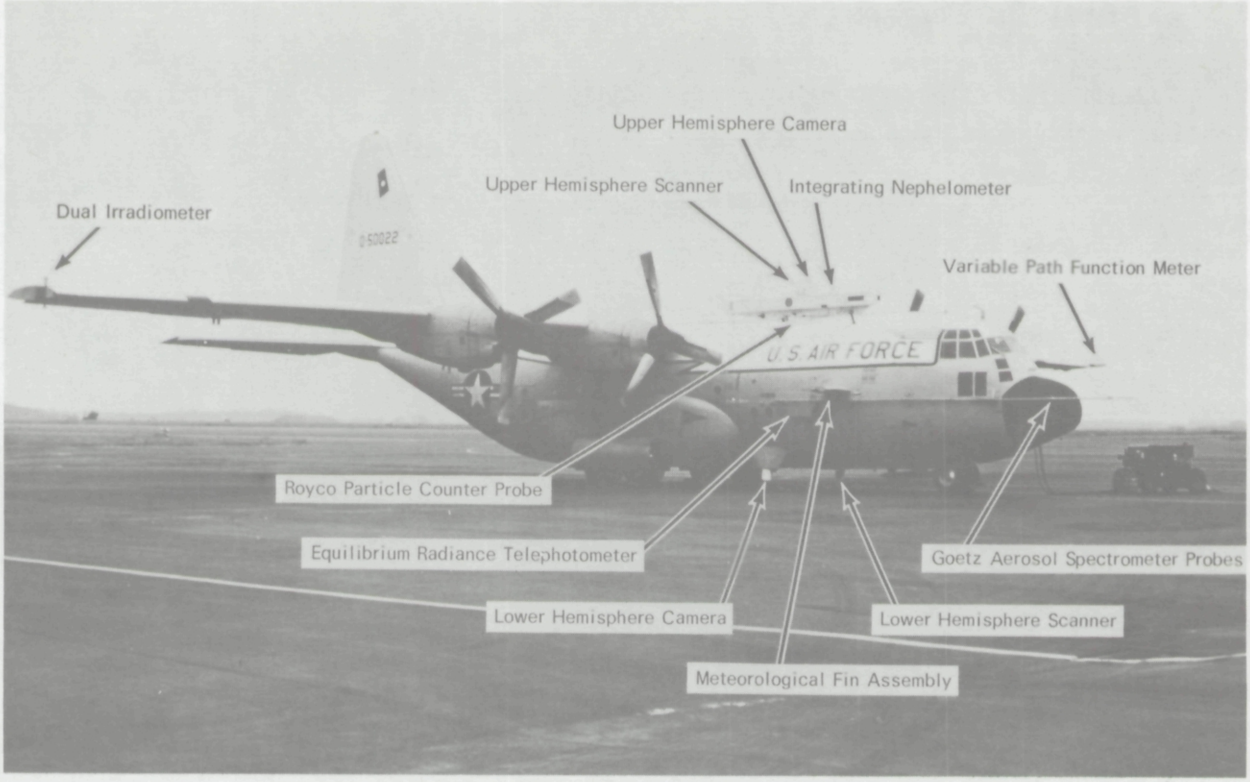

Fig. 3-1. C-130 Airborne Instrument System.

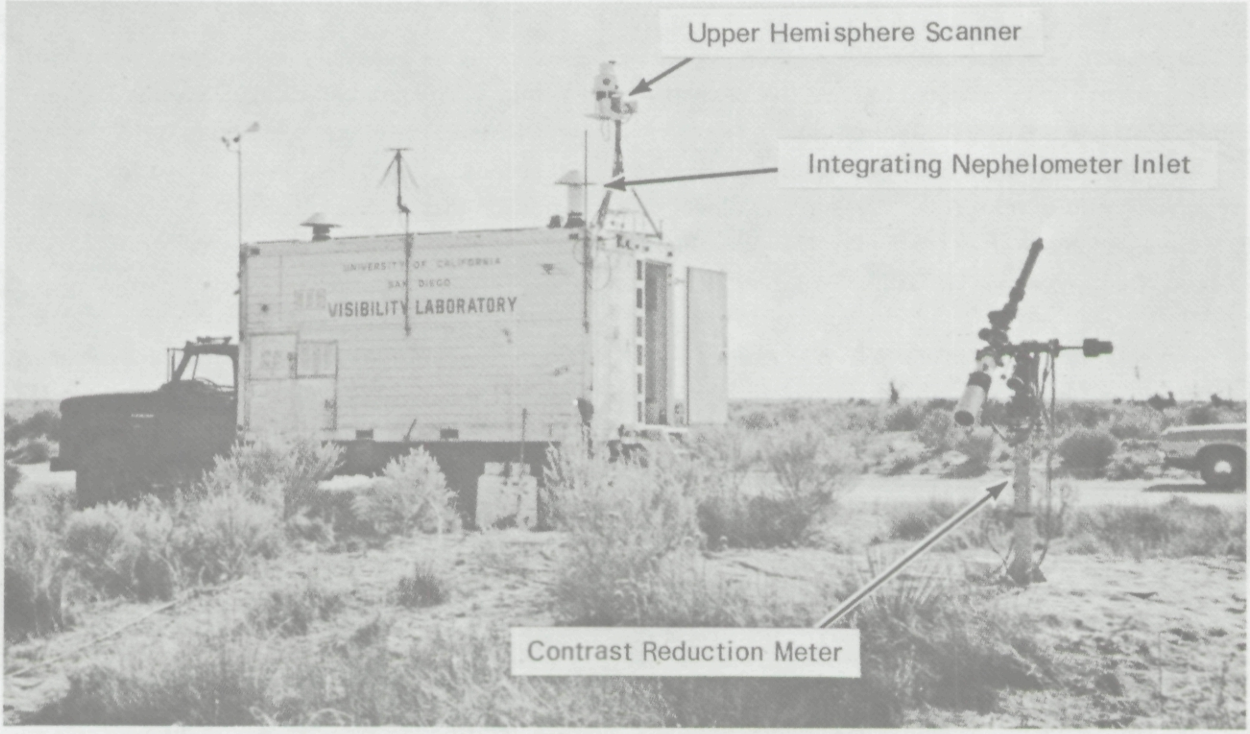

Fig. 3-2. Ground-Based Instrument System.

3.1 RADIOMETRIC SYSTEMS

A standardized radiometer, typical of those used during this data collection interval, consists of five major assemblies as listed below.

1. Multiplier Phototube Assembly
2. Temperature Control Housing Assembly
3. Optical Filter Assembly
4. Radiometer Measuring Circuit Assembly
5. Optical Collector Assembly

These assemblies are generally interchangeable between different radiometer systems, allowing easy field cannibalization in the event of a catastrophic failure of any assembly within a key system. For use in Project SEEKVAL, these five assemblies were basically unchanged from the configurations reported in AFCRL-72-0593, Duntley, *et al.* (1972c). For reader convenience, a brief description of each optical collector assembly follows.

OPTICAL COLLECTOR ASSEMBLIES

Seven basic types of collector assemblies were used in combination with the basic detector configurations described in AFCRL-74-0298, Duntley, *et al.* (1974). The only major differences between the various radiometer systems described in this report are the differences in these seven collector assemblies. The fundamental assembly differences are summarized in the following paragraphs.

Automatic 2π Scanner (UHS and LHS) Assembly. This collector assembly is essentially a small telescope that can be directed to optically scan any point within a 2π-steradian field of view. The telescope itself has a 5-degree field of view. For the SEEKVAL mission, the airborne scanners were directed in a sweep pattern which covered the full hemisphere in 180 seconds. The output is converted to an array of radiance values at selected azimuth and elevation angles, such that Δ azimuth = 6° and Δ elevation = 5° between adjacent array elements. The sweep pattern characteristics are more fully described in AFCRL-72-0593, Duntley, *et al.* (1972c).

Integrating Nephelometer (NEPH) Assembly. In order to measure and evaluate the total scattering coefficient of typical real aerosols, the Visibility Laboratory has devised and built an instrument referred to as an integrating nephelometer. This device measures the radiant flux scattered from the well-defined flux beam of a high-intensity projector. The scattered flux is collected through three different optical channels: two telescopes oriented to collect the flux scattered in the $\beta = 30°$ and $\beta = 150°$ directions, and one irradiometer assembly oriented to collect the flux scattered between the scattering angles of $\beta = 5°$ and $\beta = 170°$. From these measurements, the directional scattering functions $\sigma(30)$ and $\sigma(150)$ and the total volume scattering coefficient s may be derived.

Dual Irradiometer (DI) Assembly. The dual irradiometer assembly is a two-channel irradiometer. It has two optical input channels but only one optical output. A rotating prism subassembly allows the system operator to select either input channel for optical coupling with the output channel, while simultaneously occulting the other. The resultant time-sharing of a single detector assembly yields a device optimized for ratio type measurements.

The flat plate diffuse collector surfaces used in this assembly are mechanically corrected to yield a cosine collection characteristic within ± 2 percent for all angles of incidence between 0 and 80 degrees.

The dual irradiometer assembly is mounted on the aircraft wingtip so that the flat plate collectors are horizontal. In this configuration the upper channel receives radiant flux from the entire hemisphere above the aircraft, and the lower channel receives radiant flux from the entire hemisphere below the aircraft. These measurements of downwelling and upwelling irradiance can be used both in the calculation of directional terrain reflectances and in intersystem data validation checks.

Large Aperture Telescope (LAT) Assembly. This telescope assembly is used in the radiometer system which functions as a backup system for measuring very low flux levels. The airborne telescope assembly has a 5-degree circular field of view and an objective lens 6.2 centimeters in diameter. With this larger collection aperture, flux levels significantly lower than the detection threshold of the 2π scanner assembly can be reached and adequately measured. This system was deployed during Project SEEKVAL using a prototype integrated photometer circuit. This prototype circuit is envisioned as the next generation detector for all project radiometers.

Variable Path Function Meter (VPFM). The variable path function meter is a radiometer and shroud assembly designed to measure the radiant flux scattered by a small, well-defined volume of aerosol into a given direction when illuminated from all directions. The scattering volume is 1.27 centimeters in diameter and 22.9 centimeters in length. It is defined by the cylindrically-limited field of view of the component telephotometer and by two long cylindrical sunshades. Measurements of path function can normally be made at zenith angles between 0 and 180 degrees at azimuths corresponding to the aircraft heading. However, for the SEEKVAL deployment the VPFM was mounted in an alternative configuration which allowed measurements to be made at zenith angles between 88 degrees and 180 degrees at azimuths corresponding to either the aircraft heading or its reciprocal.

Equilibrium Radiance Telephotometer (ERT). The concept of equilibrium radiance is defined and discussed in Duntley, *et al.* (1957). In the special case of a horizontal path of sight which is optically uniform in both the composition of the aerosol and its lighting, the equilibrium radiance is equal to the horizon radiance. It is this horizon radiance which is measured by the ERT.

The ERT is basically a servo-controlled telescope. Its field of view is 1.0 degree wide and 0.2 degree high. The ERT is oriented with a horizontal path of sight and with the wide dimension of the field of view parallel to the horizon. This orientation is maintained by use of a vertical reference gyro. At the discretion of the operator, a 2.5-degree step function can be superimposed on the normal reference signal. In this condition the path of sight is alternately directed horizontally and 2.5 degrees above horizontal. The radiance measurements made at these two zenith angles determine the near horizon radiance gradient.

Contrast Reduction Meter (CRM). The function of the CRM is to measure apparent solar radiance, sky and terrain radiance, and downwelling irradiance, all with the same detector and measuring circuit. These measurements allow direct computation of earth-to-space universal contrast transmittance.

The CRM consists of a standard detector and filter changing assembly, fitted with a multiple-purpose optical collector. The optical collectors include a cosine collector for measuring the downwelling irradiance; a telescope with a 5-degree field of view for measuring sky and terrain radiances; and a Pinhole Gershun tube with a 4-minute field of view for measuring solar disk radiances.

3.2 METEOROLOGICAL SYSTEMS

All of the meteorological systems utilized in this project were purchased items; the operating characteristics of each are available in the appropriate manufacturer's brochures. For use in Project SEEKVAL, the meteorological systems were unchanged from the configurations reported in AFCRL-72-0593, Duntley, *et al.* (1972c).

The airborne meteorological package consisted of one Royco model 220 particle counter, one Cambridge model 137-C3 aircraft hygrometer system, one AN/AMQ-17 aerograph set, and two Bourns aneroid pressure transducers.

The ground-based meteorological package was less extensive, consisting of only one Royco model 220 particle counter, one Bendix model 566 aspirated hygrometer, one Science Associates windspeed and direction set, and one Taylor model SMT-5-51 aneroid barometer. The Royco system did not perform adequately during Project SEEKVAL, and thus no particle distribution data are available.

Since all of the meteorological systems were described in AFCRL-72-0255, Duntley, *et al.* (1972a) and AFCRL-72-0593, Duntley, *et al.* (1972c), no further discussion is included in this report.

3.3 CONTROL AND COMMUNICATION SYSTEMS

The basic control panels, consoles, and other support facilities listed in Table 3-1 are described fully in AFCRL-70-0137, Duntley, *et al.* (1970) and AFCRL-72-0593, Duntley, *et al.* (1972c), and the updated configurations are also reported in AFCRL-72-0593, Duntley, *et al.* (1972c). Therefore the control and communication systems are not discussed further in this report.

A problem, however, was discovered during post-deployment data analysis, which indicated that an erroneous biasing voltage had been within the control circuitry during the SEEKVAL deployment. The trouble was traced to the Visibility Studies control console. Software techniques were then utilized to correct the data on the critical altitude and heading channels, and to try to more specifically locate the source of the problem. At the same time of this report, the problem had been narrowed down to the filter control panel, but the specific circuit fault was still not identified.

3.4 PHOTOGRAPHIC SYSTEMS

Photographic documentation of the test environment performed simultaneously with the radiometric and meteorological measurements has always been a highly desirable adjunct to any field activity. For Project SEEKVAL, this photographic capability was accomplished by the Visibility Laboratory through the use of two camera systems.

AIRBORNE AUTOMAX G-1 CAMERA SYSTEM

Two 35-millimeter Automax G-1 cameras, modified to accept Traid 735 Periphoto (180-degree) lenses, were mounted on the project aircraft (Fig. 3-1). One camera was oriented to photograph the 2π upper hemisphere and the other covered the 2π lower hemisphere. Either or both cameras may be run in either cine or single-frame modes at the discretion of the operator.

The photographs from these cameras are used only as general background for the interpretation of the radiometric measurements. Thus, no special controls are placed upon the film or its processing. For this general-purpose application, the cameras are normally loaded with Kodak Ektacolor Professional S, No. 5026 film. Typical photographs from this system are used as illustrations in Section 7 of this report and were shot with a fixed f6.3 aperture in the single-frame mode.

GROUND-BASED SOLIGOR SYSTEM

The ground-site documentation photographs have historically been limited to 35-millimeter color snapshots, taken on a casual basis during lulls in the experimental sequences. For Project SEEKVAL this procedure was supplemented with a scheduled routine of site photographs using a Soligor Conversion Fisheye lens. This lens possesses almost universal adaptability to a wide variety of cameras and prime lenses. During Project SEEKVAL it was used on a Yashica, Lynx 1000.

An automatic camera system utilizing a Beatie, model D9 VARITRON was implemented during the SEEKVAL deployment in an attempt to improve the ground-based photographic documentation. Unfortunately, a magazine malfunction near the end of the deployment damaged most of the film. The system has been abandoned in favor of a more modern camera which is presently being modified as a retrofit into the basic control system.

AIRBORNE AVIONICS LABORATORY SYSTEM

Three camera systems were provided by the Air Force Avionics Laboratory for use during the Project SEEKVAL missions. They consisted of Chicago Aerial Industries KA-51A and Maurer 500 cameras. During each flight these camera systems were used to photographically document the test site as it appeared from the C-130A aircraft. The photographs from these camera systems are not included in this report.

3.5 RADIOMETRIC CALIBRATION PROCEDURES

All the radiometers used in this project are calibrated in essentially the same manner. In each case, the system is calibrated first by determining its relative flux versus high voltage characteristics over the anticipated operating span and second by establishing known absolute flux levels on this voltage curve. The entire calibration procedure is conducted by using standard photometric practices, a 3-meter optical bench, and incandescent standards of luminous intensity traceable to the National Bureau of Standards.

A detailed discussion of these calibration procedures is contained in Duntley, *et al.* (1970 and 1972a, b, and c) and is, therefore, only summarized in this report.

LINEARITY CALIBRATION PROCEDURE

The process of establishing the relative flux versus high voltage characteristic curve for each system is simple and direct. The radiometer system is positioned on the optical bench and irradiated with flux from a stabilized incandescent lamp. The mechanical and optical arrangement is such that the amount of flux presented to the detector can be readily varied in increments of 0.10 log unit. The mechanical constraints on positioning the movable lamp housing ensure compliance with the desired inverse square relationship between lamp position and flux at the detector. Therefore, through an iterative process of relocating the lamp housing at a predetermined set of locations on the optical bench and recording the resulting radiometer output signal, one can generate a set of data illustrating the system electrical response to known changes of input radiance. This set of data is commonly referred to as the system linearity calibration.

The linearity calibrations for all radiometers employed in the Project SEEKVAL task extended over a radiance span of 5 log cycles. The electrical circuitry was adjusted to yield an output signal which swung from +250 to −1000 millivolts for this five-decade swing in radiant input. The pseudo-logarithmic characteristics of the radiometer measuring circuit results in a linearity calibration curve typified in Fig. 3-3.

ABSOLUTE CALIBRATION PROCEDURE

Once the linearity calibration for the radiometer system has been established, a similar procedure is followed to convert the calibration into absolute units. For this portion of the calibration sequence, an incandescent standard of luminous intensity is used as the flux source. Then absolute levels of irradiance can be presented to the radiometer either directly or via a calibrated reflectance standard.

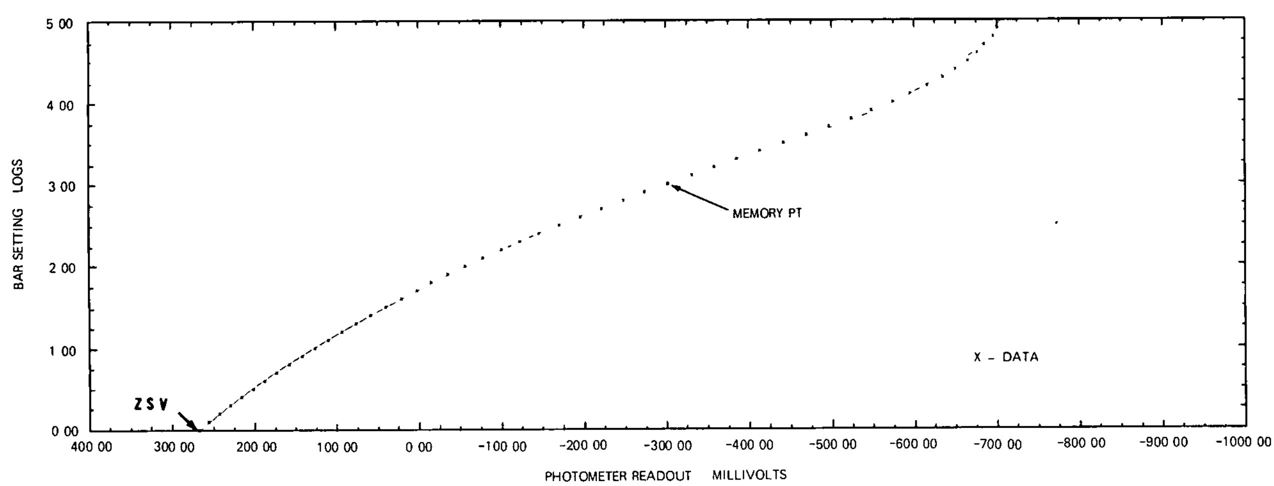

Fig. 3-3. Typical Computer-Generated Linearity Calibration Curve.

Nine determinations of the calibration constant are made during each calibration run. The average value of the nine determinations is assumed to be the most probable value for the calibration constant. Due to precision limitations, stray light, and related procedural errors, typical standard deviations for the calibration constant are on the order of ± 2 percent. Table 3-2 illustrates the quality of typical calibration constants associated with data tabulated in Section 7. It should be noted that the term "standard deviation" is not rigorously correct in this application since the calibration data set includes some obvious systematic errors due to detector dynamic response, as well as some procedural stray light errors. These systematic errors are not removed from the calibration data and, as a result, the standard deviation of the calibration constant represents a worst-case type of index.

It should also be noted that, in some cases, the basic calibration of the radiometer system is accomplished in the night mode. The conversion of the calibration constant to day mode, which allows calibrated measurements at daylight flux levels, is made by applying the day/night neutral density factor. Obviously, an error in the determination of this factor will also contribute to the overall probable error.

Table 3-2

Project SEEKVAL

Radiometer Calibration Constants (ZSV) and Related Fractional Standard Deviations (δ %) for Daylight Flights

Radiometer Identification		Calib	Calib	Filter 2		Filter 4		Filter 3		Average
System Title	MPT SN	Mode	Units	ZSV	δ %	ZSV	δ %	ZSV	δ %	δ %
CRM/SS	9861	*Out	w/Ω m²μm	1 55E+05	± 2	4 65E+04	± 2	2 93E+05	± 2	± 2
CRM/E-CAP	9861	*Out	w/ m²μm	1 64E+06	± 2	4 41E+05	± 2	2 58E+06	± 2	± 2
SCAN-1 W/FIXED	10650	*Out	w/Ω m²μm	7 59E+06	± 1	3 01E+06	± 1	1 71E+07	± 1	± 1
SCAN-1 W/FIXED	10650	Out	w/Ω m²μm	1 14E+03	± 1	4 53E+02	± 1	3 28E+03	± 1	± 1
SCAN1/E W/FIXED	10650	Out	w/ m²μm	1 41E+04	± 1	4 96E+03	± 1	3 33E+04	± 1	± 1
SCAN-3 W/FIXED	10697	*Out	w/Ω m²μm	7 83E+06	± 6	3 59E+06	± 2	1 76E+07	± 5	± 4
SCAN-3 W/FIXED	10697	Out	w/Ω m²μm	1 18E+04	± 6	3 93E+03	± 2	3 10E+04	± 5	± 4
SCAN-4 W/FIXED	9869	Out	w/Ω m²μm	1 13E+03	± 9	5 32E+02	± 1	3 31E+03	± 11	± 7
NEPH-1 SIGMA	9858	Out	w/m²μm	3 61E-01	± 1	1 33E-01	± 1	4 91E-01	± 1	± 1
NEPH-1 B30	9858	Out	w/Ω m²μm	3 11E-01	± 1	1 41E-01	± 1	5 68E-01	± 1	± 1
NEPH-3 SIGMA	14509	Out	w/m²μm	6 10E-02	± 3	2 47E-02	± 2	8 14E-02	± 2	± 2
NEPH-3 B30	14509	Out	w/Ω m²μm	6 28E-02	± 1	2 47E-02	± 1	9 14E-02	± 1	± 1
LAT 1	4463	Out	w/Ω m²μm	5 12E+00	± 1	3 46E+00	± 1	6 03E-01	± 1	± 1
D.I UPPER LEG	11783	*Out	w/ m²μm	6 87E+04	± 1	2 29E+04	± 4	6 92E+04	± 3	± 3
ERT	9846	Out	w/Ω m²μm	4 36E+02	± 1	1 73E+02	± 0	7 95E+02	± 1	± 1
VPFM	14531	Out	w/Ω m²μm	4 09E+01	± 1	2 30E+01	± 1	1 32E+02	± 1	± 1

* Indicates that the basic night mode absolute calibration was adjusted for daylight using calibrated range neutral density filter

Note LAT 1 Filter 3 is S-11.

A typical data sheet for the absolute calibration of a Project SEEKVAL radiometer is shown in Fig. 3-4. Five different levels of input radiance are used in the determination of the calibration constant for the system. The calibration constant is referred to as the zero scale value and is labeled ZSV on the calibration forms.

All procedural and precision uncertainties are, of course, independent of the absolute accuracy of the standard lamp calibration, which is assumed to be ± 3 percent.

At regular intervals during the calibration procedure, the radiometer is automatically exposed to its internal reference source, i.e., Isolite standard of luminous intensity. Since this integral, exceptionally stable source is always available for reinspection by the radiometer during subsequent measurement activities, the long term stability of the detector can be monitored and, when necessary, automatic adjustments to the calibration constant can be readily effected.

ABSOLUTE CALIBRATION FOR

(15) SCAN-3 W/FIXED (1)697 N) (RADIOMETER) TAKEN ON 6/13/74 (PRE SEEK) DEPLOYMENT

FILTER NO. 4 (DAY SKY 7000 DEGREES KELVIN)

SPAN ID	D1 CM	TOTAL DIST. CM	TOTAL DIST.SQ. CM.SQ.	CALC.TGT. B OR E *	DETEC. RAW OUTPUT	LOG OF (KO/K)	RAW ZSV	PERCENT DIFF OF RAW AVG	AVG RAW ZSV	F1 LUM. TO RAD. WATTS/LUM.	F2 COLOR MATCH	CORRECTED ZSV
1	40	141.000	1.988E 04	8.269E-03	-280	3.442	2.286E 01	1.7	2.326E 01	1.050E-03	1.263E 00	3.085E-02
2	70	171.000	2.924E 04	5.622E-03	-343	3.620	2.346E 01	-.9				
3	120	221.000	4.884E 04	3.366E-03	-427	3.843	2.345E 01	-.8				
4	200	301.000	9.060E 04	1.815E-03	-542	4.118	2.378E 01	-2.3				
5	300	401.000	1.608E 05	1.022E-03	-658	4.363	2.359E 01	-1.4				
5	300	401.000	1.608E 05	1.022E-03	-657	4.361	2.346E 01	-.8				
4	200	301.000	9.060E 04	1.815E-03	-540	4.114	2.359E 01	-1.4				
3	120	221.000	4.884E 04	3.366E-03	-424	3.836	2.308E 01	.8				
2	70	171.000	2.924E 04	5.622E-03	-339	3.609	2.286E 01	1.7				
1	40	141.000	1.988E 04	8.269E-03	-277	3.435	2.249E 01	3.3				

LINEARITY MAXIMUM = (458) APPLIED CUTOFF = (-881)
LINEARITY CALIB. END = (-881) FULL DARK = (-959) CUTOFF = (-881)

* CALCULATED LUMINANCE IN LUMENS/STERADIAN SQ.CM.

RAW ZSV STD = (4.1358E-01) FRACT. STD = (1.78) PERCENT ZSV IN WATTS SR SQ. CM. IS 3.085E-02

WITH UNIT CONVERSION FACTOR OF 127300.(0010). TO CHANGE UNITS FROM (W/SR SQ.M CM)
TO (W/SR SQ.M MICRO M) THE NEW ZSV IN WATTS/SQ. M MICRO M. IS 3.92695E 03

THIS FILTER IS PSEUDO-PHOTOPIC. TO CONVERT TO TRUE PHOTOPIC STANDARD (SEE TECHNICAL MEMORANDUM AV71-005T)
FOR DAYLIGHT DATA MULTIPLY BY 72.000LUMEN-UM / WATT. PHOTOPIC ZSV IS 2.82741E 05 LUMEN/STER SQ M.
FOR NIGHT TIME LIGHTING MULTIPLY BY 68.340LUMEN-UM / WATT. PHOTOPIC ZSV IS 2.68368E 05 LUMEN/STER SQ M.
FOR NEPHELOMETER ONLY MULTIPLY BY 72.220LUMEN-UM / WATT. PHOTOPIC ZSV IS 2.83605E 05 LUMEN/STER SQ M.

MV FLUCTUATION DATA DURING EACH CALIB MEASUREMENT

SPAN ID	STD. DEV. IN MV	FRACT STD DEV IN PERCENT
1	1.138E 00	4.070E-01
2	1.195E 00	3.489E-01
3	5.439E-01	1.274E-01
4	9.574E-01	1.767E-01
5	7.746E-01	1.178E-01
5	1.031E 00	1.570E-01
4	1.065E 00	1.971E-01
3	8.851E-01	2.087E-01
2	1.088E 00	3.212E-01
1	1.138E 00	4.105E-01

CALIBRATION LAMP IDENTIFICATION

SERIAL NUMBER = 8165-4W
LAMP INTENSITY = 538.00
DISTRIBUTION TEMPERATURE = 2854
MONITOR CURRENT CHANNEL = 4

CALIBRATION TARGET DATA

REFLECTANCE OF PATH ATTENUATOR(PERCENT) = 100.0
REFLECTANCE OF CALIBRATION TARGET(PERCENT) = 96.0
DTOTAL = LAMP DISTANCE = D1 + D2. D2(CM) = 101.0
PHOTOMETER DATA CHANNEL = 1

Fig. 3-4. Typical Absolute Calibration Form.

CALIBRATION CORRECTION FACTORS

Several calibration correction factors are used with the calibration data illustrated in Fig. 3-4 to generate the calibration constants listed in Table 3-2. In general, the factors are used at will to convert radiometric units into photometric units and reconvert them, and to adjust the value of measurements taken with an instrument having a nearly standard spectral response to the value that would have been obtained using the exact standard spectral response specified in Section 3.6.

These correction factors are discussed at length in AFCRL-70-0137 and AFCRL-72-0461, Duntley, *et al.* (1970 and 1972b). Thus, they are only summarized here in Table 3-3.

The four correction factors shown in Table 3-3 are calculated in Program SUPERCK6. Several key factors generated by Program SUPERCK6 for use with the SEEKVAL data are listed in Tables 3-4 and 3-5.

Table 3-3

Calibration Correction Factor Summary

Factor Designator	Operational Identification	Defining Equations
F1	Luminance-to-radiance conversion	$F1 = \dfrac{\Sigma_c W_\lambda \epsilon_\lambda (\overline{S_\lambda T_\lambda})\,\Delta\lambda}{680\,\Sigma_c W_\lambda \epsilon_\lambda \bar{y}\,\Delta\lambda}$
F2	Color-matching adjustment	$F2 = \dfrac{\Sigma W'_\lambda (\overline{S_\lambda T_\lambda})\,\Delta\lambda}{\Sigma W'_\lambda (S_\lambda T_\lambda)\,\Delta\lambda} \times \dfrac{\Sigma_c W_\lambda \epsilon_\lambda (S_\lambda T_\lambda)\,\Delta\lambda}{\Sigma_c W_\lambda \epsilon_\lambda (\overline{S_\lambda T_\lambda})\,\Delta\lambda}$
F3	Unit conversion	$F3 = \dfrac{10^4}{\delta\lambda} = \dfrac{10^4}{\Sigma (\overline{S_\lambda T_\lambda})\,\Delta\lambda}$
F4	Photometric reconversion	$F4 = \dfrac{680\,\Sigma W'_\lambda \bar{y}\,\Delta\lambda\,\delta\lambda\,10^{-3}}{\Sigma W'_\lambda (\overline{S_\lambda T_\lambda})\,\Delta\lambda}$

Where ${}_cW_\lambda$ = the known spectral emittance of the standard lamp used as a calibration source.

W'_λ = the approximate spectral emittance of the field scene anticipated for later measurement.

Table 3-4

Luminance-to-Radiance Conversion Factor, ${}_cW_\lambda$ at 2854°K

Factor Designator	Spectral Filter Identification				
	Filter 2 478 nm	Filter 3 664 nm	Filter 4 557 nm	Filter 5 765 nm	Filter 6 532 nm
F1 (w/lu)	1.263 E–04	7.136 E–04	1.050 E–03	1.561 E–03	2.112 E–03

Table 3-5

Radiance-to-Luminance Reconversion Factors, F4,
for Selected Typical Distribution Temperatures

Factor Designator	Distribution Temperature of Typical Data Scenes					
	4000°K	5500°K	7000°K	10 000°K	20 000°K	Night Sky
F4 (luμm/w)	7.299 E+01	7.222 E+01	7.200 E+01	7.195 E+01	7.211 E+01	6.834 E+01

CALIBRATION SUMMARY

The pre-SEEKVAL calibration data are dated June 1974. The post-SEEKVAL calibration data are dated August 1974. A review of the data related to each calibration set has led to the selection of preferred calibration constants for application to all Project SEEKVAL field data. These preferred calibration constants are those presented in Table 3-2. The determinant features leading to the selection of each instrument's calibration set are discussed in in-house reference number 111 and are not repeated here. Also, even though Filters 2, 3, and 4 were all calibrated in anticipation of Project SEEKVAL, only Filter 4, the pseudo-photopic, was utilized in the field for data collection.

IN-FLIGHT CROSS-CALIBRATION CHECK

The Project SEEKVAL deployment incorporated the standard cross-calibration (X-CAL) data sequence. During this routine the automatic 2π scanners (UHS and LHS) and the equilibrium radiance telephotometer (ERT) are manually directed to look dead ahead and parallel to the aircraft flight axis. The aircraft is put into a nose-high climb attitude, and it maintains this condition while the three forward-looking telephotometers simultaneously measure the radiance of the sky directly ahead of the aircraft. By aiming the aircraft at a reasonably uniform portion of the sky in a direction away from the sun, one obtains a data set representing the simultaneous in-flight measurement of a common scene by three different radiometer systems. These data are automatically processed to validate or, if necessary, to evaluate a potential update of the system calibration constants prior to final data processing.

A summary of the upper and lower hemisphere scanner Filter 4 cross-calibration data is presented in Table 3-6. These ratios are not corrected or adjusted and thus represent direct in-flight absolute radiance measurements. They indicate a moderate mismatch in absolute level and an unexplained irregularity from flight to flight. However, since this was an early attempt at this flight procedure and since the ratios are so irregular, no calibration updates were made to the SEEKVAL data on the basis of the X-CAL ratios.

3.6 STANDARD RESPONSE CHARACTERISTICS FOR BROAD BAND SENSORS

All the radiometric instruments both ground-based and airborne used by the Atmospheric Visibility Branch are equipped with automatic filter changing assemblies. Thus, any one of five different spectral filters can be interposed into each instrument's optical path. The combination of the sensor sensitivity S_λ and the filter transmittance T_λ is the resultant sensitivity of the filtered phototube $S_\lambda T_\lambda$. The standard responses which each optical system attempts to duplicate are indicated as $\overline{S_\lambda T_\lambda}$.

Table 3-6

Precalibration Sun Mode X-CAL Data

Flight No.	Event	UHS/LHS	ERT/UHS	ERT/LHS	ERT Position
C-351	3	1.29	0.81	1.04	Cycling
	35	1.44	1.40	2.01	
C-352	3	1.28	0.66	0.84	2.5°
	50	0.97	0.67	0.65	
C-353	60	0.85	1.31	1.11	0°
C-354	3	1.29	0.81	1.04	Cycling
	48	0.99	0.84	0.83	
C-356	56	0.99	0.70	0.70	0°
C-357	3	1.08	0.83	0.90	Cycling
	60	1.03	0.71	0.73	
C-358	3	1.40	0.80	1.12	2.5°
	49	1.04	0.78	0.82	
C-359	4	1.08	0.69	0.74	2.5°
	50	1.00	0.65	0.65	
C-360	3	1.32	0.67	0.88	2.5°
Avg		1.14	0.82	0.94	
$\overline{\lvert R_i - \bar{R} \rvert}$		0.16	0.14	0.22	

PEAK WAVELENGTH

The peak or maximum value of the standard sensor response $\overline{S_\lambda T_\lambda}$ is used to normalize the response values. The wavelength of the maximum value of the standard response is called the "peak wavelength."

MEAN WAVELENGTH

The mean wavelength $\bar{\lambda}$ is defined as

$$\bar{\lambda} = \frac{\sum\limits_{0}^{\infty} \lambda \overline{S_\lambda T_\lambda}\, \Delta \lambda}{\sum\limits_{0}^{\infty} \overline{S_\lambda T_\lambda}\, \Delta \lambda} .$$

The λ is the wavelength of the relative spectral response $\overline{S_\lambda T_\lambda}$.

RESPONSE AREA

The response area is the area under the normalized relative spectral response curve. It is equal to the width of the passband of a rectangular filter of equivalent area; hence, it is designated as $\delta\lambda$ and defined by $\delta\lambda = \Sigma(\overline{S_\lambda T_\lambda})\,\Delta\lambda$. The radiometric units of watts/m$^2\mu$m are obtained from units of watts/m^2 by dividing by the response area $\delta\lambda$ in appropriate units.

A summary of the response characteristics of the standards for Project SEEKVAL is presented in Table 3-7. The first four columns give filter code, peak wavelength, mean wavelength, and response area. The values for inherent solar properties are in columns 5, 6, and 7 and the Rayleigh limits are in columns 8, 9, and 10. The table was produced by Program RAYLIMIT.

Table 3-7

Spectral Characteristics Summary for Project SEEKVAL

Spectral Characteristics for Project SEEKVAL				Inherent Sun Properties (Johnson)			Rayleigh Atmosphere Properties (15°C)		
Filter Code No	Peak Wavelength (nm)	Mean Wavelength (nm)	Response Area (nm)	Irradiance (w/m$^2\mu$m)	Radiance (w/Ωm$^2\mu$m) Average	Radiance (w/Ωm$^2\mu$m) Center	Attenuation Length (m)	Total Scattering Coefficient (Per m)	Vertical Beam Transmittance
2	475	478	19 9	2 14E+03	3 13E+07	4 07E+07	4 84E+04	2 07E-05	0 839
3	660	664	30 2	1 57E+03	2 30E+07	2 75E+07	1 86E+05	5 41E-06	0 955
5	750	765	50 4	1 23E+03	1 80E+07	2 10E+07	3 28E+05	3 08E-06	0 974
4	550	557	78 5	1 90E+03	2 78E+07	3 47E+07	8 93E+04	1 15E-05	0 907
6	440	532	183 5	1 91E+03	2 80E+07	3 55E+07	7 22E+04	1 64E-05	0 867
9	555	560	106 9	1 89E+03	2 77E+07	3 45E+07	9 22E+04	1 15E-05	0 907

RELATIVE SPECTRAL RESPONSE OF STANDARDS

The relative spectral response of a standard $\overline{S_\lambda T_\lambda}$ curve is obtained by normalizing the curve values so that the maximum relative response is 1. Program RAYLIMIT checks to see if the input standard spectral response curve is normalized and renormalizes if necessary. It also interpolates to wavelength increments of 5 nanometers if the standard has been specified for only 10-nanometer increments. It is more reasonable to interpolate the relatively smooth response values than to ignore the fine spectral structure of the sun irradiance out of the atmosphere.

A graph of the relative spectral response of the standards used in Project SEEKVAL is presented in Fig. 1-5 and 3-5. In Fig. 3-5, which is the computer-generated plot from Program RAYLIMIT, a point is plotted for each 5 nanometers in wavelength, but an identifying symbol is printed on only every second point. The relative spectral response values are also presented in Table 3-8, from Program RAYLIMIT.

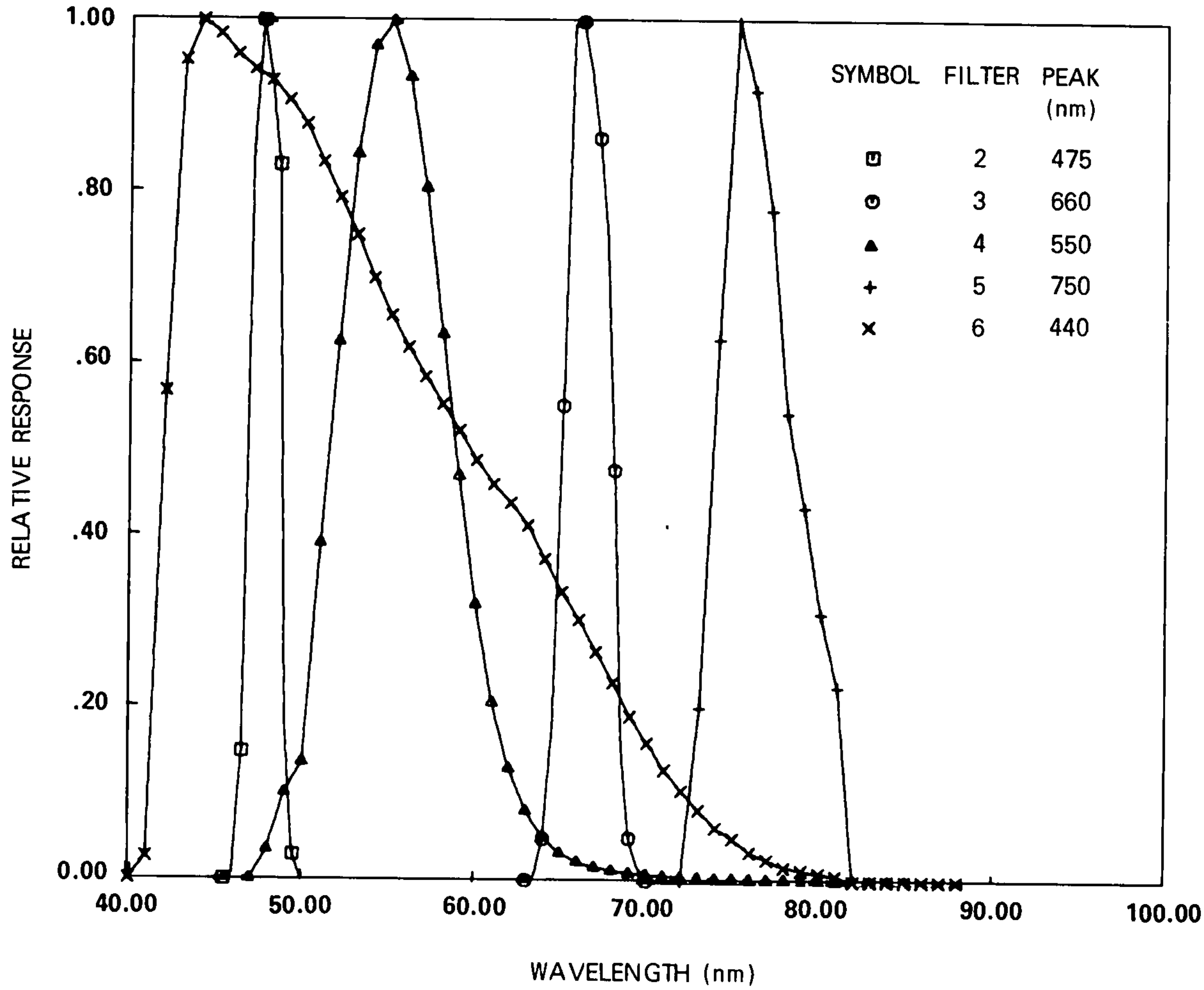

Fig. 3-5. Computer-Generated Plot of Standard Spectral Responses for Project SEEKVAL.

Table 3-8

Relative Spectral Response of Standards for Project SEEKVAL

Filter Identification and Mean Wavelength							Filter Identification and Mean Wavelength						
Wave length (nm)	No 2 Blue 478nm	No 3 Red 664nm	No 4 Pseudo Photopic 557nm	No 5 NIR 765nm	No 6 S 20 532nm	No 9 True Photopic 560nm	Wave length (nm)	No 2 Blue 478nm	No 3 Red 664nm	No 4 Pseudo Photopic 557nm	No 5 NIR 765nm	No 6 S 20 532nm	No 9 True Photopic 560nm
400	0	0	0	0	0	0 0004	615	0	0	0 1680	0	0 4500	0 4412
405	0	0	0	0	0 0129	0 0006	620	0	0	0 1300	0	0 4390	0 3810
410	0	0	0	0	0 0258	0 0012	625	0	0	0 1055	0	0 4260	0 3210
415	0	0	0	0	0 2969	0 0022	630	0	0	0 0810	0	0 4130	0 2650
420	0	0	0	0	0 5680	0 0040	635	0	0 0020	0 0657	0	0 3935	0 2170
425	0	0	0	0	0 7605	0 0073	640	0	0 0486	0 0504	0	0 3740	0 1750
430	0	0	0	0	0 9530	0 0116	645	0	0 1798	0 0411	0	0 3545	0 1382
435	0	0	0	0	0 9765	0 0168	650	0	0 5531	0 0318	0	0 3350	0 1070
440	0	0	0	0	1 0000	0 0230	655	0	0 9948	0 0268	0	0 3190	0 0816
445	0	0	0	0	0 9920	0 0298	660	0	1 0000	0 0218	0	0 3030	0 0610
450	0	0	0	0	0 9840	0 0380	665	0	0 9421	0 0188	0	0 2845	0 0446
455	0	0	0	0	0 9720	0 0480	670	0	0 8625	0 0157	0	0 2660	0 0320
460	0 0070	0	0	0	0 9600	0 0600	675	0	0 7482	0 0139	0	0 2480	0 0232
465	0 1487	0	0	0	0 9510	0 0739	680	0	0 4774	0 0120	0	0 2300	0 0170
470	0 8481	0	0	0	0 9420	0 0910	685	0	0 1585	0 0105	0	0 2105	0 0119
475	1 0000	0	0 0172	0	0 9355	0 1126	690	0	0 0495	0 0090	0	0 1910	0 0082
480	0 9329	0	0 0343	0	0 9290	0 1390	695	0	0 0166	0 0080	0	0 1755	0 0057
485	0 8304	0	0 0677	0	0 9175	0 1693	700	0	0	0 0070	0	0 1600	0 0041
490	0 1790	0	0 1010	0	0 9060	0 2080	705	0	0	0 0061	0	0 1445	0 0029
495	0 0292	0	0 1185	0	0 8920	0 2586	710	0	0	0 0053	0	0 1290	0 0021
500	0	0	0 1360	0	0 8780	0 3230	715	0	0	0 0048	0	0 1170	0 0015
505	0	0	0 2635	0	0 8560	0 4073	720	0	0	0 0042	0	0 1050	0 0010
510	0	0	0 3910	0	0 8340	0 5030	725	0	0	0 0038	0 1005	0 0938	0 0007
515	0	0	0 5085	0	0 8135	0 6082	730	0	0	0 0033	0 2010	0 0826	0 0005
520	0	0	0 6260	0	0 7930	0 7100	735	0	0	0 0030	0 4155	0 0723	0 0004
525	0	0	0 7345	0	0 7715	0 7932	740	0	0	0 0026	0 6300	0 0619	0 0003
530	0	0	0 8430	0	0 7500	0 8620	745	0	0	0 0025	0 8150	0 0558	0 0002
535	0	0	0 9065	0	0 7250	0 9149	750	0	0	0 0023	1 0000	0 0497	0 0001
540	0	0	0 9700	0	0 7000	0 9540	755	0	0	0 0020	0 9595	0 0416	0 0001
545	0	0	0 9850	0	0 6785	0 9803	760	0	0	0 0018	0 9190	0 0335	0 0001
550	0	0	1 0000	0	0 6570	0 9950	765	0	0	0 0017	0 8495	0 0292	0
555	0	0	0 9665	0	0 6385	1 0002	770	0	0	0 0016	0 7800	0 0249	0
560	0	0	0 9330	0	0 6200	0 9950	775	0	0	0 0014	0 6620	0 0206	0
565	0	0	0 8685	0	0 6030	0 9786	780	0	0	0 0013	0 5440	0 0162	0
570	0	0	0 8040	0	0 5860	0 9520	785	0	0	0 0012	0 4890	0 0144	0
575	0	0	0 7195	0	0 5700	0 9154	790	0	0	0 0012	0 4340	0 0125	0
580	0	0	0 6350	0	0 5540	0 8700	795	0	0	0 0012	0 3720	0 0107	0
585	0	0	0 5525	0	0 5385	0 8163	800	0	0	0 0011	0 3100	0 0088	0
590	0	0	0 4700	0	0 5230	0 7570	805	0	0	0 0005	0 2675	0 0075	0
595	0	0	0 3950	0	0 5060	0 6949	810	0	0	0	0 2250	0 0062	0
600	0	0	0 3200	0	0 4890	0 6310	815	0	0	0	0 1125	0 0031	0
605	0	0	0 2630	0	0 4750	0 5668	820	0	0	0	0	0	0
610	0	0	0 2060	0	0 4610	0 5030							

4. DATA COLLECTION METHODS

During Project SEEKVAL, two independent activities were maintained simultaneously. The operation of the airborne instrument system was one activity and that of the ground-based instrument system was the other. The procedural routine was for each system to run full data collection sequences at every opportunity, on a daily schedule.

4.1 AIRBORNE SYSTEM

The data collection sequence for the airborne system was broken into five standardized elements: (1) preflight warmup and calibration check, (2) straight and level sequences, (3) vertical profile sequences, (4) in-flight calibration checks, and (5) post-flight calibration check.

An illustration of our typical flight pattern, only portions of which were used for the SEEKVAL mission, is shown in Fig. 4-1. In this stylized pattern, two basic elements, the straight and level (ST & LV) and the vertical profile (V-PRO), are combined to yield the total mission flight plan. A description of these two pattern elements and the calibration elements is detailed in AFCRL-72-0593, Duntley, *et al.* (1972c), and summarized in the following paragraphs.

1. Straight and Level runs (ST & LV), Mode 03 – The ST & LV runs are primarily 2π scanner runs. The measurement of upper and lower hemisphere radiance distributions has top priority. One sky mode scanner pattern (192 seconds) plus one sun mode scanner pattern (64 seconds) are run at each altitude with each of the two optical filters.

   During ST & LV runs the aircraft should maintain a fixed heading, a constant indicated airspeed of 150 knots or less, and a 2½ degree nose-high flight attitude.

2. Vertical Profile runs (V-PRO), Mode 07 – The V-PRO runs are primarily integrating nephelometer and variable path function meter runs. The measurement of the total scattering coefficient profile has top priority. Second priority is measurement of the vertical path function profile. Each V-PRO ascent or descent is made using a single filter.

   During the V-PRO runs the aircraft should maintain a fixed heading, with the sun off the left wingtip, and a flight attitude not exceeding 4 degrees nose down or 8 degrees nose up.

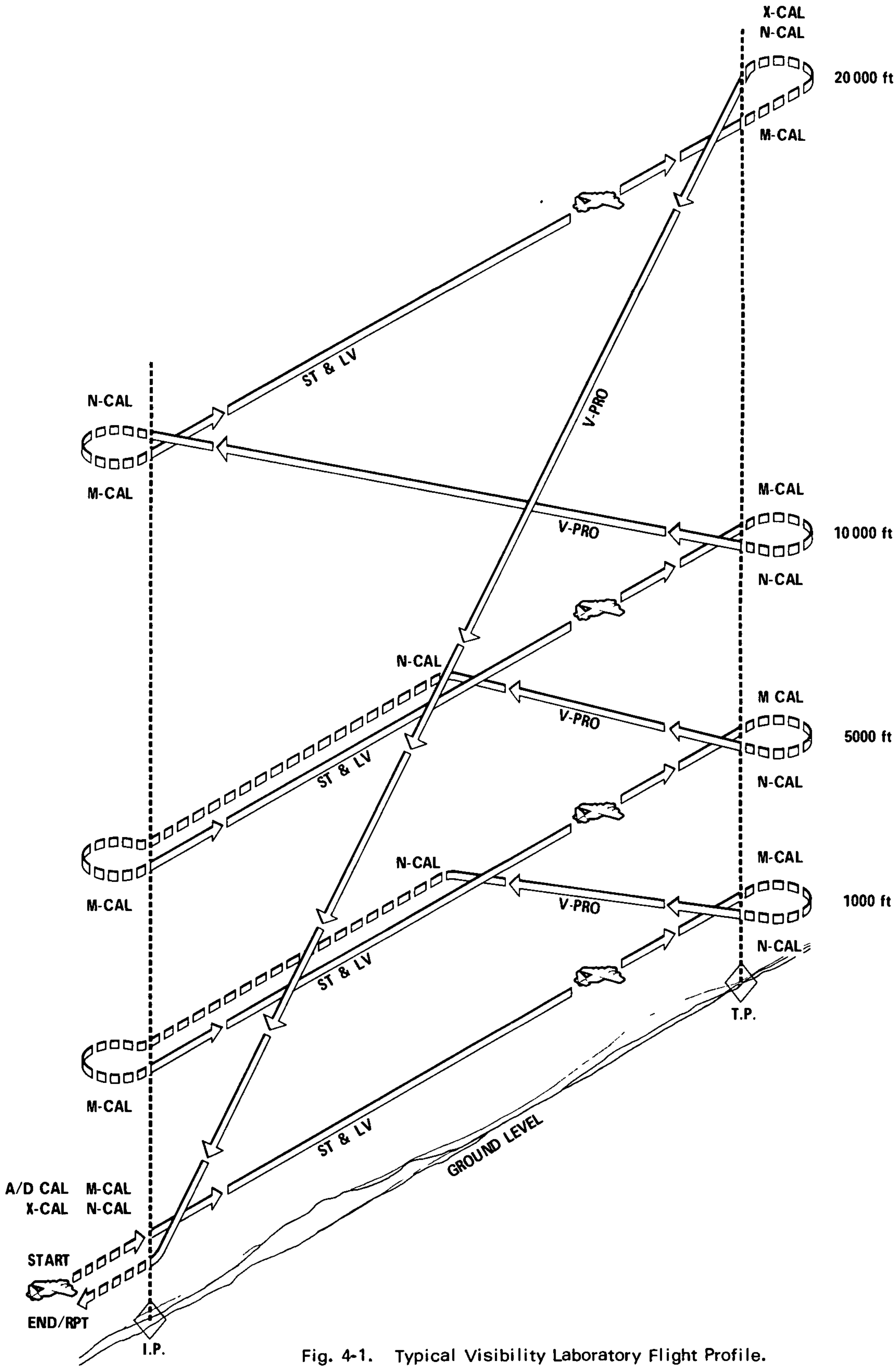

Fig. 4-1. Typical Visibility Laboratory Flight Profile.

An average rate of climb or descent of 1200 feet/minute is optimum, and airspeed is not critical, but should remain constant once established.

3. Cross-Calibration Climbs (X-CAL), Mode 08 – The X-CAL climbs are specifically designed to validate the performance of the UHS, LHS, and ERT radiometer systems. The simultaneous measurement of a common uniform segment of sky by these three radiometers has top priority. Two X-CAL climbs are associated with each standard profile, one preceding the first ST & LV run and the second following the last ST & LV run. Both sky mode and sun mode measurements are made with the UHS system.

   During the 4-minute X-CAL climb the aircraft should maintain a fixed heading, with the sun in the aft hemisphere, and a 5-degree nose-high flight attitude. The aircraft should be flown directly toward the clearest and most uniform portion of the sky as practical.

4. Calibration Blocks (A/D CAL), Mode 00, M-CAL, Mode 01, N-CAL, Mode 09 – The 32-second blocks of calibration data are inserted periodically throughout the entire data mission. They are designed to provide calibration update information to the post-flight computer processing sequences. There are 21 assorted calibration blocks associated with each (2 + 4) profile.

   During these calibration blocks there are no project-imposed requirements upon aircraft speed or attitude.

GENERAL FLIGHT PATTERN

The standard (2 + 4) profile is illustrated in Fig. 4-1. In this profile, ST & LV data runs are made using two different spectral filters at each of four altitudes. The ascent V-PRO is made using the first of the two filters, and the descent V-PRO is made using the second. After the descent V-PRO, the entire sequence is repeated using a second pair of filters.

The idealized flight profile would result in all ground tracks falling on a single line running between the Initial Point (I.P.) and the Turning Point (T.P.). See Fig. 4-1. In practice, the ST & LV elements are are actually stacked in a slab of atmosphere approximately 30 miles long, 0.5 mile wide, and 4 miles high.

Periodically, in response to specialized data requirements, as in the case of Project SEEKVAL, supplementary flight patterns are added to the mission profile. For SEEKVAL, a composite pattern made up of an AVIZ (1 + 2) special descent, i.e., one spectral filter at each of two altitudes plus assorted ST & LV and V-PRO elements, was used on all data flights. The SEEKVAL data collection flight sequence is summarized below.

SEEKVAL FLIGHT PATTERN

Courses A, B, C, and D described below, upon which the various data passes were flown, were designated by the Project Manager, who was in radio communication with the aircraft commander during each mission. The courses, in general, were at azimuths of 0, 60, 120, and 180 degrees with respect to the sun. All data passes began immediately over the Weir Prairie test site and proceeded outbound on their assigned courses for approximately 2 minutes.

During each SEEKVAL mission, an on-board camera system from the Air Force Avionics Laboratory was activated, and scene photographs from the lowered ramp were attempted.

At the conclusion of each mission, the radiometric data which were recorded and stored on magnetic tape were returned to the Visibility Laboratory for computer reduction and analysis.

4.2 GROUND-BASED SYSTEM

The ground-based data collection sequence was designed to supplement the airborne data whenever the aircraft was operating in the immediate vicinity. However, it is also complete enough to stand alone when the aircraft mission is diverted or aborted.

The ground-based instrument system has several operational responsibilities. First, it must supply a ground-level data base to allow interpolation of various measurements between ground altitude and the lowest attainable aircraft altitude. Second, it must supply long term temporal sampling of those meteorological and radiometric quantities which relate to the project task. Third, the ground system serves as a spare parts and repair facility for the entire air/ground operation. In the event of a catastrophic failure in a primary airborne instrument or assembly, the equivalent piece of instrumentation is reassigned to the aircraft from the ground-based system. The aircraft can then return to service with a minimum of "downtime" and repairs can be accomplished under the more convenient ground station conditions.

The ground-based data collection during Project SEEKVAL was accomplished through the use of a fully instrumented truck van in a manner similar to that reported in AFCRL-72-0593, Duntley, *et al.* (1972c). The ground data log and experimental procedure were revised, prior to the SEEKVAL deployment, to reflect a shortened, single filter data sequence, the "Basic Data Set." This single filter sequence is designed to simplify operational procedures and to reduce the elapsed times between the three sets of measurements used for the calculation of atmospheric beam transmittance, i.e., CRM shadow-intensity measurements, CRM solar disk measurements, and UHS sky radiance ratios.

The optimum procedure for the ground station is to complete at least one standardized Basic Data Set in each specified spectral band during the interval that the aircraft is operating overhead. Approximate elapsed times for each set is 20 minutes, with a recording time of 15 minutes 20 seconds.

The standard ground-based sequence was built around three basic patchboard arrays designed for automatic 20-channel data logging:

1. The CRM Board, primarily for solar transmissometer data
2. The UHS Board, primarily for sky and solar surround data
3. The LHS Board, primarily for terrain reflectance data

Integrating nephelometer and downwelling irradiometer measurements are made and recorded continuously throughout all three of the basic patchboard sequences listed above.

SEEKVAL GROUND-BASED DATA COLLECTION SEQUENCE

Ground-based data were collected in a fixed pattern, i.e., the Basic Data Set, on a repetitive basis during each designated data day. The Basic Data Set consists of the radiometric sequence listed below:

1. Contrast Reduction Meter (CRM) Measurements

   Total Downwelling Irradiance

   Solar Disk Radiance

   Shadow Intensity

   Sky Radiance @ β = 90 degrees

2. Upper Hemisphere Scanner Measurements

   Sky Radiances @ $2\pi\,\Omega$

3. Lower Hemisphere Scanner Measurements

   Terrain Radiances @ $2\pi\,\Omega$

4. CRM Measurements listed in step 1.

Integrating nephelometer (NEPH) and downwelling irradiometer measurements were made and recorded continuously throughout all three of the basic sequences listed above, and constitute an additional data sequence of primary importance.

The ground station data logger failed on 12 July 1974 and was under repair until 16 July 1974 when it was returned to service. During this interval, manual data were recorded when possible. Thus, only CRM and NEPH data are available for those 4 days.

At the conclusion of the deployment, the radiometric data which were recorded and stored on magnetic tape were returned to the Visibility Laboratory for computer reduction and analysis.

5. DATA PROCESSING

As in any reasonably complex, multi-input sampled data system, there is a large amount of data handling required before the scientific analyst ever sees the package. The degree of data processing sophistication utilized during this contract interval is illustrated in Fig. 5-1 and 5-2. In these generalized flow charts, the basic functional steps used in the data processing of the raw field data are clearly specified. They do not illustrate, however, all of the miscellaneous routines used for data base management and special diagnostic purposes. A more complete description of each phase of the processing sequence is contained in AFCRL-72-0255 and AFCRL-72-0593, Duntley, *et al.* (1972a and c).

5.1 AIRBORNE DATA

As described in AFCRL-72-0255, Duntley, *et al.* (1972a), several classes of data are recorded during an airborne data set: (1) radiometer outputs, (2) selector control codes, (3) transducer orientation and flight attitude signals, and (4) calibration voltages, etc. All systems, regardless of type, have been designed for an electrical output between 0 and ± 1 volt dc for full scale. The 42-channel data logger has a least count of ± 1 millivolt and records in digital format at a multiplex rate of 240 samples per second and a tape rate of 3.56 inches per second at a recording density of 200 bits per inch.

Several major improvements to the airborne data processing procedure have been implemented during the interval since AFCRL-72-0593, Duntley, *et al.* (1972c). The insertion of the programs summarized below into the general data processing schedule is illustrated in Fig. 5-1. These programs and the diagnostic capabilities their use have enabled have materially improved the quality of the upper hemisphere radiance maps, and thus the quality of all subsequently computed optical properties.

PROGRAM FLTDOC

Program FLTDOC was developed to help speed up the turnaround time required for preliminary evaluation of field data, and to provide a display to aid in the evaluation of the automatic sorting of the recorded raw data from each flight element. This program displays both tabularly and graphically each of the major flight elements (ST & LV and V-PRO) based upon the recorded identification codes, altitude, filter, and magnetic heading information. These displays permit quick classification of the flight data segments into sets which are processable and correspond to the parts of the "standard profile" described in Section 4. This early classification of the flight data permits very selective processing which insures that the analyst is provided with both an adequate representation of the flight's overall data quality and the ability to exercise close control of processing economies.

AIRBORNE DATA PROCESSING:

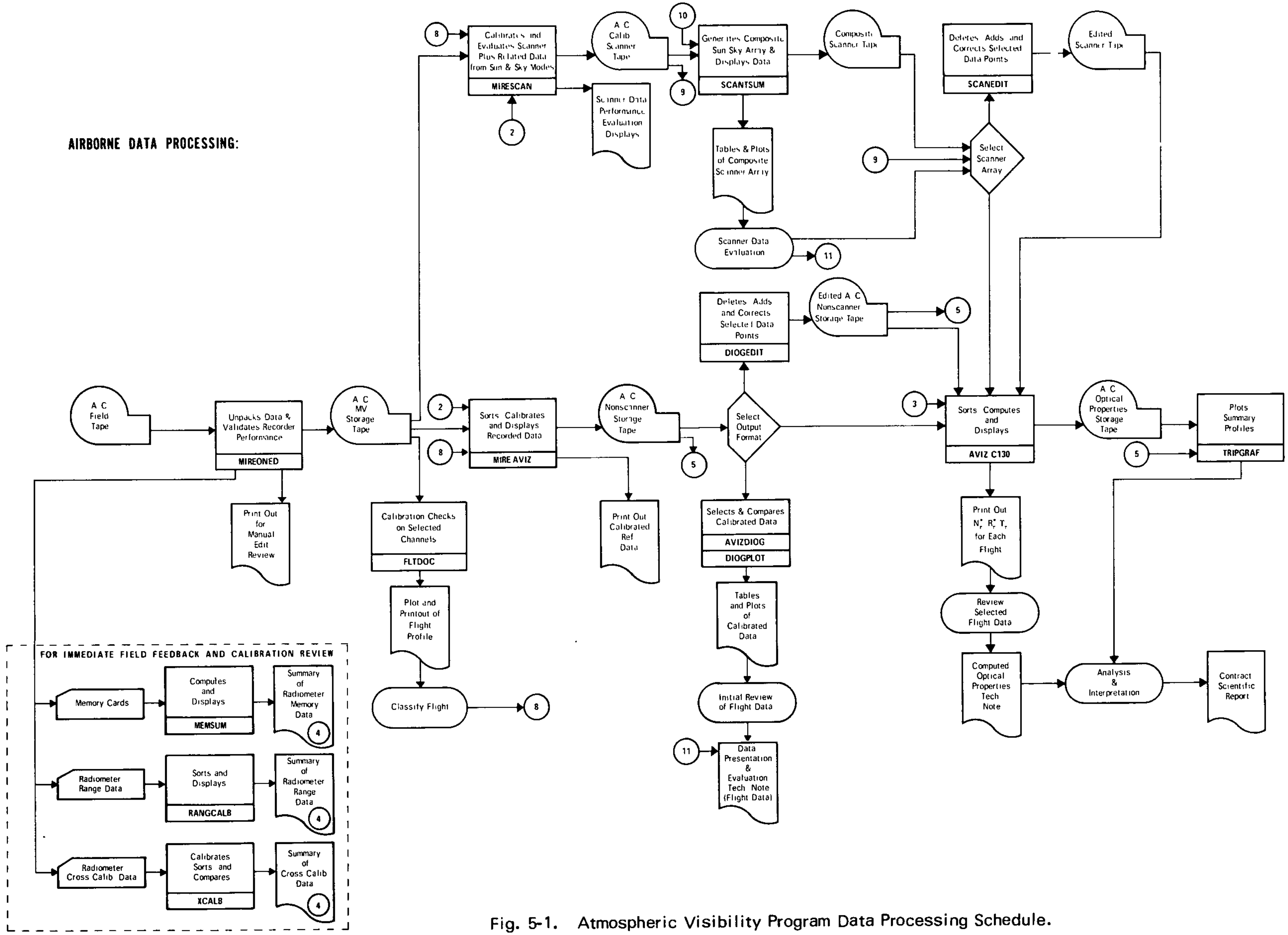

Fig. 5-1. Atmospheric Visibility Program Data Processing Schedule.

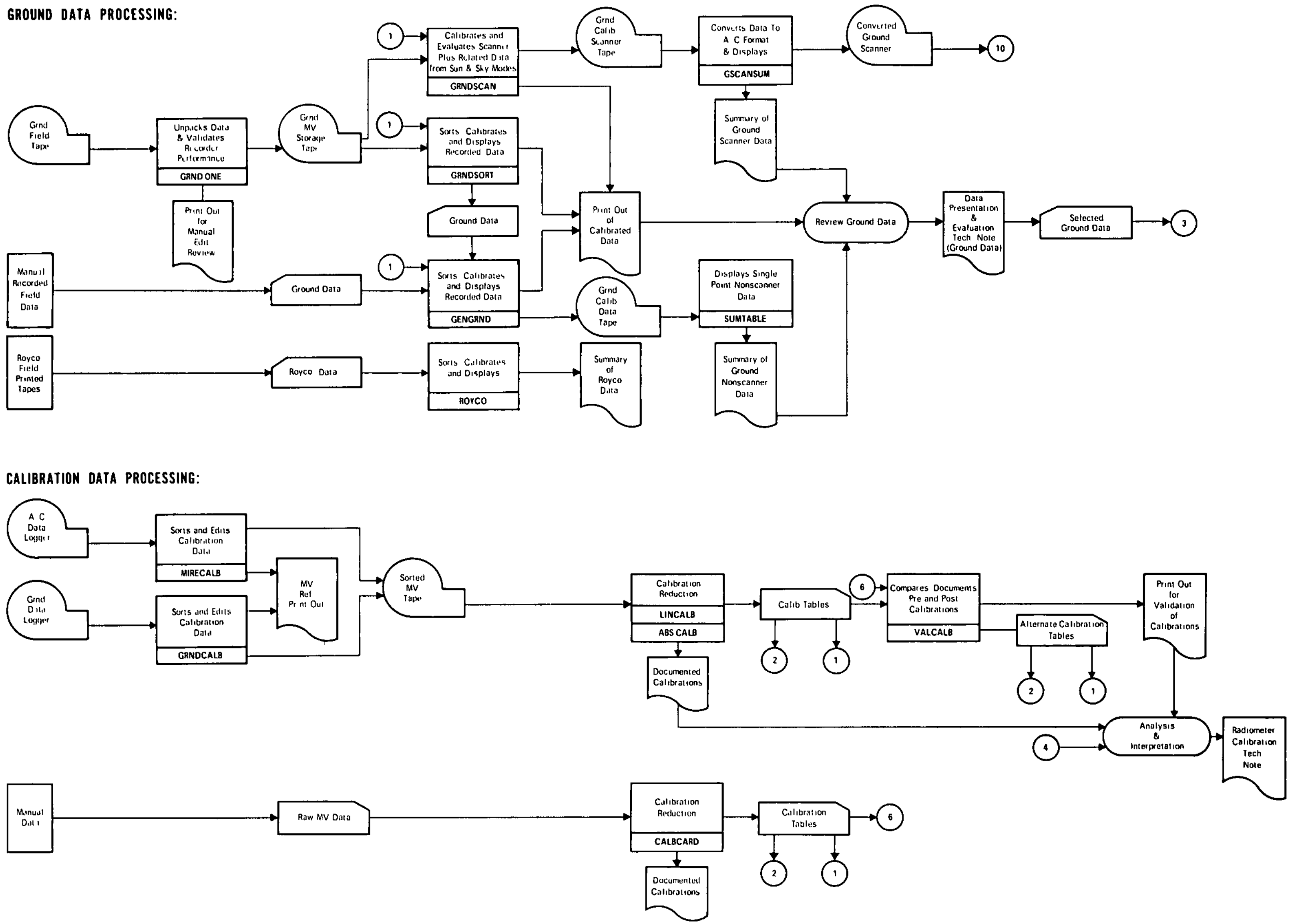

Fig. 5-2. Atmospheric Visibility Program Data Processing Schedule.

PROGRAM MIRESCAN

With the advent of the nonspiral mode of scanner data collection, which was inaugurated in February 1972, it became desirable to split the airborne data processing job into two parts. The first part involved processing all of the nonscanner-related data, which is still accomplished using the original program, MIREAVIZ. The second part involved processing all of the data directly related to the automatic 2π scanner system. Program MIRESCAN was designed to process the scanner data. Its primary function is to calibrate and sort the scanner data into a standardized array whose azimuthal axis is oriented with respect to the major light source, the sun or the moon.

PROGRAM SCANTSUM

With the advent of the sun/sky mode of scanner data collection, which was also inaugurated in February 1972, and the resultant recording of selected sky radiances in both high and low sensitivity ranges, it became necessary to devise additional software sophistications. Specifically, a procedure was required to combine the sun mode measurements and the sky mode measurements into a single composite data array. This standardized composite array would represent a complete 2π map of the sky's radiance distribution, all points of which were within the combined sun and sky mode calibrated radiometric span of the scanner system. Program SCANTSUM selects measured data from the sun mode data array and combines it with the basic sky mode data array. It provides displays of the initial data and the composite data, as well as diagnostic data for evaluation by the analyst.

5.2 GROUND-BASED DATA

The data processing associated with the ground-based data set is similar in concept to that applied to the airborne data. The primary differences are the result of a different recording format between the two data loggers and the significantly lesser amount of data resulting from the ground station. As noted in AFCRL-72-0255, Duntley, *et al.* (1972a), the same general classes of data are handled, but in much smaller quantities. Again, all systems, regardless of type, have been designed for an electrical output between 0 and ± 1 volt dc for full scale. The data logger is normally adjusted for a least count of ± 0.1 millivolt. It also records in digital format; however, the normal incremental sample rate is relatively slow, approximately eight samples per second.

Since the ground-based automatic 2π scanner system is operationally equivalent to the airborne, a similar data processing update was required to efficiently handle the sun/sky mode data from the ground-based upper hemisphere scanner. Consequently, Programs GRNDSCAN and GSCANSUM were developed to convert the ground scanner data, which are recorded at a much slower rate than the airborne data, into a format compatible with the airborne data processing routines. Subsequent to conversion, Program SCANTSUM can now be used to generate the composite array of ground-based sun and sky radiance data in the same manner as it does for the airborne data. Thus, in subsequent computational routines, data arrays from either airborne or ground-based upper hemisphere scanner systems can be used interchangeably.

The insertion of the programs discussed above into the general data processing schedule is illustrated in Fig. 5-2.

5.3 CALIBRATION DATA

The calibration data are the heart of the data processing system in that any data processed are only as good as the calibrations applied to them. The calibration data are recorded on tape in an effort to eliminate the human bias and are handled in a phased procedure similar to that used in the general data processing technique. The data can be recorded on either the airborne or the ground data logging system. In an initial procedure, these data go through Program MIRECALB or GRNDCALB, according to the recording system used, to verify the electrical quality of the radiometer data and associated monitored parameters. For final processing, the data are sorted and stored in set fashion.

Programs LINCALB and ABSCALB perform the data reduction of all raw radiometer calibration data which have been recorded on magnetic tapes, and Program CALBCARD performs the same function on manually recorded data. These programs generate "standard radiometer calibration" card decks which are used in the documentation and comparison modes of Program VALCALB. The documentation and comparison mode outputs are used to describe the quality of each pre-deployment and post-deployment set of calibration data generated, and to aid in the selection of the preferred calibration data which are ultimately applied to the field measurements.

Since many of the radiometer systems can be calibrated and used in either a high or low sensitivity range, a procedure is required to adjust the calibration constants whenever a field measurement is made in a different mode from that used during calibration. Program VALCALB handles this procedure by generating an "alternate radiometer calibration" card deck which has the high/low sensitivity range change for each radiometer built in. Thus field data from any radiometer can be correctly processed regardless of which sensitivity range was actually used by merely specifying the "standard" or "alternate" calibration card deck.

5.4 DATA TAPES

The data processing sequences discussed in the previous paragraphs produce output tapes containing a broad catalog of calibrated data. These tapes are useable as data inputs to a multiplicity of diverse problems requiring a knowledge of atmospheric optical properties. To simplify future retrieval, the data tape numbers, the in-house descriptions of the data, and the computed properties reported herein have been summarized in Table 5-1.

Table 5-1

Processed Data Library Tapes

SEEKVAL Flight No.	MIREAVIZ Tape No. VL-338F File No.	MIRESCAN Tape No. VL-339F File No.	Data Presentation No.	AVIZC130 Tape No. VL-337F File No.	Computed Properties No.
C-351	1	1	116	1	124
C-352	2	2	117	2	125
C-354	3	3	113	3	114
C-357	4	4	118	4	126
C-358	5	5	119	5	127
C-359	6	6	120	6	128
C-360A	7	7	121	7	129
C-360B	8	8	115	8	123

6. WEATHER

6.1 SUMMARY

Meteorological data for this analysis were gathered from several sources. Daily surface and 500-millibar charts for 7:00 AM, EST (1200 GMT) were obtained from the Department of Commerce, National Oceanic and Atmospheric Administration (NOAA), Environmental Data Service. Portions of these charts have been reproduced as figures 6-1. Two sets of facsimile charts issued by the National Meteorological Center were obtained from the Lindbergh Field NOAA office. They were the 3-hourly surface charts, and the daily 500-millibar charts for 0000 GMT and 1200 GMT. Also available for the period of the deployment were the hourly and special reports made by the weather offices at McChord Air Force Base and Gray Army Air Field. Radiosonde observations were taken at Gray Army Air Field on some of the days when data flights were made by the project aircraft, however, the flight track was located approximately 20 miles southwest of McChord and 13 miles southwest of Gray.

This section includes a discussion of the surface and 500-millibar charts for all of the days of the deployment, as well as for all the days on which data were acquired. Listed in tabular form are the hourly and special reports made by the observers at McChord Air Force Base and Gray Army Air Field.

Also included in this section are graphical representations of ambient temperature and relative humidity profiles measured during each reported data flight (Fig. 6-2 and 6-3). The temperatures were measured continuously by an AN/AMQ-17 aerograph system described briefly in AFCRL-70-0137, Duntley, *et al.* (1970) and more completely in USNAF TP-133. The relative humidities were computed using these measured ambient temperatures and dewpoint temperatures which were measured by a Cambridge model 137-C3 aircraft hygrometer. The profile identification symbols used in Fig. 6-2 and 6-3 are related to the spectral filter sequence during which the data were measured; i.e., the temperature profile identified with the Filter 4A symbol was taken during the same time interval as the Filter 4A radiometric measurements; the temperatures coded as Filter 4B were taken simultaneously with the Filter 4B radiometric measurements, etc. Users should be aware that these profiles represent conditions associated with a specific flight track which was 20 miles from the meteorological station at McChord Air Force Base.

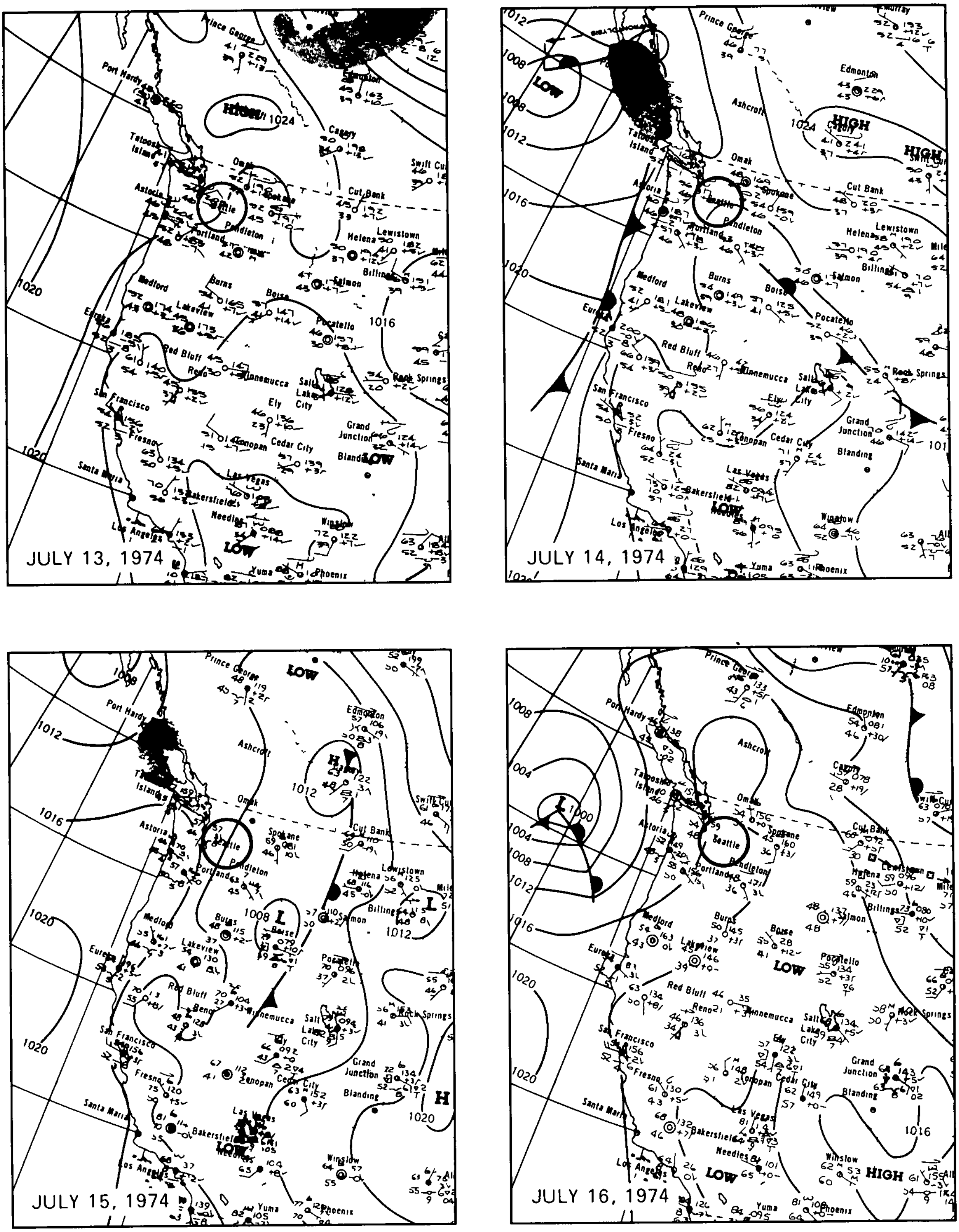

Fig. 6-1. Synoptic Charts of Seattle Area During Project SEEKVAL.

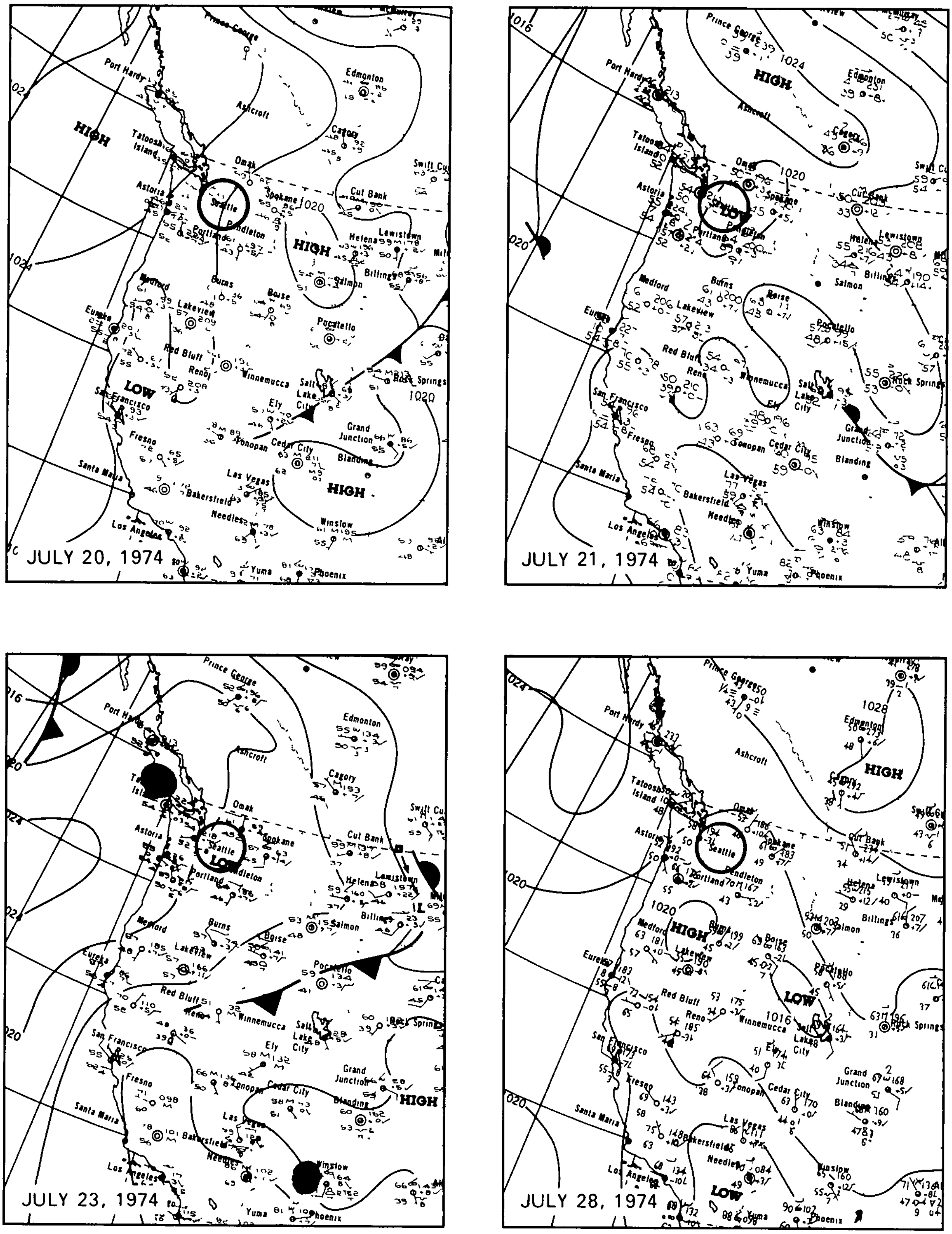

Fig. 6-1 (cont.). Synoptic Charts of Seattle Area During Project SEEKVAL.

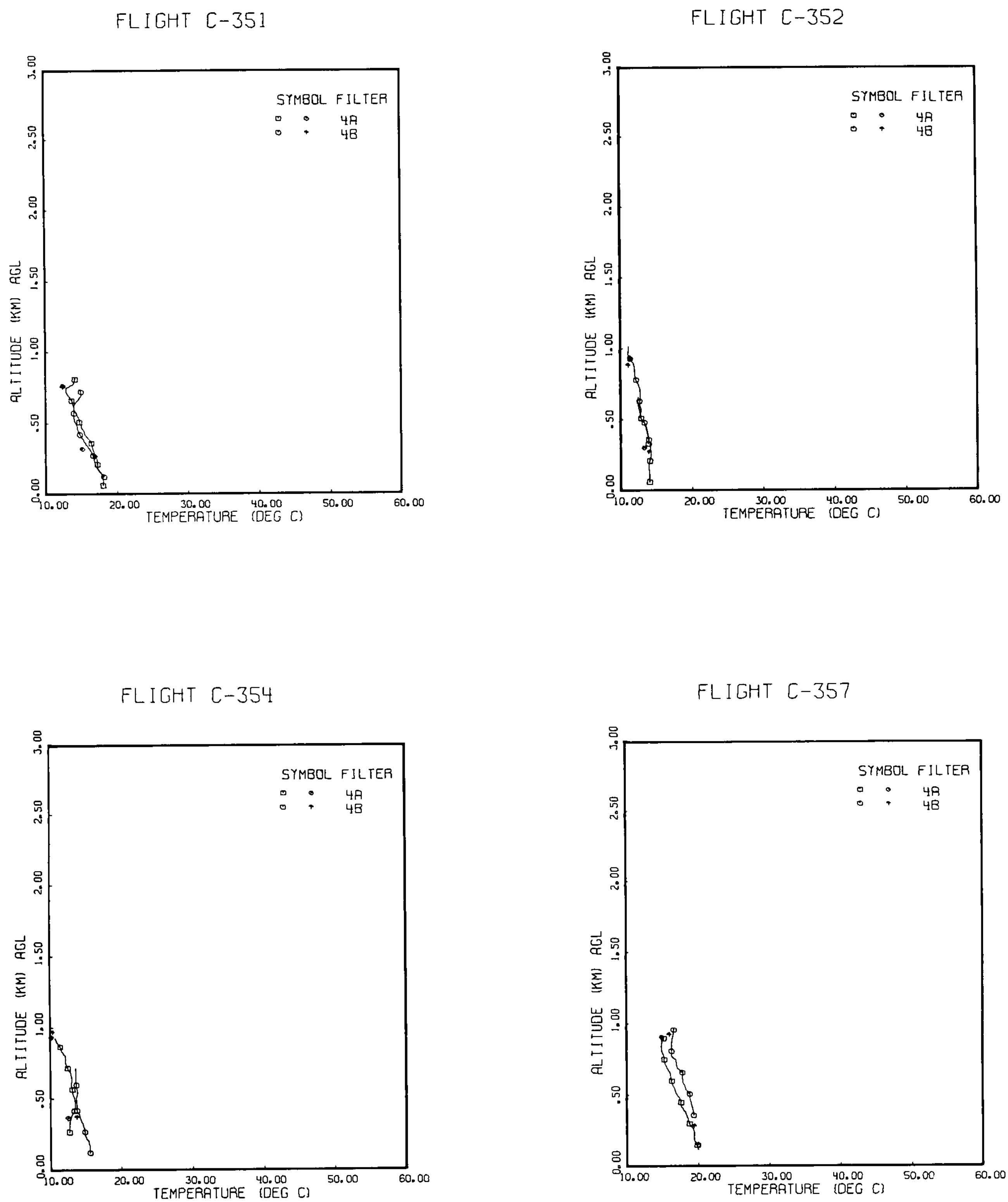

Fig. 6-2. Temperature Versus Altitude for Eight Project SEEKVAL Flights.

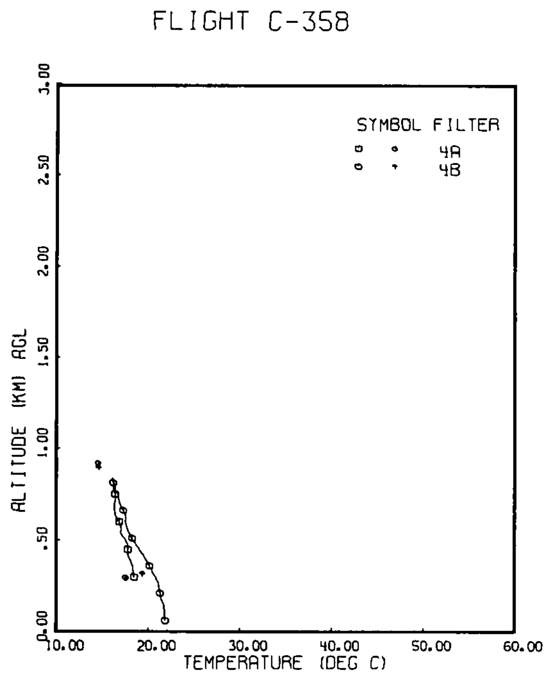

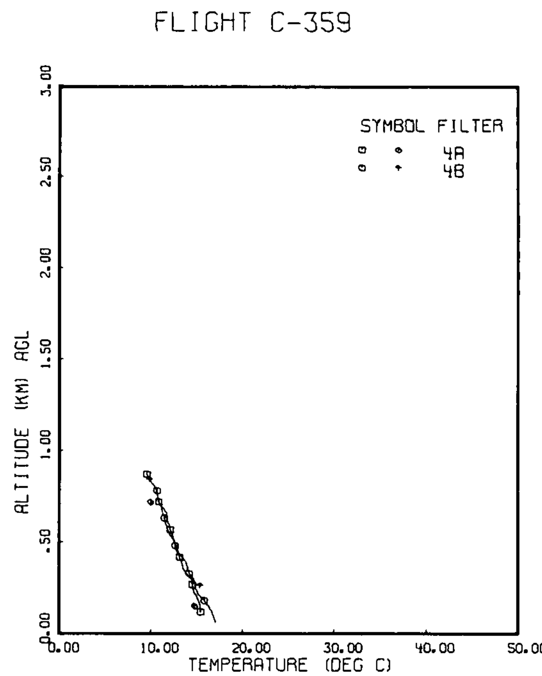

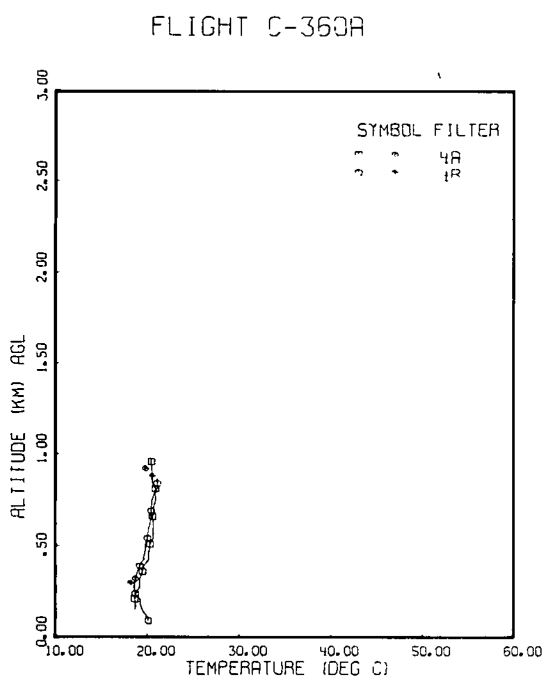

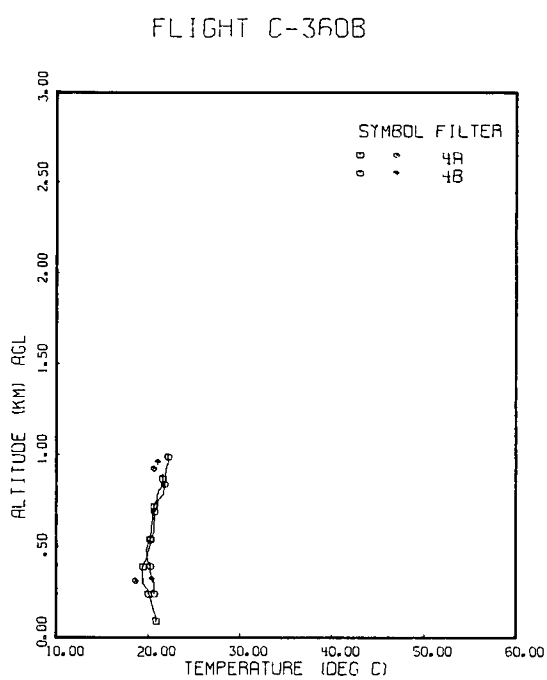

Fig. 6-2 (cont.). Temperature Versus Altitude for Eight Project SEEKVAL Flights.

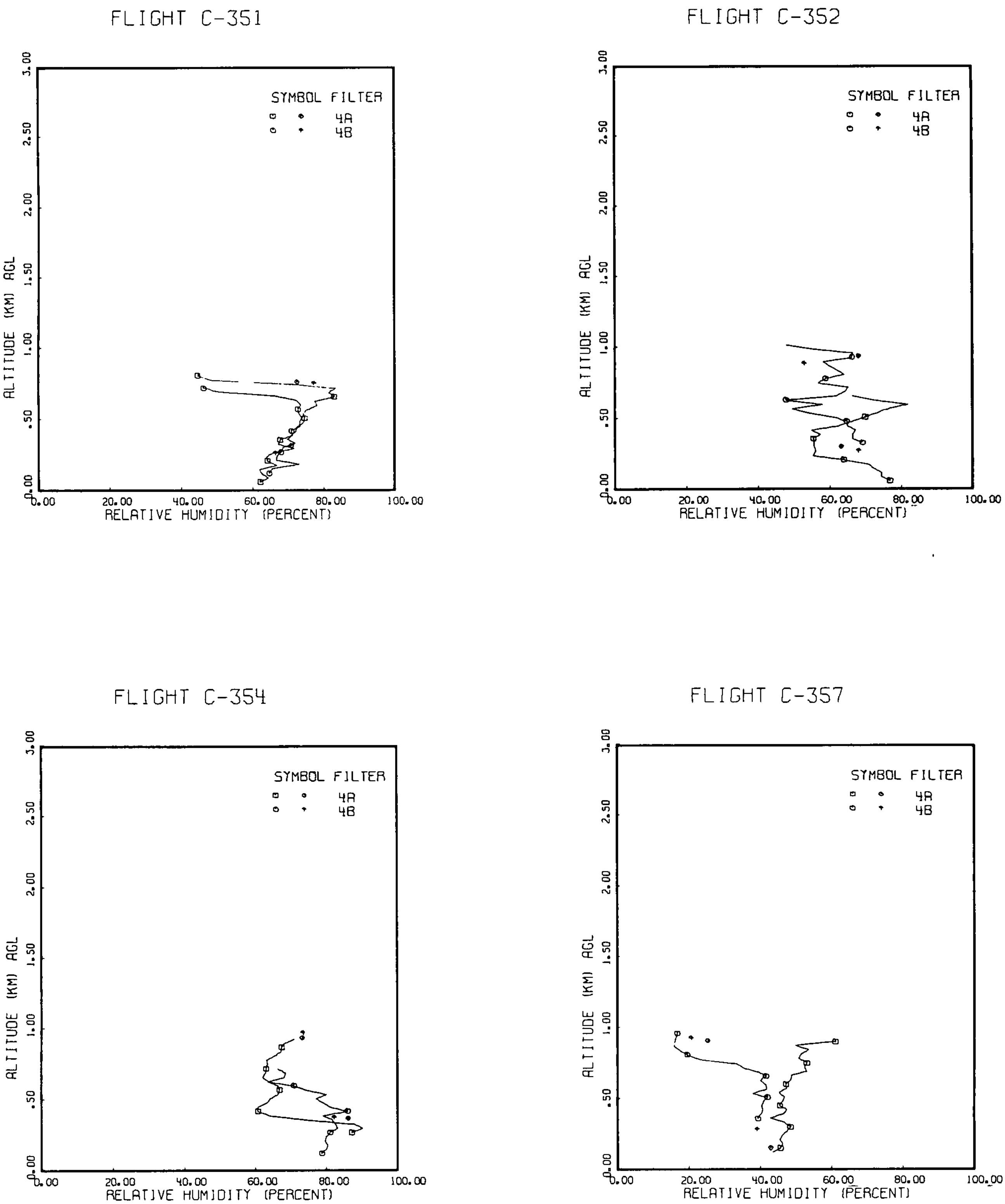

Fig. 6-3. Relative Humidity Versus Altitude for Eight Project SEEKVAL Flights.

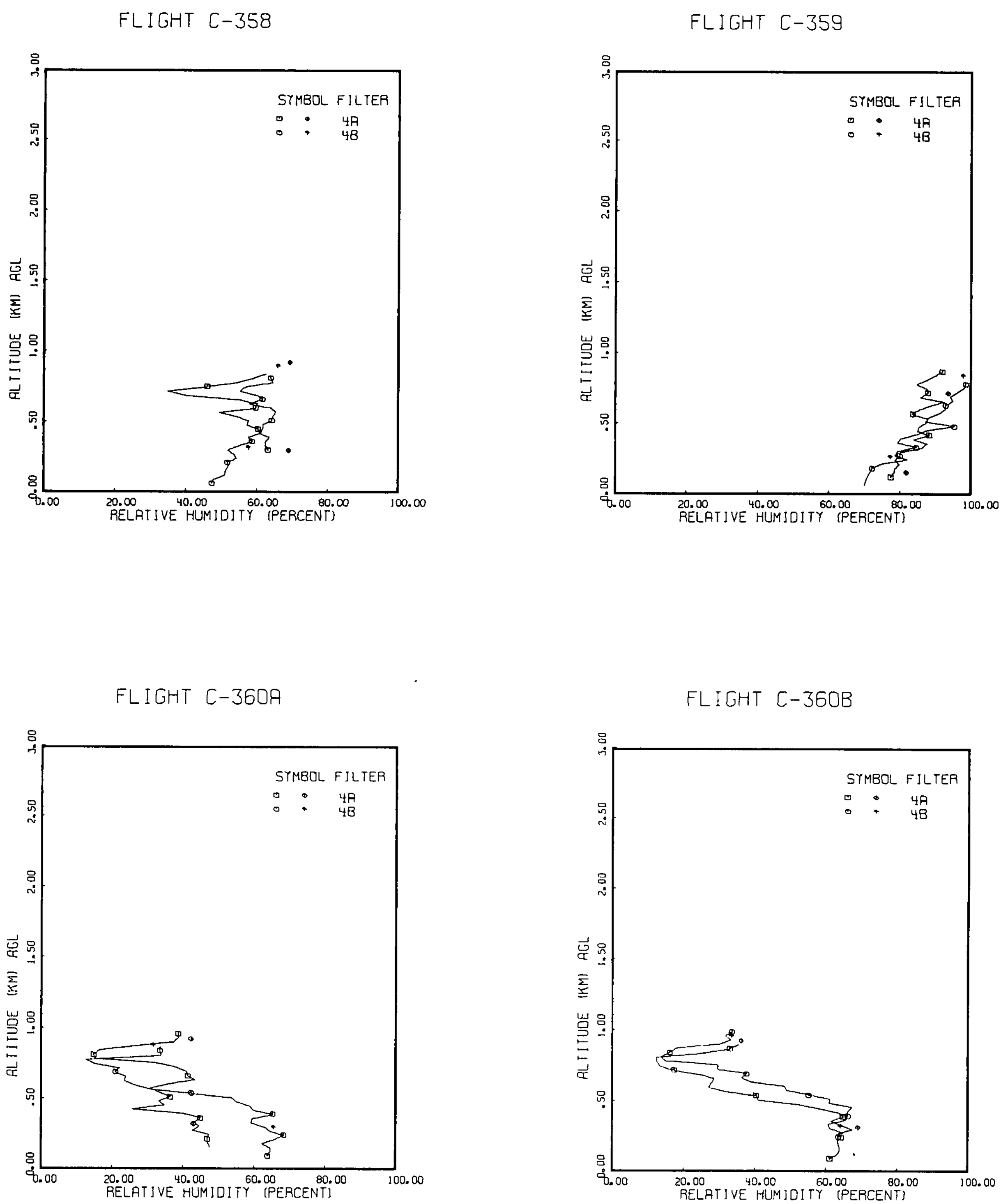

Fig. 6-3 (cont.). Relative Humidity Versus Altitude for Eight Project SEEKVAL Flights.

6.2 SYNOPTIC CONDITIONS

FLIGHT C-350 – 12 JULY 1974

The surface charts showed a ridge of high pressure over Washington, Oregon, and Idaho that changed little in intensity through the day. At 500 millibars, there was a low in the Gulf of Alaska with a trough extending southeastward to northern California and Nevada, the winds were moderate southwesterly, and a slight warming trend was noted.

FLIGHT C-351 – 13 JULY 1974

A weak ridge remained over Washington with a 1024-millibar high centered in southern British Columbia. A 1012-millibar low was situated off the West Coast centered at 44° N. 131.5° W. at 1800 GMT. This low center had an associated frontal system. At 500 millibars at 1200 GMT there was a low centered at 52° N. 140.5° W. with a trough extending southsoutheastward from the center. Winds aloft were moderate southwesterly, and the temperature had risen 7° C in 24 hours. Flow from Canada at low levels was bringing continental polar air.

FLIGHT C-352 – 14 JULY 1974

The 1200 GMT surface chart showed an occluded front approaching the Pacific coast. By 1800 GMT the front was passing over the coasts of Washington and Oregon, and had passed McChord at 2100 GMT. Only scattered clouds and a wind shift marked the frontal passage. At 500 millibars there was slight ridging in western Washington and Oregon which served to keep the low off the coast stationary. There were strong southwesterly winds and slowly rising temperatures at this level. The airmass was maritime polar with low-level flow from the ocean.

FLIGHT C-353 – 15 JULY 1974

The surface charts showed weak ridging from the Pacific high, along the coast from Washington to northern California and behind the front of the day before. At 500 millibars there was a low centered at 50° N. 135° W. There was a high centered in New Mexico with a ridge from Montana to Great Bear Lake. There were strong southwesterly winds. The airmass was maritime polar.

FLIGHT C-354 – 16 JULY 1974

The surface charts showed a weakening in the ridging along the coast with an approaching frontal system in the western Pacific. At 500 millibars there was a low centered over Queen Charlotte Islands with a trough southward. There also was a high centered in the Texas Panhandle with ridging northward to Saskatchewan. The winds were moderate southwesterly. The airmass was maritime polar.

FLIGHT C-355 – 17 JULY 1974

The surface charts showed that an occluded front, preceded and accompanied by showers, moved across Washington passing Tacoma about 0900 GMT. Rain showers continued throughout the day.

At 500 millibars there remained a low over Queen Charlotte Islands with a trough southward. There was ridging from the Dakotas into Manitoba. The winds were moderately strong southwesterly. The airmass was maritime polar.

NO FLIGHT OR GROUND DATA – 18 JULY 1974

Following the frontal passage of the 17th, the surface charts showed weak ridging from the Pacific high. The pressure gradient was very weak over Washington. At 500 millibars the low off the Canadian coast was stationary and filling, with the center at 52° N. 132° W. at 1200 GMT. The winds were moderately strong southwesterly. The airmass was modified maritime polar.

FLIGHT C-356 – 19 JULY 1974

The surface charts showed a weak ridging from the Pacific high, along the Washington and Oregon coasts. At 500 millibars there was a low off British Columbia with a trough southsouthwest. There also was ridging from a high in Kansas north to the Arctic circle. The winds were strong southwesterly. The airmass was modified maritime polar.

FLIGHT C-357 – 20 JULY 1974

On the surface charts, high pressure was centered off northwestern Washington with ridging along the coast of Washington and Oregon. This situation remained unchanged throughout the day. At 500 millibars the trough had moved into British Columbia, and there was weak ridging off the coast. The winds were moderate westsouthwesterly. The airmass was continental polar.

FLIGHT C-358 – 21 JULY 1974

The surface charts showed a 1019-millibar low over eastern Washington. The gradient over the wesern part of the state was very weak. A frontal system was associated with a deepening low centered at 46° N. 131° W. at 1800 GMT. At 500 millibars there was weak ridging from Nevada northwest to British Columbia. The winds were westsouthwesterly of moderate force. The airmass was modified continental polar.

NO FLIGHT OR GROUND DATA – 22 JULY 1974

The surface charts showed that a cold front crossed the Washington coast at 1200 GMT accompanied by rain. At 500 millibars there was a trough from the Gulf of Alaska southeast to the Washington and Oregon coasts. The winds were moderately strong southwesterly. The airmass was maritime polar.

FLIGHT C-359 – 23 JULY 1974

The surface charts showed weak ridging from the Pacific high over the Pacific Northwest. The cold front which moved in over Washington the day before continued to move southeastward. A weakening occlusion was off the coast of British Columbia at 1800 GMT. At 500 millibars there was a weakening trough from British Columbia to northern California. The winds were moderate westerly. The airmass was maritime polar.

GROUND DATA ONLY – 24 JULY 1974

The surface charts showed increased ridging from the Pacific high, over the western third of the nation. At 500 millibars there was a very weak ridge off the Washington and Oregon coasts. The winds were westnorthwesterly of moderate force. The airmass was continental polar.

NO FLIGHT OR GROUND DATA – 25 JULY 1974

The surface charts showed that ridging continued over Washington and Oregon. At 500 millibars there was slight ridging along the coast of Washington and Oregon. The winds were moderate westnorthwesterly.

NO FLIGHT OR GROUND DATA – 26 JULY 1974

The surface charts showed that the ridge weakened through the day and that there was a low over eastern Washington. At 500 millibars there was slight ridging over Washington and British Columbia.

NO FLIGHT OR GROUND DATA – 27 JULY 1974

The surface charts showed a very weak gradient over western Washington and a weak low in the eastern part of the state. At 500 millibars there was a high in New Mexico and moderate ridging northnorthwest to British Columbia.

FLIGHT C-360 – 28 JULY 1974

The surface charts showed a weak gradient with weak ridging in northwestern Washington. At 500 millibars there was a high in Utah with ridging to British Columbia. The winds were moderate westsouthwesterly. The airmass was continental polar.

GROUND DATA ONLY – 29 JULY 1974

The surface charts showed weak ridging in western Washington and an inverted trough in central Washington and Oregon. At 500 millibars there was a weak trough along the coasts of Washington and Oregon. In addition there was ridging from a high in Nevada to central and eastern Washington. The winds were moderate southwesterly. The airmass was continental polar.

6.3 TABULAR SUMMARY AND GLOSSARY

A summary of the daily meteorological observations taken at McChord Air Force Base and Gray Army Air Field on the days during which data flights were made is presented in Table 6-1. A glossary of the most often used symbols is also included. All data were reported in Pacific standard time (p.s.t.) but have been changed to Greenwich civil time (g.c.t.) to coincide with ground and flight logs.

METEOROLOGICAL GLOSSARY AND ABBREVIATIONS

SKY AND CEILING

Sky cover symbols are in ascending order Figures preceding symbols are heights in hundreds of feet above station Sky cover symbols are

○	Clear less than 0 1 sky cover
⦶	Scattered 0 1 to less than 0 6 sky cover
⦷	Broken 0 6 to 0 9 sky cover
⊕	Overcast more than 0 9 sky cover
-	Thin (when prefixed), light (when suffixed)
--	Very light (when suffixed)
-X	Partial obscuration 0 1 to less than 1 0 sky hidden by precipitation or obstruction to vision (bases at surface)
X	Obscuration 1 0 sky hidden by precipitation or obstruction to vision (bases at surface)

Letter preceding height of layer identifies ceiling layer and indicates how ceiling height was obtained Thus

A	Aircraft
B	Balloon (pilot or ceiling)
D	Estimated height of cirriform clouds on basis of persistency
E	Estimated height of noncirriform clouds
M	Measured
R	Radiosonde balloon or radar
U	Height of cirriform ceiling layer unknown
V	Immediately following numerical value indicates a varying ceiling (also used with varying visibility)
W	Indefinite, sky obscured by surface base phenomenon. e.g. fog, blowing dust, snow

RELATIVE HUMIDITY (RH)

Reported in percent and computed from temperature and dewpoint

VISIBILITY (VV)

Reported in statute miles

WEATHER AND OBSTRUCTION TO VISION SYMBOLS

A	Hail	IF	Ice fog
AP	Small hail	K	Smoke
BD	Blowing dust	L	Drizzle
BN	Blowing sand	R	Rain
BS	Blowing snow	RW	Rain showers
D	Dust	S	Snow
E	Sleet	SG	Snow grains
EW	Sleet showers	SP	Snow pellets
F	Fog	SW	Snow showers
GF	Ground fog	T	Thunderstorms
H	Haze	ZL	Freezing drizzle
IC	Ice crystals	ZR	Freezing rain

CLOUD ABBREVIATIONS

Ac	Altocumulus	Cs	Cirrostratus
As	Altostratus	Cu	Cumulus
Cb	Cumulonimbus	Ns	Nimbostratus
Cc	Cirrocumulus	Sc	Stratocumulus
Ci	Cirrus	St	Stratus

WIND

Direction in ten's of degrees from true north, speed in knots A "0000" indicates calm A "G" indicates gusty A "Q" indicates squall Peak speed of gusts, when reported, follows G or Q The contraction WSHFT in remarks followed by time group (GMT) indicates wind shift and its time of occurrence

Examples 0129 is 010 degrees, 29 knots

3627G40 is 360 degrees, 27 knots, peak speed in gusts of 40 knots

Table 6-1

STANDARD METEOROLOGICAL DATA SHEET
12 July 1974

Data Source: McChord Air Force Base
Flight No. C-350

Field Site: Rainier, Washington
Lat. 46° 55' N – Long. 122° 42' W – El. 158 m

Time p.s.t.	Time g.c.t.	Sky and Ceiling (Hundreds of Feet)	Visibility (miles)	Weather and Obstructions To Vision	Temp. (°F)	Dewpoint (°F)	Rel. Hum. %	Wind Direction (00–36)	Wind Speed (Kt)	Cloud Type	Total Sky Cover
0755	1555	12⦶ 25⦶ E40⦶ 100⦶	15		57	51	80	12	01	Cu Ac	0.9
0829	1629	12⦶ M17⦶ 40⦶ 100⦶	10	RW–				00	00	Cu Ac	0.9
0855	1655	12⦶ M17⦶ 40⦶ 100⊕	10	RW–	58	52	80	00	00	Cu Ac	1.0
0955	1755	12⦶ M17⦶ 40⦶ 100⊕	10	RW–	57	51	80	00	00	Cu Ac	1.0
1023	1823	12⦶ M21⦶ 40⦶ 100⊕	10							Cu Ac	1.0
1055	1855	12⦶ E21⦶ 40⦶ 100⊕	10	RW–	59	50	72	30	03	Cu Ac	1.0
1118	1918	12⦶ 21⦶ E40⦶ 100⦶	15							Cu Ac	0.8
1155	1955	20⦶ E40⦶ 100⦶	20		63	50	62	00	00	Cu Ac	0.8
1255	2055	30⦶ E50⦶	20		63	47	55	00	00	Cu Sc	0.7

Gray Army Air Field

Time p.s.t.	Time g.c.t.	Sky and Ceiling (Hundreds of Feet)	Visibility (miles)	Weather and Obstructions To Vision	Temp. (°F)	Dewpoint (°F)	Rel. Hum. %	Wind Direction (00–36)	Wind Speed (Kt)	Cloud Type	Total Sky Cover
0755	1555	8⦶ 12⦶ 25⦶ E40⦶ 100⦶	10		55	47	74	00	00		
0850	1650	8⦶ 12⦶ E25⦶ 40⦶ 100⊕	10					00	00		
0855	1655	8⦶ 12⦶ E25⦶ 40⦶ 100⊕	10		56	47	71	00	00		
0955	1755	8⦶ 12⦶ M23⦶ 40⊕	10		56	47	71	30	02		
1055	1855	12⦶ 25⦶ E40⦶ 80⦶	10		58	49	71	04	04		
1155	1955	25⦶ 40⦶ E80⦶	10		61	47	60	00	00		
1255	2055	25⦶ 40⦶ E80⦶	20		63	47	55	36	05		

Table 6-1 (cont.)

STANDARD METEOROLOGICAL DATA SHEET
13 July 1974

Data Source: McChord Air Force Base
Flight C-351

Field Site: Rainier, Washington
Lat. 46° 55' N – Long. 122° 42' W – El. 158 m

Time p.s.t.	Time g.c.t.	Sky and Ceiling (Hundreds of Feet)	Visibility (miles)	Weather and Obstructions To Vision	Temp. (°F)	Dewpoint (°F)	Hum. %	Wind Direction (00–36)	Wind Speed (Kt)	Cloud Type	Total Sky Cover
0855	1655	200⦶	30		60	49	66	02	02	Cs	0.1
0955	1755		30		63	50	62	01	04		0
1055	1855		30		67	51	56	35	06		0
1155	1955	250–⦶	30		67	51	56	02	08	Ci	0.1
1255	2055	250–⦶	30		71	51	49	03	06	Ci	0.1
1355	2155	250–⦶	30		72	48	42	03	06	Ci	0.1

Gray Army Air Field

Time p.s.t.	Time g.c.t.	Sky and Ceiling (Hundreds of Feet)	Visibility (miles)	Weather and Obstructions To Vision	Temp. (°F)	Dewpoint (°F)	Hum. %	Wind Direction (00–36)	Wind Speed (Kt)	Cloud Type	Total Sky Cover
0855	1655	200⦶	35		60	47	62	31	03		
0955	1755	200⦶	35		62	49	62	02	04		
1055	1855	200⦶	35		65	49	56	35	06		
1155	1955	200⦶	35		68	50	52	36	08		
1255	2055	200⦶	35		69	49	48	36	06		
1355	2155	35⦶ 200⦶	35		71	49	45	04	05		

Table 6-1 (cont.)

STANDARD METEOROLOGICAL DATA SHEET
14 July 1974

Data Source: McChord Air Force Base
Flight No. C-352

Field Site: Rainier, Washington
Lat. 46° 55' N – Long. 122° 42' W – El. 158 m

Time p.s.t.	Time g.c.t.	Sky and Ceiling (Hundreds of Feet)	Visibility (miles)	Weather and Obstructions To Vision	Temp. (°F)	Dewpoint (°F)	Rel. Hum. %	Wind Direction (00–36)	Wind Speed (Kt)	Cloud Type	Total Sky Cover
0555	1355	E100⦷	15		56	53	89	18	01	Ac	0.6
0655	1455	100⦶	30		60	48	64	23	01	Ac	0.5
0755	1555	100⦶	30		64	48	56	25	04	Ac	0.4
0855	1655	90⦶	30		66	47	50	26	06	Ac	0.3
0955	1755	90⦶	30		67	46	46	28	05	Ac	0.1
Gray Army Air Field											
0558	1358	35⦶ 100⦶	10		54	48	80	00	00		
0658	1458	E100⦷	35		60	46	59	23	03		
0755	1555	100⦶	35		62	46	54	25	06		
0855	1655	100⦶	35		64	46	52	25	06		
0955	1755	100⦶	35		67	44	43	22	05		

Table 6-1 (cont.)

STANDARD METEOROLOGICAL DATA SHEET
15 July 1974

Data Source: McChord Air Force Base
Flight No. C-353

Field Site: Rainier, Washington
Lat. 46° 55' N – Long. 122° 42' W – El. 158 m

Time p.s.t.	Time g.c.t.	Sky and Ceiling (Hundreds of Feet)	Visibility (miles)	Weather and Obstructions To Vision	Temp. (°F)	Dewpoint (°F)	Rel. Hum. %	Wind Direction (00–36)	Wind Speed (Kt)	Cloud Type	Total Sky Cover
1354	2154	E25 ⦷	15		59	51	74	25	08	Sc	0.9
1455	2255	M28 ⦷	15		62	48	59	28	08	Sc	0.9
1555	2355	E35 ⦷ 80 ⦷	15		63	47	55	23	06	Sc Ac	0.8
1655	0055	E35 ⦷ 80 ⦷	15		62	53	72	26	07	Sc Ac	0.7
1755	0155	35 ⦶ E80 ⦷	15		61	50	66	26	07	Sc Ac	0.6
1855	0255	35 ⦶ E80 ⦷ 250 ⦷	15		61	50	66	24	06	Sc Ac Cs	0.7

Gray Army Air Field

Time p.s.t.	Time g.c.t.	Sky and Ceiling (Hundreds of Feet)	Visibility (miles)	Weather and Obstructions To Vision	Temp. (°F)	Dewpoint (°F)	Rel. Hum. %	Wind Direction (00–36)	Wind Speed (Kt)	Cloud Type	Total Sky Cover
1355	2155	E35 ⦷ 200 ⦷	7		64	46	52	24	10		
1455	2255	E35 ⦷ 200 ⦷	7		62	48	60	26	05		
1555	2355	E35 ⦷ 200 ⦷	7		63	48	58	24	08		
1620	0020	E35 ⦷ 200 ⦷	7	RW–				23	06		
1637	0037	E35 ⦷ 200 ⦷	7					30	10		
1655	0055	25 ⦶ 35 ⦶ E200 ⦷	7		62	49	62	32	07		
1755	0155	25 ⦶ 35 ⦶ E80 ⦷ 200 ⦷	7		61	49	64	30	08		
1855	0255	25 ⦶ E35 ⦷ 80 ⦷ 200 ⦷	7		59	48	66	26	05		

Table 6-1 (cont.)

STANDARD METEOROLOGICAL DATA SHEET
16 July 1974

Data Source: McChord Air Force Base
Flight No. C-354

Field Site: Rainier, Washington
Lat. 46° 55' N – Long. 122° 42' W – El. 158 m

Time p.s.t.	Time g.c.t.	Sky and Ceiling (Hundreds of Feet)	Visibility (miles)	Weather and Obstructions To Vision	Temp. (°F)	Dewpoint (°F)	Rel. Hum. %	Wind Direction (00–36)	Wind Speed (Kt)	Cloud Type	Total Sky Cover
0855	1655	70⌽ E110⊕	15		60	51	71	00	00	Ac	1.0
0955	1755	80⌽ E110⊕	15		62	49	62	36	01	Ac	1.0
1057	1857	E70⦷ 120⊕	15		65	47	51	04	02	Ac	1.0
1155	1955	E65⦷ 100⊕	15		67	48	50	36	01	Ac	1.0
1257	2057	E60⦷ 100⊕	7		65	53	65	31	03	Ac	1.0

Gray Army Air Field

Time p.s.t.	Time g.c.t.	Sky and Ceiling (Hundreds of Feet)	Visibility (miles)	Weather and Obstructions To Vision	Temp. (°F)	Dewpoint (°F)	Rel. Hum. %	Wind Direction (00–36)	Wind Speed (Kt)	Cloud Type	Total Sky Cover
0855	1655	E60⦷ 100⊕	10		59	49	69	00	00		
0955	1755	E60⦷ 100⦷ 200⊕	10		60	49	66	00	00		
1055	1855	E60⦷ 80⊕	10		62	49	62	00	00		
1155	1955	E60⊕	10		64	50	60	00	00		
1240	2040	E60⦷ 100⊕	7	RW–				33	03		
1255	2055	E60⦷ 100⊕	7	RW–	63	51	64	34	02		

Table 6-1 (cont.)

STANDARD METEOROLOGICAL DATA SHEET
17 July 1974

Data Source: McChord Air Force Base
Flight No. C-355

Field Site: Rainier, Washington
Lat. 46° 55' N – Long. 122° 42' W – El. 158 m

Time p.s.t.	Time g.c.t.	Sky and Ceiling (Hundreds of Feet)	Visibility (miles)	Weather and Obstructions To Vision	Temp. (°F)	Dewpoint (°F)	Rel. Hum. %	Wind Direction (00–36)	Wind Speed (Kt)	Cloud Type	Total Sky Cover
1055	1855	11⦶ E30⦷ 50⊕	10	RW–	68	62	81	20	06		
1155	1955	14⦶ E30⦷ 50⦷ 80⦷	10		70	61	72	20	06		

Gray Army Air Force

Time p.s.t.	Time g.c.t.	Sky and Ceiling (Hundreds of Feet)	Visibility (miles)	Weather and Obstructions To Vision	Temp. (°F)	Dewpoint (°F)	Rel. Hum. %	Wind Direction (00–36)	Wind Speed (Kt)	Cloud Type	Total Sky Cover
1055	1855	15⦶ E25⦷ 50⊕	7	R–	66	58	75	21	04		
1130	1930	15⦶ E25⦷ 50⊕	7					17	06		
1155	1955	15⦶ E25⊕	7		68	59	73	20	05		

Table 6-1 (cont.)

STANDARD METEOROLOGICAL DATA SHEET
19 July 1974

Data Source: McChord Air Force Base
Flight No. C-356

Field Site: Rainier, Washington
Lat. 46° 55' N – Long. 122° 42' W – El. 158 m

Time p.s.t.	Time g.c.t.	Sky and Ceiling (Hundreds of Feet)	Visibility (miles)	Weather and Obstructions To Vision	Temp. (°F)	Dewpoint (°F)	Rel. Hum. %	Wind Direction (00–36)	Wind Speed (Kt)	Cloud Type	Total Sky Cover
1055	1855	20⦶ E30⊕	7		61	46	58	04	05	Sc	1.0
1155	1955	25⦶ E45⦷	7		64	47	54	02	03	Sc	0.9
1255	2055	50⦶ E80⦷	15		66	48	52	36	02	Sc Ac	0.7
1355	2155	50⦶ 80⦶	15		67	50	54	36	04	Sc Ac	0.4
1455	2255	50⦶ 80⦶	15		69	48	57	03	02	Sc Ac	0.3
Gray Army Air Field											
1040	1840	15⦶ E35⊕	10					06	05		
1055	1855	E35⊕	10		61	45	55	02	05		
1155	1955	E35⦷	10		63	45	51	36	04		
1255	2055	E35⦷	10		64	47	54	35	04		
1355	2155	40⦶ 250⦶	35		67	49	52	04	02		
1455	2255	40⦶ 250–⦷	20		69	49	48	31	04		

Table 6-1 (cont.)

STANDARD METEOROLOGICAL DATA SHEET
20 July 1974

Data Source: McChord Air Force Base
Flight No. C-357

Field Site: Rainier, Washington
Lat. 46° 55' N – Long. 122° 42' W – El. 158 m

Time p.s.t.	Time g.c.t.	Sky and Ceiling (Hundreds of Feet)	Visibility (miles)	Weather and Obstructions To Vision	Temp. (°F)	Dewpoint (°F)	Rel. Hum. %	Wind Direction (00–36)	Wind Speed (Kt)	Cloud Type	Total Sky Cover
1355	2155	140⌽ 250–⦷	40		73	43	34	02	08	Ac Cs	0.7
1455	2255	160⌽ 250–⦷	20		73	45	36	36	04	Ac Cs	0.7
1555	2355	160⌽ 250–⊕	20		75	44	32	02	05	Ac Cs	1.0
1655	0055	160⌽ 250–⦷	20		74	38	27	35	05	Ac Cs	0.7
1755	0155	160⌽ 250–⦷	20		73	44	35	02	04	Ac Cs	0.7
1855	0255	160⌽ 250–⦷	20		71	43	36	02	05	Ac Cs	0.7
Gray Army Air Force											
1355	2155	170⌽ 250–⦷	35		75	49	40	05	05		
1455	2255	120⌽ 250–⦷	35		76	47	36	03	06		
1555	2355	200–⦷	35		76	47	36	36	03		
1655	0055	200–⦷	35		75	47	37	05	06		
1755	0155	200–⦷	35		71	44	37	03	03		
1855	0255	200–⦷	35		69	43	39	04	04		

Table 6-1 (cont.)

STANDARD METEOROLOGICAL DATA SHEET
21 July 1974

Data Source: McChord Air Force Base
Flight No. C-358

Field Site: Rainier, Washington
Lat. 46° 55' N – Long. 122° 42' W – El. 158 m

Time p.s.t.	Time g.c.t.	Sky and Ceiling (Hundreds of Feet)	Visibility (miles)	Weather and Obstructions To Vision	Temp. (°F)	Dewpoint (°F)	Rel. Hum. %	Wind Direction (00–36)	Wind Speed (Kt)	Cloud Type	Total Sky Cover
0955	1755	200⦶ 250–⊕	15		70	52	52	00	00	Cs	1.0
1055	1855	E180⦷ 250⊕	15		72	53	51	00	00	Cs	1.0
1155	1955	180⦶ 250–⊕	15		74	54	49	32	03	Cs	1.0
1255	2055	180⦶ 250–⊕	15		76	51	41	29	03	Cs	1.0
Gray Army Air Field											
0955	1755	120⦶ 250–⊕	35		68	48	49	00	00		
1055	1855	200–⊕	35		71	50	47	00	00		
1155	1955	200–⊕	35		72	52	49	00	00		
1255	2055	200–⊕	35		75	51	42	25	03		

Table 6-1 (cont.)

STANDARD METEOROLOGICAL DATA SHEET
23 July 1974

Data Source: McChord Air Force Base
Flight No. C-359

Field Site: Rainier, Washington
Lat. 46° 55' N – Long. 122° 42' W – El. 158 m

Time p.s.t.	Time g.c.t.	Sky and Ceiling (Hundreds of Feet)	Visibility (miles)	Weather and Obstructions To Vision	Temp. (°F)	Dewpoint (°F)	Rel. Hum. %	Wind Direction (00–36)	Wind Speed (Kt)	Cloud Type	Total Sky Cover
1155	1955	E26⦷ 50⦷ 80⦷	10		64	57	78	29	02	Sc	0.9
1255	2055	E28⦷ 50⦷	10		67	53	60	02	03	Sc	0.9
1326	2126	30⦶ E40⦷	15					36	03	Sc	0.9
1355	2155	30⦶ E40⦷	15		68	53	58	00	00	Sc	0.9
1455	2255	30⦶ E40⦷	15		67	52	58	23	02	Sc	0.9
1557	2355	30⦶ E40⦷	15		68	52	56	31	02	Sc	0.6
Gray Army Air Field											
1155	1955	15⦶ E25⦷ 40⊕	10		63	53	70	02	02		
1234	2034	25⦶ E40⊕	10					33	02		
1256	2056	30⦶ E40⦷	10		65	53	65	30	04		
1355	2155	30⦶ E40⦷	10		66	52	60	24	03		
1455	2255	30⦶ E40⦷	10		66	53	63	00	00		
1555	2355	E40⦷	10		68	54	60	03	04		

Table 6-1 (cont.)

STANDARD METEOROLOGICAL DATA SHEET
28 July 1974

Data Source: McChord Air Force Base
Flight No. C-360

Field Site: Rainier, Washington
Lat. 46° 55' N – Long. 122° 42' W – El. 158 m

Time p.s.t.	Time g.c.t.	Sky and Ceiling (Hundreds of Feet)	Visibility (miles)	Weather and Obstructions To Vision	Temp. (°F)	Dewpoint (°F)	Rel. Hum. %	Wind Direction (00–36)	Wind Speed (Kt)	Cloud Type	Total Sky Cover
0555	1355	250⦶	15		57	53	86	00	00	Cc	0.3
0657	1457	250⦶	15		64	54	69	00	00	Cc	0.2
0757	1557	150⦶ 250⦶	15		70	51	53	02	03	Cc	0.2
0857	1657	200⦶	15		72	54	53	36	04	Cc	0.1
0956	1756	200⦶	15		73	55	53	35	05	Cc	0.1
1057	1857	200⦶	15		77	56	48	02	06	Cc	0.1
Gray Army Air Field											
0555	1355	150⦶ 200–⦶	35		58	52	80	00	00		
0655	1455	150⦶ 200–⦶	35		64	54	69	00	00		
0755	1555	150⦶ 200–⦶	35		68	51	54	02	07		
0858	1658	200⦶	35		72	52	49	05	04		
0957	1757	200⦶	35		75	54	48	03	06		
1055	1855	200⦶	35		77	54	44	04	05		

7. DATA PRESENTATION

7.1 AIRBORNE DATA AND FLIGHT SUMMARY

Between 12 and 28 July 1974, 10 flights resulting in numerous data profiles were made in western Washington. An eleventh flight, C-355, was attempted, but instrument malfunction caused the flight to be terminated without obtaining any data. Data for eight double profiles from seven flights are included in this report. Data for the remaining three flights were of inadequate quality to justify complete processing. During these three flights the nephelometer system was optically contaminated, and the highly variable lighting conditions, as evidenced by an irregular downwelling irradiance profile, precluded recovery of the attenuation coefficient from measured path function and computed equilibrium radiance values.

All of the measurements were made with the pseudo-photopic filter, Filter 4, of mean wavelength 557 nanometers. Each flight contained numerous sets of assorted flight elements consisting of straight and level flight elements at both high altitude (900 meters AGL) and low altitude (300 meters AGL) and vertical profile elements taken during ascents and descents. From these, elements comprising two (1 + 2) profiles were selected for processing and labeled chronologically as Filter 4A and Filter 4B. One flight, Flight C-360, was also divided into two portions, Flight C-360A and C-360B, and double profiles were selected for each of these flight portions.

The flights were conducted in the vicinity of Rainier, Washington, in support of SEEKVAL Project ID1. The purpose of the field test was to determine suitable instrumentation for recording ground-scene characteristics as seen by aircraft observers, and for measuring atmospheric factors which degrade those characteristics. The flight track was over the test site at 122.7° W. longitude, 46.92° N. latitude, 158 meters mean sea level. The test site containing the visual scene was in an open meadow or prairie surrounded by pine woods.

PHOTOGRAPHIC DOCUMENTATION

Sky and terrain conditions encountered during each of the data flights were documented photographically during each straight and level flight sequence. These documentary photographs were taken simultaneously with the measurements of sky and terrain radiance at each of two designated altitudes.

The photographs illustrating sky and terrain conditions during each of the eight double profiles have been examined and classified with respect to discernible cloud conditions. A summary of these general cloud and terrain descriptions is presented in Table 7-1.

There are four profiles for which the pictures show clear skies at all altitudes. There are six profiles with scattered clouds above the highest flight altitude, but with the sun unobscured during most or all of each profile. Two additional profiles are for broken clouds with the sun partially obscured by the clouds during much of each profile. The remaining four profiles have skies completely overcast.

Table 7-1

SUMMARY OF HEMISPHERICAL PICTURES

Flight No.	General Description Pictures for Flight	Filter	Upper Hemisphere		Lower Hemisphere*	
			Low Altitude	High Altitude	Low Altitude	High Altitude
C-351	Clear, no clouds	4A	Clear	–	Mostly prairie fields ahead	–
		4B	Clear	Clear	Mostly prairie	Woods, fields, prairie
C-352	Scattered small high clouds at first, then clear sky	4A	Scattered high clouds, sun in clouds near horizon	Sun visible in scattered clouds near horizon	Broken shadow, mostly prairie	Clear, mostly woods and prairie
		4B	Clear	–	Clear, prairie with trees	–
C-354	Solid overcast, sun rarely visible as bright spot	4A	Solid thin overcast	Slightly thicker overcast	Shadow, woods	Shadow, mostly woods
		4B	Solid overcast	Solid overcast	Shadow, prairie and target	Shadow, fields, woods
C-357	High, very thin-to-wispy cirrus clouds	4A	Scattered clouds, one less tenuous cloud near sun	Scattered clouds, may have clouds before sun	Clear, woods and fields	Clear, woods and fields
		4B	Scattered to broken, sun near clouds	Scattered wispy clouds	Clear, prairie and woods	Clear, woods
C-358	White overcast, some thinner areas, sun visible through clouds	4A	Overcast, small amount of blue visible	Solid overcast	Diffuse, fields	Diffuse, fields and woods
		4B	Overcast with 1/2 of sky bluish	Overcast except for one patch of bluish sky	Clear, prairie surrounded by woods	Diffuse, mostly woods, some fields
C-359	Varying from heavy overcast to clear, clouds well-defined	4A	Broken, sun spot visible through clouds	Heavy, solid overcast	Scattered shadow, woods	Broken deep shadow, mostly woods
		4B	Broken, sun in clear portion of sky	Broken, sun not visible	Clear, woods	Broken shadow, woods
C-360A	Blue sky overhead with clouds at horizon	4A	Clouds on horizon, near sun	Clouds on horizon, sun may be in clouds	Clear, woods	Clear, woods and fields
		4B	Clouds on horizon, sun possibly above clouds	Clouds on horizon, sun above clouds	Clear, woods mostly	Clear, fields and woods
C-360B	Clear overhead with clouds at horizon at first, then clear sky	4A	Clouds near horizon, sun above them	Clouds near horizon, sun above them	Clear, woods and fields	Clear, woods and fields
		4B	Clear	Clear	Clear, mostly woods	Clear, mostly woods

* In the lower hemisphere, the term "clear" means there are no distinct, well-defined cloud shadows.

Photographs illustrating typical sky and terrain conditions during four of the eight double profiles reported herein are shown in Fig. 7-1 and 7-2. In each instance, the picture on the left represents the sky (upper hemisphere) as seen through a 180-degree lens, and the picture on the right represents the terrain (lower hemisphere). The photographs were taken from both the high and low flight altitudes for each of the four flight profiles. The pictures representing flight profile C-358, Filter 4B, illustrate the full overcast condition. Those representing Flight C-359, Filter 4B, depict the broken cloud situation. The pictures representing Flight C-360A, Filter 4A, indicate the scattered clouds with unobscured sun, and those for C-360B, Filter 4B, are typical of the clear skies.

RADIOMETRIC DOCUMENTATION

Table 7-2 contains a summary of pertinent descriptive information on the eight flight profiles for which radiometric data are reported herein. The flight numbers are sequential. The times under the Total Time of Data-Taking column are Greenwich mean time (GMT) and Pacific daylight time (PDT). The PDT is equal to GMT-7. The sun zenith angles are tabulated for the time when sky radiance data-taking began, at the time of sun transit (minimum sun zenith angle), and at the conclusion of the sky radiance data-taking. The average sun zenith angles in column 11 were used in Eq. 2.6, 2.22, and 2.36 during the calculations leading to the derivation of path radiance and path reflectance. The maximum flight altitude is noted in column 12.

Table 7-2

FLIGHT DATA SUMMARY

Flight No.	Date (1974)	Total Time of Data-Taking				Filter	Sun Zenith Angle (degrees)				Maximum Flight Altitude (meters AGL)
		Start		End							
		GMT	PDT	GMT	PDT		Start	Transit	End	Average	
C-351	13 July	1933	1233	1956	1256	4A	26.6	-	25.5	26.0	810
		2039	1339	2056	1356	4B	25.5	-	26.2	26.0	753
C-352	14 July	1510	0810	1537	0837	4A	65.4	-	61.1	63.2	937
		1707	1007	1725	1025	4B	45.7	-	43.0	44.4	1020
C-354	16 July	1748	1048	1805	1105	4A	39.4	-	37.2	38.3	936
		1901	1201	1922	1222	4B	29.8	-	28.7	29.3	973
C-357	20 July	2324	1624	2342	1642	4A	46.0	-	48.6	47.3	909
		0154	1854	0212	1912	4B	71.3	-	74.0	72.6	960
C-358	21 July	1839	1139	1855	1155	4A	33.2	-	31.5	32.3	920
		2007	1307	2024	1324	4B	26.6	26.5	26.5	26.5	895
C-359	23 July	2124	1424	2143	1443	4A	30.2	-	31.8	31.0	870
		2324	1624	2344	1644	4B	46.3	-	49.4	47.8	843
C-360A	28 July	1455	0755	1511	0811	4A	69.8	-	67.5	68.7	960
		1641	0941	1702	1002	4B	52.0	-	50.3	51.1	880
C-360B	28 July	1704	1004	1725	1025	4A	48.2	-	46.5	47.3	926
		1818	1118	1833	1133	4B	37.0	-	35.4	36.2	990

FLIGHT C-358
Filter 4B

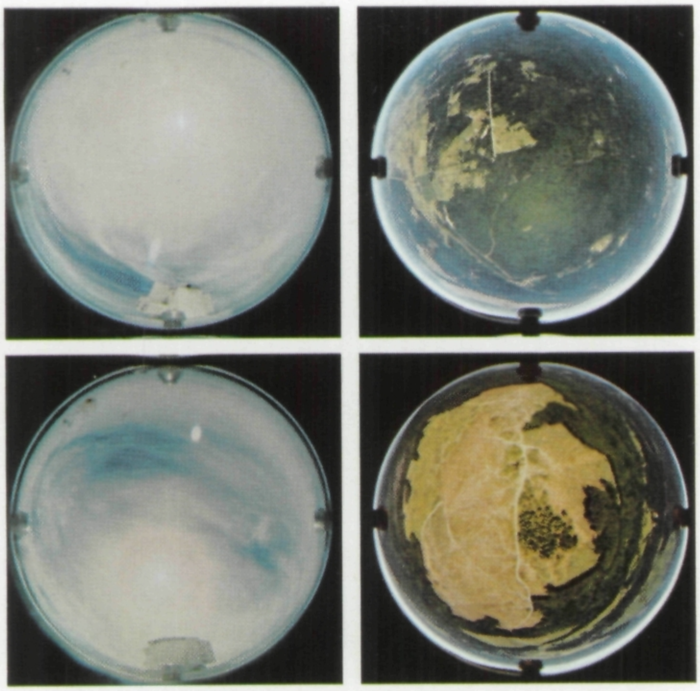

Upper and Lower Hemisphere
895 m AGL 2007 GMT

Upper and Lower Hemisphere
318 m AGL 2021 GMT

Fig. 7-1. Typical Sky and Terrain Photographs for Flights C-358 and C-359.

FLIGHT C-359
Filter 4B

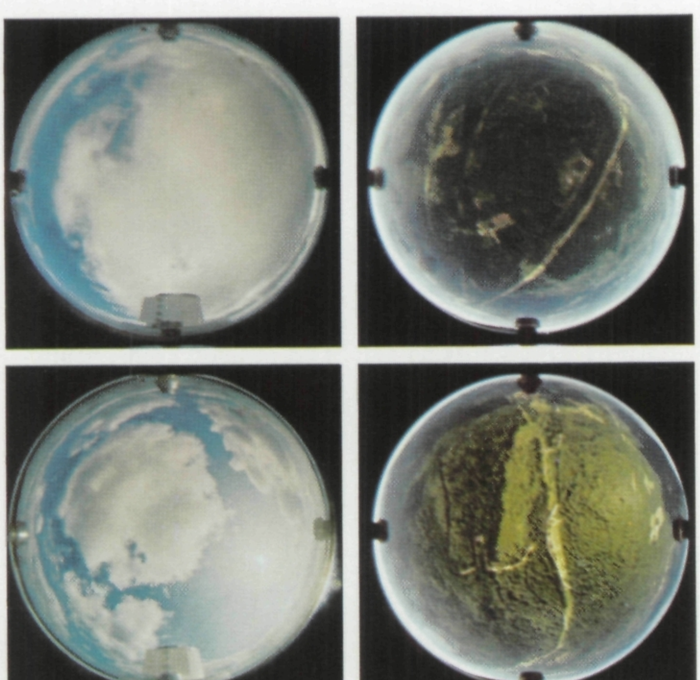

Upper and Lower Hemisphere
843m AGL 2323 GMT

Upper and Lower Hemisphere
264m AGL 2342 GMT

FLIGHT C-360A
Filter 4A

Upper and Lower Hemisphere
923 m AGL 1455 GMT

Upper and Lower Hemisphere
320 m AGL 1508 GMT

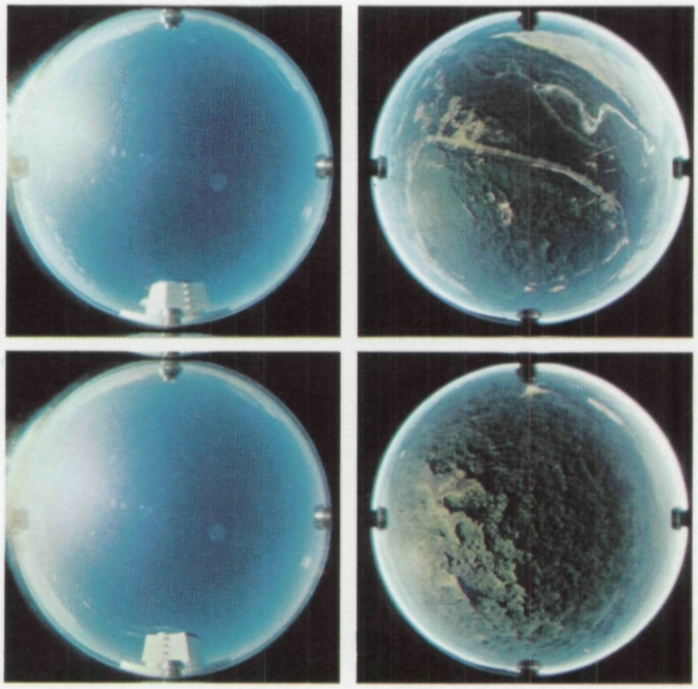

Fig. 7-2. Typical Sky and Terrain Photographs for Flight C-360A and C-360B.

FLIGHT C-360B
Filter 4B

Upper and Lower Hemisphere
963 m AGL 1818 GMT

Upper and Lower Hemisphere
320 m AGL 1830 GMT

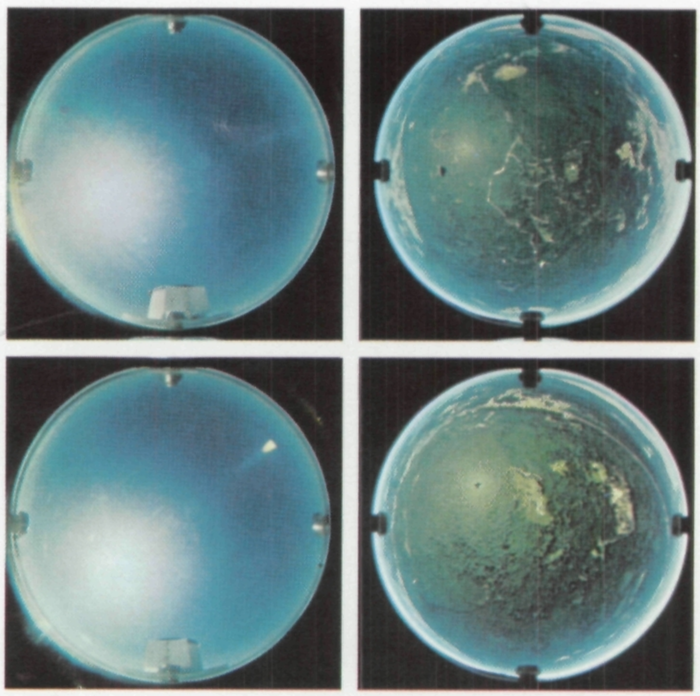

Radiometric data for the seven flights representing eight double profiles are presented tabularly and graphically in Section 7.3 in sets by flight number. A detailed description and report of weather characteristics are given as the introductory page of each data set.

Whenever the sky is clear at the highest altitude, the beam transmittance is extrapolated from space to the highest altitude of flight from sky radiance ratios as described in Section 2.1. It was possible to use this method for Flight C-351, Filters 4A and 4B, and C-360B, Filter 4B. The value of space-to-altitude transmittance obtained from C-360B, Filter 4B, was used throughout the entire flight since it compared well with the values obtained from the ground-based contrast reduction meter combined with the airborne nephelometer data. The space-to-altitude transmittances for Flights C-352 and C-357 were specified on the basis of the ground-based contrast reduction meter measurement coupled with the airborne total scattering coefficient values. Two flights had the sun partially obscured by clouds but it was possible to obtain estimates of space-to-altitude transmittance, which included the cloud effect, from sun mode radiance measurements for Flight C-358 and from downwelling irradiance measurements for Flight C-359. The eighth double profile, C-354, had such a thick overcast that the sun was not visible through the clouds.

These values of space-to-altitude transmittance are not included in the standard sets of data tables by flight. These values and the resultant space-to-ground beam transmittance, when combined with the beam transmittance based on the total scattering coefficient profile, are presented for seven double profiles in Table 7-3.

Table 7-3

VERTICAL BEAM TRANSMITTANCE, SPACE TO 1200 METERS AND SPACE TO GROUND

		Space-to-1200 Meters Beam Transmittance		Space-to-Ground Beam Transmittance	
Flight No.	Date (1974)	Filter 4A	Filter 4B	Filter 4A	Filter 4B
C-351	13 July	0.900	0.886	0.812	0.801
C-352	14 July	0.853	0.862	0.801	0.798
C-357	20 July	0.881	0.881	0.822	0.810
C-358	21 July	0.228	0.556	0.208	0.516
C-359	23 July	0.347	0.289	0.302	0.245
C-360A	28 July	0.840	0.840	0.802	0.798
C-360B	28 July	0.840	0.840	0.795	0.787

7.2 DESCRIPTION OF AIRBORNE DATA TABLES AND GRAPHS

DATA TABLES

Data are presented in tables of:

- Irradiance
- Directional Reflectance of Terrain
- Total Scattering Coefficient
- Equivalent Attenuation Length from Ground to Altitude
- Beam Transmittance from Ground to Altitude
- Path Radiance from Ground to Altitude
- Directional Path Reflectance from Ground to Altitude

Each optical property is tabulated in the tables as a function of altitude above ground level except for the directional reflectance of terrain which is tabulated as a function of zenith angle. The data are further divided by optical filters which are given in chronological order except for Flight C-357. The tables of directional reflectance of terrain, path radiance from ground to altitude, and directional path reflectance from ground to altitude are presented in four sets of four azimuths, with respect to the sun, of 0, 90, 180, and 270 degrees.

Irradiance. The downwelling irradiances H(z,d) and upwelling irradiances H(z,u), albedos H(z,u)/H(z,d), scalar irradiances ${}_s h(z)$, ${}_k h(z,d)$, h(z,u), and h(z), and scalar albedos h(z,u)/h(z,d) are presented in columnar form as a function of altitude. The irradiances are computed from measurements of sky and terrain radiance made by the airborne 2π scanner system at each of the flight profile level altitudes.

The altitudes are given in meters above ground level for the altitudes of flight. There are two tables of irradiance for each flight, one table for each optical filter. The dimensions and units for the irradiances are "$wm^{-2}\mu m^{-1}$". Albedos are, of course, dimensionless.

The irradiances for Filter 4 (4A or 4B) can be converted to illuminance values in units of lumens per square meter by multiplying each irradiance by the factor 72.0 lμm/w.

Directional Reflectance of Terrain. The directional terrain reflectance $R_o(z,\theta,\phi)$ is tabulated by zenith angle in two columns for the optical filters. A table is presented for each of the four azimuthal points. Reflectance is dimensionless. These reflectances are based on the apparent terrain radiance and the downwelling irradiance measured at the minimum aircraft altitude.

It should be stressed again that the reflectances presented in this section are typical of the average terrain beneath the flight path. The lower hemisphere scanner has a 5-degree circular field of view and during the data-taking interval, the aircraft is traveling at approximately 150 knots. Both of these characteristics contribute to the optical smearing of the measurement area and the attendant radiometric averaging.

The background reflectance required as input to a contrast transmittance computation must represent the actual background at the immediate boundary of the target object. This will not necessarily be the same as the average reflectance of the surrounding area.

Inherent and Apparent Terrain Radiances. The terrain radiance is not included in these tables. The inherent radiance of the terrain $N_o(z_t,\theta,\phi)$ immediately surrounding the target may be computed from the directional reflectance of the terrain $R_o(z_t,\theta,\phi)$ and the downwelling irradiance $H(z_t,d)$:

$$N_o(z_t,\theta,\phi) = \frac{1}{\pi} R_o(z_t,\theta,\phi) H(z_t,d) \ . \tag{7.1}$$

The downwelling irradiance at the lowest flight altitude for each filter may be used as the ground-level irradiance with reasonable accuracy [Duntley, *et al.* (1970), p. 7-25]. The apparent terrain radiance $N_r(z,\theta,\phi)$ at the sensor altitude z can be computed as follows:

$$N_r(z,\theta,\phi) = N_o(z_t,\theta,\phi) T_r(z,\theta) + N_r^*(z,\theta,\phi) \ . \tag{7.2}$$

The beam transmittances $T_r(z,\theta)$ and the path radiances $N_r^*(z,\theta,\phi)$ from ground to altitude are given in the tables to be described later.

The terrain radiances for Filter 4 may be converted to luminance values in units of $lu/\Omega m^2$ by multiplying the radiance by the factor 72.0 $lu\mu m/w$.

Total Scattering Coefficient. The total volume scattering coefficient $s(z)$ is tabulated by altitude in two columns for the two optical filters. The altitude is given in meters, above ground level, at 30-meter (98.4-foot) increments. The measurement unit for the total scattering coefficient is "m^{-1}".

At the bottom of the total scattering coefficient table are given the first and last data altitudes. This is the lowest and highest altitude of data measurements. When ground-based measurements of total scattering coefficient are available, the first data altitude is ground level.

The total scattering coefficient is used for the calculation of atmospheric beam transmittance in the next set of tables using the equations of the Theory, Section 2.

Equivalent Attenuation Length from Ground to Altitude. The equivalent attenuation length $\bar{L}(z)$ is a pseudo-attenuation length which, when combined with its altitude z, can be used directly in Eq. 2.12 to compute beam transmittance. The equivalent attenuation length permits easy calculation of the atmospheric beam transmittance between ground level and altitude z above ground level for a downward path of sight, or between altitude and ground level for the upward path of sight.

The equivalent attenuation length $\bar{L}(z)$ is tabulated by altitude for the path of sight between ground and the altitude shown in two columns for the two optical filters. The altitude is given in meters, above ground level, at 300-meter (984-foot) increments. The measurement unit for the equivalent attenuation length is "km".

Beam Transmittance from Ground to Altitude. The atmospheric beam transmittance $T_r(z,\theta)$ is tabulated in two types of tables: one for the vertical path of sight and one for the slant paths of sight.

The beam transmittance is tabulated for the vertical path of sight, between ground and the altitude shown, in two columns for the two optical filters. The altitude is given in meters, above ground level, at 300-meter (984-foot) increments. This property is dimensionless.

The atmospheric beam transmittance for the relatively clear days is tabulated for the slant paths of sight, between ground and the altitude shown, for the six zenith angles from 95 to 180 degrees. There are two tables, one for each optical filter. This property is dimensionless.

The beam transmittance is computed from measurements of total scattering coefficient. The assumption is made that there is no significant atmospheric absorption in the pass bands of the measurements, whence the atmospheric attenuation coefficient $\alpha(z)$ is assumed equivalent to the scattering coefficient $s(z)$.

Path Radiance from Ground to Altitude. Path radiance $N_r^*(z,\theta,\phi)$ is tabulated for the slant paths of sight, between ground and the altitude shown, for the six zenith angles from 95 to 180 degrees. The path radiance is computed from measurements of total scattering coefficient, measurements of sky and terrain radiances, and a catalog of proportional directional scattering coefficients based upon the work of Barteneva (1960).

There are four sets of data tables, one set for each of the four cardinal azimuths from the sun, 0, 90, 180, and 270 degrees. Each set is listed on a single sheet and contains two tables, one for each filter. The measurement units are "$w\Omega^{-1}\ m^{-2}\ \mu m^{-1}$".

The path radiance values for Filter 4 may be converted to path luminance values with units of $lu/\Omega m^2$ by multiplying the radiance by the factor 72.0 $lu\mu m/w$.

Directional Path Reflectance from Ground to Altitude. Directional path reflectance $R_r^*(z,\theta,\phi)$ is also tabulated for the downward-looking slant paths of sight, between ground and the altitude shown, for the six zenith angles from 95 to 180 degrees. The directional path reflectance is computed from the previously derived values of path radiance, beam transmittance, and total downwelling irradiance.

There are four sets of data tables, one set for each of the four cardinal azimuths from the sun, 0, 90, 180, and 270 degrees. Each set is listed on a single sheet and contains two tables, one for each filter. This property is dimensionless.

Contrast Transmittance. Contrast transmittance ${}_b\tau_r(z,\theta,\phi)$ is not tabulated. This optical property is a function of the directional path reflectance and the directional background reflectance against which an object is viewed. The directional terrain reflectance reported herein is measured by the airborne radiometer. Thus, it is the average reflectance of many individual areas integrated into one value by the 5-degree circular field of the radiometer. The background reflectance against which the object is viewed will probable never be the same as the reflectance of the average terrain. If the area of the background is sufficiently small, its reflectance will have no appreciable effect on the path reflectance. In such cases, decoupling exists between the object background area and the atmospheric path reflectance and the contrast transmittance may be calculated by Eq. 3 of Duntley (1969) repeated below:

$$ {}_b\tau_r(z,\theta,\phi) = \left\{1 + [\,R_r^*(z,\theta,\phi)/{}_bR_o(z_t,\theta,\phi)]\right\}^{-1} \quad . \tag{7.3}$$

DATA GRAPHS

Data are also presented in graphs of:

Downwelling Irradiance
Total Scattering Coefficient
Equivalent Attenuation Length from Ground to Altitude
Vertical Beam Transmittance from Ground to Altitude
Path Radiance from Ground to Altitude
Directional Path Reflectance from Ground to Altitude

Downwelling Irradiance. The downwelling irradiance $H(z,d)$ is graphed as a function of altitude AGL. These irradiances are from column 2 of the irradiance table. They are computed from the sky measurements and the sun irradiance at each of the flight profile level altitudes.

Total Scattering Coefficient. The total volume scattering coefficient $s(z)$ in m^{-1} is graphed using a single average value for each 30-meter change in altitude. Identifying symbols for the spectral filters appear at every fifth data point, or at 150-meter intervals. These same data were tabulated in the total scattering coefficient table.

Equivalent Attenuation Length from Ground to Altitude. The equivalent attenuation length $\bar{L}(z)$ in kilometers, for the path between ground and altitude, is graphed for each 30-meter change in altitude. Spectral identifying symbols appear at 150-meter intervals or every fifth data point.

Vertical Beam Transmittance from Ground to Altitude. The vertical beam transmittance $T_r(0,0)$ or $T_r(z,180)$ between ground and altitude is graphed for each 30-meter interval. Spectral identifying symbols appear at 150-meter intervals or every fifth data point. This represents smaller altitude increments than in the tabular display of beam transmittance.

Path Radiance from Ground to Altitude. The path radiance $N_r^*(z,\theta,\phi)$ is graphed for downward-looking slant paths between ground and the altitude shown. Each graph is for one path of sight for both optical filters. The first graph is for the vertical downward path of sight, the second and third are for zenith angles 120 and 100 degrees toward the azimuth of the sun. These are data selected from the path radiance tables.

Directional Path Reflectance from Ground to Altitude. The directional path reflectance $R_r^*(z,\theta,\phi)$ is also graphed for downward-looking slant paths between ground and the altitude shown. Each graph is for one path of sight and two optical filters. The first graph is for the vertical downward path of sight, the second and third are for zenith angles 120 and 100 degrees toward the azimuth of the sun. These selected paths of sight are the same as for the path radiance graphs. The data were selected from the many paths of sight tabulated in the directional path reflectance tables.

7.3 PRESENTATION OF AIRBORNE DATA

Tabular listings and graphical displays of the data discussed in Section 7.2 are presented in the pages immediately following. Users should be aware that regardless of the display format, the data values are valid to, at best, only three significant figures. The tables of beam transmittance and directional reflectance of the terrain, in particular, should be rounded off to two digits prior to further application.

It should also be remembered that all values in the data tables except scattering coefficient are computed values based upon the measured values of upper and lower hemisphere radiances. All other direct radiometric measurements made by the airborne data systems are used only for corroboration and cross-checking.

All altitudes presented in the data tables, in the flight description, and in the graphs are given as above ground level (AGL) unless otherwise specified.

FLIGHT C-351 – 13 JULY 1974 – DESCRIPTION OF FLIGHT AND WEATHER CHARACTERISTICS

It was a clear, sunlit morning. The flight was conducted over flat grassy prairie surrounded by thick pine woods. The data-taking for the first profile, Filter 4A, started at 1933 GMT and continued until 1956 GMT. The data-taking for the second flight profile, Filter 4B, started at 2039 GMT and continued until 2056 GMT. The sun zenith angle during sky radiance data-taking for Filter 4A was 26.6 degrees at the beginning and 25.5 degrees at the end, and for Filter 4B it was 25.5 degrees at the beginning and 26.2 degrees at the end. The maximum altitude for the Filter 4A profile was 810 meters, and the maximum altitude for the Filter 4B profile was 753 meters. Average terrain elevation was 158 meters.

The ground station reported that it was a beautiful clear day with the snowcaps on Mt. Rainier (40 miles or 64 kilometers) clearly visible.

At the beginning of the flight, McChord Air Force Base was reporting clear skies and 30-mile (48-kilometer) visibility, while Gray Army Air Field reported scattered clouds at 20 000 feet (6000 meters) and 35-mile (56-kilometer) visibility. At the end of the flight, McChord Air Force Base reported 0.1 thin scattered clouds at 25 000 feet (7500 meters) and 30-mile (48-kilometer) visibility. Gray Army Air Field reported scattered clouds at 3500 feet (1050 meters), scattered clouds at 20 000 feet (6000 meters), and 35-mile (56-kilometer) visibility.

The flight log entry was clear, low haze, with some cirrus building.

The surface charts showed that a weak ridge remained over Washington with a 1024-millibar high centered in southern British Columbia. A 1012-millibar low was situated off the West Coast centered at 44° N. 131.5° W. at 1800 GMT. This low center had an associated frontal system. At 500 millibars at 1200 GMT there was a low centered at 52° N. 140.5° W. with a trough extending southsoutheastward from the center. Winds aloft were moderate southwesterly, and the temperature had risen 7° Centigrade in 24 hours. Flow from Canada at low levels was bringing in continental polar air.

These data were taken from the 3-hourly surface facsimile charts issued by the National Meteorological Center and obtained from the Lindbergh Field NOAA office. The 500-millibar charts were for 0000 GMT and 1200 GMT, and were obtained from the same source.

FLIGHT NO. C-351

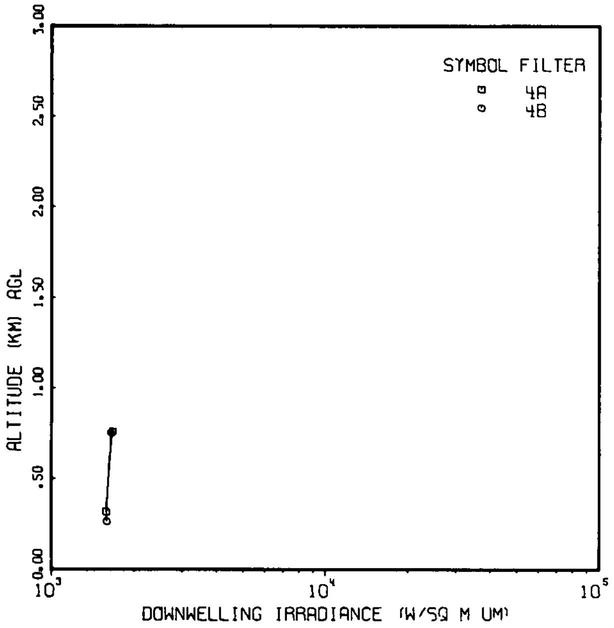

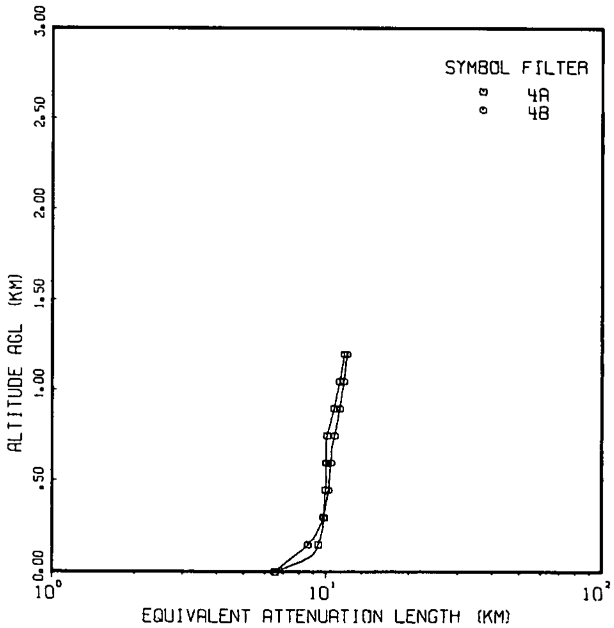

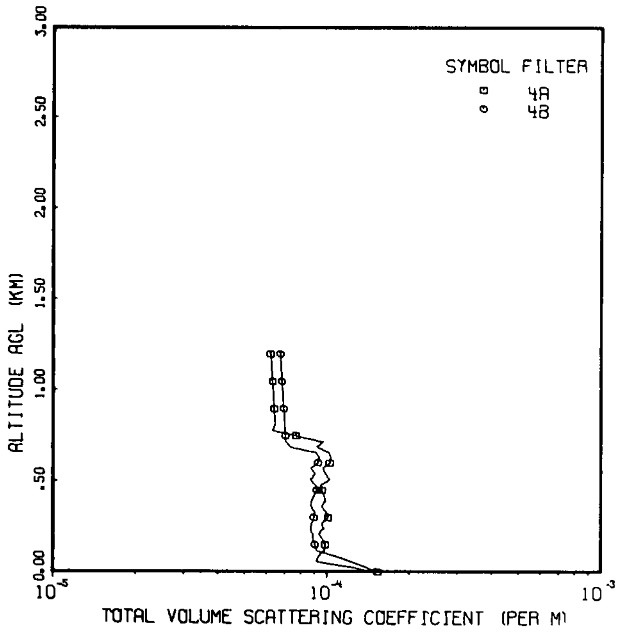

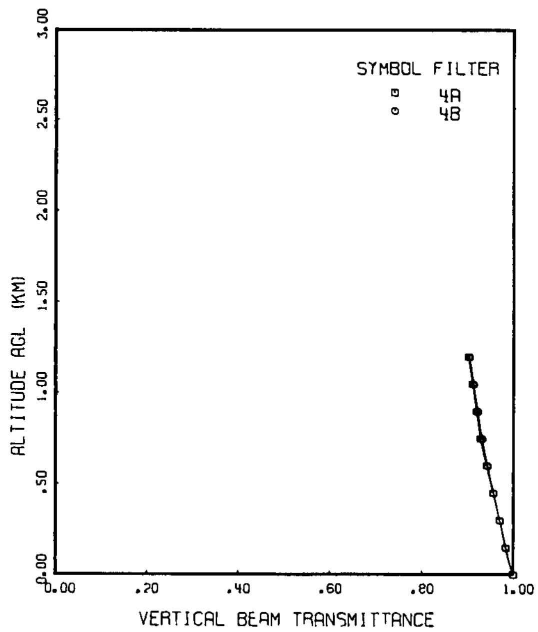

FLIGHT NO. C-351

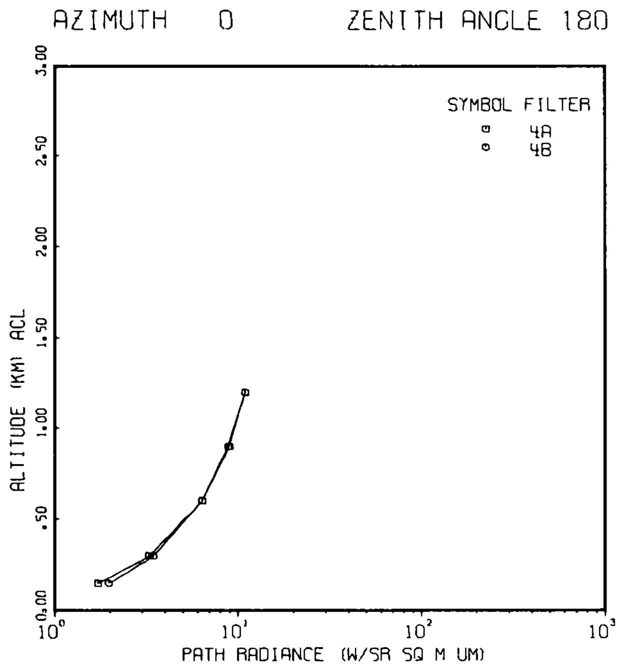

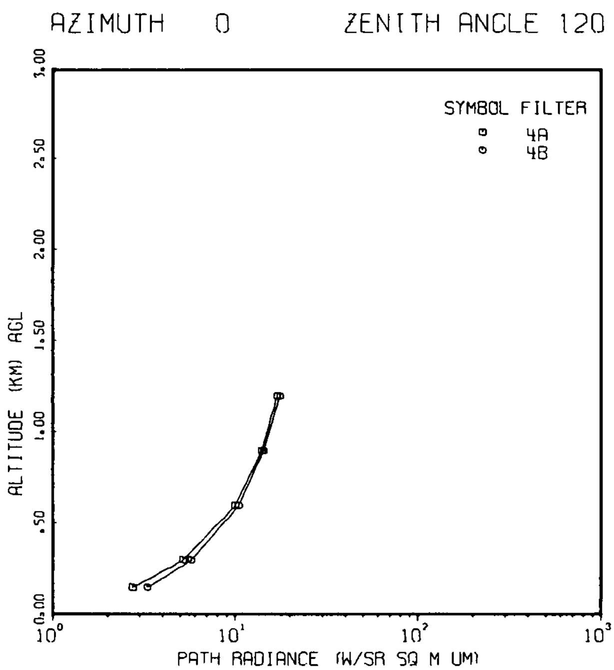

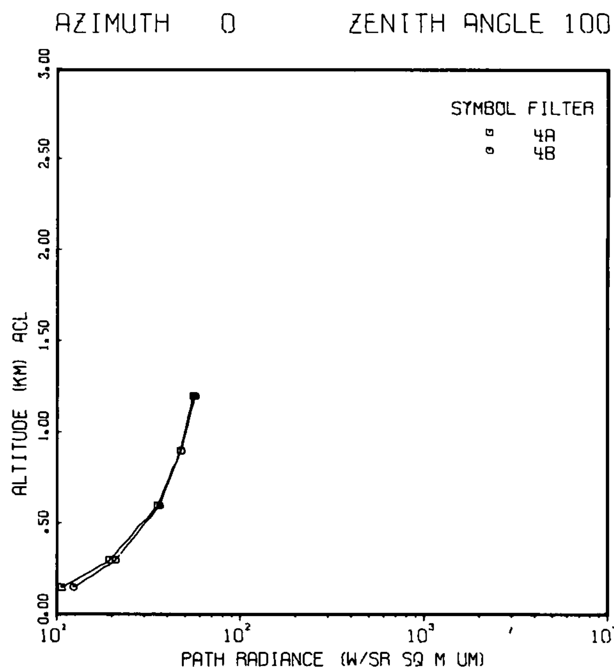

FLIGHT NO. C-351

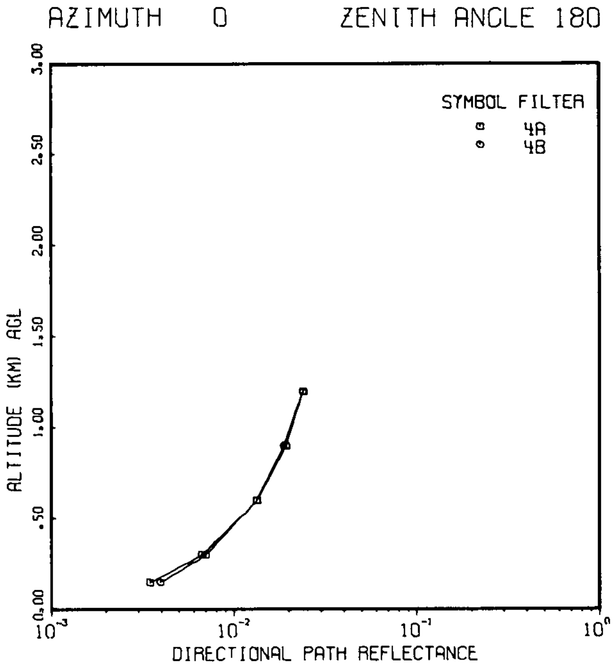

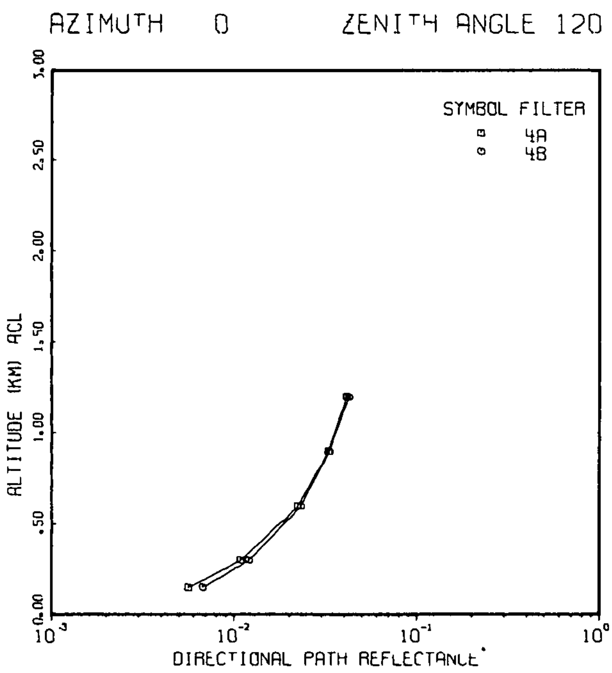

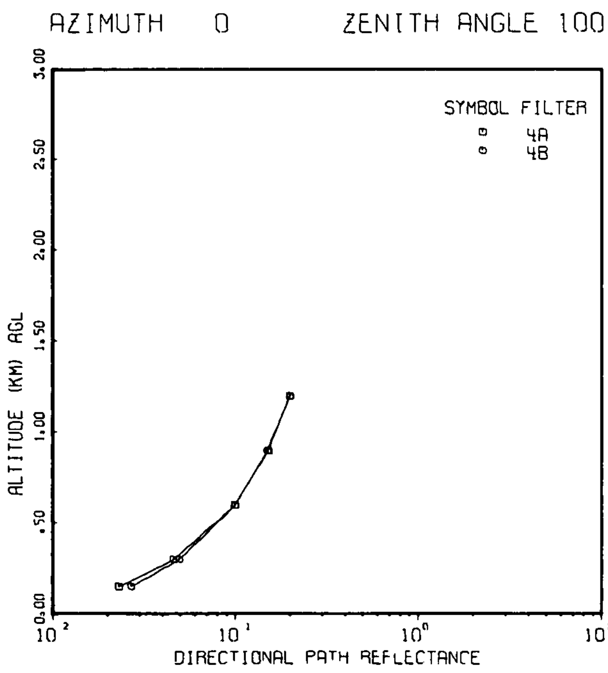

FLIGHT NO. C-351
IRRADIANCE

(JOB 5800 DATE 05/19/75)
FLIGHT NO.C-351 FILTER NO. 4A SUN ZENITH ANGLE 26.0
IRRADIANCE (W/SQ M UM)

ALTITUDE (METERS)	DOWN-WELLING	UP-WELLING	ALBEDO	SCALAR SUN	SCALAR SKY	SCALAR UPWELLING	SCALAR TOTAL	SCALAR ALBEDO
318	1.59E 03	7.74E 01	.049	1.51E 03	4.63E 02	1.66E 02	2.14E 03	.084
763	1.67E 03	8.96E 01	.054	1.58E 03	4.64E 02	1.98E 02	2.25E 03	.097

FLIGHT NO.C-351 FILTER NO. 4B SUN ZENITH ANGLE 26.0
IRRADIANCE (W/SQ M UM)

ALTITUDE (METERS)	DOWN-WELLING	UP-WELLING	ALBEDO	SCALAR SUN	SCALAR SKY	SCALAR UPWELLING	SCALAR TOTAL	SCALAR ALBEDO
266	1.59E 03	8.81E 01	.055	1.48E 03	5.22E 02	1.82E 02	2.19E 03	.091
753	1.65E 03	9.65E 01	.058	1.55E 03	4.77E 02	2.26E 02	2.26E 03	.111

FLIGHT NO. C-351
DIRECTIONAL REFLECTANCE OF TERRAIN

(JOB 5800 DATE 5/19/75)

FLIGHT NO. C-351
AZIMUTH OF PATH OF SIGHT = 0
DIRECTIONAL REFLECTANCE OF TERRAIN

ZENITH ANGLE	FILTERS 4A	4B
95	.0717	.0985
100	.0356	.0731
105	.0285	.0537
120	.0297	.0633
150	.0610	.0574
180	.0678	.0376

FLIGHT NO. C-351
AZIMUTH OF PATH OF SIGHT = 90
DIRECTIONAL REFLECTANCE OF TERRAIN

ZENITH ANGLE	FILTERS 4A	4B
95	.0733	.0596
100	.0712	.0507
105	.0748	.0490
120	.0338	.0587
150	.0580	.0493
180	.0678	.0376

FLIGHT NO. C-351
AZIMUTH OF PATH OF SIGHT = 180
DIRECTIONAL REFLECTANCE OF TERRAIN

ZENITH ANGLE	FILTERS 4A	4B
95	.0854	.0900
100	.0721	.0769
105	.0438	.0487
120	.0430	.0616
150	.0989	.0728
180	.0678	.0376

FLIGHT NO. C-351
AZIMUTH OF PATH OF SIGHT = 270
DIRECTIONAL REFLECTANCE OF TERRAIN

ZENITH ANGLE	FILTERS 4A	4B
95	.1476	.0739
100	.0461	.0622
105	.0277	.0403
120	.0266	.0816
150	.0727	.0522
180	.0678	.0376

FLIGHT NO. C-351
TOTAL VOLUME SCATTERING COEFFICIENT

(JOB 5800 DATE 05/19/75)
DATE 71374 FLIGHT NO. C-351 GROUND LEVEL ALTITUDE (M)= 158

ALTITUDE (M)	TOTAL VOLUME SCATTERING COEFFICIENT (PER M) FILTERS 4A	4B
0	1.53E-04	1,53E-04
30	1.22E-04	1,38E-04
60	9.18E-05	1,22E-04
90	9.35E-05	1,07E-04
120	9.80E-05	9,17E-05
150	9.85E-05	9,02E-05
180	9.65E-05	8,89E-05
210	9.34E-05	8,89E-05
240	9.74E-05	8,69E-05
270	9.56E-05	8,82E-05
300	1.01E-04	8,96E-05
330	9.96E-05	9,04E-05
360	9.56E-05	8,74E-05
390	9.89E-05	8.80E-05
420	9.74E-05	8,96E-05
450	9.59E-05	9,18E-05
480	9.5[illegible]E-05	9,09E-05
510	1.02E-04	8,69E-05
540	9.89E-05	9,06E-05
570	9.68E-05	8,72E-05
600	1.02E-04	9,26E-05
630	1.04E-04	9,42E-05
660	1.01E-04	9,06E-05
690	9.18E-05	7,35E-05
720	9.68E-05	7,06E-05
750	7.70E-05	7,04E-05
780	6.3[illegible]E-05	7,02E-05
810	6.45E-05	7,00E-05
840	6.43E-05	6,97E-05
870	6.41E-05	6,95E-05
900	6.39E-05	6,93E-05
930	6.37E-05	6,91E-05
960	6.36E-05	6.89E-05
990	6.34E-05	6,87E-05
1020	6.32E-05	6,85E-05
1050	6.30E-05	6,83E-05
1080	6.28E-05	6.81E-05
1110	6.26E-05	6,79E-05
1140	6.24E-05	6,77E-05
1170	6.22E-05	6,75E-05
1200	6.21E-05	6,73E-05
FIRST DATA ALT	0	0
LAST DATA ALT	810	720

FLIGHT NO. C-351
BEAM TRANSMITTANCE FROM GROUND TO ALTITUDE

(JOB 5800 DATE 05/19/75)

FLIGHT NO. C-351 FILTER NO. 4A
BEAM TRANSMITTANCE FROM GROUND TO ALTITUDE

ALTITUDE	ZENITH ANGLE OF PATH OF SIGHT (DEG)					
M	95	100	105	120	150	180
150	8.33E-01	9.12E-01	9.4[illegible]E-01	9.69E-01	9.82E-01	9.84E-01
300	7.05E-01	8.39E-01	8.89E-01	9.41E-01	9.65E-01	9.70E-01
600	5.01E-01	7.08E-01	7.93E-01	8.87E-01	9.33E-01	9.42E-01
900	3.[illegible]7E-01	6.16E-01	7.22E-01	8.45E-01	9.07E-01	9.19E-01
1200	3.02E-01	5.52E-01	6.72E-01	8.14E-01	8.88E-01	9.02E-01

FLIGHT NO. C-351 FILTER NO. 4B
BEAM TRANSMITTANCE FROM GROUND TO ALTITUDE

ALTITUDE	ZENITH ANGLE OF PATH OF SIGHT (DEG)					
M	95	100	1[illegible]5	120	150	180
150	8.19E-01	9.05E-01	9.35E-01	9.66E-01	9.80E-01	9.83E-01
300	7.02E-01	8.38E-01	8.88E-01	9.40E-01	9.65E-01	9.70E-01
600	5.15E-01	7.18E-01	8.[illegible]1E-01	8.91E-01	9.36E-01	9.44E-01
900	3.95E-01	6.30E-01	7.33E-01	8.52E-01	9.11E-01	9.23E-01
1200	3.1[illegible]E-01	5.60E-01	6.77E-01	8.17E-01	8.90E-01	9.04E-01

FLIGHT NO. C-351
PATH RADIANCE FROM GROUND TO ALTITUDE
AZIMUTH OF PATH OF SIGHT = 0

(JOB 5800 DATE 05/19/75)
AZIMUTH OF PATH OF SIGHT = 0

FLIGHT NO. C-351 FILTER NO. 4A
PATH RADIANCE FROM GROUND TO ALTITUDE (W/SR SQ M UM)

ALTITUDE	ZENITH ANGLE OF PATH OF SIGHT (DEG)					
M	95	100	105	120	150	180
150	2.30E 01	1.06E 01	6.48E 00	2.75E 00	1.52E 00	1.72E 00
300	4.06E 01	1.94E 01	1.20E 01	5.17E 00	2.87E 00	3.26E 00
600	6.86E 01	3.55E 01	2.26E 01	1.00E 01	5.61E 00	6.38E 00
900	8.57E 01	4.73E 01	3.08E 01	1.40E 01	7.89E 00	8.96E 00
1200	9.60E 01	5.55E 01	3.67E 01	1.70E 01	9.63E 00	1.09E 01

FLIGHT NO. C-351 FILTER NO. 4B
PATH RADIANCE FROM GROUND TO ALTITUDE (W/SR SQ M UM)

ALTITUDE	ZENITH ANGLE OF PATH OF SIGHT (DEG)					
M	95	100	105	120	150	180
150	2.59E 01	1.23E 01	7.60E 00	3.30E 00	1.78E 00	1.97E 00
300	4.24E 01	2.09E 01	1.31E 01	5.74E 00	3.12E 00	3.44E 00
600	6.92E 01	3.64E 01	2.33E 01	1.05E 01	5.76E 00	6.37E 00
900	8.63E 01	4.78E 01	3.12E 01	1.43E 01	7.93E 00	8.79E 00
1200	9.84E 01	5.68E 01	3.77E 01	1.76E 01	9.84E 00	1.09E 01

FLIGHT NO. C-351
PATH RADIANCE FROM GROUND TO ALTITUDE
AZIMUTH OF PATH OF SIGHT = 90

(JOB 5800 DATE 5/19/75)
AZIMUTH OF PATH OF SIGHT = 90

FLIGHT NO. C-351 FILTER NO. 4A
PATH RADIANCE FROM GROUND TO ALTITUDE (W/SR SQ M UM)

ALTITUDE	ZENITH ANGLE OF PATH OF SIGHT (DEG)					
M	95	100	105	120	150	180
150	1.64E 01	8.12E 00	5.38E 00	2.69E 00	1.75E 00	1.72E 00
300	2.88E 01	1.49E 01	9.98E 00	5.06E 00	3.31E 00	3.26E 00
600	4.87E 01	2.72E 01	1.88E 01	9.77E 00	6.47E 00	6.38E 00
900	6.13E 01	3.63E 01	2.55E 01	1.36E 01	9.09E 00	8.96E 00
1200	6.90E 01	4.26E 01	3.04E 01	1.65E 01	1.11E 01	1.09E 01

FLIGHT NO. C-351 FILTER NO. 4B
PATH RADIANCE FROM GROUND TO ALTITUDE (W/SR SQ M UM)

ALTITUDE	ZENITH ANGLE OF PATH OF SIGHT (DEG)					
M	95	100	105	120	150	180
150	1.84E 01	9.32E 00	6.19E 00	3.13E 00	2.03E 00	1.97E 00
300	3.01E 01	1.58E 01	1.06E 01	5.45E 00	3.55E 00	3.44E 00
600	4.91E 01	2.75E 01	1.90E 01	9.95E 00	6.56E 00	6.37E 00
900	6.13E 01	3.62E 01	2.54E 01	1.36E 01	9.04E 00	8.79E 00
1200	6.98E 01	4.30E 01	3.07E 01	1.67E 01	1.12E 01	1.09E 01

FLIGHT NO. C-351
PATH RADIANCE FROM GROUND TO ALTITUDE
AZIMUTH OF PATH OF SIGHT = 180

(JOB 5800 DATE 05/19/75)
AZIMUTH OF PATH OF SIGHT = 180

FLIGHT NO. C-351 FILTER NO. 4A
PATH RADIANCE FROM GROUND TO ALTITUDE (W/SR SQ M UM)

ALTITUDE	ZENITH ANGLE OF PATH OF SIGHT (DEG)					
M	95	100	105	120	150	180
150	1.59E 01	8.29E 00	5.73E 00	3.29E 00	2,46E 00	1.72E 00
300	2.80E 01	1.52E 01	1.06E 01	6.18E 00	4,65E 00	3.26E 00
600	4.76E 01	2.79E 01	2.00E 01	1.20E 01	9,09E 00	6.38E 00
900	6.02E 01	3.73E 01	2.73E 01	1.67E 01	1.28E 01	8.96E 00
1200	6.80E 01	4.39E 01	3.26E 01	2.02E 01	1.56E 01	1.09E 01

FLIGHT NO. C-351 FILTER NO. 4B
PATH RADIANCE FROM GROUND TO ALTITUDE (W/SR SQ M UM)

ALTITUDE	ZENITH ANGLE OF PATH OF SIGHT (DEG)					
M	95	100	105	120	150	180
150	1.83E 01	9.74E 00	6.74E 00	3.86E 00	2,82E 00	1,97E 00
300	3.00E 01	1.65E 01	1.16E 01	6.72E 00	4.93E 00	3,44E 00
600	4.89E 01	2.88E 01	2.06E 01	1.23E 01	9,09E 00	6,37E 00
900	6.10E 01	3.78E 01	2.76E 01	1.67E 01	1.25E 01	8.79E 00
1200	6.95E 01	4.50E 01	3.34E 01	2.06E 01	1,56E 01	1.09E 01

FLIGHT NO. C-351
PATH RADIANCE FROM GROUND TO ALTITUDE
AZIMUTH OF PATH OF SIGHT = 270

(JOB 5800 DATE 5/19/75)
AZIMUTH OF PATH OF SIGHT = 270

FLIGHT NO. C-351 FILTER NO. 4A
PATH RADIANCE FROM GROUND TO ALTITUDE (W/SR SQ M UM)

ALTITUDE M	ZENITH ANGLE OF PATH OF SIGHT (DEG) 95	100	105	120	150	180
150	1.63E 01	8.24E 0	5.33E 00	2.65E 00	1.74E 00	1.72E 00
300	2.88E 01	1.51E 01	9.89E 00	4.99E 00	3.29E 00	3.26E 00
600	4.86E 01	2.74E 01	1.86E 01	9.64E 00	6.44E 00	6.38E 00
900	6.07E 01	3.61E 01	2.52E 01	1.34E 01	9.07E 00	8.96E 00
1200	6.8[illegible]E 01	4.21E 01	3.01E 01	1.63E 01	1.11E 01	1.09E 01

FLIGHT NO. C-351 FILTER NO. 4B
PATH RADIANCE FROM GROUND TO ALTITUDE (W/SR SQ M UM)

ALTITUDE M	ZENITH ANGLE OF PATH OF SIGHT (DEG) 95	100	105	120	150	180
150	1.85E 01	9.44E 00	6.29E 00	3.19E 00	2.05E 00	1.94E 00
300	3.04E 01	1.60E 01	1.08E 01	5.55E 00	3.58E 00	3.39E 00
600	4.96E 01	2.79E 01	1.93E 01	1.01E 01	6.61E 00	6.30E 00
900	6.18E 01	3.66E 01	2.58E 01	1.38E 01	9.11E 00	8.76E 00
1200	7.05E 01	4.36E 01	3.12E 01	1.70E 01	1.13E 01	1.09E 01

FLIGHT NO. C-351
DIRECTIONAL PATH REFLECTANCE FROM GROUND TO ALTITUDE
AZIMUTH OF PATH OF SIGHT = 0

(JOB 5800 DATE 05/19/75)
AZIMUTH OF PATH OF SIGHT = 0

FLIGHT NO. C-351 FILTER NO. 4A
DIRECTIONAL PATH REFLECTANCE FROM GROUND TO ALTITUDE

ALTITUDE	ZENITH ANGLE OF PATH OF SIGHT (DEG)					
M	95	100	105	120	150	180
150	5.48E-02	2.30E-02	1.37E-02	5.62E-03	3.06E-03	3.46E-03
300	1.14E-01	4.59E-02	2.68E-02	1.09E-02	5.90E-03	6.66E-03
600	2.71E-01	9.94E-02	5.64E-02	2.24E-02	1.19E-02	1.34E-02
900	4.50E-01	1.52E-01	8.44E-02	3.28E-02	1.72E-02	1.93E-02
1200	6.30E-01	1.99E-01	1.08E-01	4.14E-02	2.15E-02	2.40E-02

FLIGHT NO. C-351 FILTER NO. 4B
DIRECTIONAL PATH REFLECTANCE FROM GROUND TO ALTITUDE

ALTITUDE	ZENITH ANGLE OF PATH OF SIGHT (DEG)					
M	95	100	105	120	150	180
150	6.23E-02	2.69E-02	1.60E-02	6.74E-03	3.59E-03	3.95E-03
300	1.19E-01	4.92E-02	2.90E-02	1.21E-02	6.38E-03	7.01E-03
600	2.65E-01	1.00E-01	5.74E-02	2.32E-02	1.21E-02	1.33E-02
900	4.32E-01	1.50E-01	8.39E-02	3.32E-02	1.72E-02	1.88E-02
1200	6.26E-01	2.00E-01	1.10E-01	4.25E-02	2.18E-02	2.38E-02

FLIGHT NO. C-351
DIRECTIONAL PATH REFLECTANCE FROM GROUND TO ALTITUDE
AZIMUTH OF PATH OF SIGHT = 90

(JOB 5800 DATE 05/19/75)
AZIMUTH OF PATH OF SIGHT = 90

FLIGHT NO. C-351 FILTER NO, 4A
DIRECTIONAL PATH REFLECTANCE FROM GROUND TO ALTITUDE

ALTITUDE	ZENITH ANGLE OF PATH OF SIGHT (DEG)					
M	95	100	105	120	150	180
150	3.89E-02	1.76E-02	1.13E-02	5.50E-03	3.53E-03	3.46E-03
300	8.08E-02	3.51E-02	2.22E-02	1.06E-02	6.79E-03	6.66E-03
600	1.93E-01	7.61E-02	4.68E-02	2.18E-02	1.37E-02	1.34E-02
900	3.22E-01	1.17E-01	7.00E-02	3.19E-02	1.99E-02	1.93E-02
1200	4.53E-01	1.53E-01	8.97E-02	4.02E-02	2.48E-02	2.40E-02

FLIGHT NO. C-351 FILTER NO, 4B
DIRECTIONAL PATH REFLECTANCE FROM GROUND TO ALTITUDE

ALTITUDE	ZENITH ANGLE OF PATH OF SIGHT (DEG)					
M	95	100	105	120	150	180
150	4.42E-02	2.03E-02	1.31E-02	6.40E-03	4.09E-03	3.95E-03
300	8.46E-02	3.73E-02	2.37E-02	1.14E-02	7.26E-03	7.01E-03
600	1.88E-01	7.57E-02	4.68E-02	2.20E-02	1.38E-02	1.33E-02
900	3.06E-01	1.13E-01	6.84E-02	3.15E-02	1.96E-02	1.88E-02
1200	4.44E-01	1.52E-01	8.95E-02	4.03E-02	2.49E-02	2.38E-02

FLIGHT NO. C-351
DIRECTIONAL PATH REFLECTANCE FROM GROUND TO ALTITUDE
AZIMUTH OF PATH OF SIGHT = 180

(JOB 5800 DATE 05/19/75)
AZIMUTH OF PATH OF SIGHT = 180

FLIGHT NO. C-351 FILTER NO. 4A
DIRECTIONAL PATH REFLECTANCE FROM GROUND TO ALTITUDE

ALTITUDE	ZENITH ANGLE OF PATH OF SIGHT (DEG)					
M	95	100	105	120	150	180
150	3.79E-02	1.80E-02	1.21E-02	6.73E-03	4.96E-03	3.46E-03
300	7.88E-02	3.59E-02	2.37E-02	1.30E-02	9.54E-03	6.66E-03
600	1.88E-01	7.80E-02	5.00E-02	2.67E-02	1.93E-02	1.34E-02
900	3.16E-01	1.20E-01	7.50E-02	3.91E-02	2.79E-02	1.93E-02
1200	4.46E-01	1.58E-01	9.63E-02	4.93E-02	3.48E-02	2.40E-02

FLIGHT NO. C-351 FILTER NO. 4B
DIRECTIONAL PATH REFLECTANCE FROM GROUND TO ALTITUDE

ALTITUDE	ZENITH ANGLE OF PATH OF SIGHT (DEG)					
M	95	100	105	120	150	180
150	4.40E-02	2.12E-02	1.42E-02	7.89E-03	5.67E-03	3.95E-03
300	8.43E-02	3.90E-02	2.57E-02	1.41E-02	1.01E-02	7.01E-03
600	1.87E-01	7.91E-02	5.09E-02	2.72E-02	1.92E-02	1.33E-02
900	3.05E-01	1.18E-01	7.44E-02	3.88E-02	2.71E-02	1.88E-02
1200	4.42E-01	1.59E-01	9.74E-02	4.97E-02	3.45E-02	2.38E-02

FLIGHT NO. C-351
DIRECTIONAL PATH REFLECTANCE FROM GROUND TO ALTITUDE
AZIMUTH OF PATH OF SIGHT = 270

(JOB 5800 DATE 5/19/75)
AZIMUTH OF PATH OF SIGHT = 270

FLIGHT NO. C-351 FILTER NO. 4A
DIRECTIONAL PATH REFLECTANCE FROM GROUND TO ALTITUDE

ALTITUDE	ZENITH ANGLE OF PATH OF SIGHT (DEG)					
M	95	100	105	120	150	180
150	3.88E-02	1.79E-02	1.12E-02	5.42E-03	3.51E-03	3.46E-03
300	8.09E-02	3.56E-02	2.20E-02	1.05E-02	6.76E-03	6.66E-03
600	1.92E-01	7.67E-02	4.64E-02	2.15E-02	1.37E-02	1.34E-02
900	3.18E-01	1.16E-01	6.92E-02	3.15E-02	1.98E-02	1.93E-02
1200	4.46E-01	1.51E-01	8.87E-02	3.97E-02	2.47E-02	2.40E-02

FLIGHT NO. C-351 FILTER NO. 4B
DIRECTIONAL PATH REFLECTANCE FROM GROUND TO ALTITUDE

ALTITUDE	ZENITH ANGLE OF PATH OF SIGHT (DEG)					
M	95	100	105	120	150	180
150	4.47E-02	2. 6E-02	1.33E-02	6.51E-03	4.12E-03	3.89E-03
300	8.54E-02	3.78E-02	2.40E-02	1.16E-02	7.33E-03	6.90E-03
600	1.90E-01	7.67E-02	4.75E-02	2.24E-02	1.39E-02	1.32E-02
900	3.09E-01	1.15E-01	6.94E-02	3.20E-02	1.97E-02	1.87E-02
120	4.49E-01	1.54E-01	9.09E-02	4.11E-02	2.51E-02	2.39E-02

FLIGHT C-352 – 14 JULY 1974 – DESCRIPTION OF FLIGHT AND WEATHER CHARACTERISTICS

It was a sunlit morning. There were scattered clouds during the first flight profile, and it was clear during the second profile. The flight was conducted over flat grassy prairie surrounded by thick pine woods. The data-taking for the first profile, Filter 4A, started at 1510 GMT and continued until 1537 GMT. The data-taking for the second flight profile, Filter 4B, started at 1707 GMT and continued until 1725 GMT. The sun zenith angle during sky radiance data-taking for Filter 4A was 65.4 degrees at the beginning and 61.1 degrees at the end, and for Filter 4B it was 45.7 degrees at the beginning and 43.0 degrees at the end. The maximum altitude for the Filter 4A profile was 937 meters, and for the Filter 4B profile it was 1020 meters. Average elevation of the terrain was 158 meters.

> The ground station reported that clouds formed in the morning around 5000 feet (1500 meters) with 30 to 40 percent sky cover. As the day progressed there was almost complete clearing by local noon.
>
> At the beginning of the flight, McChord Air Force Base was reporting 0.6 altocumulus at 10 000 feet (3000 meters) with 15-mile (24-kilometer) visibility. At the same time Gray Army Air Field recorded scattered clouds at 3500 feet (1050 meters), scattered clouds at 10 000 feet (3000 meters), and 10-mile (16-kilometer) visibility. At the end of the flight, McChord Air Force Base was reporting 0.1 altocumulus at 9000 feet (2700 meters) with 30-mile (48-kilometer) visibility; Gray Army Air Field was reporting scattered clouds at 10 000 feet (3000 meters) and 35-mile (56-kilometer) visibility.
>
> At 1533 GMT, the flight log noted scattered cumulus at approximately 4000 feet (1200 meters) and moderate haze. At 1706 GMT, the log noted light clouds at about 10 000 feet (3000 meters).

The 1200 GMT surface chart showed an occluded front approaching the Pacific coast. By 1800 GMT the front was passing over the coasts of Washington and Oregon, and had passed McChord Air Force Base at 2100 GMT. Only scattered clouds and a wind shift marked the frontal passage. At 500 millibars there was slight ridging in western Washington and Oregon which served to keep the low off the coast stationary. There were strong southwesterly winds and slowly rising temperatures at this level. The airmass was maritime polar with low-level flow from the ocean.

These data were taken from the 3-hourly surface facsimile charts issued by the National Meteorological Center and obtained from the Lindbergh Field NOAA office. The 500-millibar charts were for 0000 GMT and 1200 GMT, and were obtained from the same source.

FLIGHT NO. C-352

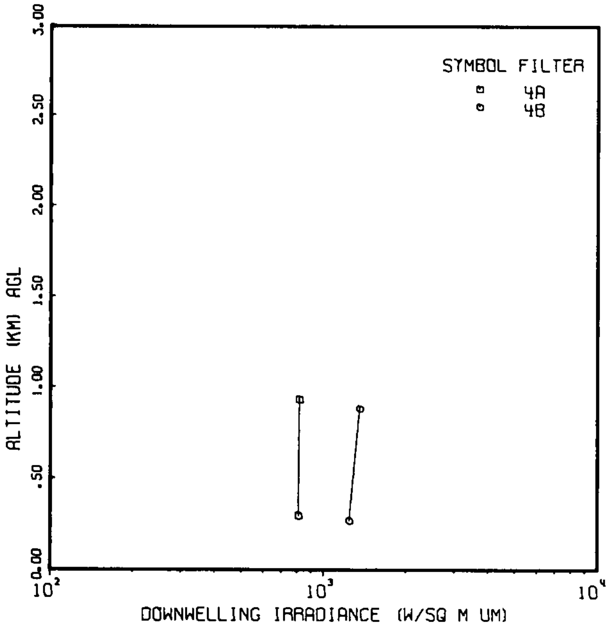

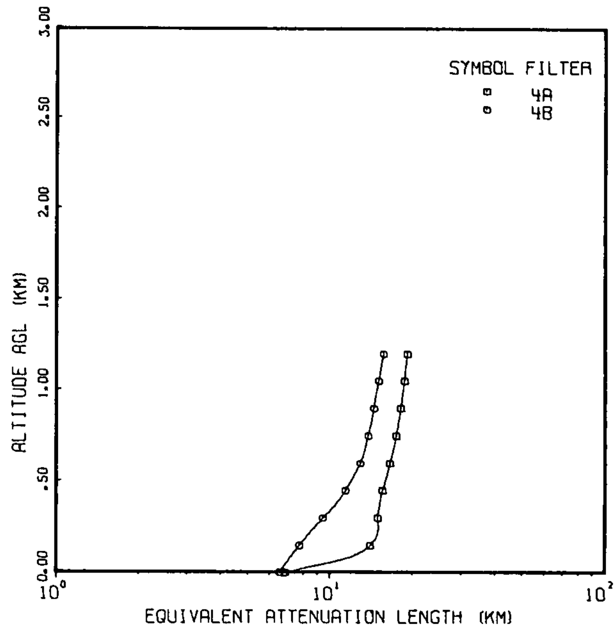

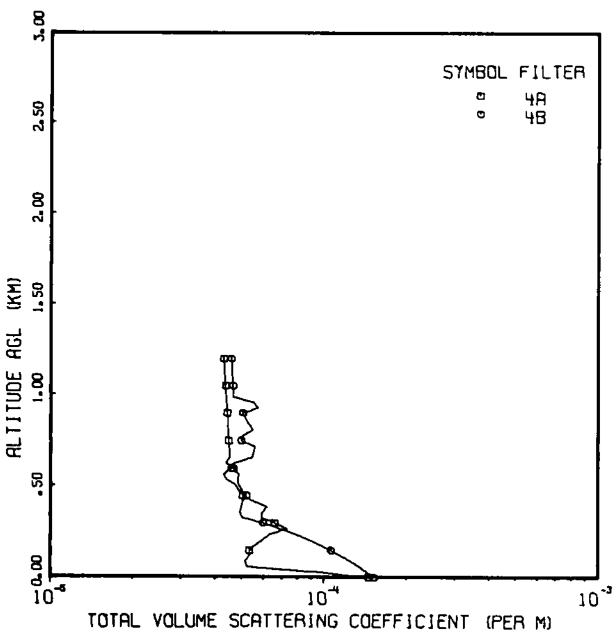

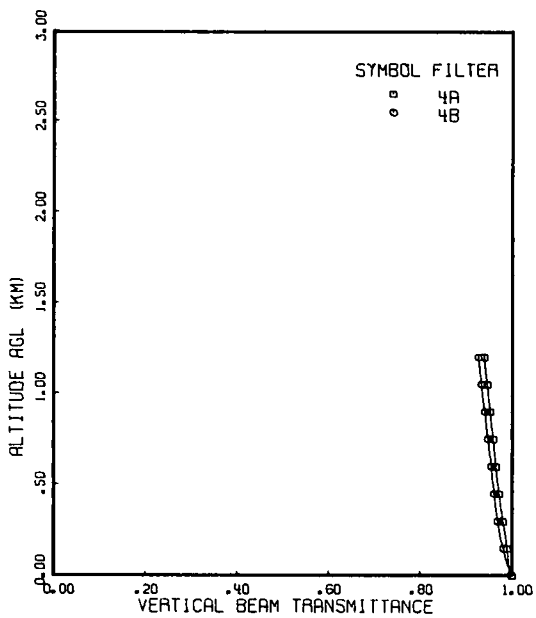

FLIGHT NO. C-352

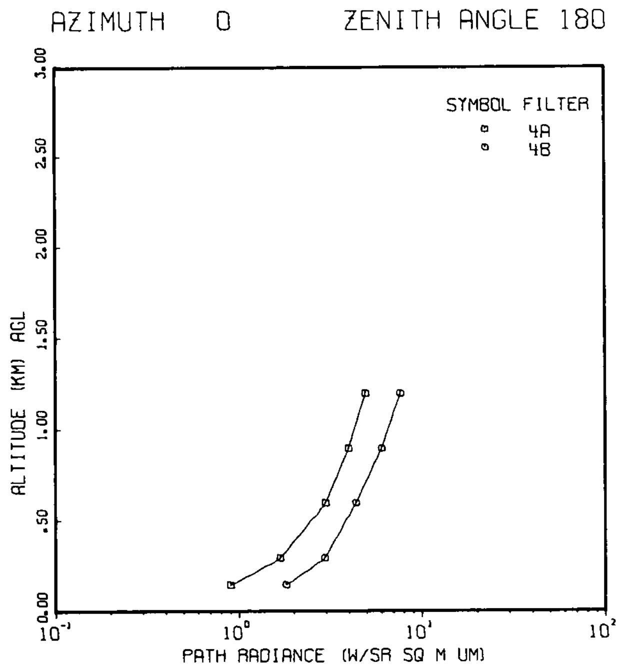

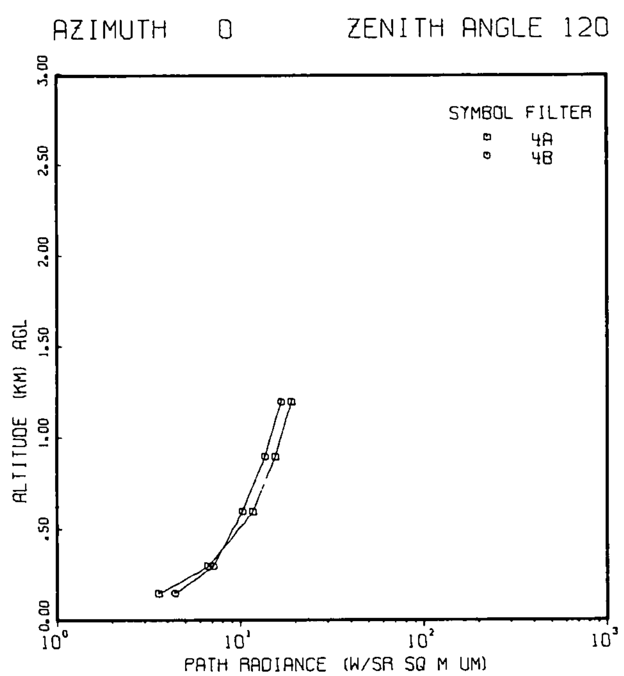

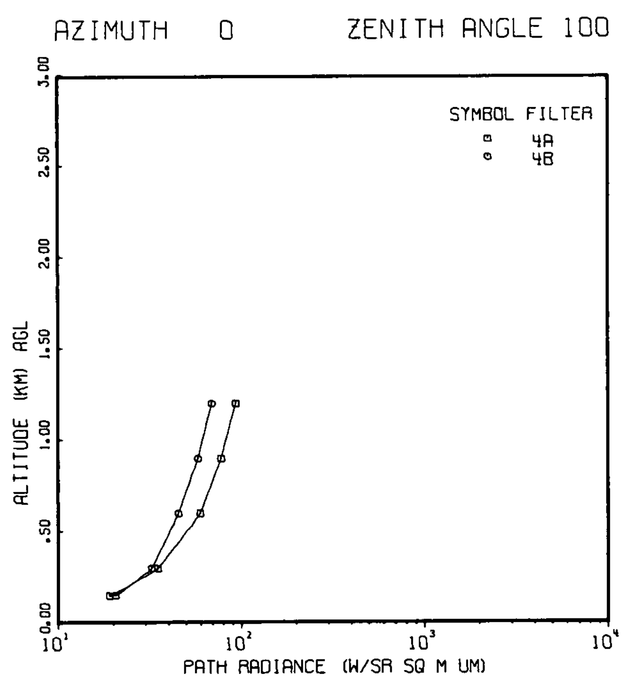

FLIGHT NO. C-352

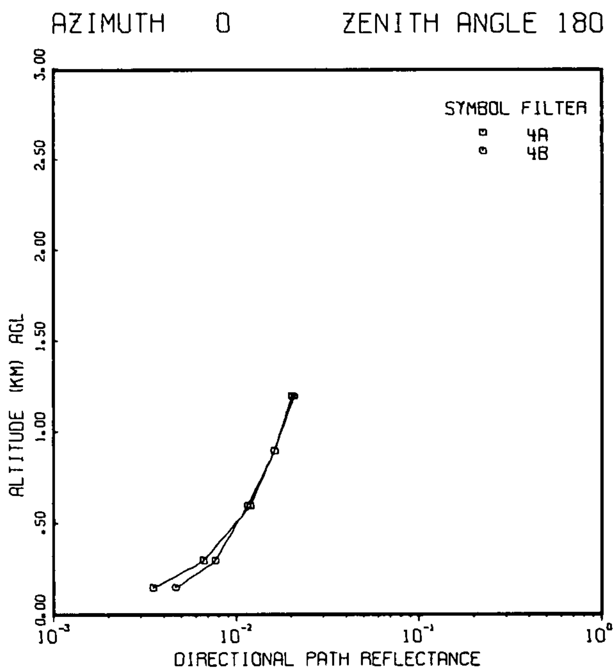

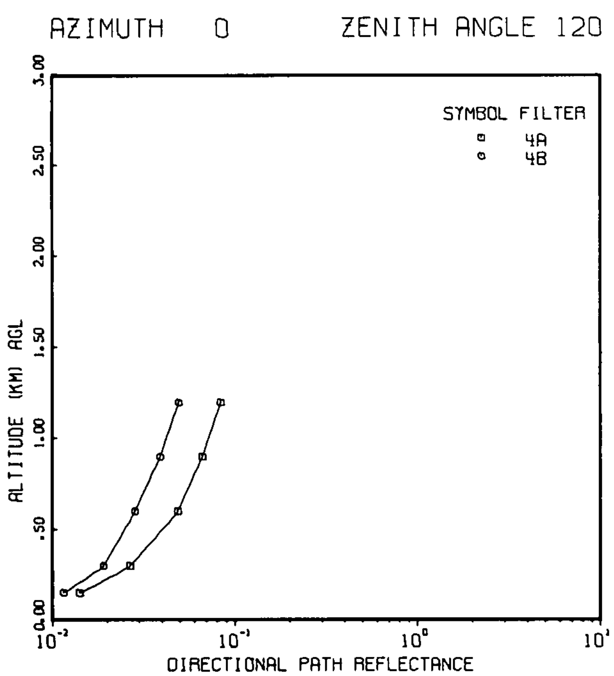

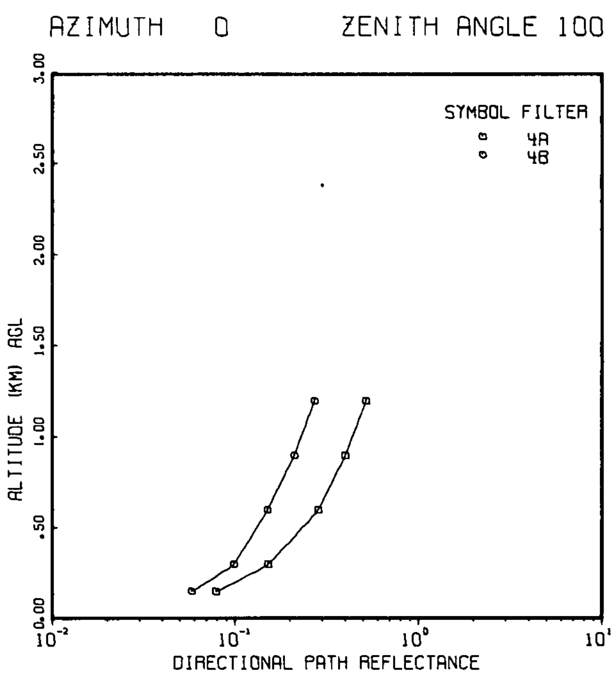

FLIGHT NO. C-352
IRRADIANCE

(JOR 4875 DATE 05/30/75)

FLIGHT NO.C-352 FILTER NO. 4A SUN ZENITH ANGLE 63.2

IRRADIANCE (W/SQ M UM)

ALTITUDE (METERS)	DOWN-WELLING	UP-WELLING	ALBEDO	SCALAR SUN	SCALAR SKY	SCALAR UPWELLING	SCALAR TOTAL	SCALAR ALBEDO
303	8.12E 02	3.76E 01	.046	1.18E 03	7.68E 02	1.03E 02	2.05E 03	.053
937	8.18E 02	5.63E 01	.069	1.25E 03	5.93E 02	1.54E 02	2.01E 03	.083

FLIGHT NO.C-352 FILTER NO. 4B SUN ZENITH ANGLE 44.4

IRRADIANCE (W/SQ M UM)

ALTITUDE (METERS)	DOWN-WELLING	UP-WELLING	ALBEDO	SCALAR SUN	SCALAR SKY	SCALAR UPWELLING	SCALAR TOTAL	SCALAR ALBEDO
272	1.24E 03	6.88E 01	.055	1.40E 03	5.92E 02	1.44E 02	2.14E 03	.072
886	1.35E 03	7.28E 1	.054	1.46E 03	6.02E 02	1.87E 02	2.25E 03	.090

FLIGHT NO. C-352
DIRECTIONAL REFLECTANCE OF TERRAIN

(JOB 4875 DATE 5/30/75)

FLIGHT NO. C-352
AZIMUTH OF PATH OF SIGHT = 0
DIRECTIONAL REFLECTANCE OF TERRAIN

ZENITH ANGLE	FILTERS 4A	4B
95	.2572	.1052
100	.0944	.0512
105	. 459	.034[illegible]
120	.0220	.0412
150	. 400	.0199
180	.0352	.0296

FLIGHT NO. C-352
AZIMUTH OF PATH OF SIGHT = 90
DIRECTIONAL REFLECTANCE OF TERRAIN

ZENITH ANGLE	FILTERS 4A	4B
95	.0578	.0567
100	.0503	.0395
105	. 500	.0294
120	.0199	.0308
150	. 436	.0459
180	. 352	.0296

FLIGHT NO. C-352
AZIMUTH OF PATH OF SIGHT = 180
DIRECTIONAL REFLECTANCE OF TERRAIN

ZENITH ANGLE	FILTERS 4A	4B
95	.1300	.1401
100	.1440	.0961
105	.1274	.0766
120	.051[illegible]	.0688
150	. 443	.0783
180	.0352	.0296

FLIGHT NO. C-352
AZIMUTH OF PATH OF SIGHT = 270
DIRECTIONAL REFLECTANCE OF TERRAIN

ZENITH ANGLE	FILTERS 4A	4B
95	.1599	.0453
100	. 653	. 316
105	.05[illegible]0	.0351
120	.0444	.024[illegible]
150	.0278	.0579
180	.0352	.0296

FLIGHT NO. C-352
TOTAL VOLUME SCATTERING COEFFICIENT

(JOB 4875 DATE 05/30/75)
DATE 71474 FLIGHT NO. C-352 GROUND LEVEL ALTITUDE (M)= 158

ALTITUDE (M)	TOTAL VOLUME SCATTERING COEFFICIENT (PER M) FILTERS 4A	4B
0	1.46E-04	1,52E-04
30	9.91E-05	1,43E-04
60	5.25E-05	1,34E-04
90	5.14E-05	1,25E-04
120	5.34E-05	1,15E-04
150	5.34E-05	1,06E-04
180	5.62E-05	9,69E-05
210	5.99E-05	8,76E-05
240	6.35E-05	7,83E-05
270	7.29E-05	6,91E-05
300	6.61E-05	5,98E-05
330	5.92E-05	5,05E-05
360	5.96E-05	4,93E-05
390	6.19E-05	5,01E-05
420	5.51E-05	5,04E-05
450	5.34E-05	5,20E-05
480	5.01E-05	4,86E-05
510	4.86E-05	4,74E-05
540	4.87E-05	4,40E-05
570	4.88E-05	4,28E-05
600	4.66E-05	4,59E-05
630	4.37E-05	4,68E-05
660	4.53E-05	5,43E-05
690	4.51E-05	5,55E-05
720	4.50E-05	5,59E-05
750	4.49E-05	4,98E-05
780	4.47E-05	5,07E-05
810	4.46E-05	5,49E-05
840	4.45E-05	5,31E-05
870	4.44E-05	5,17E-05
900	4.42E-05	5,04E-05
930	4.41E-05	5,74E-05
960	4.40E-05	5,52E-05
990	4.38E-05	4,65E-05
1020	4.37E-05	4,66E-05
1050	4.36E-05	4,65E-05
1080	4.34E-05	4,63E-05
1110	4.33E-05	4,62E-05
1140	4.32E-05	4,60E-05
1170	4.31E-05	4,59E-05
1200	4.29E-05	4,58E-05
FIRST DATA ALT	0	0
LAST DATA ALT	660	1020

FLIGHT NO. C-352
BEAM TRANSMITTANCE FROM GROUND TO ALTITUDE

(JOB 4875 DATE 05/30/75)

FLIGHT NO. C-352 FILTER NO. 4A
BEAM TRANSMITTANCE FROM GROUND TO ALTITUDE

ALTITUDE M	ZENITH ANGLE OF PATH OF SIGHT (DEG) 95	100	105	120	150	180
150	8.85E-01	9.40E-01	9.60E-01	9.79E-01	9.88E-01	9.89E-01
300	7.94E-01	8.91E-01	9.25E-01	9.61E-01	9.77E-01	9.80E-01
600	6.58E-01	8.12E-01	8.69E-01	9.30E-01	9.59E-01	9.64E-01
900	5.63E-01	7.51E-01	8.26E-01	9.06E-01	9.44E-01	9.52E-01
1200	4.83E-01	6.97E-01	7.85E-01	8.82E-01	9.30E-01	9.39E-01

FLIGHT NO. C-352 FILTER NO. 4B
BEAM TRANSMITTANCE FROM GROUND TO ALTITUDE

ALTITUDE M	ZENITH ANGLE OF PATH OF SIGHT (DEG) 95	100	105	120	150	180
150	8.00E-01	8.94E-01	9.28E-01	9.62E-01	9.78E-01	9.81E-01
300	6.93E-01	8.32E-01	8.84E-01	9.38E-01	9.64E-01	9.69E-01
600	5.84E-01	7.65E-01	8.36E-01	9.11E-01	9.48E-01	9.55E-01
900	4.87E-01	6.99E-01	7.87E-01	8.83E-01	9.31E-01	9.40E-01
1200	4.10E-01	6.43E-01	7.44E-01	8.58E-01	9.15E-01	9.26E-01

FLIGHT NO. C-352
PATH RADIANCE FROM GROUND TO ALTITUDE
AZIMUTH OF PATH OF SIGHT = 0

(JOB 4875 DATE 05/30/75)
AZIMUTH OF PATH OF SIGHT = 0

FLIGHT NO. C-352 FILTER NO. 4A
PATH RADIANCE FROM GROUND TO ALTITUDE (W/SR SQ M UM)

ALTITUDE	ZENITH ANGLE OF PATH OF SIGHT (DEG)					
M	95	100	105	120	150	180
150	4.21E 01	1.91E 01	1.09E 01	3.58E 00	1.11E 00	8.98E-01
300	7.51E 01	3.50E 01	2.01E 01	6.65E 00	2.07E 00	1.68E 00
600	1.25E 02	5.98E 01	3.50E 01	1.17E 01	3.67E 00	2.98E 00
900	1.59E 02	7.79E 01	4.61E 01	1.56E 01	4.91E 00	3.98E 00
1200	1.89E 02	9.36E 01	5.61E 01	1.91E 01	6.06E 00	4.92E 00

FLIGHT NO. C-352 FILTER NO. 4B
PATH RADIANCE FROM GROUND TO ALTITUDE (W/SR SQ M UM)

ALTITUDE	ZENITH ANGLE OF PATH OF SIGHT (DEG)					
M	95	100	105	120	150	180
150	4.46E 01	2.05E 01	1.21E 01	4.37E 00	1.87E 00	1.80E 00
300	6.85E 01	3.25E 01	1.94E 01	7.09E 00	3.04E 00	2.94E 00
600	9.27E 01	4.55E 01	2.75E 01	1.03E 01	4.46E 00	4.36E 00
900	1.15E 02	5.83E 01	3.57E 01	1.36E 01	6.06E 00	6.03E 00
1200	1.32E 02	6.91E 01	4.29E 01	1.67E 01	7.56E 00	7.64E 00

FLIGHT NO. C-352
PATH RADIANCE FROM GROUND TO ALTITUDE
AZIMUTH OF PATH OF SIGHT = 90

(JOB 4875 DATE 05/30/75)
AZIMUTH OF PATH OF SIGHT = 90

FLIGHT NO. C-352 FILTER NO. 4A
PATH RADIANCE FROM GROUND TO ALTITUDE (W/SR SQ M UM)

ALTITUDE	ZENITH ANGLE OF PATH OF SIGHT (DEG)					
M	95	100	105	120	150	180
150	1.19E 01	6.06E 00	3.97E 00	1.91E 00	1.03E 00	8.98E-01
300	2.12E 01	1.11E 01	7.33E 00	3.56E 00	1.93E 00	1.68E 00
600	3.51E 01	1.90E 01	1.28E 01	6.29E 00	3.43E 00	2.98E 00
900	4.50E 01	2.49E 01	1.69E 01	8.43E 00	4.60E 00	3.98E 00
1200	5.32E 01	3.02E 01	2.07E 01	1.04E 01	5.69E 00	4.92E 00

FLIGHT NO. C-352 FILTER NO. 4B
PATH RADIANCE FROM GROUND TO ALTITUDE (W/SR SQ M UM)

ALTITUDE	ZENITH ANGLE OF PATH OF SIGHT (DEG)					
M	95	100	105	120	150	180
150	2.05E 01	1.03E 01	6.81E 00	3.39E 00	2.00E 00	1.80E 00
300	3.14E 01	1.63E 01	1.09E 01	5.50E 00	3.25E 00	2.94E 00
600	4.28E 01	2.32E 01	1.57E 01	8.03E 00	4.79E 00	4.36E 00
900	5.37E 01	3.03E 01	2.08E 01	1.08E 01	6.57E 00	6.03E 00
1200	6.26E 01	3.66E 01	2.55E 01	1.35E 01	8.26E 00	7.64E 00

FLIGHT NO. C-352
PATH RADIANCE FROM GROUND TO ALTITUDE
AZIMUTH OF PATH OF SIGHT = 180

(JOB 4875 DATE 05/30/75)
AZIMUTH OF PATH OF SIGHT = 180

FLIGHT NO. C-352 FILTER NO. 4A
PATH RADIANCE FROM GROUND TO ALTITUDE (W/SR SQ M UM)

ALTITUDE	ZENITH ANGLE OF PATH OF SIGHT (DEG)					
M	95	100	105	120	150	180
150	1.81E 01	9.64E 01	6.83E 00	3.50E 00	1.37E 00	8.98E-01
300	3.21E 01	1.76E 01	1.26E 01	6.52E 00	2.55E 00	1.68E 00
600	5.20E 01	2.98E 01	2.16E 01	1.14E 01	4.51E 00	2.98E 00
900	6.41E 01	3.81E 01	2.78E 01	1.49E 01	6.02E 00	3.98E 00
1200	7.51E 01	4.49E 01	3.31E 01	1.80E 01	7.41E 00	4.92E 00

FLIGHT NO. C-352 FILTER NO. 4B
PATH RADIANCE FROM GROUND TO ALTITUDE (W/SR SQ M UM)

ALTITUDE	ZENITH ANGLE OF PATH OF SIGHT (DEG)					
M	95	100	105	120	150	180
150	2.41E 01	1.28E 01	8.95E 00	5.24E 00	2.86E 00	1.80E 00
300	3.68E 01	2.63E 01	1.44E 01	8.49E 00	4.67E 00	2.94E 00
600	5.05E 01	2.90E 01	2.18E 01	1.25E 01	6.98E 00	4.36E 00
900	6.41E 01	3.84E 01	2.79E 01	1.72E 01	9.83E 00	6.03E 00
1200	7.54E 01	4.68E 01	3.45E 01	2.17E 01	1.26E 01	7.64E 00

FLIGHT NO. C-352
PATH RADIANCE FROM GROUND TO ALTITUDE
AZIMUTH OF PATH OF SIGHT = 270

(JOB 4875 DATE 05/30/75)
AZIMUTH OF PATH OF SIGHT = 270

FLIGHT NO. C-352 FILTER NO. 4A
PATH RADIANCE FROM GROUND TO ALTITUDE (W/SR SQ M UM)

ALTITUDE	ZENITH ANGLE OF PATH OF SIGHT (DEG)					
M	95	100	105	120	150	180
150	1.22E 01	6.04E 00	3.99E 00	1.95E 00	1,06E 00	8,98E-01
300	2.17E 01	1.10E 01	7.36E 00	3.63E 00	1,97E 00	1,68E 00
600	3.55E 01	1.89E 01	1.28E 01	6.38E 00	3,49E 00	2,98E 00
900	4.47E 01	2.47E 01	1.69E 01	8.50E 00	4,67E 00	3,98E 00
1200	5.20E 01	2.97E 01	2.05E 01	1.04E 01	5,75E 00	4,92E 00

FLIGHT NO. C-352 FILTER NO. 4B
PATH RADIANCE FROM GROUND TO ALTITUDE (W/SR SQ M UM)

ALTITUDE	ZENITH ANGLE OF PATH OF SIGHT (DEG)					
M	95	100	105	120	150	180
150	2.01E 01	1.02E 01	6.74E 00	3.40E 00	2,02E 00	1,80E 00
300	3.08E 01	1.61E 01	1.08E 01	5.52E 00	3,30E 00	2,94E 00
600	4.20E 01	2.29E 01	1.56E 01	8.05E 00	4.86E 00	4,36E 00
900	5.30E 01	3.10E 01	2.07E 01	1,09E 01	6,65E 00	6,03E 00
1200	6.19E 01	3.63E 01	2.54E 01	1,35E 01	8.35E 00	7,64E 00

FLIGHT NO. C-352
DIRECTIONAL PATH REFLECTANCE FROM GROUND TO ALTITUDE
AZIMUTH OF PATH OF SIGHT = 0

(JOB 4875 DATE 5/30/75)
AZIMUTH OF PATH OF SIGHT = 0

FLIGHT NO. C-352 FILTER NO. 4A
DIRECTIONAL PATH REFLECTANCE FROM GROUND TO ALTITUDE

ALTITUDE	ZENITH ANGLE OF PATH OF SIGHT (DEG)					
M	95	100	105	120	150	180
150	1.84E-01	7.87E-02	4.40E-02	1.41E-02	4.34E-03	3.51E-03
300	3.66E-01	1.52E-01	8.41E-02	2.68E-02	8.19E-03	6.62E-03
600	7.32E-01	2.85E-01	1.56E-01	4.87E-02	1.48E-02	1.19E-02
900	1.10E 00	4.01E-01	2.16E-01	6.64E-02	2.01E-02	1.62E-02
1200	1.51E 00	5.19E-01	2.76E-01	8.36E-02	2.52E-02	2.03E-02

FLIGHT NO. C-352 FILTER NO. 4B
DIRECTIONAL PATH REFLECTANCE FROM GROUND TO ALTITUDE

ALTITUDE	ZENITH ANGLE OF PATH OF SIGHT (DEG)					
M	95	100	105	120	150	180
150	1.41E-01	5.79E-02	3.29E-02	1.15E-02	4.82E-03	4.65E-03
300	2.50E-01	9.86E-02	5.54E-02	1.91E-02	7.98E-03	7.68E-03
600	4.01E-01	1.50E-01	8.32E-02	2.85E-02	1.19E-02	1.16E-02
900	5.95E-01	2.11E-01	1.15E-01	3.90E-02	1.65E-02	1.62E-02
1200	8.11E-01	2.72E-01	1.46E-01	4.93E-02	2.09E-02	2.08E-02

FLIGHT NO. C-352
DIRECTIONAL PATH REFLECTANCE FROM GROUND TO ALTITUDE
AZIMUTH OF PATH OF SIGHT = 90

(JOB 4875 DATE 05/30/75)
AZIMUTH OF PATH OF SIGHT = 90

FLIGHT NO. C-352 FILTER NO. 4A
DIRECTIONAL PATH REFLECTANCE FROM GROUND TO ALTITUDE

ALTITUDE	ZENITH ANGLE OF PATH OF SIGHT (DEG)					
M	95	100	105	120	150	180
150	5.20E-02	2.49E-02	1.60E-02	7.56E-03	4.05E-03	3.51E-03
300	1.03E-01	4.81E-02	3.06E-02	1.43E-02	7.64E-03	6.62E-03
600	2.06E-01	9.07E-02	5.68E-02	2.62E-02	1.38E-02	1.19E-02
900	3.09E-01	1.28E-01	7.93E-02	3.60E-02	1.88E-02	1.62E-02
1200	4.27E-01	1.68E-01	1.02E-01	4.57E-02	2.37E-02	2.03E-02

FLIGHT NO. C-352 FILTER NO. 4B
DIRECTIONAL PATH REFLECTANCE FROM GROUND TO ALTITUDE

ALTITUDE	ZENITH ANGLE OF PATH OF SIGHT (DEG)					
M	95	100	105	120	150	180
150	6.48E-02	2.91E-02	1.85E-02	8.91E-03	5.16E-03	4.65E-03
300	1.14E-01	4.96E-02	3.12E-02	1.48E-02	8.53E-03	7.68E-03
600	1.85E-01	7.65E-02	4.75E-02	2.23E-02	1.28E-02	1.16E-02
900	2.79E-01	1.10E-01	6.70E-02	3.10E-02	1.78E-02	1.62E-02
1200	3.86E-01	1.44E-01	8.67E-02	3.97E-02	2.28E-02	2.08E-02

FLIGHT NO. C-352
DIRECTIONAL PATH REFLECTANCE FROM GROUND TO ALTITUDE
AZIMUTH OF PATH OF SIGHT = 180

(JOB 4875 DATE 05/30/75)
AZIMUTH OF PATH OF SIGHT = 180

FLIGHT NO. C-352 FILTER NO. 4A
DIRECTIONAL PATH REFLECTANCE FROM GROUND TO ALTITUDE

ALTITUDE	ZENITH ANGLE OF PATH OF SIGHT (DEG)					
M	95	100	105	120	150	180
150	7.90E-02	3.96E-02	2.75E-02	1.38E-02	5.35E-03	3.51E-03
300	1.57E-01	7.65E-02	5.26E-02	2.62E-02	1.01E-02	6.62E-03
600	3.05E-01	1.42E-01	9.61E-02	4.73E-02	1.82E-02	1.19E-02
900	4.40E-01	1.96E-01	1.30E-01	6.37E-02	2.47E-02	1.62E-02
1200	5.86E-01	2.49E-01	1.63E-01	7.91E-02	3.08E-02	2.03E-02

FLIGHT NO. C-352 FILTER NO. 4B
DIRECTIONAL PATH REFLECTANCE FROM GROUND TO ALTITUDE

ALTITUDE	ZENITH ANGLE OF PATH OF SIGHT (DEG)					
M	95	100	105	120	150	180
150	7.60E-02	3.62E-02	2.44E-02	1.38E-02	7.40E-03	4.65E-03
300	1.34E-01	6.17E-02	4.10E-02	2.29E-02	1.22E-02	7.68E-03
600	2.18E-01	9.57E-02	6.28E-02	3.47E-02	1.86E-02	1.16E-02
900	3.33E-01	1.39E-01	8.98E-02	4.93E-02	2.67E-02	1.62E-02
1200	4.65E-01	1.84E-01	1.17E-01	6.40E-02	3.48E-02	2.08E-02

FLIGHT NO. C-352
DIRECTIONAL PATH REFLECTANCE FROM GROUND TO ALTITUDE
AZIMUTH OF PATH OF SIGHT = 270

(JOB 4875 DATE 05/30/75)
AZIMUTH OF PATH OF SIGHT = 270

FLIGHT NO. C-352 FILTER NO. 4A
DIRECTIONAL PATH REFLECTANCE FROM GROUND TO ALTITUDE

ALTITUDE	ZENITH ANGLE OF PATH OF SIGHT (DEG)					
M	95	100	105	120	150	180
150	5.34E-02	2.49E-02	1.61E-02	7.70E-03	4.14E-03	3.51E-03
300	1.06E-01	4.79E-02	3.08E-02	1.46E-02	7.81E-03	6.62E-03
600	2.09E-01	9.02E-02	5.69E-02	2.66E-02	1.41E-02	1.19E-02
900	3.07E-01	1.27E-01	7.90E-02	3.63E-02	1.91E-02	1.62E-02
1200	4.16E-01	1.65E-01	1.01E-01	4.58E-02	2.39E-02	2.03E-02

FLIGHT NO. C-352 FILTER NO. 4B
DIRECTIONAL PATH REFLECTANCE FROM GROUND TO ALTITUDE

ALTITUDE	ZENITH ANGLE OF PATH OF SIGHT (DEG)					
M	95	100	105	120	150	180
150	6.35E-02	2.87E-02	1.84E-02	8.93E-03	5.23E-03	4.65E-03
300	1.12E-01	4.89E-02	3.09E-02	1.49E-02	8.65E-03	7.68E-03
600	1.82E-01	7.55E-02	4.71E-02	2.23E-02	1.30E-02	1.16E-02
900	2.75E-01	1.08E-01	6.66E-02	3.12E-02	1.81E-02	1.62E-02
1200	3.82E-01	1.43E-01	8.64E-02	3.99E-02	2.31E-02	2.08E-02

FLIGHT C-354 – 16 JULY 1974 – DESCRIPTION OF FLIGHT AND WEATHER CHARACTERISTICS

It was an overcast morning. The sun was generally not visible through the clouds. The flight was conducted over flat grassy prairie surrounded by thick pine woods. The data-taking for the first flight profile, Filter 4A, started at 1748 GMT and continued until 1805 GMT. The data-taking for the second flight profile, Filter 4B, started at 1901 GMT and continued until 1922 GMT. The sun zenith angle during sky radiance data-taking for Filter 4A was 39.4 degrees at the beginning and 37.2 degrees at the end, and for Filter 4B it was 29.8 degrees at the beginning and 28.7 degrees at the end. The maximum altitude for the Filter 4A profile was 936 meters, and for the Filter 4B profile it was 973 meters. Average elevation of terrain was 158 meters.

> The ground station reported complete overcast. There were broken clouds at low altitudes with high overcast above. There was some light rain about 2022 GMT.
>
> At the beginning of the flight, McChord Air Force Base was reporting scattered altocumulus clouds at 7000 feet (2100 meters) and overcast altocumulus estimated at 11 000 feet (3300 meters), with a visibility of 15 miles (24 kilometers). At the same time, Gray Army Air Field was reporting broken clouds estimated at 6000 feet (1800 meters) and overcast at 10 000 feet (3000 meters) with 10-mile (16-kilometer) visibility. At the end of the flight, McChord Air Force Base was reporting broken altocumulus estimated at 6000 feet (1800 meters) and overcast altocumulus at 10 000 feet (3000 meters), with a visibility of 7 miles (11.2 kilometers). At this time, Gray Army Air Field reported similar conditions and, in addition, a light rain shower.
>
> The flight log entry read full overcast, clear below, light horizon haze, with visibility greater than 20 miles (32 kilometers).

The surface charts showed a weakening in the ridging along the coast with an approaching frontal system in the western Pacific. At 500 millibars there was a low centered over Queen Charlotte Islands with a trough southward. There was also a high centered in the Texas Panhandle with ridging northward to Saskatchewan. The winds were moderate southwesterly. The airmass was maritime polar.

These data were taken from the 3-hourly surface facsimile charts issued by the National Meteorological Center and obtained from the Lindbergh Field NOAA office. The 500-millibar charts were for 0000 GMT and 1200 GMT, and were obtained from the same source.

FLIGHT NO. C-354

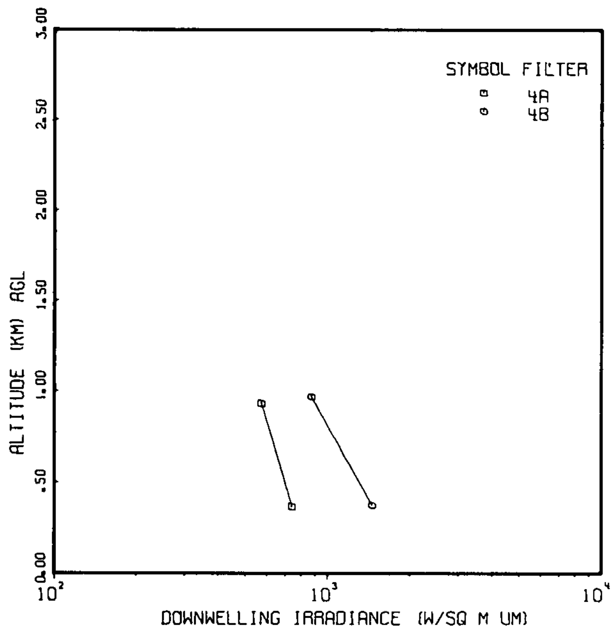

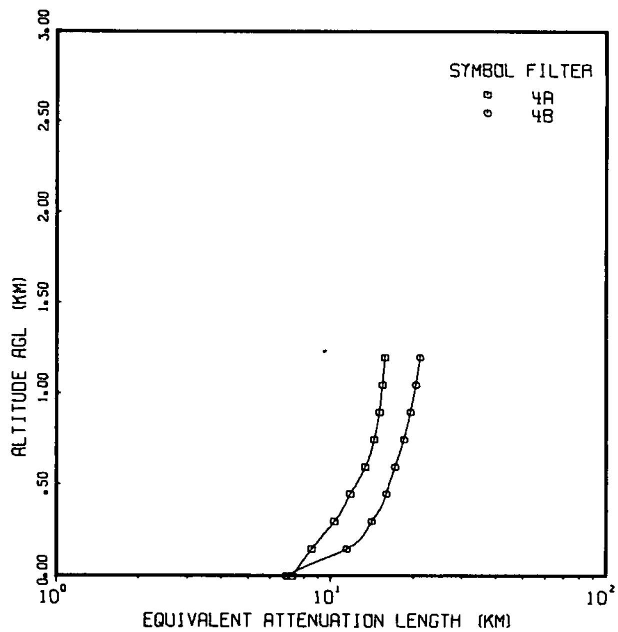

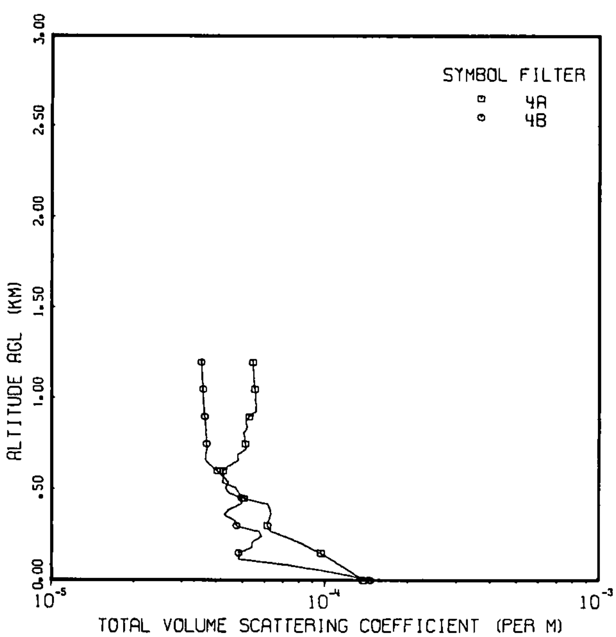

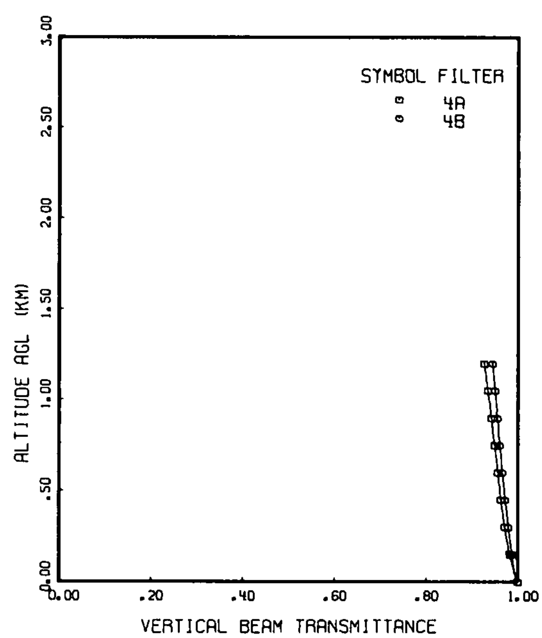

FLIGHT NO. C-354

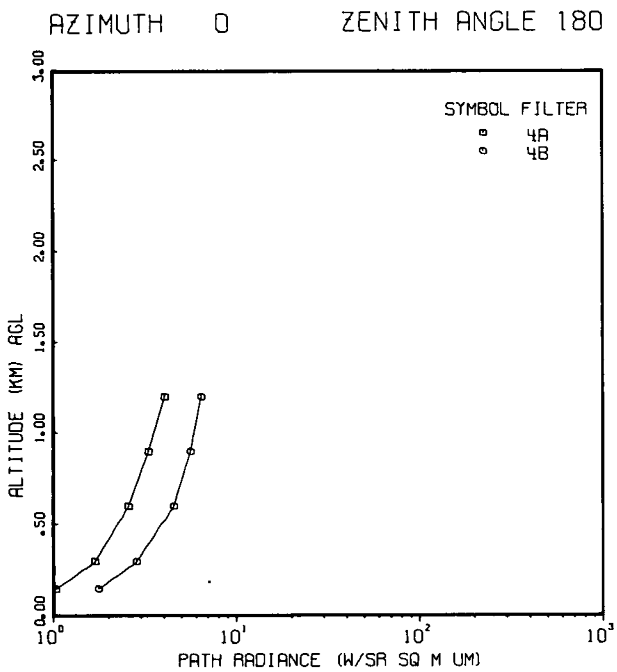

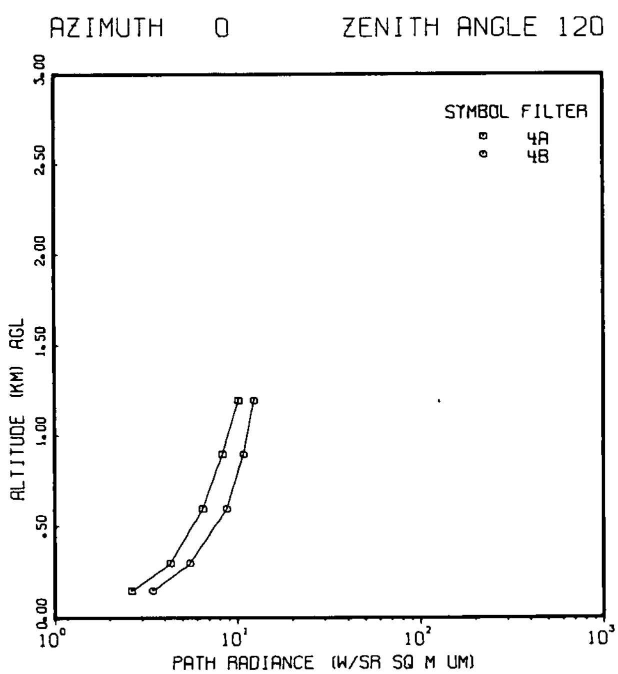

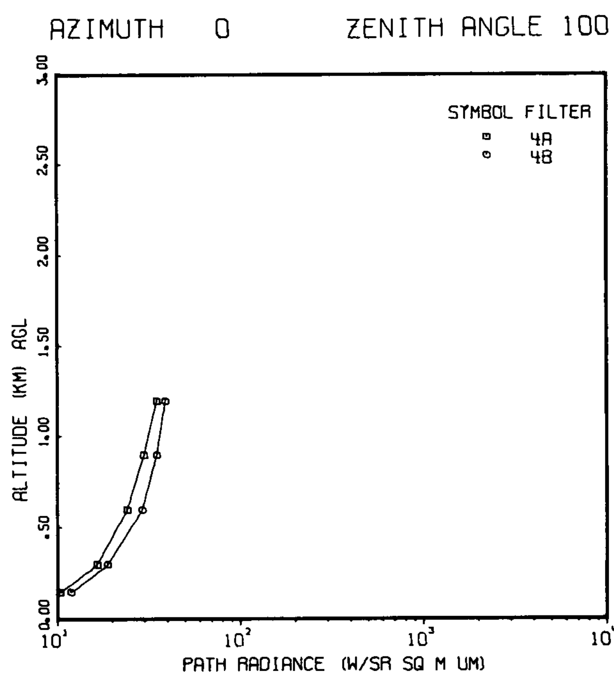

FLIGHT NO. C-354

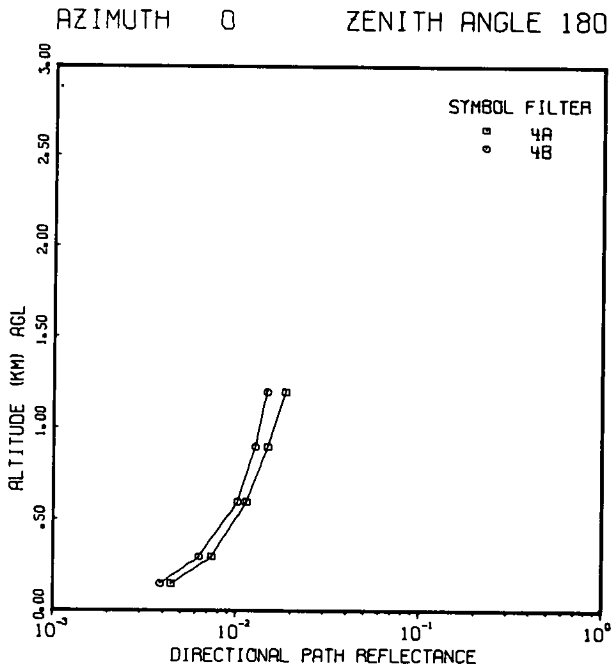

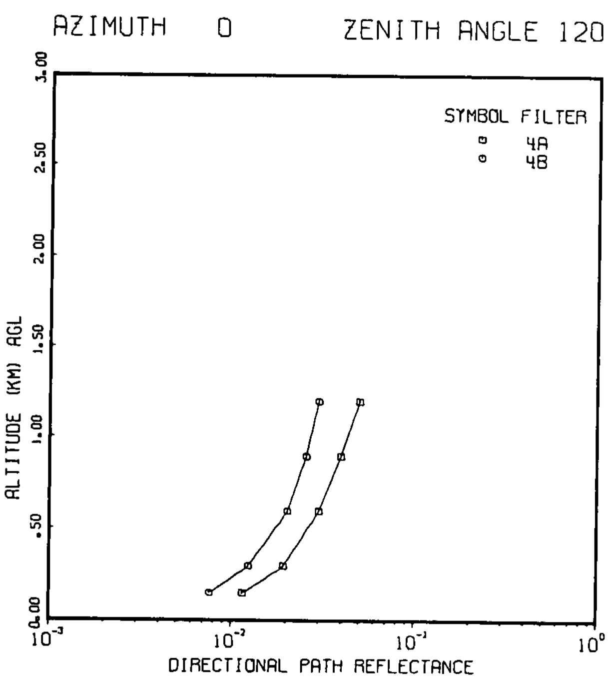

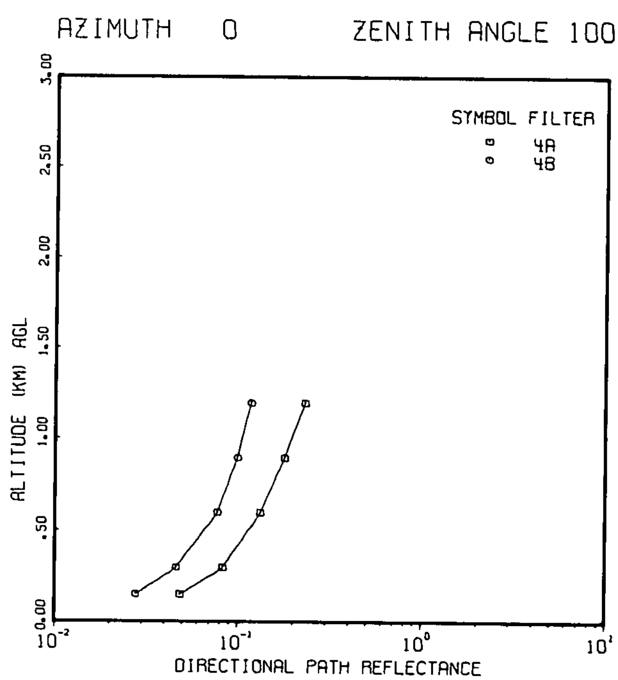

FLIGHT NO. C-354
IRRADIANCE

(JOB 5810 DATE 05/21/75)

FLIGHT NO.C-354 FILTER NO. 4A SUN ZENITH ANGLE 38.3

IRRADIANCE (W/SQ M UM)

ALTITUDE (METERS)	DOWN- WELLING	UP- WELLING	ALBEDO	SCALAR SUN	SCALAR SKY	SCALAR UPWELLING	SCALAR TOTAL	SCALAR ALBEDO
369	7.40E 02	2.56E 01	.035		1.36E 03	5.97E 01	1.42E 03	.044
936	5.73E 02	2.70E 01	.047		1.13E 03	7.38E 01	1.20E 03	.065

FLIGHT NO.C-354 FILTER NO. 4B SUN ZENITH ANGLE 29.3

IRRADIANCE (W/SQ M UM)

ALTITUDE (METERS)	DOWN- WELLING	UP- WELLING	ALBEDO	SCALAR SUN	SCALAR SKY	SCALAR UPWELLING	SCALAR TOTAL	SCALAR ALBEDO
375	1.45E 03	6.05E 01	.042		2.29E 03	1.22E 02	2.41E 03	.053
973	8.73E 02	3.75E 01	.043		1.42E 03	9.61E 01	1.52E 03	.068

FLIGHT NO. C-354
DIRECTIONAL REFLECTANCE OF TERRAIN

(JOB 5810 DATE 05/21/75)

FLIGHT NO. C-354
AZIMUTH OF PATH OF SIGHT = 0
DIRECTIONAL REFLECTANCE OF TERRAIN

ZENITH ANGLE	FILTERS 4A	4B
95	.0794	.0588
100	.0867	.0462
105	.0378	.0256
120	.0302	.0430
150	.0255	.0457
180	.0533	.0257

FLIGHT NO. C-354
AZIMUTH OF PATH OF SIGHT = 90
DIRECTIONAL REFLECTANCE OF TERRAIN

ZENITH ANGLE	FILTERS 4A	4B
95	.0754	.0731
100	.0522	.0349
105	.0490	.0388
120	.0453	.0500
150	.0240	.0480
180	.0533	.0257

FLIGHT NO. C-354
AZIMUTH OF PATH OF SIGHT = 180
DIRECTIONAL REFLECTANCE OF TERRAIN

ZENITH ANGLE	FILTERS 4A	4B
95	.0613	.0684
100	.0611	.0373
105	.0589	.0263
120	.0335	.0546
150	.0253	.0691
180	.0533	.0257

FLIGHT NO. C-354
AZIMUTH OF PATH OF SIGHT = 270
DIRECTIONAL REFLECTANCE OF TERRAIN

ZENITH ANGLE	FILTERS 4A	4B
95	.0583	.0453
100	.0425	.0271
105	.0386	.0202
120	.0309	.0396
150	.0248	.0374
180	.0533	.0257

FLIGHT NO. C-354
TOTAL VOLUME SCATTERING COEFFICIENT

(JOB 5810 DATE 05/21/75)
DATE 71674 FLIGHT NO. C-354 GROUND LEVEL ALTITUDE (M)= 158

ALTITUDE (M)	TOTAL VOLUME SCATTERING COEFFICIENT (PER M) FILTERS 4A	4B
0	1.38E-04	1.46E-04
30	1.30E-04	1.22E-04
60	1.21E-04	9.71E-05
90	1.13E-04	7.27E-05
120	1.05E-04	4.83E-05
150	9.66E-05	4.83E-05
180	8.83E-05	5.41E-05
210	8.00E-05	5.45E-05
240	7.17E-05	5.86E-05
270	6.34E-05	5.72E-05
300	6.16E-05	4.75E-05
330	6.24E-05	4.69E-05
360	6.34E-05	4.27E-05
390	6.30E-05	4.48E-05
420	6.16E-05	4.95E-05
450	5.04E-05	4.96E-05
480	4.46E-05	4.84E-05
510	4.32E-05	4.72E-05
540	4.46E-05	4.22E-05
570	4.25E-05	4.26E-05
600	4.24E-05	4.04E-05
630	4.48E-05	3.82E-05
660	4.83E-05	3.66E-05
690	4.79E-05	3.66E-05
720	5.13E-05	3.70E-05
750	5.11E-05	3.69E-05
780	5.11E-05	3.68E-05
810	5.04E-05	3.67E-05
840	5.23E-05	3.66E-05
870	5.13E-05	3.65E-05
900	5.28E-05	3.64E-05
930	5.60E-05	3.63E-05
960	5.58E-05	3.62E-05
990	5.57E-05	3.61E-05
1020	5.55E-05	3.60E-05
1050	5.53E-05	3.59E-05
1080	5.52E-05	3.58E-05
1110	5.50E-05	3.56E-05
1140	5.48E-05	3.55E-05
1170	5.47E-05	3.54E-05
1200	5.45E-05	3.53E-05

FIRST DATA ALT 0 0

LAST DATA ALT 930 720

FLIGHT NO. C-354
BEAM TRANSMITTANCE FROM GROUND TO ALTITUDE

(JOB 5810 DATE 05/21/75)

FLIGHT NO. C-354 FILTER NO. 4A
BEAM TRANSMITTANCE FROM GROUND TO ALTITUDE

ALTITUDE	ZENITH ANGLE OF PATH OF SIGHT (DEG)					
M	95	100	105	120	150	180
150	8.17E-01	9.04E-01	9.34E-01	9.65E-01	9.80E-01	9.83E-01
300	7.16E-01	8.46E-01	8.94E-01	9.44E-01	9.67E-01	9.71E-01
600	5.95E-01	7.72E-01	8.41E-01	9.14E-01	9.49E-01	9.56E-01
900	5.00E-01	7.09E-01	7.94E-01	8.87E-01	9.33E-01	9.42E-01
1200	4.12E-01	6.44E-01	7.45E-01	8.58E-01	9.16E-01	9.27E-01

FLIGHT NO. C-354 FILTER NO. 4B
BEAM TRANSMITTANCE FROM GROUND TO ALTITUDE

ALTITUDE	ZENITH ANGLE OF PATH OF SIGHT (DEG)					
M	95	100	105	120	150	180
150	8.60E-01	9.27E-01	9.51E-01	9.74E-01	9.85E-01	9.87E-01
300	7.83E-01	8.85E-01	9.21E-01	9.58E-01	9.76E-01	9.79E-01
600	6.67E-01	8.17E-01	8.73E-01	9.32E-01	9.60E-01	9.66E-01
900	5.86E-01	7.67E-01	8.37E-01	9.12E-01	9.48E-01	9.55E-01
1200	5.16E-01	7.21E-01	8.03E-01	8.92E-01	9.36E-01	9.45E-01

FLIGHT NO. C-354
PATH RADIANCE FROM GROUND TO ALTITUDE
AZIMUTH OF PATH OF SIGHT = 0

(J08 5810 DATE 05/21/75)
AZIMUTH OF PATH OF SIGHT = 0

FLIGHT NO. C-354 FILTER NO. 4A
PATH RADIANCE FROM GROUND TO ALTITUDE (W/SR SQ M UM)

ALTITUDE	ZENITH ANGLE OF PATH OF SIGHT (DEG)					
M	95	1C0	105	120	150	180
150	2.20E 01	1.03E 01	6.38E 00	2.63E 00	1.21E 00	1.03E 00
300	3.41E C1	1.65E 01	1.03E 01	4.29E 00	1.99E 00	1.69E 00
600	4.77E 01	2.41E 01	1.53E 01	6.48E 00	3.02E 00	2.58E 00
900	5.63E 01	2.98E 01	1.92E 01	8.29E 00	3.90E 00	3.31E 00
1200	6.30E 01	3.50E 01	2.30E 01	1.01E 01	4.80E 00	4.07E 00

FLIGHT NO. C-354 FILTER NO. 4B
PATH RADIANCE FROM GROUND TO ALTITUDE (W/SR SQ M UM)

ALTITUDE	ZENITH ANGLE OF PATH OF SIGHT (DEG)					
M	95	1C0	105	120	150	180
150	2.51E 01	1.19E 01	7.54E 00	3.42E 00	1.86E 00	1.77E 00
300	3.89E 01	1.89E 01	1.21E 01	5.50E 00	3.01E 00	2.85E 00
600	5.77E 01	2.92E 01	1.89E 01	8.75E 00	4.82E 00	4.56E 00
900	6.69E 01	3.51E 01	2.30E 01	1.08E 01	5.97E 00	5.63E 00
1200	7.18E 01	3.91E 01	2.60E 01	1.24E 01	6.87E 00	6.44E 00

FLIGHT NO. C-354
PATH RADIANCE FROM GROUND TO ALTITUDE
AZIMUTH OF PATH OF SIGHT = 90

(JOB 5810 CATE 05/21/75)
AZIMUTH OF PATH OF SIGHT = 90

FLIGHT NO. C-354 FILTER NO. 4A
PATH RADIANCE FROM GROUND TO ALTITUDE (W/SR SQ M UM)

ALTITUDE	ZENITH ANGLE OF PATH OF SIGHT (DEG)					
M	95	1C0	105	120	150	180
150	1.73E 01	8.44E 00	5.49E 00	2.45E 00	1.23E 00	1.03E 00
300	2.69E 01	1.35E 01	8.87E 00	4.01E 00	2.02E 00	1.69E 00
600	3.83E 01	2.00E 01	1.33E 01	6.06E 00	3.06E 00	2.58E 00
900	4.73E C1	2.55E 01	1.70E 01	7.83E 00	3.94E 00	3.31E 00
1200	5.57E 01	3.12E 01	2.09E 01	9.66E 00	4.83E 00	4.07E 00

FLIGHT NO. C-354 FILTER NO. 4B
PATH RADIANCE FROM GROUND TO ALTITUDE (W/SR SQ M UM)

ALTITUDE	ZENITH ANGLE OF PATH OF SIGHT (DEG)					
M	95	1C0	105	120	150	180
150	2.22E 01	1.08E 01	7.04E 00	3.41E 00	1.97E 00	1.77E 00
300	3.43E 01	1.71E 01	1.12E 01	5.50E 00	3.19E 00	2.85E 00
600	5.11E C1	2.65E 01	1.77E 01	8.74E 00	5.09E 00	4.56E 00
900	5.97E 01	3.21E 01	2.16E 01	1.08E 01	6.28E 00	5.63E 00
1200	6.49E 01	3.61E 01	2.45E 01	1.23E 01	7.18E 00	6.44E 00

FLIGHT NO. C-354
PATH RADIANCE FROM GROUND TO ALTITUDE
AZIMUTH OF PATH OF SIGHT = 180

(JOB 5810 CATE 05/21/75)
AZIMUTH OF PATH OF SIGHT = 180

FLIGHT NO. C-354 FILTER NO. 4A
PATH RADIANCE FROM GROUND TO ALTITUDE (W/SR SQ M UM)

ALTITUDE	ZENITH ANGLE OF PATH OF SIGHT (DEG)					
M	95	100	105	120	150	180
150	1.58E 01	7.83E 00	5.17E 00	2.43E 00	1.25E 00	1.03E 00
300	2.45E 01	1.25E 01	8.36E 00	3.97E 00	2.06E 00	1.69E 00
600	3.49E 01	1.85E 01	1.25E 01	6.01E 00	3.13E 00	2.58E 00
900	4.31E 01	2.37E 01	1.60E 01	7.76E 00	4.02E 00	3.31E 00
1200	5.07E 01	2.89E 01	1.97E 01	9.56E 00	4.93E 00	4.07E 00

FLIGHT NO. C-354 FILTER NO. 4B
PATH RADIANCE FROM GROUND TO ALTITUDE (W/SR SQ M UM)

ALTITUDE	ZENITH ANGLE OF PATH OF SIGHT (DEG)					
M	95	100	105	120	150	180
150	2.10E 01	1.05E 01	7.03E 00	3.67E 00	2.22E 00	1.77E 00
300	3.25E 01	1.66E 01	1.12E 01	5.90E 00	3.58E 00	2.85E 00
600	4.84E 01	2.58E 01	1.76E 01	9.37E 00	5.70E 00	4.56E 00
900	5.64E 01	3.12E 01	2.15E 01	1.15E 01	6.99E 00	5.63E 00
1200	6.12E 01	3.49E 01	2.43E 01	1.31E 01	7.93E 00	6.44E 00

FLIGHT NO. C-354
PATH RADIANCE FROM GROUND TO ALTITUDE
AZIMUTH OF PATH OF SIGHT = 270

(JOB 5810 CATE 05/21/75)
AZIMUTH OF PATH OF SIGHT = 270

FLIGHT NO. C-354 FILTER NO. 4A
PATH RADIANCE FROM GROUND TO ALTITUDE (W/SR SQ M UM)

ALTITUDE	ZENITH ANGLE OF PATH OF SIGHT (DEG)					
M	95	1C0	105	120	150	180
150	1.80E 01	8.63E 00	5.47E 00	2.42E 00	1.21E 00	1.03E 00
300	2.79E 01	1.38E 01	8.84E 00	3.95E 00	1.98E 00	1.69E 00
600	3.91E 01	2.02E 01	1.32E 01	5.97E 00	3.01E 00	2.58E 00
900	4.66E 01	2.52E 01	1.66E 01	7.68E 00	3.89E 00	3.31E 00
1200	5.27E 01	2.99E 01	2.01E 01	9.43E 00	4.80E 00	4.07E 00

FLIGHT NO. C-354 FILTER NO. 4B
PATH RADIANCE FROM GROUND TO ALTITUDE (W/SR SQ M UM)

ALTITUDE	ZENITH ANGLE OF PATH OF SIGHT (DEG)					
M	95	100	105	120	150	180
150	2.13E 01	1.04E 01	6.84E 00	3.37E 00	1.98E 00	1.77E 00
300	3.30E 01	1.66E 01	1.09E 01	5.43E 00	3.20E 00	2.85E 00
600	4.91E 01	2.57E 01	1.72E 01	8.63E 00	5.11E 00	4.56E 00
900	5.73E 01	3.10E 01	2.10E 01	1.07E 01	6.32E 00	5.63E 00
1200	6.20E 01	3.48E 01	2.38E 01	1.22E 01	7.25E 00	6.44E 00

FLIGHT NO. C-354
DIRECTIONAL PATH REFLECTANCE FROM GROUND TO ALTITUDE
AZIMUTH OF PATH OF SIGHT = 0

(JOB 5810 CATE 05/21/75)
AZIMUTH OF PATH OF SIGHT = 0

FLIGHT NO. C-354 FILTER NO. 4A
DIRECTIONAL PATH REFLECTANCE FROM GROUND TO ALTITUDE

ALTITUDE	ZENITH ANGLE OF PATH OF SIGHT (DEG)					
M	95	1C0	105	120	150	180
150	1.14E-01	4.84E-02	2.90E-02	1.16E-02	5.25E-03	4.46E-03
300	2.02E-01	8.28E-02	4.90E-02	1.93E-02	8.74E-03	7.41E-03
600	3.40E-01	1.33E-01	7.74E-02	3.01E-02	1.35E-02	1.14E-02
900	4.78E-01	1.79E-01	1.03E-01	3.97E-02	1.77E-02	1.49E-02
1200	6.49E-01	2.31E-01	1.31E-01	5.01E-02	2.23E-02	1.86E-02

FLIGHT NO. C-354 FILTER NO. 4B
DIRECTIONAL PATH REFLECTANCE FROM GROUND TO ALTITUDE

ALTITUDE	ZENITH ANGLE OF PATH OF SIGHT (DEG)					
M	95	1C0	105	120	150	180
150	6.32E-02	2.77E-02	1.72E-02	7.59E-03	4.10E-03	3.87E-03
300	1.07E-01	4.61E-02	2.83E-02	1.24E-02	6.68E-03	6.31E-03
600	1.87E-01	7.73E-02	4.68E-02	2.03E-02	1.09E-02	1.02E-02
900	2.47E-01	9.90E-02	5.95E-02	2.56E-02	1.36E-02	1.28E-02
1200	3.01E-01	1.17E-01	7.01E-02	3.00E-02	1.59E-02	1.48E-02

FLIGHT NO. C-354
DIRECTIONAL PATH REFLECTANCE FROM GROUND TO ALTITUDE
AZIMUTH OF PATH OF SIGHT = 90

(JOB 5810 DATE 05/21/75)
AZIMUTH OF PATH OF SIGHT = 90

FLIGHT NO. C-354 FILTER NO. 4A
DIRECTIONAL PATH REFLECTANCE FROM GROUND TO ALTITUDE

ALTITUDE	ZENITH ANGLE OF PATH OF SIGHT (DEG)					
M	95	1C0	105	120	150	180
150	9.01E-02	3.97E-02	2.49E-02	1.08E-02	5.33E-03	4.46E-03
300	1.60E-C1	6.78E-02	4.22E-02	1.80E-02	8.86E-03	7.41E-03
600	2.73E-01	1.10E-01	6.70E-02	2.82E-02	1.37E-02	1.14E-02
900	4.02E-01	1.53E-01	9.10E-02	3.75E-02	1.79E-02	1.49E-02
1200	5.74E-01	2.05E-01	1.19E-01	4.78E-02	2.24E-02	1.86E-02

FLIGHT NO. C-354 FILTER NO. 4B
DIRECTIONAL PATH REFLECTANCE FROM GROUND TO ALTITUDE

ALTITUDE	ZENITH ANGLE OF PATH OF SIGHT (DEG)					
M	95	1C0	105	120	150	180
150	5.57E-02	2.52E-02	1.60E-02	7.58E-03	4.34E-03	3.87E-03
300	9.48E-02	4.18E-02	2.64E-02	1.24E-02	7.07E-03	6.31E-03
600	1.66E-01	7.03E-02	4.38E-02	2.03E-02	1.15E-02	1.02E-02
900	2.21E-01	9.06E-02	5.58E-02	2.55E-02	1.43E-02	1.28E-02
1200	2.72E-01	1.08E-01	6.61E-02	2.98E-02	1.66E-02	1.48E-02

FLIGHT NO. C-354
DIRECTIONAL PATH REFLECTANCE FROM GROUND TO ALTITUDE
AZIMUTH OF PATH OF SIGHT = 180

(JOB 5810 CATE 05/21/75)
AZIMUTH OF PATH OF SIGHT = 180

FLIGHT NO. C-354 FILTER NO. 4A
DIRECTIONAL PATH REFLECTANCE FROM GROUND TO ALTITUDE

ALTITUDE	ZENITH ANGLE OF PATH OF SIGHT (DEG)					
M	95	1C0	105	120	150	180
150	8.21E-02	3.68E-02	2.35E-02	1.07E-02	5.44E-03	4.46E-03
300	1.46E-01	6.28E-02	3.97E-02	1.79E-02	9.04E-03	7.41E-03
600	2.49E-01	1.02E-01	6.31E-02	2.79E-02	1.40E-02	1.14E-02
900	3.66E-01	1.42E-01	8.58E-02	3.71E-02	1.83E-02	1.49E-02
1200	5.23E-C1	1.90E-01	1.12E-01	4.73E-02	2.28E-02	1.86E-02

FLIGHT NO. C-354 FILTER NO. 4B
DIRECTIONAL PATH REFLECTANCE FROM GROUND TO ALTITUDE

ALTITUDE	ZENITH ANGLE OF PATH OF SIGHT (DEG)					
M	95	1C0	105	120	150	180
150	5.27E-02	2.45E-02	1.60E-02	8.14E-03	4.87E-03	3.87E-03
300	8.97E-C2	4.07E-02	2.64E-02	1.33E-02	7.94E-03	6.31E-03
600	1.57E-C1	6.83E-C2	4.37E-02	2.17E-02	1.29E-02	1.02E-02
900	2.C8E-01	8.79E-02	5.56E-02	2.73E-02	1.60E-02	1.28E-02
1200	2.57E-01	1.05E-01	6.56E-02	3.16E-02	1.83E-02	1.48E-02

FLIGHT NO. C-354
DIRECTIONAL PATH REFLECTANCE FROM GROUND TO ALTITUDE
AZIMUTH OF PATH OF SIGHT = 270

(JOB 5810 DATE 05/21/75)
AZIMUTH OF PATH OF SIGHT = 270

FLIGHT NO. C-354 FILTER NO. 4A
DIRECTIONAL PATH REFLECTANCE FROM GROUND TO ALTITUDE

ALTITUDE	ZENITH ANGLE OF PATH OF SIGHT (DEG)					
M	95	100	105	120	150	180
150	9.36E-02	4.05E-02	2.49E-02	1.06E-02	5.23E-03	4.46E-03
300	1.65E-01	6.93E-02	4.20E-02	1.78E-02	8.71E-03	7.41E-03
600	2.79E-01	1.11E-01	6.65E-02	2.77E-02	1.35E-02	1.14E-02
900	3.95E-01	1.51E-01	8.91E-02	3.67E-02	1.77E-02	1.49E-02
1200	5.43E-01	1.97E-01	1.14E-01	4.66E-02	2.22E-02	1.86E-02

FLIGHT NO. C-354 FILTER NO. 4B
DIRECTIONAL PATH REFLECTANCE FROM GROUND TO ALTITUDE

ALTITUDE	ZENITH ANGLE OF PATH OF SIGHT (DEG)					
M	95	100	105	120	150	180
150	5.36E-02	2.43E-02	1.56E-02	7.48E-03	4.35E-03	3.87E-03
300	9.13E-02	4.05E-02	2.57E-02	1.22E-02	7.09E-03	6.31E-03
600	1.59E-01	6.79E-02	4.25E-02	2.00E-02	1.15E-02	1.02E-02
900	2.11E-01	8.75E-02	5.43E-02	2.53E-02	1.44E-02	1.28E-02
1200	2.60E-01	1.04E-01	6.41E-02	2.96E-02	1.67E-02	1.48E-02

FLIGHT C-357 – 20 JULY 1974 – DESCRIPTION OF FLIGHT AND WEATHER CHARACTERISTICS

It was a sunlit afternoon. There were scattered high thin cirrus clouds. The flight was conducted over flat grassy prairie surrounded by thick pine woods. The data-taking for the first flight profile, Filter 4A, started at 2324 GMT and continued until 2342 GMT. The data-taking for the second flight profile, Filter 4B, started at 0154 GMT and continued until 0212 GMT. The sun zenith angle during sky radiance data-taking for Filter 4A was 46.0 degrees at the beginning and 48.6 degrees at the end, and for Filter 4B it was 71.3 degrees at the beginning and 74.0 degrees at the end. The maximum altitude for the Filter 4A profile was 909 meters, and for the Filter 4B profile it was 960 meters. The average elevation of the terrain was 158 meters.

The ground station reported scattered cirrus clouds.

At the beginning of the flight, McChord Air Force Base was reporting scattered altocumulus at 16 000 feet (4800 meters) and thin broken cirrostratus at 25 000 feet (7500 meters) (total cloud amount 0.7), with 20-mile (32-kilometer) visibility. At the same time Gray Army Air Field was reporting scattered clouds at 12 000 feet (3600 meters) and then broken clouds at 2500 feet (7500 meters) with 35-mile (56-kilometer) visibility. At the end of the flight, McChord Air Force Base reported scattered altocumulus at 16 000 feet (4800 meters) and thin broken cirrostratus at 25 000 feet (7500 meters) (total cloud amount 0.7), with 20-mile (32-kilometer) visibility. Gray Army Air Field reported thin broken clouds at 20 000 feet (6000 meters) with 35-mile (56-kilometer) visibility.

The flight log entry read clear, light cirrus in streaks, with a visibility of 20+ miles (32+ kilometers).

On the surface charts, high pressure was centered off northwestern Washington with ridging along the coast of Washington and Oregon. This situation remained unchanged throughout the day. At 500 millibars the trough had moved into British Columbia, and there was weak ridging off the coast. The winds were moderate westsouthwesterly. The airmass was continental polar.

These data were taken from the 3-hourly surface facsimile charts issued by the National Meteorological Center and obtained from the Lindbergh Field NOAA office. The 500-millibar charts were for 0000 GMT and 1200 GMT, and were obtained from the same source.

FLIGHT NO. C-357

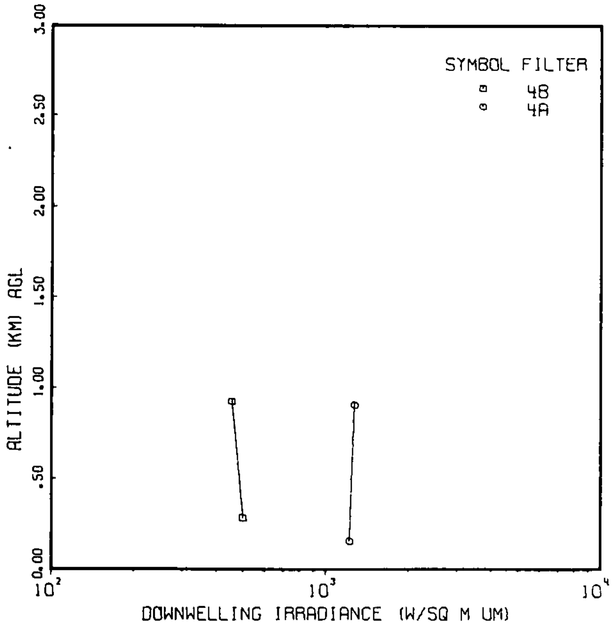

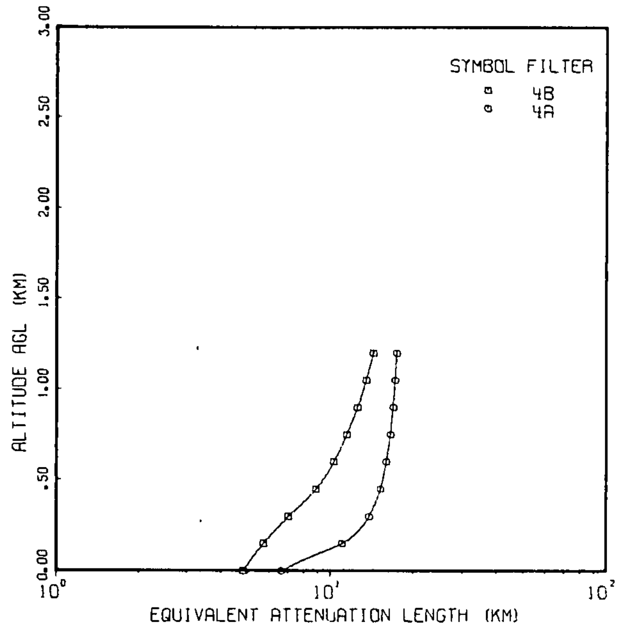

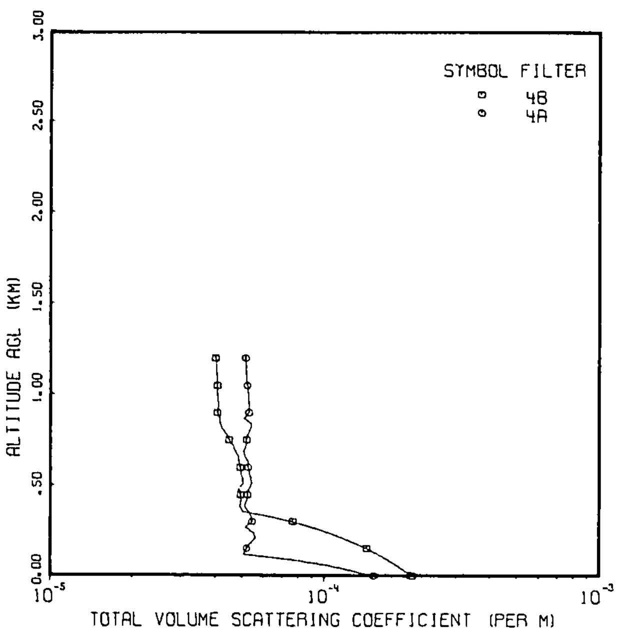

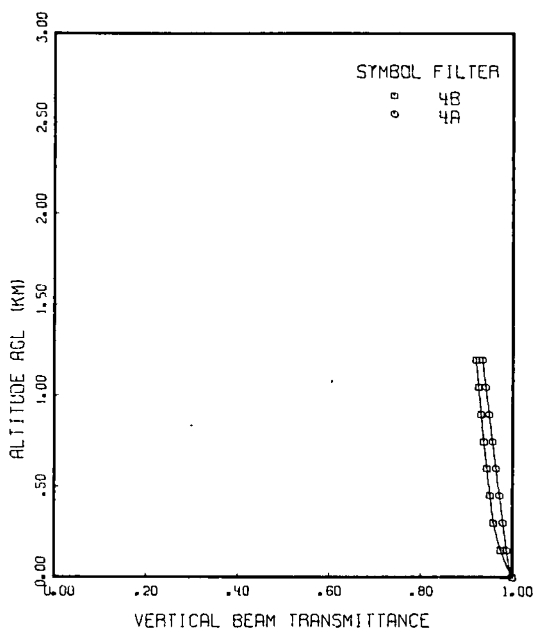

FLIGHT NO. C-357

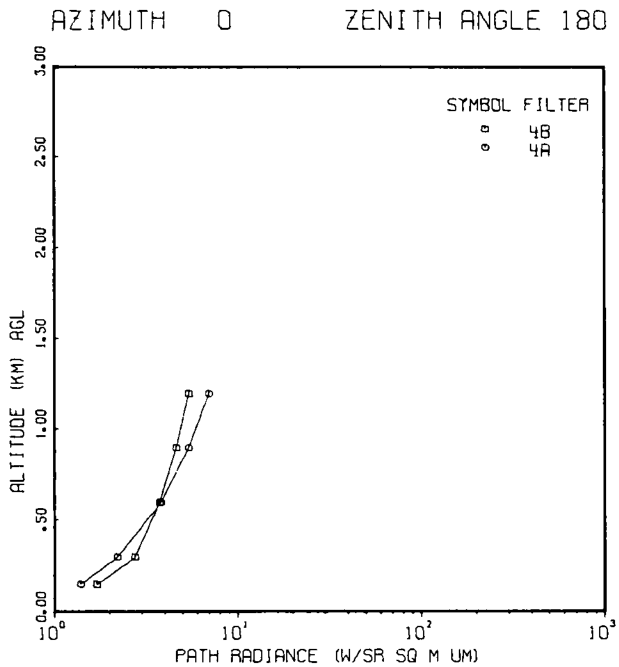

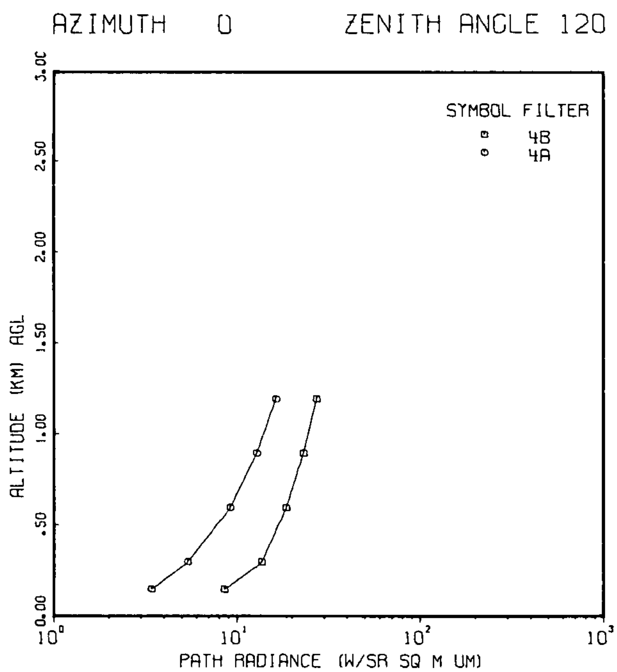

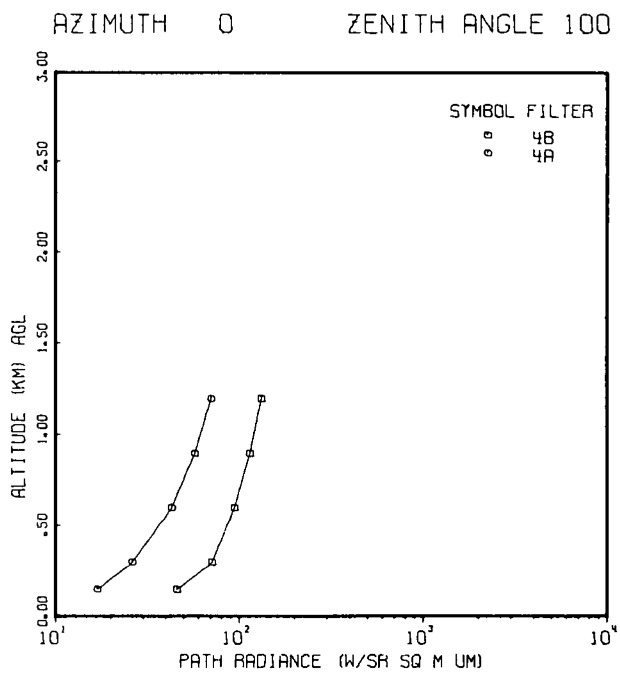

FLIGHT NO. C-357

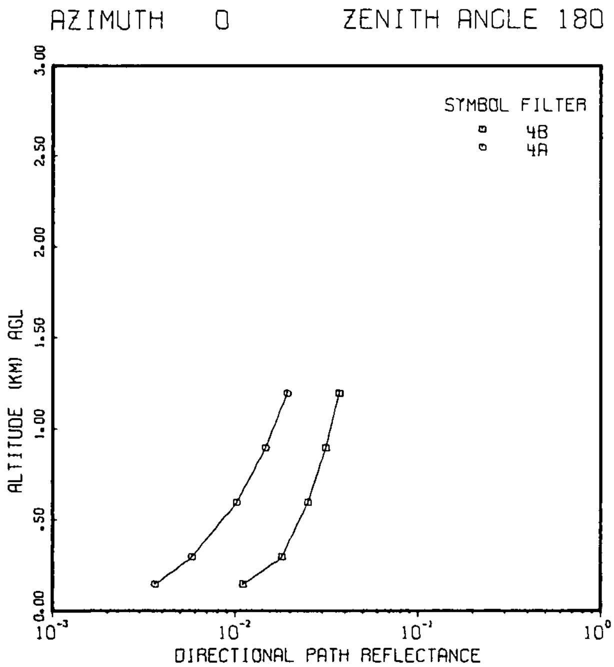

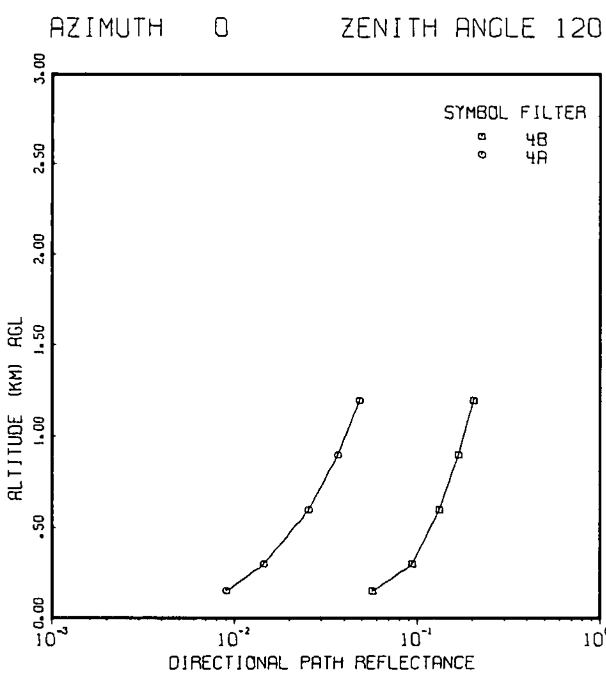

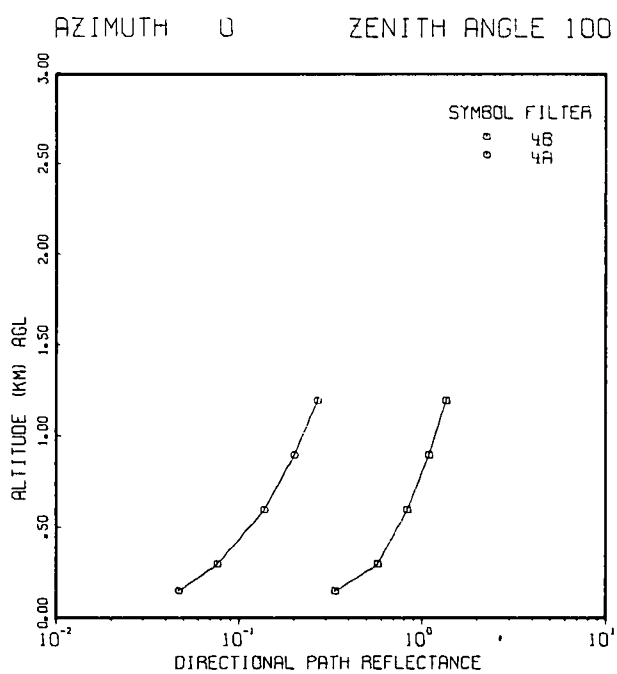

FLIGHT NO. C-357
IRRADIANCE

(JOB 5812 CATE 05/21/75)

FLIGHT NO.C-357 FILTER NO. 4B SUN ZENITH ANGLE 72.6

IRRADIANCE (W/SQ M UM)

ALTITUDE (METERS)	DOWN-WELLING	UP-WELLING	ALBEDO	SCALAR SUN	SCALAR SKY	SCALAR UPWELLING	SCALAR TOTAL	SCALAR ALBEDO
284	4.98E 02	2.97E 01	.060	1.05E 03	5.13E 02	8.79E 01	1.65E 03	.056
928	4.54E 02	3.07E 01	.068	1.17E 03	4.70E 02	1.10E 02	1.75E 03	.067

FLIGHT NO.C-357 FILTER NO. 4A SUN ZENITH ANGLE 47.3

IRRADIANCE (W/SQ M UM)

ALTITUDE (METERS)	DOWN-WELLING	UP-WELLING	ALBEDO	SCALAR SUN	SCALAR SKY	SCALAR UPWELLING	SCALAR TOTAL	SCALAR ALBEDO
154	1.22E 03	4.75E 01	.039	1.41E 03	6.87E 02	1.21E 02	2.22E 03	.058
909	1.27E 03	6.74E 01	.053	1.49E 03	5.56E 02	1.73E 02	2.22E 03	.084

FLIGHT NO. C-357
DIRECTIONAL REFLECTANCE OF TERRAIN

(JOB 5812 DATE 05/21/75)

FLIGHT NO. C-357
AZIMUTH OF PATH OF SIGHT = 0
DIRECTIONAL REFLECTANCE OF TERRAIN

ZENITH ANGLE	FILTERS 4B	4A
95	.3660	.1531
100	.1843	.0545
105	.0995	.0345
120	.0383	.0203
150	.0576	.0173
180	.0244	.0703

FLIGHT NO. C-357
AZIMUTH OF PATH OF SIGHT = 90
DIRECTIONAL REFLECTANCE OF TERRAIN

ZENITH ANGLE	FILTERS 4B	4A
95	.1742	.1033
100	.0719	.0552
105	.0568	.0484
120	.0386	.0217
150	.0729	.0225
180	.0244	.0703

FLIGHT NO. C-357
AZIMUTH OF PATH OF SIGHT = 180
DIRECTIONAL REFLECTANCE OF TERRAIN

ZENITH ANGLE	FILTERS 4B	4A
95	.2415	.1724
100	.2259	.1502
105	.2282	.0792
120	.1180	.0785
150	.0985	.0388
180	.0244	.0703

FLIGHT NO. C-357
AZIMUTH OF PATH OF SIGHT = 270
DIRECTIONAL REFLECTANCE OF TERRAIN

ZENITH ANGLE	FILTERS 4B	4A
95	.1153	.0523
100	.0720	.0389
105	.0497	.0302
120	.0368	.0250
150	.0673	.0219
180	.0244	.0703

FLIGHT NO. C-357
TOTAL VOLUME SCATTERING COEFFICIENT

(JOB 5812 DATE 05/21/75)
DATE 72074 FLIGHT NO. C-357 GROUND LEVEL ALTITUDE (M)= 158

ALTITUDE (M)	TOTAL VOLUME SCATTERING COEFFICIENT (PER M) FILTERS 4B	4A
0	2.08E-04	1.51E-04
30	1.95E-04	1.26E-04
60	1.82E-04	1.01E-04
90	1.69E-04	7.56E-C5
120	1.55E-04	5.05E-05
150	1.42E-04	5.20E-05
180	1.29E-04	5.38E-05
210	1.16E-04	5.63E-C5
240	1.03E-04	5.48E-05
270	8.96E-05	5.15E-05
300	7.65E-05	5.44E-05
330	6.33E-05	5.40E-05
360	5.02E-05	5.28E-05
390	4.90E-05	5.11E-05
420	4.97E-05	5.22E-05
450	4.94E-05	5.25E-05
480	4.85E-05	5.31E-05
510	5.06E-05	5.44E-05
540	5.01E-05	5.38E-05
570	4.95E-C5	5.33E-C5
600	4.92E-05	5.26E-05
630	4.86E-05	5.28E-05
660	4.87E-05	5.15E-05
690	4.71E-05	5.07E-C5
720	4.65E-05	5.19E-05
750	4.47E-05	5.21E-05
780	4.39E-05	5.27E-05
810	4.25E-05	5.38E-C5
840	4.16E-05	5.44E-05
870	4.13E-05	5.08E-05
900	4.06E-05	5.30E-05
930	4.11E-05	5.28E-05
960	4.1CE-05	5.27E-05
990	4.09E-05	5.25E-05
1020	4.08E-05	5.24E-05
1050	4.07E-05	5.22E-05
1080	4.05E-05	5.21E-05
1110	4.04E-05	5.19E-05
1140	4.03E-05	5.18E-05
1170	4.02E-05	5.16E-C5
12C0	4.01E-05	5.14E-05
FIRST DATA ALT	0	0
LAST DATA ALT	960	9C0

FLIGHT NO. C-357
BEAM TRANSMITTANCE FROM GROUND TO ALTITUDE

(JOB 5812 CATE 05/21/75)

FLIGHT NO. C-357 FILTER NO. 4B
BEAM TRANSMITTANCE FROM GROUND TO ALTITUDE

ALTITUDE	ZENITH ANGLE OF PATH OF SIGHT (DEG)					
M	95	1C0	105	120	150	180
150	7.39E-01	8.60E-01	9.03E-01	9.49E-01	9.70E-01	9.74E-01
300	6.12E-01	7.82E-C1	8.48E-01	9.18E-01	9.52E-01	9.58E-01
600	5.09E-01	7.15E-01	7.98E-01	8.90E-01	9.35E-01	9.43E-01
900	4.34E-01	6.61E-01	7.58E-01	8.66E-01	9.20E-01	9.31E-01
1200	3.76E-01	6.16E-01	7.23E-01	8.45E-01	9.08E-01	9.19E-01

FLIGHT NO. C-357 FILTER NO. 4A
BEAM TRANSMITTANCE FROM GROUND TO ALTITUDE

ALTITUDE	ZENITH ANGLE OF PATH OF SIGHT (DEG)					
M	95	1C0	105	120	150	180
150	8.55E-01	9.25E-01	9.49E-01	9.73E-01	9.84E-01	9.86E-01
300	7.79E-01	8.82E-01	9.20E-01	9.58E-01	9.75E-01	9.79E-01
600	6.48E-01	8.05E-01	8.65E-01	9.27E-01	9.57E-01	9.63E-01
900	5.39E-01	7.36E-01	8.14E-01	8.99E-01	9.40E-01	9.48E-01
1200	4.49E-01	6.72E-01	7.66E-01	8.71E-01	9.23E-01	9.33E-01

FLIGHT NO. C-357
PATH RADIANCE FROM GROUND TO ALTITUDE
AZIMUTH OF PATH OF SIGHT = 0

(JOB 5812 CATE 05/21/75)
AZIMUTH OF PATH OF SIGHT = 0

FLIGHT NO. C-357 FILTER NO. 4B
PATH RADIANCE FROM GROUND TO ALTITUDE (W/SR SQ M UM)

ALTITUDE	ZENITH ANGLE OF PATH OF SIGHT (DEG)					
M	95	1C0	105	120	150	180
150	1.C2E 02	4.59E 01	2.69E 01	8.53E 00	2.29E 00	1.70E 00
300	1.51E 02	7.12E 01	4.23E 01	1.36E 01	3.69E 00	2.74E 00
600	1.92E 02	9.43E 01	5.68E 01	1.86E 01	5.04E 00	3.74E 00
900	2.25E 02	1.14E 02	6.95E 01	2.31E 01	6.26E 00	4.62E 00
1200	2.53E 02	1.32E 02	8.10E 01	2.72E 01	7.38E 00	5.42E 00

FLIGHT NO. C-357 FILTER NO. 4A
PATH RADIANCE FROM GROUND TO ALTITUDE (W/SR SQ M UM)

ALTITUDE	ZENITH ANGLE OF PATH OF SIGHT (DEG)					
M	95	1C0	105	120	150	180
150	3.89E 01	1.68E 01	9.89E 00	3.40E 00	1.42E 00	1.38E 00
300	5.89E 01	2.61E 01	1.55E 01	5.38E 00	2.25E 00	2.20E 00
600	9.19E 01	4.2CE 01	2.57E 01	9.17E 00	3.87E 00	3.81E 00
900	1.17F 02	5.74E 01	3.49E 01	1.28E 01	5.44E 00	5.40E 00
1200	1.37E 02	7.03E 01	4.33E 01	1.63E 01	6.97E 00	6.98F 00

FLIGHT NO. C-357
PATH RADIANCE FROM GROUND TO ALTITUDE
AZIMUTH OF PATH OF SIGHT = 90

(JOB 5812 DATE 05/21/75)
AZIMUTH OF PATH OF SIGHT = 90

FLIGHT NO. C-357 FILTER NO. 4B
PATH RADIANCE FROM GROUND TO ALTITUDE (W/SR SQ M UM)

ALTITUDE	ZENITH ANGLE OF PATH OF SIGHT (DEG)					
M	95	1C0	105	120	150	180
150	2.23E 01	1.15E 01	7.69E 00	3.74E 00	2.00E 00	1.70E 00
300	3.32E 01	1.79E 01	1.21E 01	5.98E 00	3.21E 00	2.74E 00
600	4.19E 01	2.35E 01	1.62E 01	8.11E 00	4.38E 00	3.74E 00
900	4.86E 01	2.82E 01	1.96E 01	9.96E 00	5.40E 00	4.62E 00
1200	5.39E 01	3.22E 01	2.26E 01	1.16E 01	6.34E 00	5.42E 00

FLIGHT NO. C-357 FILTER NO. 4A
PATH RADIANCE FROM GROUND TO ALTITUDE (W/SR SQ M UM)

ALTITUDE	ZENITH ANGLE OF PATH OF SIGHT (DEG)					
M	95	1C0	105	120	150	180
150	1.61E 01	8.17E 00	5.39E 00	2.66E 00	1.55E 00	1.38E 00
300	2.46E 01	1.27E 01	8.46E 00	4.20E 00	2.46E 00	2.20E 00
600	3.93E 01	2.11E 01	1.42E 01	7.17E 00	4.22E 00	3.81E 00
900	5.13E 01	2.86E 01	1.96E 01	1.00E 01	5.93E 00	5.40E 00
1200	6.14E 01	3.55E 01	2.46E 01	1.28E 01	7.60E 00	6.98E 00

FLIGHT NO. C-357
PATH RADIANCE FROM GROUND TO ALTITUDE
AZIMUTH OF PATH OF SIGHT = 180

(JOB 5812 CATE 05/21/75)
AZIMUTH OF PATH OF SIGHT = 180

FLIGHT NO. C-357 FILTER NO. 4B
PATH RADIANCE FROM GROUND TO ALTITUDE (W/SR SQ M UM)

ALTITUDE	ZENITH ANGLE OF PATH OF SIGHT (DEG)					
M	95	1C0	105	120	150	180
150	3.66E 01	2.02E 01	1.40E 01	6.79E 00	2.51E 00	1.70E 00
300	5.43E C1	3.13E 01	2.21E 01	1.09E 01	4.05E 00	2.74E 00
600	6.91E 01	4.14E 01	2.96E 01	1.47E 01	5.51E 00	3.74E 00
900	8.09E 01	4.99E 01	3.61E 01	1.80E 01	6.78E 00	4.62E 00
1200	9.07E 01	5.73E C1	4.18E 01	2.09E 01	7.93E 00	5.42E 00

FLIGHT NO. C-357 FILTER NO. 4A
PATH RADIANCE FROM GROUND TO ALTITUDE (W/SR SQ M UM)

ALTITUDE	ZENITH ANGLE OF PATH OF SIGHT (DEG)					
M	95	1C0	105	120	150	180
150	2.02E 01	1.09E 01	7.93E 00	4.80E 00	2.39E 00	1.38E 00
300	3.08E 01	1.70E 01	1.24E 01	7.60E 00	3.80E 00	2.20E 00
600	4.91E 01	2.82E C1	2.07E 01	1.30E 01	6.59E 00	3.81E 00
900	6.42E 01	3.82E 01	2.83E 01	1.81E 01	9.35E 00	5.40E 00
1200	7.68E 01	4.74E 01	3.53E 01	2.30E 01	1.21E 01	6.98E 00

FLIGHT NO. C-357
PATH RADIANCE FROM GROUND TO ALTITUDE
AZIMUTH OF PATH OF SIGHT = 270

(JOB 5812 CATE 05/21/75)
AZIMUTH OF PATH OF SIGHT = 270

FLIGHT NO. C-357 FILTER NO. 4B
PATH RADIANCE FROM GROUND TO ALTITUDE (W/SR SQ M UM)

ALTITUDE	ZENITH ANGLE OF PATH OF SIGHT (DEG)					
M	95	1CO	105	120	150	180
150	2.13E 01	1.10E 01	7.42E 00	3.68E 00	2.00E 00	1.70E 00
300	3.16E 01	1.71E 01	1.17E 01	5.88E 00	3.22E 00	2.74E 00
600	4.COE 01	2.26E 01	1.56E 01	7.96E 00	4.39E 00	3.74E 00
900	4.64E 01	2.71E 01	1.89E 01	9.78E 00	5.41E 00	4.62E 00
1200	5.16E 01	3.10E 01	2.19E 01	1.14E 01	6.35E 00	5.42E 00

FLIGHT NO. C-357 FILTER NO. 4A
PATH RADIANCE FROM GROUND TO ALTITUDE (W/SR SQ M UM)

ALTITUDE	ZENITH ANGLE OF PATH OF SIGHT (DEG)					
M	95	100	105	120	150	180
150	1.55E 01	7.88E OC	5.23E 00	2.64E 00	1.57E 00	1.38E 00
300	2.36E 01	1.23E C1	8.21E 00	4.17E 00	2.48E 00	2.20E 00
600	3.76E 01	2.03E 01	1.38E 01	7.11E 00	4.27E 00	3.81E 00
900	4.92E 01	2.76E 01	1.90E 01	9.92E 00	5.99E 00	5.40E 00
1200	5.89E 01	3.42E 01	2.39E 01	1.26E 01	7.68E 00	6.98E 00

FLIGHT NO. C-357
DIRECTIONAL PATH REFLECTANCE FROM GROUND TO ALTITUDE
AZIMUTH OF PATH OF SIGHT = 0

(JOB 5812 CATE 05/21/75)
AZIMUTH OF PATH OF SIGHT = 0

FLIGHT NO. C-357 FILTER NO. 4B
DIRECTIONAL PATH REFLECTANCE FROM GROUND TO ALTITUDE

ALTITUDE	ZENITH ANGLE OF PATH OF SIGHT (DEG)					
M	95	1C0	105	120	150	180
150	8.68E-01	3.36E-01	1.87E-01	5.67E-02	1.49E-02	1.10E-02
300	1.56E 00	5.74E-01	3.15E-01	9.36E-02	2.44E-02	1.81E-02
600	2.38E 00	8.32E-01	4.49E-01	1.32E-01	3.40E-02	2.50E-02
900	3.27E 00	1.09E 00	5.79E-01	1.68E-01	4.29E-02	3.13E-02
1200	4.24E 00	1.35E 00	7.07E-01	2.03E-01	5.13E-02	3.72E-02

FLIGHT NO. C-357 FILTER NO. 4A
DIRECTIONAL PATH REFLECTANCE FROM GROUND TO ALTITUDE

ALTITUDE	ZENITH ANGLE OF PATH OF SIGHT (DEG)					
M	95	1C0	105	120	150	180
150	1.17E-01	4.69E-02	2.69E-02	9.00E-03	3.72E-03	3.62E-03
300	1.95E-01	7.64E-02	4.34E-02	1.45E-02	5.95E-03	5.79E-03
600	3.66E-01	1.37E-01	7.67E-02	2.55E-02	1.04E-02	1.02E-02
900	5.60E-01	2.01E-01	1.10E-01	3.67E-02	1.49E-02	1.47E-02
1200	7.89E-01	2.69E-01	1.46E-01	4.82E-02	1.94E-02	1.93E-02

FLIGHT NO. C-357
DIRECTIONAL PATH REFLECTANCE FROM GROUND TO ALTITUDE
AZIMUTH OF PATH OF SIGHT = 90

(JOB 5812 CATE 05/21/75)
AZIMUTH OF PATH OF SIGHT = 90

FLIGHT NO. C-357 FILTER NO. 4B
DIRECTIONAL PATH REFLECTANCE FROM GROUND TO ALTITUDE

ALTITUDE	ZENITH ANGLE OF PATH OF SIGHT (DEG)					
M	95	1C0	105	120	150	180
150	1.91E-01	8.45E-02	5.37E-02	2.49E-02	1.30E-02	1.10E-02
300	3.42E-01	1.44E-01	9.01E-02	4.11E-02	2.13E-02	1.81E-02
600	5.19E-01	2.08E-01	1.28E-01	5.75E-02	2.95E-02	2.50E-02
900	7.05E-01	2.69E-01	1.63E-01	7.25E-02	3.70E-02	3.13E-02
1200	9.05E-01	3.30E-01	1.98E-01	8.68E-02	4.40E-02	3.72E-02

FLIGHT NO. C-357 FILTER NO. 4A
DIRECTIONAL PATH REFLECTANCE FROM GROUND TO ALTITUDE

ALTITUDE	ZENITH ANGLE OF PATH OF SIGHT (DEG)					
M	95	1C0	105	120	150	180
150	4.87E-02	2.28E-02	1.46E-02	7.04E-03	4.06E-03	3.62E-03
300	8.15E-02	3.72E-02	2.37E-02	1.13E-02	6.49E-03	5.79E-03
600	1.56E-01	6.75E-02	4.24E-02	1.99E-02	1.14E-02	1.02E-02
900	2.45E-01	1.00E-01	6.20E-02	2.87E-02	1.62E-02	1.47E-02
1200	3.53E-01	1.36E-01	8.27E-02	3.77E-02	2.12E-02	1.93E-02

FLIGHT NO. C-357
DIRECTIONAL PATH REFLECTANCE FROM GROUND TO ALTITUDE
AZIMUTH OF PATH OF SIGHT = 180

(JOB 5812 DATE 05/21/75)
AZIMUTH OF PATH OF SIGHT = 180

FLIGHT NO. C-357 . FILTER NO. 4B
DIRECTIONAL PATH REFLECTANCE FROM GROUND TO ALTITUDE

ALTITUDE	ZENITH ANGLE OF PATH OF SIGHT (DEG)					
M	95	1C0	105	120	150	180
150	3.12E-01	1.48E-01	9.80E-02	4.51E-02	1.63E-02	1.10E-02
300	5.60E-01	2.53E-01	1.64E-01	7.46E-02	2.68E-02	1.81E-02
600	8.55E-01	3.65E-01	2.34E-01	1.04E-01	3.71E-02	2.50E-02
900	1.17E 00	4.76E-01	3.00E-01	1.31E-01	4.64E-02	3.13E-02
1200	1.52E 00	5.86E-01	3.65E-01	1.56E-01	5.51E-02	3.72E-02

FLIGHT NO. C-357 FILTER NO. 4A
DIRECTIONAL PATH REFLECTANCE FROM GROUND TO ALTITUDE

ALTITUDE	ZENITH ANGLE OF PATH OF SIGHT (DEG)					
M	95	1C0	105	120	150	180
150	6.08E-02	3.04E-02	2.15E-02	1.27E-02	6.27E-03	3.62E-03
300	1.02E-01	4.96E-02	3.48E-02	2.04E-02	1.01E-02	5.79E-03
600	1.95E-01	9.02E-02	6.18E-02	3.60E-02	1.77E-02	1.02E-02
900	3.07E-01	1.34E-01	8.96E-02	5.18E-02	2.56E-02	1.47E-02
1200	4.41E-01	1.82E-01	1.19E-01	6.81E-02	3.37E-02	1.93E-02

FLIGHT NO. C-357
DIRECTIONAL PATH REFLECTANCE FROM GROUND TO ALTITUDE
AZIMUTH OF PATH OF SIGHT = 270

(JOB 5812 CATE 05/21/75)
AZIMUTH OF PATH OF SIGHT = 270

FLIGHT NO. C-357 FILTER NO. 4B
DIRECTIONAL PATH REFLECTANCE FROM GROUND TO ALTITUDE

ALTITUDE	ZENITH ANGLE OF PATH OF SIGHT (DEG)					
M	95	100	105	120	150	180
150	1.82E-01	8.10E-02	5.18E-02	2.44E-02	1.30E-02	1.10E-02
300	3.26E-01	1.38E-01	8.69E-02	4.04E-02	2.13E-02	1.81E-02
600	4.95E-01	1.99E-01	1.23E-01	5.64E-02	2.96E-02	2.50E-02
900	6.73E-01	2.58E-01	1.58E-01	7.12E-02	3.71E-02	3.13E-02
1200	8.65E-01	3.17E-01	1.91E-01	8.52E-02	4.41E-02	3.72E-02

FLIGHT NO. C-357 FILTER NO. 4A
DIRECTIONAL PATH REFLECTANCE FROM GROUND TO ALTITUDE

ALTITUDE	ZENITH ANGLE OF PATH OF SIGHT (DEG)					
M	95	100	105	120	150	180
150	4.66E-02	2.20E-02	1.42E-02	6.98E-03	4.10E-03	3.62E-03
300	7.81E-02	3.58E-02	2.30E-02	1.12E-02	6.56E-03	5.79E-03
600	1.50E-01	6.51E-02	4.11E-02	1.97E-02	1.15E-02	1.02E-02
900	2.35E-01	9.67E-02	6.02E-02	2.84E-02	1.64E-02	1.47E-02
1200	3.38E-01	1.31E-01	8.03E-02	3.74E-02	2.14E-02	1.93E-02

FLIGHT C-358 – 21 JULY 1974 – DESCRIPTION OF FLIGHT AND WEATHER CHARACTERISTICS

It was an overcast morning but the sun was visible through the clouds. The flight was conducted over flat grassy prairie surrounded by thick pine woods. The data-taking for the first profile, Filter 4A, started at 1839 GMT and continued until 1855 GMT. The data-taking for the second flight profile, Filter 4B, started at 2007 GMT and continued until 2024 GMT. The sun zenith angle during sky radiance data-taking for Filter 4A was 33.2 degrees at the beginning and 31.5 degrees at the end, and for Filter 4B it was 26.6 degrees at the beginning and 26.5 degrees during transit and at the end. The maximum altitude for the Filter 4A profile was 920 meters, and for the Filter 4B profile it was 895 meters. The average elevation of the terrain was 158 meters.

> The ground station reported high cirrus overcast. Also, they were able to see Mt. Rainier with some haze obscuration.
>
> At the beginning of the flight, McChord Air Force Base was reporting two layers cirrostratus, scattered at 20 000 feet (6000 meters) and thin overcast at 25 000 feet (7500 meters) (total amount 1.0), with a visibility of 15 miles (24 kilometers). At the same time, Gray Army Air Field was reporting scattered clouds at 12 000 feet (3600 meters) and thin overcast at 25 000 feet (7500 meters) with a visibility of 35 miles (56 kilometers). At the end of the flight, McChord Air Force Base reported two layers of cirrostratus, scattered at 18 000 feet (5400 meters) and thin overcast at 25 000 feet (7500 meters), while visibility remained at 15 miles (24 kilometers). Gray Army Air Field was reporting thin overcast at 20 000 feet (6000 meters) and 35-mile (56-kilometer) visibility.
>
> The flight log read overcast, moderate to heavy haze. At 2020 GMT the thin overcast was thinner than at the start of the flight.

The surface charts showed a 1019-millibar low over eastern Washington. The gradient over the western part of the state was very weak. A frontal system was associated with a deepening low centered at 46° N. 131° W. at 1800 GMT. At 500 millibars there was weak ridging from Nevada northwest to British Columbia. The winds were westsouthwesterly of moderate force. The airmass was modified continental polar.

These data were taken from the 3-hourly surface facsimile charts issued by the National Meteorological Center and obtained from the Lindbergh Field NOAA office. The 500-millibar charts were for 0000 GMT and 1200 GMT, and were obtained from the same source.

FLIGHT NO. C-358

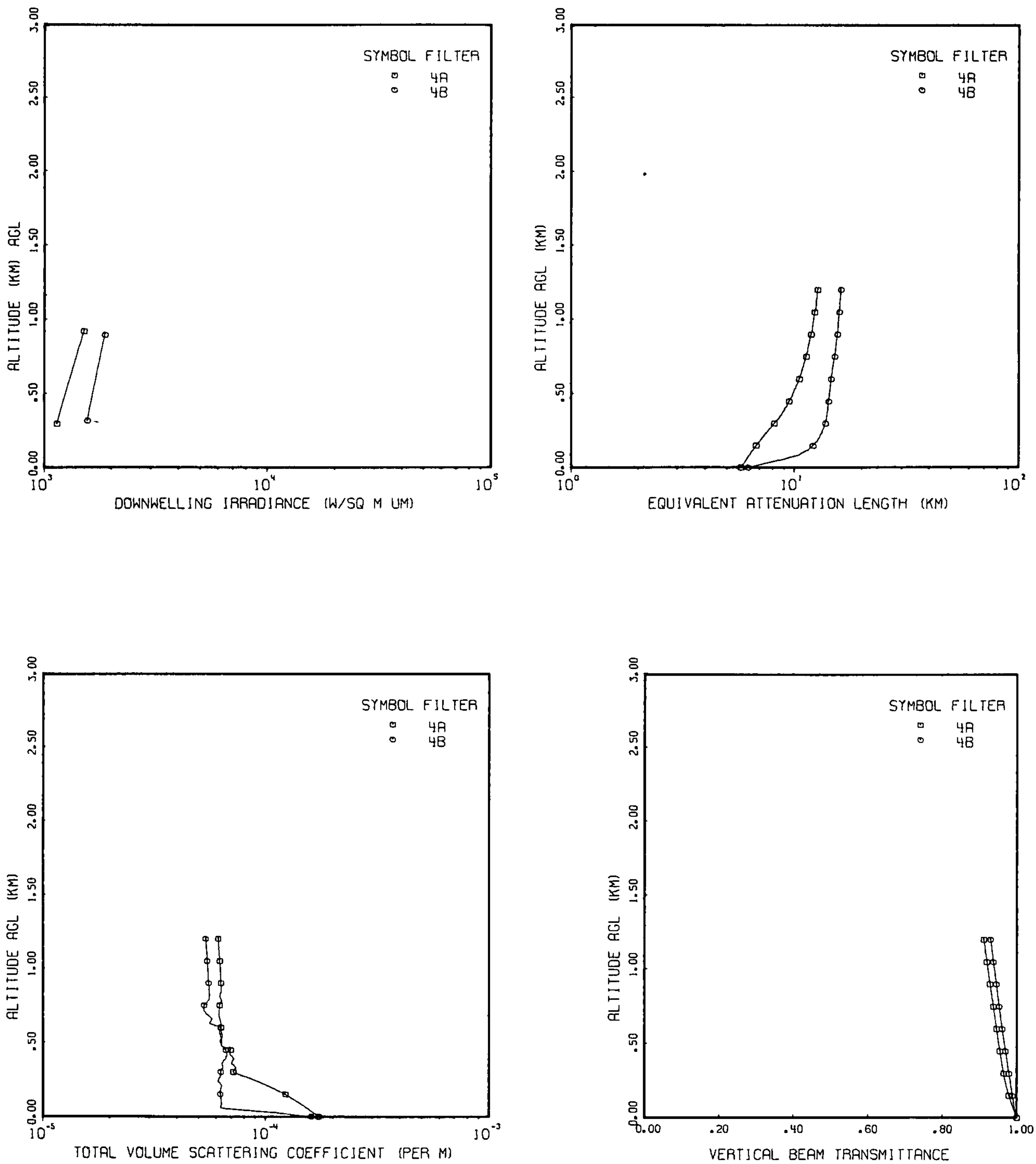

FLIGHT NO. C-358

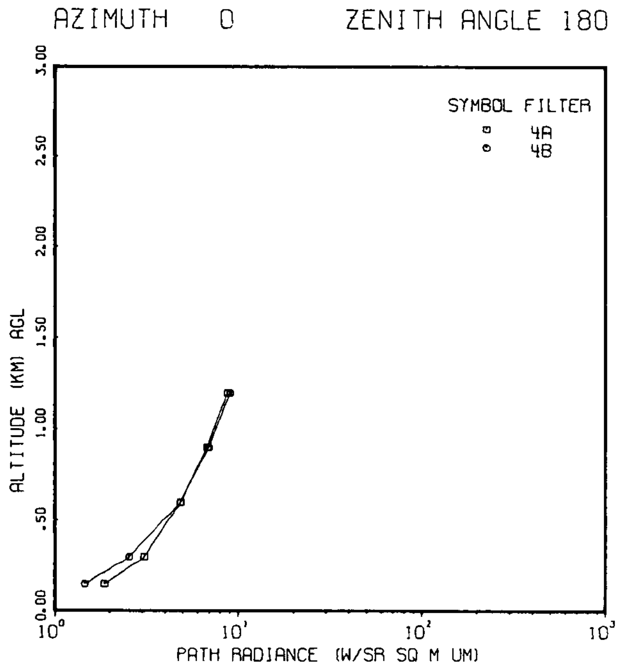

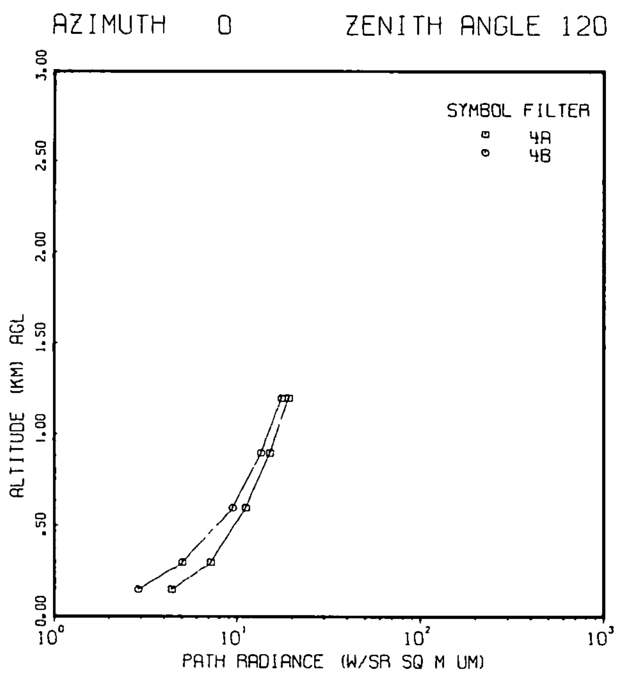

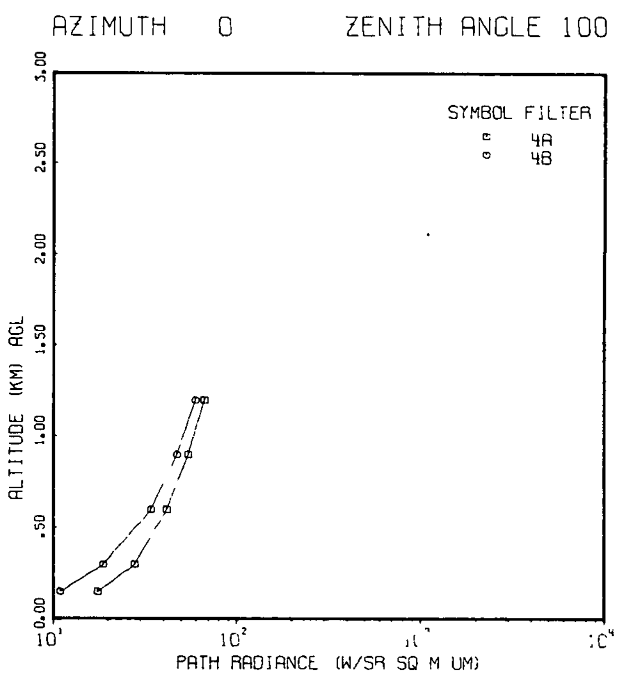

FLIGHT NO. C-358

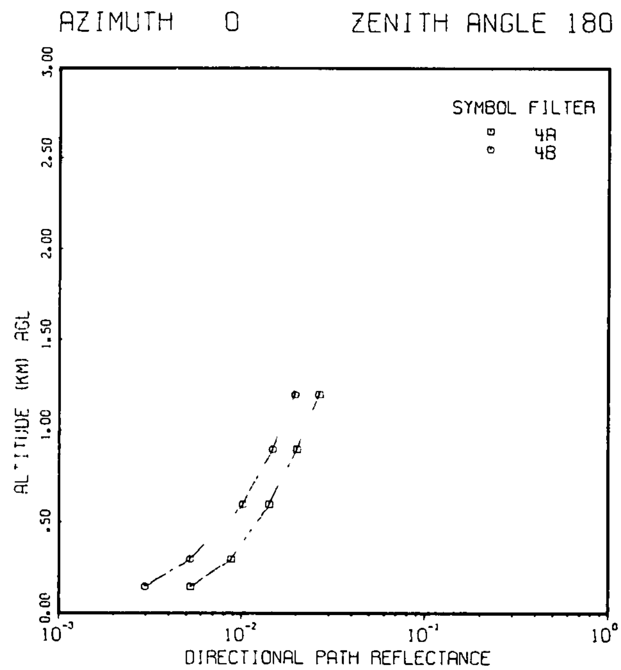

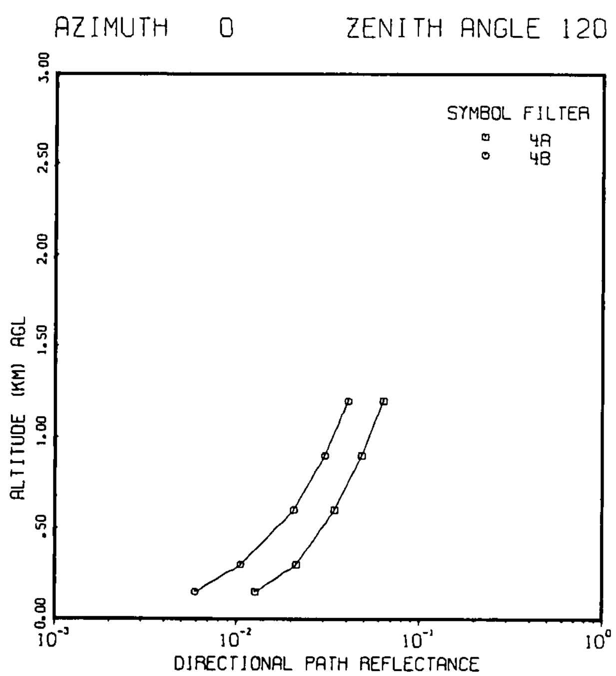

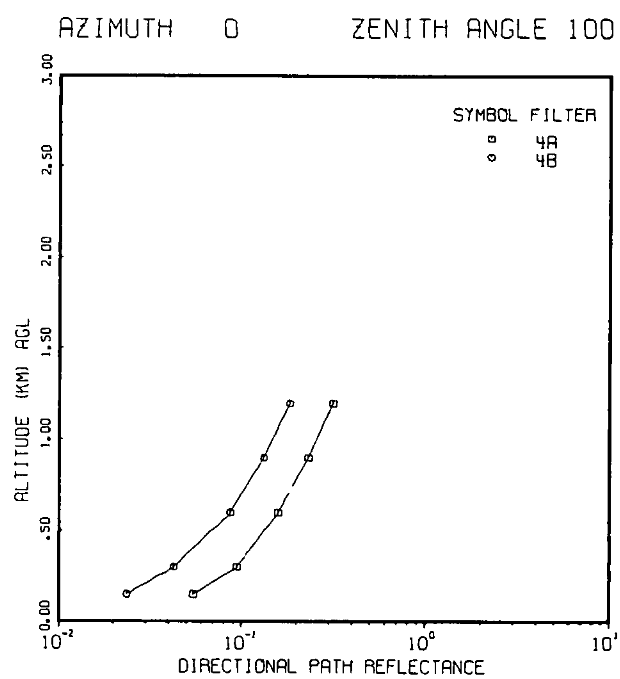

FLIGHT NO. C-358
IRRADIANCE

(JOB 4858 DATE 05/21/75)

FLIGHT NO.C-358 FILTER NO. 4A SUN ZENITH ANGLE 32.3

IRRADIANCE (W/SQ M UM)

ALTITUDE (METERS)	DOWN-WELLING	UP-WELLING	ALBEDO	SCALAR SUN	SCALAR SKY	SCALAR UPWELLING	SCALAR TOTAL	SCALAR ALBEDO
297	1.14E 03	5.64E 01	.049	3.00E 02	1.62E 03	1.35E 02	2.06E 03	.070
920	1.51E 03	6.68E 01	.044	3.15E 02	2.05E 03	1.76E 02	2.54E 03	.074

FLIGHT NO.C-358 FILTER NO. 4B SUN ZENITH ANGLE 26.5

IRRADIANCE (W/SQ M UM)

ALTITUDE (METERS)	DOWN-WELLING	UP-WELLING	ALBEDO	SCALAR SUN	SCALAR SKY	SCALAR UPWELLING	SCALAR TOTAL	SCALAR ALBEDO
318	1.57E 03	7.67E 01	.049	9.04E 02	1.42E 03	1.74E 02	2.50E 03	.075
895	1.88E 03	7.98E 01	.042	9.39E 02	1.81E 03	2.00E 02	2.95E 03	.073

FLIGHT NO. C-358
DIRECTIONAL REFLECTANCE OF TERRAIN

(JOB 4858 DATE 05/21/75)

FLIGHT NO. C-358

AZIMUTH OF PATH OF SIGHT = 0

DIRECTIONAL REFLECTANCE CF TERRAIN

ZENITH ANGLE	FILTERS 4A	4B
95	.1259	.0870
100	.0662	.0706
105	.0457	.0642
120	.0302	.0528
150	.0387	.0319
180	.0390	.0603

FLIGHT NO. C-358

AZIMUTH OF PATH OF SIGHT = 90

DIRECTIONAL REFLECTANCE OF TERRAIN

ZENITH ANGLE	FILTERS 4A	4B
95	.1247	.0535
100	.0656	.0558
105	.0582	.0798
120	.0308	.0508
150	.0386	.0366
180	.0390	.0603

FLIGHT NO. C-358

AZIMUTH OF PATH OF SIGHT = 180

DIRECTIONAL REFLECTANCE OF TERRAIN

ZENITH ANGLE	FILTERS 4A	4B
95	.1115	.0649
100	.0812	.0568
105	.0634	.081C
120	.0556	.0715
150	.0605	.0634
180	.0390	.0603

FLIGHT NO. C-358

AZIMUTH OF PATH OF SIGHT = 270

DIRECTIONAL REFLECTANCE OF TERRAIN

ZENITH ANGLE	FILTERS 4A	4B
95	.1550	.125C
100	.0658	.0634
105	.0450	.0637
120	.0546	.0281
150	.0446	.0418
180	.0390	.0603

FLIGHT NO. C-358
TOTAL VOLUME SCATTERING COEFFICIENT

(JOB 4858 DATE 05/21/75)
DATE 72174 FLIGHT NO. C-358 GROUND LEVEL ALTITUDE (M)= 158

ALTITUDE (M)	TOTAL VOLUME SCATTERING COEFFICIENT (PER M) FILTERS 4A	4B
0	1.73E-04	1.61E-04
30	1.63E-04	1.12E-04
60	1.53E-04	6.26E-05
90	1.43E-04	6.33E-05
120	1.32E-04	6.29E-05
150	1.22E-04	6.25E-05
180	1.12E-04	6.27E-05
210	1.02E-04	6.38E-05
240	9.18E-05	6.10E-05
270	8.16E-05	6.28E-05
300	7.15E-05	6.28E-05
330	7.38E-05	6.46E-05
360	6.99E-05	6.35E-05
390	7.24E-05	6.63E-05
420	6.91E-05	6.71E-05
450	6.96E-05	6.60E-05
480	6.32E-05	6.36E-05
510	6.36E-05	6.22E-05
540	6.28E-05	6.39E-05
570	6.18E-05	6.32E-05
600	6.30E-05	6.30E-05
630	6.30E-05	5.59E-05
660	6.20E-05	5.77E-05
690	6.14E-05	5.45E-05
720	6.18E-05	5.26E-05
750	6.21E-05	5.29E-05
780	6.36E-05	5.54E-05
810	6.20E-05	5.58E-05
840	6.33E-05	5.57E-05
870	6.31E-05	5.55E-05
900	6.29E-05	5.54E-05
930	6.27E-05	5.52E-05
960	6.25E-05	5.50E-05
990	6.23E-05	5.49E-05
1020	6.22E-05	5.47E-05
1050	6.20E-05	5.45E-05
1080	6.18E-05	5.44E-05
1110	6.16E-05	5.42E-05
1140	6.14E-05	5.40E-05
1170	6.12E-05	5.39E-05
1200	6.10E-05	5.37E-05
FIRST DATA ALT	0	0
LAST DATA ALT	840	810

FLIGHT NO. C-358
BEAM TRANSMITTANCE FROM GROUND TO ALTITUDE

(JOB 4858 DATE 05/21/75)

FLIGHT NO. C-358 FILTER NO. 4A
BEAM TRANSMITTANCE FROM GROUND TO ALTITUDE

ALTITUDE	ZENITH ANGLE OF PATH OF SIGHT (DEG)					
M	95	100	105	120	150	180
150	7.75E-01	8.80E-01	9.18E-01	9.57E-01	9.75E-01	9.78E-01
300	6.56E-01	8.10E-01	8.68E-01	9.29E-01	9.59E-01	9.64E-01
600	5.18E-01	7.21E-01	8.03E-01	8.92E-01	9.36E-01	9.45E-01
900	4.16E-01	6.47E-01	7.47E-01	8.60E-01	9.16E-01	9.27E-01
1200	3.34E-01	5.81E-01	6.95E-01	8.28E-01	8.97E-01	9.10E-01

FLIGHT NO. C-358 FILTER NO. 4B
BEAM TRANSMITTANCE FROM GROUND TO ALTITUDE

ALTITUDE	ZENITH ANGLE OF PATH OF SIGHT (DEG)					
M	95	100	105	120	150	180
150	8.68E-01	9.31E-01	9.53E-01	9.76E-01	9.86E-01	9.88E-01
300	7.79E-01	8.82E-01	9.19E-01	9.57E-01	9.75E-01	9.78E-01
600	6.23E-01	7.89E-01	8.53E-01	9.21E-01	9.54E-01	9.60E-01
900	5.13E-01	7.17E-01	8.00E-01	8.91E-01	9.36E-01	9.44E-01
1200	4.23E-01	6.53E-01	7.51E-01	8.62E-01	9.18E-01	9.29E-01

FLIGHT NO. C-358
PATH RADIANCE FROM GROUND TO ALTITUDE
AZIMUTH OF PATH OF SIGHT = 0

(JOB 4858 DATE 05/21/75)
AZIMUTH OF PATH OF SIGHT = 0

FLIGHT NO. C-358 FILTER NO. 4A
PATH RADIANCE FROM GROUND TO ALTITUDE (W/SR SQ M UM)

ALTITUDE	ZENITH ANGLE OF PATH OF SIGHT (DEG)					
M	95	1C0	105	120	150	180
150	3.74E 01	1.75E 01	1.08E 01	4.41E 00	2.05E 00	1.88E 00
300	5.71E 01	2.79E 01	1.74E 01	7.20E 00	3.37E 00	3.09E 00
600	8.10E 01	4.16E 01	2.64E 01	1.12E 01	5.31E 00	4.89E 00
900	1.01E 02	5.44E 01	3.51E 01	1.51E 01	7.33E 00	6.80E 00
1200	1.19E 02	6.66E 01	4.36E 01	1.92E 01	9.43E 00	8.81E 00

FLIGHT NO. C-358 FILTER NO. 4B
PATH RADIANCE FROM GROUND TO ALTITUDE (W/SR SQ M UM)

ALTITUDE	ZENITH ANGLE OF PATH OF SIGHT (DEG)					
M	95	1C0	105	120	150	180
150	2.37E 01	1.09E 01	6.77E 00	2.88E 00	1.46E 00	1.46E 00
300	3.95E 01	1.87E 01	1.17E 01	5.02E 00	2.55E 00	2.56E 00
600	6.82E 01	3.41E 01	2.17E 01	9.47E 00	4.86E 00	4.86E 00
900	9.06E 01	4.73E 01	3.04E 01	1.35E 01	7.00E 00	6.97E 00
1200	1.10E 02	5.96E 01	3.89E 01	1.75E 01	9.15E 00	9.08E 00

FLIGHT NO. C-358
PATH RADIANCE FROM GROUND TO ALTITUDE
AZIMUTH OF PATH OF SIGHT = 90

(JOB 4858 CATE 05/21/75)
AZIMUTH OF PATH OF SIGHT = 90

FLIGHT NO. C-358 FILTER NO. 4A
PATH RADIANCE FROM GROUND TO ALTITUDE (W/SR SQ M UM)

ALTITUDE	ZENITH ANGLE OF PATH OF SIGHT (DEG)					
M	95	100	105	120	150	180
150	2.93E 01	1.43E 01	9.15E 00	4.12E 00	2.14E 00	1.88E 00
300	4.48E 01	2.27E 01	1.47E 01	6.73E 00	3.52E 00	3.09E 00
600	6.34E 01	3.39E 01	2.24E 01	1.05E 01	5.55E 00	4.89E 00
900	7.91E 01	4.43E 01	2.98E 01	1.42E 01	7.68E 00	6.80E 00
1200	9.27E 01	5.42E 01	3.70E 01	1.80E 01	9.92E 00	8.81E 00

FLIGHT NO. C-358 FILTER NO. 4B
PATH RADIANCE FROM GROUND TO ALTITUDE (W/SR SQ M UM)

ALTITUDE	ZENITH ANGLE OF PATH OF SIGHT (DEG)					
M	95	100	105	120	150	180
150	1.92E 01	9.26E 00	5.98E 00	2.81E 00	1.59E 00	1.46E 00
300	3.21E 01	1.59E 01	1.03E 01	4.90E 00	2.78E 00	2.56E 00
600	5.58E 01	2.91E 01	1.93E 01	9.26E 00	5.28E 00	4.86E 00
900	7.51E 01	4.07E 01	2.73E 01	1.33E 01	7.59E 00	6.97E 00
1200	9.20E 01	5.17E 01	3.51E 01	1.72E 01	9.91E 00	9.08E 00

FLIGHT NO. C-358
PATH RADIANCE FROM GROUND TO ALTITUDE
AZIMUTH OF PATH OF SIGHT = 180

(JOB 4858 DATE 05/21/75)
AZIMUTH OF PATH OF SIGHT = 180

FLIGHT NO. C-358 FILTER NO. 4A
PATH RADIANCE FROM GROUND TO ALTITUDE (W/SR SQ M UM)

ALTITUDE	ZENITH ANGLE OF PATH OF SIGHT (DEG)					
M	95	100	105	120	150	180
150	2.77E 01	1.39E 01	9.21E 00	4.55E 00	2.54E 00	1.88E 00
300	4.23E 01	2.22E 01	1.48E 01	7.42E 00	4.17E 00	3.09E 00
600	6.02E 01	3.32E 01	2.27E 01	1.16E 01	6.58E 00	4.89E 00
900	7.61E 01	4.39E 01	3.04E 01	1.58E 01	9.13E 00	6.80E 00
1200	9.01E 01	5.41E 01	3.80E 01	2.01E 01	1.18E 01	8.81E 00

FLIGHT NO. C-358 FILTER NO. 4B
PATH RADIANCE FROM GROUND TO ALTITUDE (W/SR SQ M UM)

ALTITUDE	ZENITH ANGLE OF PATH OF SIGHT (DEG)					
M	95	100	105	120	150	180
150	1.90E 01	9.42E 00	6.26E 00	3.22E 00	1.99E 00	1.46E 00
300	3.17E 01	1.61E 01	1.08E 01	5.61E 00	3.49E 00	2.56E 00
600	5.46E 01	2.93E 01	2.00E 01	1.06E 01	6.62E 00	4.86E 00
900	7.22E 01	4.05E 01	2.80E 01	1.50E 01	9.45E 00	6.97E 00
1200	8.72E 01	5.09E 01	3.57E 01	1.94E 01	1.23E 01	9.08E 00

FLIGHT NO. C-358
PATH RADIANCE FROM GROUND TO ALTITUDE
AZIMUTH OF PATH OF SIGHT = 270

(JOB 4858 DATE 05/21/75)
AZIMUTH OF PATH OF SIGHT = 270

FLIGHT NO. C-358 FILTER NO. 4A
PATH RADIANCE FROM GROUND TO ALTITUDE (W/SR SQ M UM)

ALTITUDE	ZENITH ANGLE OF PATH OF SIGHT (DEG)					
M	95	100	105	120	150	180
150	2.91E 01	1.43E 01	9.19E 00	4.20E 00	2.20E 00	1.88E 00
300	4.45E 01	2.27E 01	1.48E 01	6.85E 00	3.61E 00	3.09E 00
600	6.31E 01	3.40E 01	2.25E 01	1.06E 01	5.68E 00	4.89E 00
900	7.91E 01	4.45E 01	3.00E 01	1.44E 01	7.83E 00	6.80E 00
1200	9.31E 01	5.45E 01	3.73E 01	1.83E 01	1.01E 01	8.81E 00

FLIGHT NO. C-358 FILTER NO. 4B
PATH RADIANCE FROM GROUND TO ALTITUDE (W/SR SQ M UM)

ALTITUDE	ZENITH ANGLE OF PATH OF SIGHT (DEG)					
M	95	100	105	120	150	180
150	1.94E 01	9.37E 00	6.05E 00	2.84E 00	1.61E 00	1.46E 00
300	3.24E 01	1.61E 01	1.05E 01	4.95E 00	2.82E 00	2.56E 00
600	5.60E 01	2.92E 01	1.94E 01	9.34E 00	5.36E 00	4.86E 00
900	7.43E 01	4.05E 01	2.72E 01	1.33E 01	7.69E 00	6.97E 00
1200	9.01E 01	5.10E 01	3.48E 01	1.73E 01	1.00E 01	9.08E 00

FLIGHT NO. C-358
DIRECTIONAL PATH REFLECTANCE FROM GROUND TO ALTITUDE
AZIMUTH OF PATH OF SIGHT = 0

(JOB 4858 CATE 05/21/75)
AZIMUTH OF PATH OF SIGHT = 0

FLIGHT NO. C-358 FILTER NO. 4A
DIRECTIONAL PATH REFLECTANCE FROM GROUND TO ALTITUDE

ALTITUDE	ZENITH ANGLE OF PATH OF SIGHT (DEG)					
M	95	100	105	120	150	180
150	1.32E-01	5.46E-02	3.22E-02	1.27E-02	5.79E-03	5.28E-03
300	2.39E-01	9.45E-02	5.49E-02	2.13E-02	9.66E-03	8.80E-03
600	4.29E-01	1.59E-01	9.04E-02	3.44E-02	1.56E-02	1.42E-02
900	6.69E-01	2.31E-01	1.29E-01	4.84E-02	2.20E-02	2.01E-02
1200	9.78E-01	3.15E-01	1.72E-01	6.35E-02	2.89E-02	2.66E-02

FLIGHT NO. C-358 FILTER NO. 4B
DIRECTIONAL PATH REFLECTANCE FROM GROUND TO ALTITUDE

ALTITUDE	ZENITH ANGLE OF PATH OF SIGHT (DEG)					
M	95	100	105	120	150	180
150	5.48E-02	2.36E-02	1.42E-02	5.92E-03	2.97E-03	2.97E-03
300	1.02E-01	4.26E-02	2.55E-02	1.05E-02	5.25E-03	5.24E-03
600	2.20E-01	8.68E-02	5.09E-02	2.06E-02	1.02E-02	1.02E-02
900	3.55E-01	1.32E-01	7.63E-02	3.04E-02	1.50E-02	1.48E-02
1200	5.21E-01	1.83E-01	1.04E-01	4.07E-02	2.00E-02	1.96E-02

FLIGHT NO. C-358
DIRECTIONAL PATH REFLECTANCE FROM GROUND TO ALTITUDE
AZIMUTH OF PATH OF SIGHT = 90

(JOB 4858 DATE 05/21/75)
AZIMUTH OF PATH OF SIGHT = 90

FLIGHT NO. C-358 FILTER NO. 4A
DIRECTIONAL PATH REFLECTANCE FROM GROUND TO ALTITUDE

ALTITUDE	ZENITH ANGLE OF PATH OF SIGHT (DEG)					
M	95	1C0	105	120	150	180
150	1.04E-01	4.46E-02	2.74E-02	1.18E-02	6.03E-03	5.28E-03
300	1.88E-01	7.71E-02	4.66E-02	1.99E-02	1.01E-02	8.80E-03
600	3.36E-01	1.29E-01	7.67E-02	3.22E-02	1.63E-02	1.42E-02
900	5.22E-01	1.88E-01	1.10E-01	4.54E-02	2.30E-02	2.01E-02
1200	7.60E-01	2.56E-01	1.46E-01	5.98E-02	3.03E-02	2.66E-02

FLIGHT NO. C-358 FILTER NO. 4B
DIRECTIONAL PATH REFLECTANCE FROM GROUND TO ALTITUDE

ALTITUDE	ZENITH ANGLE OF PATH OF SIGHT (DEG)					
M	95	1C0	105	120	150	180
150	4.45E-02	1.99E-02	1.26E-02	5.78E-03	3.23E-03	2.97E-03
300	8.26E-02	3.61E-02	2.26E-02	1.03E-02	5.72E-03	5.24E-03
600	1.80E-01	7.39E-02	4.53E-02	2.02E-02	1.11E-02	1.02E-02
900	2.94E-C1	1.14E-01	6.84E-02	2.98E-02	1.63E-02	1.48E-02
1200	4.36E-01	1.59E-01	9.36E-02	4.01E-02	2.16E-02	1.96E-02

FLIGHT NO. C-358
DIRECTIONAL PATH REFLECTANCE FROM GROUND TO ALTITUDE
AZIMUTH OF PATH OF SIGHT = 180

(JOB 4858 CATE 05/21/75)
AZIMUTH OF PATH OF SIGHT = 180

FLIGHT NO. C-358 FILTER NO. 4A
DIRECTIONAL PATH REFLECTANCE FROM GROUND TO ALTITUDE

ALTITUDE	ZENITH ANGLE OF PATH OF SIGHT (DEG)					
M	95	1CO	105	120	150	180
150	9.80E-02	4.34E-02	2.75E-02	1.30E-02	7.14E-03	5.28E-03
300	1.77E-01	7.51E-02	4.69E-02	2.19E-02	1.19E-02	8.80E-03
600	3.19E-01	1.27E-01	7.75E-02	3.56E-02	1.93E-02	1.42E-02
900	5.02E-01	1.86E-01	1.12E-01	5.04E-02	2.74E-02	2.01E-02
1200	7.39E-01	2.55E-01	1.50E-01	6.67E-02	3.61E-02	2.66E-02

FLIGHT NO. C-358 FILTER NO. 4B
DIRECTIONAL PATH REFLECTANCE FROM GROUND TO ALTITUDE

ALTITUDE	ZENITH ANGLE OF PATH OF SIGHT (DEG)					
M	95	1CO	105	120	150	180
150	4.39E-02	2.03E-02	1.32E-02	6.61E-03	4.06E-03	2.97E-03
300	8.16E-02	3.67E-02	2.36E-02	1.18E-02	7.18E-03	5.24E-03
600	1.76E-01	7.46E-02	4.71E-02	2.30E-02	1.39E-02	1.02E-02
900	2.82E-01	1.13E-01	7.03E-02	3.38E-02	2.03E-02	1.48E-02
1200	4.13E-01	1.56E-01	9.54E-02	4.51E-02	2.68E-02	1.96E-02

FLIGHT NO. C-358
DIRECTIONAL PATH REFLECTANCE FROM GROUND TO ALTITUDE
AZIMUTH OF PATH OF SIGHT = 270

(JOB 4858 DATE 05/21/75)
AZIMUTH OF PATH OF SIGHT = 270

FLIGHT NO. C-358 FILTER NO. 4A
DIRECTIONAL PATH REFLECTANCE FROM GROUND TO ALTITUDE

ALTITUDE M	ZENITH ANGLE OF PATH OF SIGHT (DEG) 95	100	105	120	150	180
150	1.03E-01	4.45E-02	2.75E-02	1.20E-02	6.19E-03	5.28E-03
300	1.86E-01	7.70E-02	4.69E-02	2.02E-02	1.03E-02	8.80E-03
600	3.34E-01	1.29E-01	7.71E-02	3.27E-02	1.66E-02	1.42E-02
900	5.22E-01	1.89E-01	1.10E-01	4.61E-02	2.34E-02	2.01E-02
1200	7.64E-01	2.57E-01	1.47E-01	6.06E-02	3.08E-02	2.66E-02

FLIGHT NO. C-358 FILTER NO. 4B
DIRECTIONAL PATH REFLECTANCE FROM GROUND TO ALTITUDE

ALTITUDE M	ZENITH ANGLE OF PATH OF SIGHT (DEG) 95	100	105	120	150	180
150	4.50E-02	2.02E-02	1.27E-02	5.84E-03	3.28E-03	2.97E-03
300	8.35E-02	3.65E-02	2.28E-02	1.04E-02	5.80E-03	5.24E-03
600	1.80E-01	7.43E-02	4.56E-02	2.03E-02	1.13E-02	1.02E-02
900	2.91E-01	1.13E-01	6.83E-02	3.00E-02	1.65E-02	1.48E-02
1200	4.27E-01	1.57E-01	9.29E-02	4.02E-02	2.19E-02	1.96E-02

FLIGHT C-359 – 23 JULY 1974 – DESCRIPTION OF FLIGHT AND WEATHER CHARACTERISTICS

It was an afternoon with scattered to broken clouds. The sun was partially obscured by clouds during much of both profiles. The flight was conducted over flat grassy prairie surrounded by thick pine woods. The data-taking for the first flight profile, Filter 4A, started at 2124 GMT and continued until 2143 GMT. The data-taking for the second profile, Filter 4B, started at 2324 GMT and continued until 2344 GMT. The sun zenith angle during sky radiance data-taking for Filter 4A was 30.2 degrees at the beginning and 31.8 degrees at the end, and for Filter 4B it was 46.3 degrees at the beginning and 49.4 degrees at the end. The maximum altitude for the Filter 4A profile was 870 meters, and for the Filter 4B profile it was 843 meters. Average elevation of terrain was 158 meters.

> The ground station reported broken cumulus clouds estimated at 2500 feet (750 meters).
>
> At the beginning of the flight, McChord Air Force Base was reporting broken cumulus at 2800 feet (840 meters) and 5000 feet (1500 meters) (total amount 0.9) with 10-mile (16 kilometer) visibility. Gray Army Air Field was reporting scattered clouds at 3000 feet (900 meters) and broken clouds at 4000 feet (1200 meters), with 10-mile (16-kilometer) visibility. At the end of the flight, McChord Air Force Base reported scattered clouds at 3000 feet (900 meters) and broken cumulus clouds at 4000 feet (1200 meters) (total amount 0.6), with a visibility of 15 miles (24 kilometers). At the same time, Gray Army Air Field reported broken clouds at 4000 feet (1200 meters) and 10-mile (16-kilometer) visibility.
>
> The flight log read scattered to broken clouds with bases at 4000 feet (1200 meters) and haze. During the mission, the flight crew estimated the visibility to be 20 miles (32 kilometers) to the north and 7 to 10 miles (11 to 16 kilometers) to the east. At 2310 GMT, the flight log read "Picking up lots of haze from forest fire."

The surface charts showed weak ridging from the Pacific high over the Pacific Northwest. The cold front which moved in over Washington the day before continued to move southeastward. A weakening occlusion was off the coast of British Columbia at 1800 GMT. At 500 millibars there was a weakening trough from British Columbia to northern California. The winds were moderate westerly. The airmass was maritime polar.

These data were taken from the 3-hourly facsimile charts issued by the National Meteorological Center and obtained from the Lindbergh Field NOAA office. The 500 millibar charts are for 0000 GMT and 1200 GMT, and were obtained from the same source.

FLIGHT NO. C-359

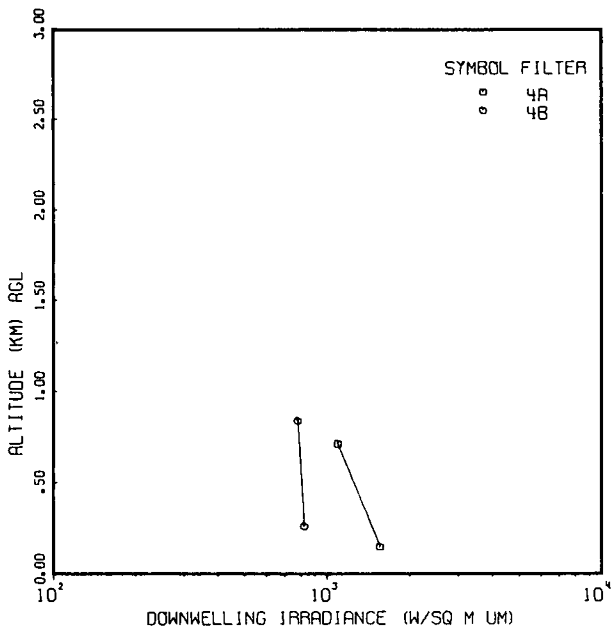

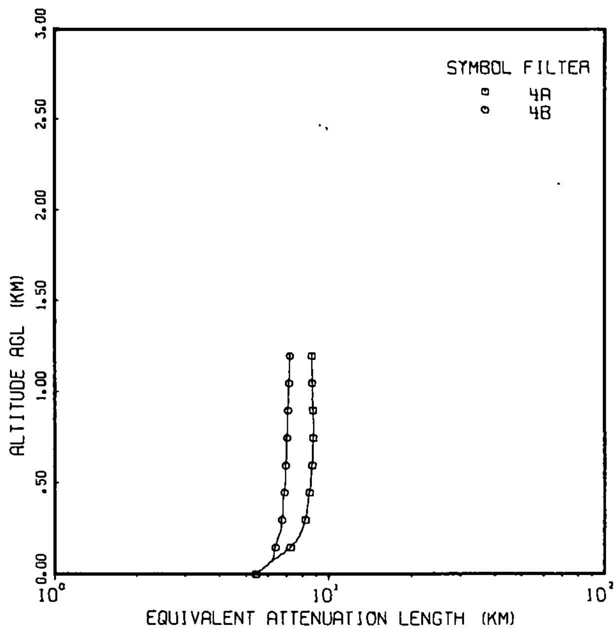

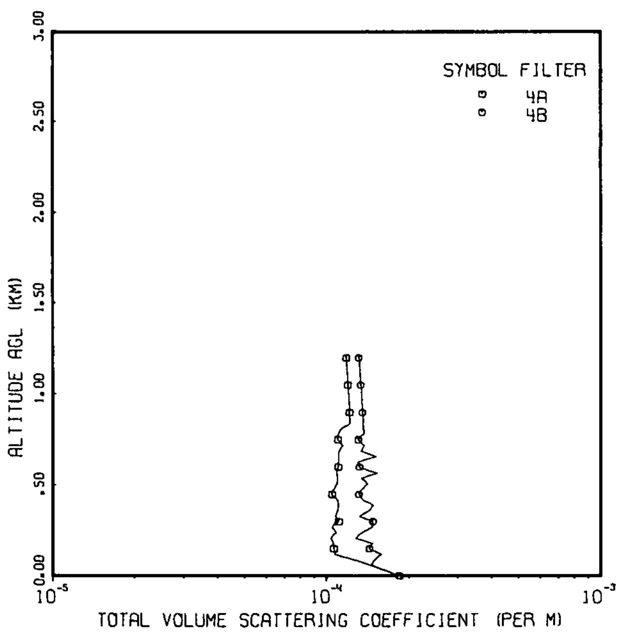

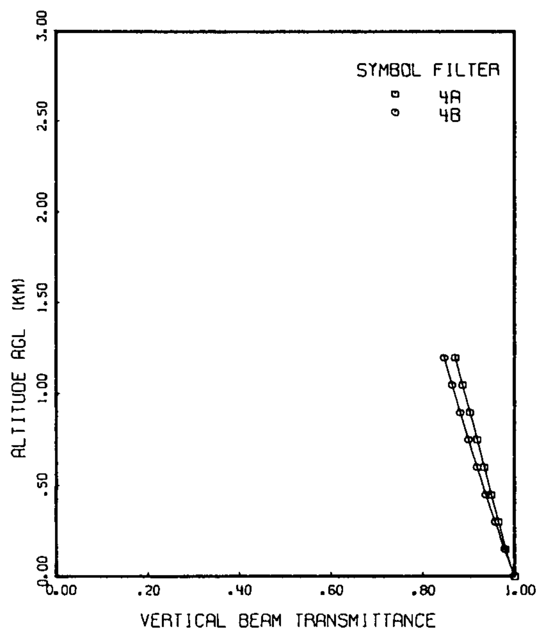

FLIGHT NO. C-359

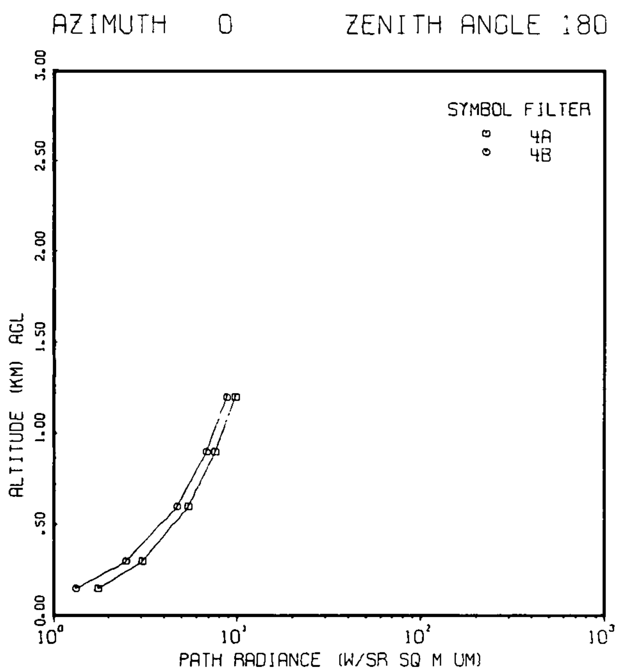

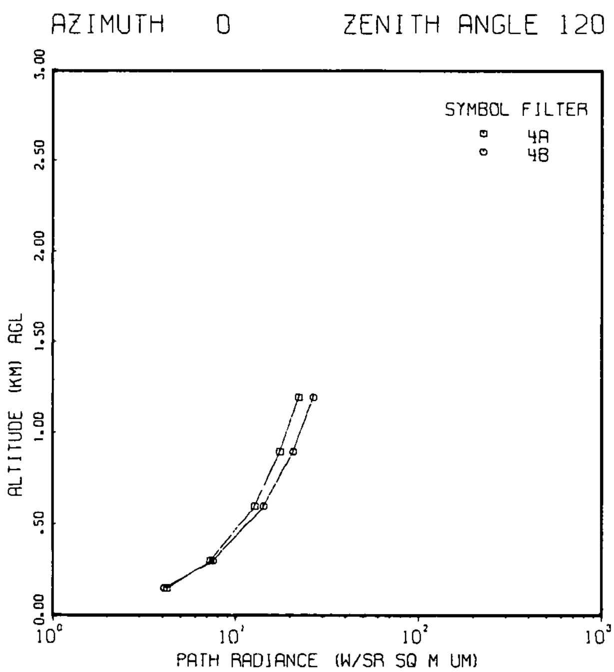

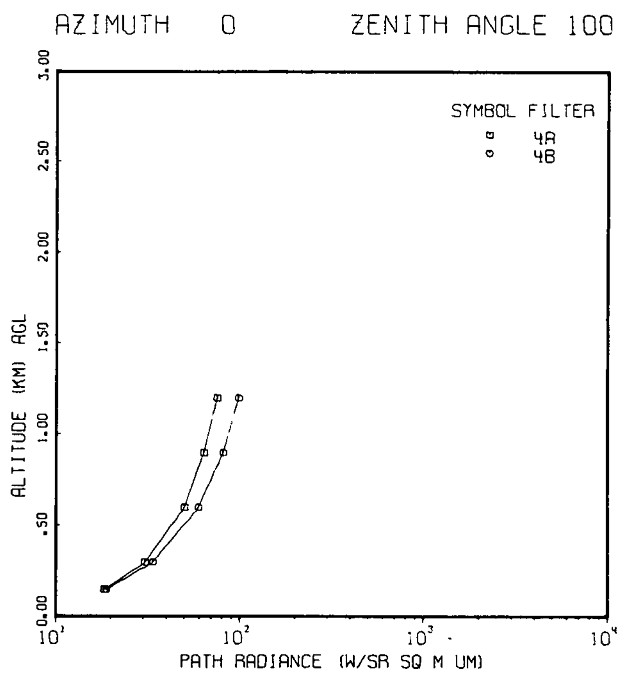

FLIGHT NO. C-359

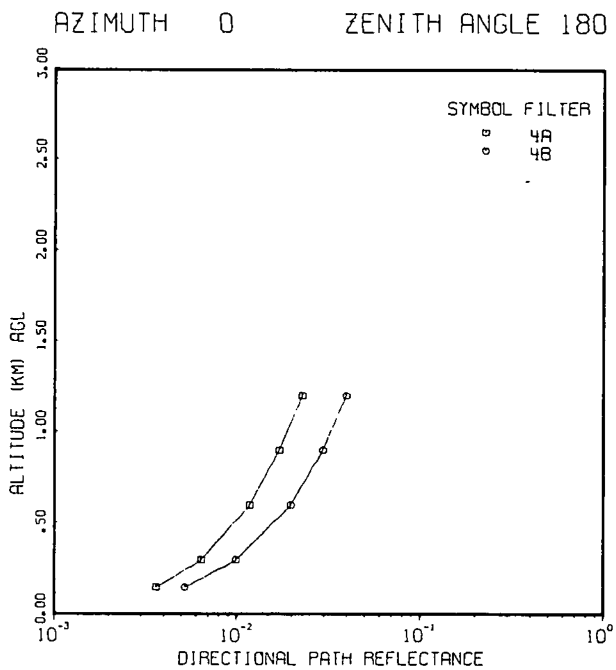

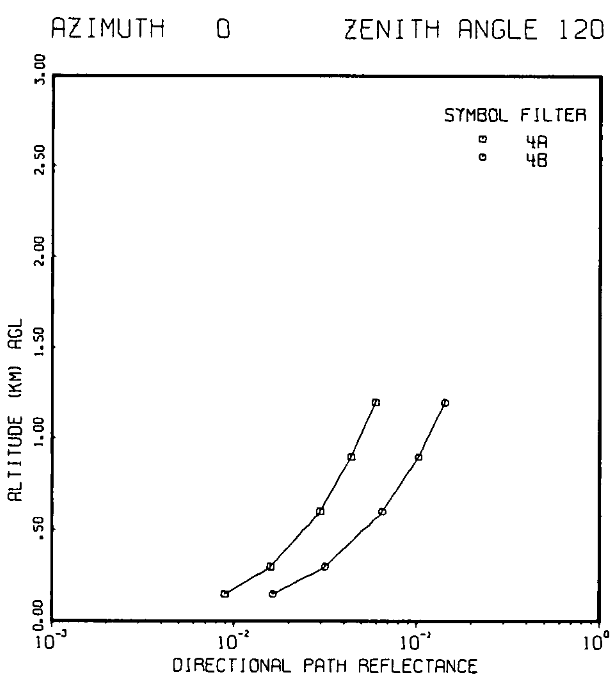

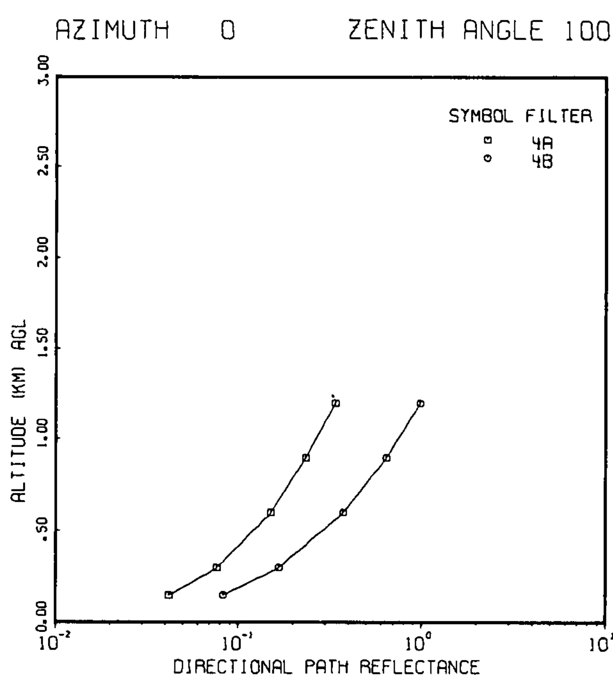

FLIGHT NO. C-359
IRRADIANCE

(JOB 4860 CATE 05/21/75)

FLIGHT NO.C-359 FILTER NO. 4A SUN ZENITH ANGLE 31.0

IRRADIANCE (W/SQ M UM)

ALTITUDE (METERS)	DOWN-WELLING	UP-WELLING	ALBEDO	SCALAR SUN	SCALAR SKY	SCALAR UPWELLING	SCALAR TOTAL	SCALAR ALBEDO
151	1.55E 03	5.70E 01	.037	4.67E 02	1.84E 03	1.31E 02	2.44E 03	.057
717	1.09E 03	7.74E 01	.071	5.02E 02	1.14E 03	1.98E 02	1.84E 03	.121

FLIGHT NO.C-359 FILTER NO. 4B SUN ZENITH ANGLE 47.8

IRRADIANCE (W/SQ M UM)

ALTITUDE (METERS)	DOWN-WELLING	UP-WELLING	ALBEDO	SCALAR SUN	SCALAR SKY	SCALAR UPWELLING	SCALAR TOTAL	SCALAR ALBEDO
264	8.22E 02	5.93E 01	.072	2.41E 02	1.25E 03	1.38E 02	1.63E 03	.092
843	7.77E 02	7.17E 01	.092	2.71E 02	1.20E 03	1.93E 02	1.66E 03	.131

FLIGHT NO. C-359
DIRECTIONAL REFLECTANCE OF TERRAIN

(JOB 4860 DATE 05/21/75)

FLIGHT NO. C-359

AZIMUTH OF PATH OF SIGHT = 0

DIRECTIONAL REFLECTANCE OF TERRAIN

ZENITH ANGLE	FILTERS 4A	4B
95	.0507	.2656
100	.0291	.1521
105	.0212	.1018
120	.0390	.0199
150	.0457	.0411
180	.0155	.0566

FLIGHT NO. C-359

AZIMUTH OF PATH OF SIGHT = 90

DIRECTIONAL REFLECTANCE OF TERRAIN

ZENITH ANGLE	FILTERS 4A	4B
95	.1003	.1811
100	.0450	.0834
105	.0382	.0586
120	.0288	.0225
150	.0472	.0531
180	.0155	.0566

FLIGHT NO. C-359

AZIMUTH OF PATH OF SIGHT = 180

DIRECTIONAL REFLECTANCE OF TERRAIN

ZENITH ANGLE	FILTERS 4A	4B
95	.0955	.1315
100	.0405	.0577
105	.0402	.0512
120	.1001	.0503
150	.0341	.0530
180	.0155	.0566

FLIGHT NO. C-359

AZIMUTH OF PATH OF SIGHT = 270

DIRECTIONAL REFLECTANCE OF TERRAIN

ZENITH ANGLE	FILTERS 4A	4B
95	.0527	.0955
100	.0369	.0759
105	.0301	.0602
120	.0590	.0782
150	.0176	.0882
180	.0155	.0566

FLIGHT NO. C-359
TOTAL VOLUME SCATTERING COEFFICIENT

(JOB 4860 DATE 05/21/75)
DATE 72374 FLIGHT NO. C-359 GROUND LEVEL ALTITUDE (M)= 158

ALTITUDE (M)	TOTAL VOLUME SCATTERING COEFFICIENT (PER M) FILTERS 4A	4B
0	1.84E-04	1.84E-04
30	1.65E-04	1.65E-04
60	1.45E-04	1.45E-04
90	1.26E-04	1.50E-04
120	1.07E-04	1.58E-04
150	1.06E-04	1.43E-04
180	1.05E-04	1.47E-04
210	1.03E-04	1.27E-04
240	1.08E-04	1.34E-04
270	1.04E-04	1.46E-04
300	1.10E-04	1.47E-04
330	1.07E-04	1.31E-04
360	1.10E-04	1.42E-04
390	1.10E-04	1.49E-04
420	1.10E-04	1.36E-04
450	1.04E-04	1.31E-04
480	1.06E-04	1.34E-04
510	1.09E-04	1.41E-04
540	1.09E-04	1.34E-04
570	1.08E-04	1.53E-04
600	1.10E-04	1.31E-04
630	1.10E-04	1.30E-04
660	1.10E-04	1.51E-04
690	1.11E-04	1.34E-04
720	1.15E-04	1.37E-04
750	1.10E-04	1.30E-04
780	1.10E-04	1.36E-04
810	1.13E-04	1.36E-04
840	1.22E-04	1.36E-04
870	1.21E-04	1.35E-04
900	1.21E-04	1.35E-04
930	1.21E-04	1.34E-04
960	1.20E-04	1.34E-04
990	1.20E-04	1.34E-04
1020	1.20E-04	1.33E-04
1050	1.19E-04	1.33E-04
1080	1.19E-04	1.32E-04
1110	1.19E-04	1.32E-04
1140	1.18E-04	1.32E-04
1170	1.18E-04	1.31E-04
1200	1.18E-04	1.31E-04
FIRST DATA ALT	0	0
LAST DATA ALT	870	780

FLIGHT NO. C-359
BEAM TRANSMITTANCE FROM GROUND TO ALTITUDE

(JOB 4860 CATE 05/21/75)

FLIGHT NO. C-359 FILTER NO. 4A
BEAM TRANSMITTANCE FROM GROUND TO ALTITUDE

ALTITUDE	ZENITH ANGLE OF PATH OF SIGHT (DEG)					
M	95	1C0	105	120	150	180
150	7.89E-01	8.88E-01	9.23E-01	9.60E-01	9.76E-01	9.80E-01
300	6.57E-01	8.10E-01	8.68E-01	9.30E-01	9.59E-01	9.64E-01
600	4.51E-01	6.72E-01	7.66E-01	8.71E-01	9.23E-01	9.33E-01
900	3.03E-01	5.52E-01	6.71E-01	8.14E-01	8.88E-01	9.02E-01
1200	2.00E-01	4.49E-01	5.85E-01	7.57E-01	8.52E-01	8.70E-01

FLIGHT NO. C-359 FILTER NO. 4B
BEAM TRANSMITTANCE FROM GROUND TO ALTITUDE

ALTITUDE	ZENITH ANGLE OF PATH OF SIGHT (DEG)					
M	95	1C0	105	120	150	180
150	7.64E-01	8.74E-01	9.13E-01	9.54E-01	9.73E-01	9.77E-01
300	6.00E-01	7.74E-01	8.42E-01	9.15E-01	9.50E-01	9.57E-01
600	3.70E-01	6.09E-01	7.17E-01	8.42E-01	9.05E-01	9.17E-01
900	2.30E-01	4.82E-01	6.12E-01	7.76E-01	8.64E-01	8.81E-01
1200	1.44E-01	3.83E-01	5.25E-01	7.16E-01	8.25E-01	8.46E-01

FLIGHT NO. C-359
PATH RADIANCE FROM GROUND TO ALTITUDE
AZIMUTH OF PATH OF SIGHT = 0

(JOB 4860 DATE 05/21/75)
AZIMUTH OF PATH OF SIGHT = 0

FLIGHT NO. C-359 FILTER NO. 4A
PATH RADIANCE FROM GROUND TO ALTITUDE (W/SR SQ M UM)

ALTITUDE	ZENITH ANGLE OF PATH OF SIGHT (DEG)					
M	95	1C0	105	120	150	180
150	4.C6E 01	1.84E 01	1.11E 01	4.23E 00	1.91E 00	1.76E 00
300	6.47E 01	3.07E 01	1.87E 01	7.28E 00	3.30E 00	3.05E 00
600	9.57E 01	5.00E 01	3.16E 01	1.28E 01	5.86E 00	5.43E 00
900	1.11E 02	6.38E 01	4.18E 01	1.76E 01	8.18E 00	7.61E 00
1200	1.21E 02	7.54E 01	5.10E 01	2.23E 01	1.05E 01	9.80E 00

FLIGHT NO. C-359 FILTER NO. 4B
PATH RADIANCE FROM GROUND TO ALTITUDE (W/SR SQ M UM)

ALTITUDE	ZENITH ANGLE OF PATH OF SIGHT (DEG)					
M	95	1C0	105	120	150	180
150	4.15E 01	1.88E 01	1.13E 01	4.06E 00	1.58E 00	1.33E 00
300	7.01E 01	3.37E 01	2.05E 01	7.53E 00	2.95E 00	2.48E 00
600	1.12E 02	5.95E 01	3.75E 01	1.43E 01	5.64E 00	4.72E 00
900	1.40E 02	8.12E 01	5.27E 01	2.08E 01	8.22E 00	6.81E 00
1200	1.58E 02	9.85E 01	6.58E 01	2.67E 01	1.07E 01	8.78E 00

FLIGHT NO. C-359
PATH RADIANCE FROM GROUND TO ALTITUDE
AZIMUTH OF PATH OF SIGHT = 90

(JOB 4860 DATE 05/21/75)
AZIMUTH OF PATH OF SIGHT = 90

FLIGHT NO. C-359 FILTER NO. 4A
PATH RADIANCE FROM GROUND TO ALTITUDE (W/SR SQ M UM)

ALTITUDE	ZENITH ANGLE OF PATH OF SIGHT (DEG)					
M	95	1C0	105	120	150	180
150	2.63E 01	1.27E 01	8.12E 00	3.69E 00	2.00E 00	1.76E 00
300	4.20E 01	2.13E 01	1.38E 01	6.37E 00	3.47E 00	3.05E 00
600	6.36E 01	3.53E 01	2.36E 01	1.12E 01	6.15E 00	5.43E 00
900	7.61E 01	4.61E 01	3.18E 01	1.56E 01	8.59E 00	7.61E 00
1200	8.46E 01	5.52E 01	3.92E 01	1.98E 01	1.10E 01	9.80E 00

FLIGHT NO. C-359 FILTER NO. 4B
PATH RADIANCE FROM GROUND TO ALTITUDE (W/SR SQ M UM)

ALTITUDE	ZENITH ANGLE OF PATH OF SIGHT (DEG)					
M	95	1C0	105	120	150	180
150	2.34E 01	1.14E 01	7.26E 00	3.20E 00	1.58E 00	1.33E 00
300	3.95E 01	2.04E 01	1.32E 01	5.93E 00	2.96E 00	2.48E 00
600	6.25E 01	3.57E 01	2.40E 01	1.11E 01	5.60E 00	4.72E 00
900	7.74E 01	4.80E 01	3.33E 01	1.59E 01	8.06E 00	6.81E 00
1200	8.68E 01	5.78E 01	4.12E 01	2.03E 01	1.04E 01	8.78E 00

FLIGHT NO. C-359
PATH RADIANCE FROM GROUND TO ALTITUDE
AZIMUTH OF PATH OF SIGHT = 180

(JOB 4860 CATE 05/21/75)
AZIMUTH OF PATH OF SIGHT = 180

FLIGHT NO. C-359 FILTER NO. 4A
PATH RADIANCE FROM GROUND TO ALTITUDE (W/SR SQ M UM)

ALTITUDE	ZENITH ANGLE OF PATH OF SIGHT (DEG)					
M	95	1C0	105	120	150	180
150	2.48E 01	1.25E 01	8.33E 00	4.18E 00	2.36E 00	1.76E 00
300	3.96E 01	2.09E 01	1.41E 01	7.19E 00	4.10E 00	3.05E 00
600	5.95E 01	3.44E 01	2.39E 01	1.26E 01	7.30E 00	5.43E 00
900	7.02E 01	4.43E 01	3.19E 01	1.74E 01	1.02E 01	7.61E 00
1200	7.75E 01	5.27E 01	3.91E 01	2.20E 01	1.32E 01	9.80E 00

FLIGHT NO. C-359 FILTER NO. 4B
PATH RADIANCE FROM GROUND TO ALTITUDE (W/SR SQ M UM)

ALTITUDE	ZENITH ANGLE OF PATH OF SIGHT (DEG)					
M	95	1C0	105	120	150	180
150	2.15E 01	1.08E 01	7.16E 00	3.56E 00	1.76E 00	1.33E 00
300	3.63E 01	1.94E 01	1.30E 01	6.60E 00	3.30E 00	2.48E 00
600	5.74E 01	3.39E 01	2.36E 01	1.23E 01	6.24E 00	4.72E 00
900	7.10E 01	4.55E 01	3.27E 01	1.74E 01	8.98E 00	6.81E 00
1200	7.95E 01	5.47E 01	4.04E 01	2.20E 01	1.15E 01	8.78E 00

FLIGHT NO. C-359
PATH RADIANCE FROM GROUND TO ALTITUDE
AZIMUTH OF PATH OF SIGHT = 270

(JOB 4860 DATE 05/21/75)
AZIMUTH OF PATH OF SIGHT = 270

FLIGHT NO. C-359 FILTER NO. 4A
PATH RADIANCE FROM GROUND TO ALTITUDE (W/SR SQ M UM)

ALTITUDE	ZENITH ANGLE OF PATH OF SIGHT (DEG)					
M	95	1C0	105	120	150	180
150	2.63E 01	1.28E 01	8.21E 00	3.78E 00	2.03E 00	1.76E 00
300	4.22E 01	2.15E 01	1.40E 01	6.52E 00	3.51E 00	3.05E 00
600	6.46E 01	3.59E 01	2.41E 01	1.16E 01	6.26E 00	5.43E 00
900	7.82E 01	4.72E 01	3.27E 01	1.61E 01	8.80E 00	7.61E 00
1200	8.75E 01	5.69E 01	4.04E 01	2.06E 01	1.13E 01	9.80E 00

FLIGHT NO. C-359 FILTER NO. 4B
PATH RADIANCE FROM GROUND TO ALTITUDE (W/SR SQ M UM)

ALTITUDE	ZENITH ANGLE OF PATH OF SIGHT (DEG)					
M	95	1C0	105	120	150	180
150	2.14E 01	1.05E 01	6.77E 00	3.09E 00	1.59E 00	1.32E 00
300	3.62E 01	1.88E 01	1.23E 01	5.74E 00	2.98E 00	2.47E 00
600	5.77E 01	3.32E 01	2.25E 01	1.08E 01	5.65E 00	4.69E 00
900	7.24E 01	4.53E 01	3.17E 01	1.57E 01	8.13E 00	6.80E 00
1200	8.18E 01	5.49E 01	3.96E 01	2.01E 01	1.04E 01	8.78E 00

FLIGHT NO. C-359
DIRECTIONAL PATH REFLECTANCE FROM GROUND TO ALTITUDE
AZIMUTH OF PATH OF SIGHT = 0

(JOB 4860 CATE 05/21/75)
AZIMUTH OF PATH OF SIGHT = 0

FLIGHT NO. C-359 FILTER NO. 4A
DIRECTIONAL PATH REFLECTANCE FROM GROUND TO ALTITUDE

ALTITUDE	ZENITH ANGLE OF PATH OF SIGHT (DEG)					
M	95	1C0	105	120	150	180
150	1.04E-01	4.19E-02	2.42E-02	8.91E-03	3.95E-03	3.63E-03
300	1.99E-01	7.65E-02	4.36E-02	1.58E-02	6.96E-03	6.40E-03
600	4.29E-01	1.50E-01	8.34E-02	2.96E-02	1.28E-02	1.18E-02
900	7.41E-01	2.34E-01	1.26E-01	4.37E-02	1.86E-02	1.71E-02
1200	1.23E 00	3.39E-01	1.76E-01	5.95E-02	2.49E-02	2.28E-02

FLIGHT NO. C-359 FILTER NO. 4B
DIRECTIONAL PATH REFLECTANCE FROM GROUND TO ALTITUDE

ALTITUDE	ZENITH ANGLE OF PATH OF SIGHT (DEG)					
M	95	1C0	105	120	150	180
150	2.08E-01	8.24E-02	4.71E-02	1.63E-02	6.19E-03	5.19E-03
300	4.47E-01	1.66E-01	9.30E-02	3.15E-02	1.19E-02	9.93E-03
600	1.15E C0	3.73E-01	2.00E-01	6.48E-02	2.38E-02	1.97E-02
900	2.33E 00	6.44E-01	3.29E-01	1.02E-01	3.64E-02	2.96E-02
1200	4.19E 00	9.84E-01	4.79E-01	1.43E-01	4.94E-02	3.96E-02

FLIGHT NO. C-359
DIRECTIONAL PATH REFLECTANCE FROM GROUND TO ALTITUDE
AZIMUTH OF PATH OF SIGHT = 90

(JOB 4860 DATE 05/21/75)
AZIMUTH OF PATH OF SIGHT = 90

FLIGHT NO. C-359 FILTER NO. 4A
DIRECTIONAL PATH REFLECTANCE FROM GROUND TO ALTITUDE

ALTITUDE	ZENITH ANGLE OF PATH OF SIGHT (DEG)					
M	95	1C0	105	120	150	180
150	6.73E-02	2.89E-02	1.78E-02	7.78E-03	4.14E-03	3.63E-03
300	1.29E-01	5.31E-02	3.21E-02	1.38E-02	7.31E-03	6.40E-03
600	2.85E-01	1.06E-01	6.24E-02	2.60E-02	1.35E-02	1.18E-02
900	5.07E-01	1.6SE-01	9.58E-02	3.87E-02	1.96E-02	1.71E-02
1200	8.57E-01	2.48E-01	1.36E-01	5.28E-02	2.62E-02	2.28E-02

FLIGHT NO. C-359 FILTER NO. 4B
DIRECTIONAL PATH REFLECTANCE FROM GROUND TO ALTITUDE

ALTITUDE	ZENITH ANGLE OF PATH OF SIGHT (DEG)					
M	95	1C0	105	120	150	180
150	1.17E-01	4.9SE-02	3.04E-02	1.28E-02	6.21E-03	5.19E-03
300	2.52E-01	1.01E-01	6.C0E-02	2.48E-02	1.19E-02	9.93E-03
600	6.46E-01	2.24E-01	1.28E-01	5.05E-02	2.36E-02	1.97E-02
900	1.28E 00	3.81E-01	2.08E-01	7.84E-02	3.57E-02	2.96E-02
1200	2.30E 00	5.77E-01	3.00E-01	1.08E-01	4.80E-02	3.96E-02

FLIGHT NO. C-359
DIRECTIONAL PATH REFLECTANCE FROM GROUND TO ALTITUDE
AZIMUTH OF PATH OF SIGHT = 180

(JOB 4860 DATE 05/21/75)
AZIMUTH OF PATH OF SIGHT = 180

FLIGHT NO. C-359 FILTER NO. 4A
DIRECTIONAL PATH REFLECTANCE FROM GROUND TO ALTITUDE

ALTITUDE	ZENITH ANGLE OF PATH OF SIGHT (DEG)					
M	95	100	105	120	150	180
150	6.37E-02	2.85E-02	1.82E-02	8.80E-03	4.89E-03	3.63E-03
300	1.22E-01	5.21E-02	3.29E-02	1.56E-02	8.64E-03	6.40E-03
600	2.67E-01	1.03E-01	6.32E-02	2.92E-02	1.60E-02	1.18E-02
900	4.68E-01	1.62E-01	9.60E-02	4.31E-02	2.33E-02	1.71E-02
1200	7.85E-01	2.37E-01	1.35E-01	5.86E-02	3.13E-02	2.28E-02

FLIGHT NO. C-359 FILTER NO. 4B
DIRECTIONAL PATH REFLECTANCE FROM GROUND TO ALTITUDE

ALTITUDE	ZENITH ANGLE OF PATH OF SIGHT (DEG)					
M	95	100	105	120	150	180
150	1.08E-01	4.74E-02	3.00E-02	1.43E-02	6.92E-03	5.19E-03
300	2.31E-01	9.56E-02	5.91E-02	2.76E-02	1.33E-02	9.93E-03
600	5.93E-01	2.13E-01	1.26E-01	5.58E-02	2.64E-02	1.97E-02
900	1.18E 00	3.61E-01	2.04E-01	8.57E-02	3.98E-02	2.96E-02
1200	2.10E 00	5.46E-01	2.94E-01	1.17E-01	5.35E-02	3.96E-02

FLIGHT NO. C-359
DIRECTIONAL PATH REFLECTANCE FROM GROUND TO ALTITUDE
AZIMUTH OF PATH OF SIGHT = 270

(JOB 4860 DATE 05/21/75)
AZIMUTH OF PATH OF SIGHT = 270

FLIGHT NO. C-359 FILTER NO. 4A
DIRECTIONAL PATH REFLECTANCE FROM GROUND TO ALTITUDE

ALTITUDE	ZENITH ANGLE OF PATH OF SIGHT (DEG)					
M	95	100	105	120	150	180
150	6.74E-02	2.91E-02	1.80E-02	7.96E-03	4.19E-03	3.63E-03
300	1.30E-01	5.35E-02	3.25E-02	1.42E-02	7.41E-03	6.40E-03
600	2.90E-01	1.08E-01	6.36E-02	2.68E-02	1.37E-02	1.18E-02
900	5.21E-01	1.73E-01	9.83E-02	4.01E-02	2.00E-02	1.71E-02
1200	8.87E-01	2.56E-01	1.40E-01	5.49E-02	2.69E-02	2.28E-02

FLIGHT NO. C-359 FILTER NO. 4B
DIRECTIONAL PATH REFLECTANCE FROM GROUND TO ALTITUDE

ALTITUDE	ZENITH ANGLE OF PATH OF SIGHT (DEG)					
M	95	100	105	120	150	180
150	1.07E-01	4.61E-02	2.83E-02	1.24E-02	6.26E-03	5.15E-03
300	2.31E-01	9.29E-02	5.60E-02	2.40E-02	1.20E-02	9.85E-03
600	5.96E-01	2.09E-01	1.20E-01	4.92E-02	2.38E-02	1.96E-02
900	1.20E 00	3.59E-01	1.98E-01	7.73E-02	3.60E-02	2.95E-02
1200	2.17E 00	5.48E-01	2.88E-01	1.07E-01	4.84E-02	3.97E-02

FLIGHT C-360A – 28 JULY 1974 – DESCRIPTION OF FLIGHT AND WEATHER CHARACTERISTICS

It was a sunlit morning with scattered clouds on the horizon. The flight was conducted over flat grassy prairie surrounded by thick pine woods. The data-taking for the first flight profile, Filter 4A, started at 1455 GMT and continued until 1511 GMT. The data-taking for the second profile, Filter 4B, started at 1641 GMT and continued until 1702 GMT. The sun zenith angle during sky radiance data-taking for Filter 4A was 69.8 degrees at the beginning and 67.5 degrees at the end, and for Filter 4B it was 52.0 at the beginning and 50.3 degrees at the end. The maximum altitude for the Filter 4A profile was 960 meters, and for the Filter 4B profile it was 880 meters. The average elevation of the terrain was 158 meters.

> The ground station reported clear, few cirrus on the horizon, and unlimited visibility.
>
> At the beginning of Flight C-360A, McChord Air Force Base was reporting 0.3 scattered cirrocumulus clouds at 25000 feet (7500 meters) and 15-mile (24-kilometer) visibility. At the same time, Gray Army Air Field was reporting scattered clouds at 15000 feet (4500 meters) and thin scattered clouds at 20000 feet (6000 meters), with 35-mile (56-kilometer) visibility. At the end of Flight C-360B, McChord Air Force Base was reporting 0.1 cirrocumulus at 20000 feet (6000 meters) and 15-mile (24-kilometer) visibility. Gray Army Air Field reported scattered clouds at 20000 feet (6000 meters) and 35-mile (56-kilometer) visibility.
>
> The flight log read light to moderate haze, with no significant clouds.

The surface charts showed a weak gradient with weak ridging in northwestern Washington. At 500 millibars there was a high in Utah with ridging to British Columbia. The winds were moderate westsouthwesterly. The airmass was continental polar.

These data were taken from the 3-hourly surface facsimile charts issued by the National Meteorological Center and obtained from the Lindbergh Field NOAA office. The 500-millibar charts were for 0000 GMT and 1200 GMT, and were obtained from the same source.

FLIGHT NO. C-360A

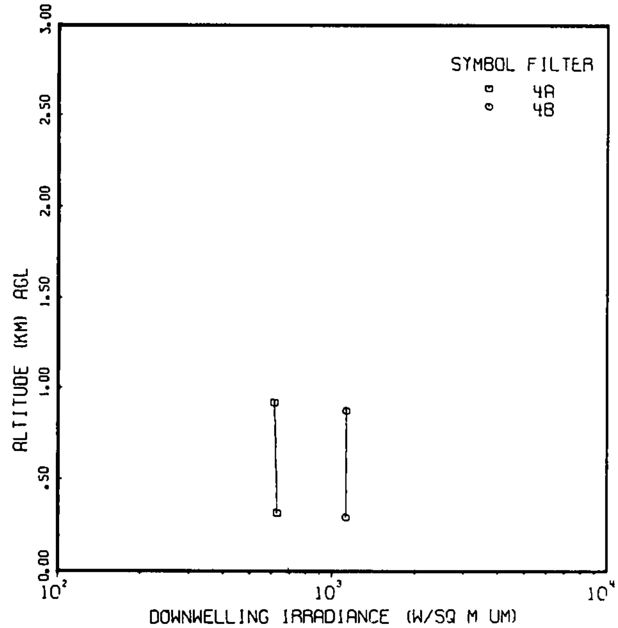

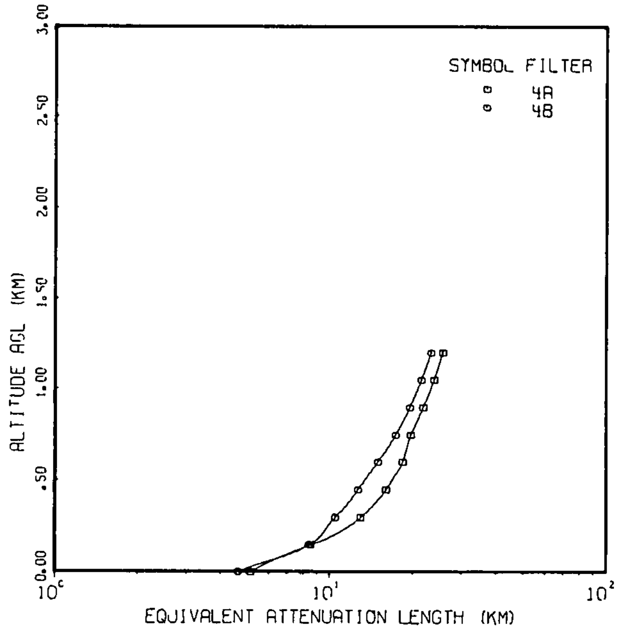

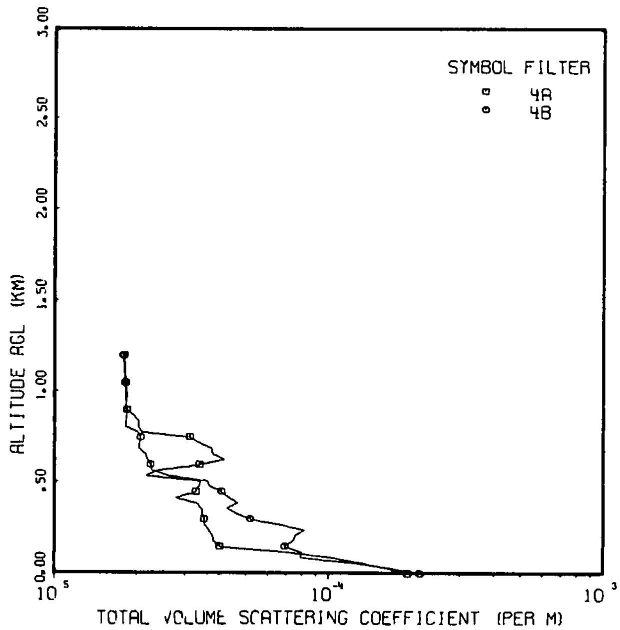

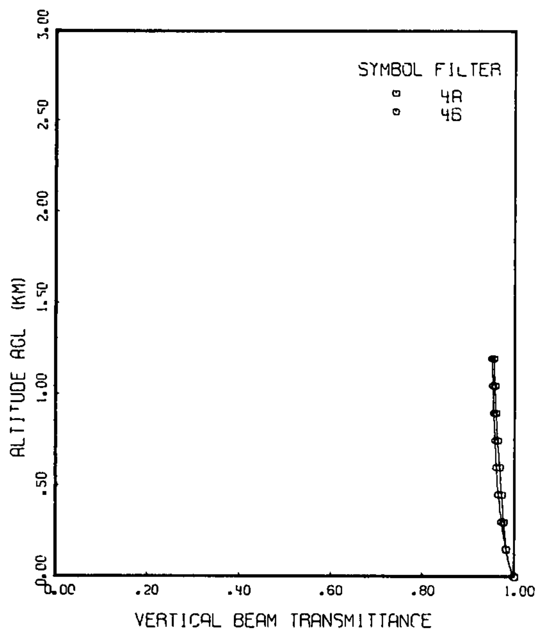

FLIGHT NO. C-360A

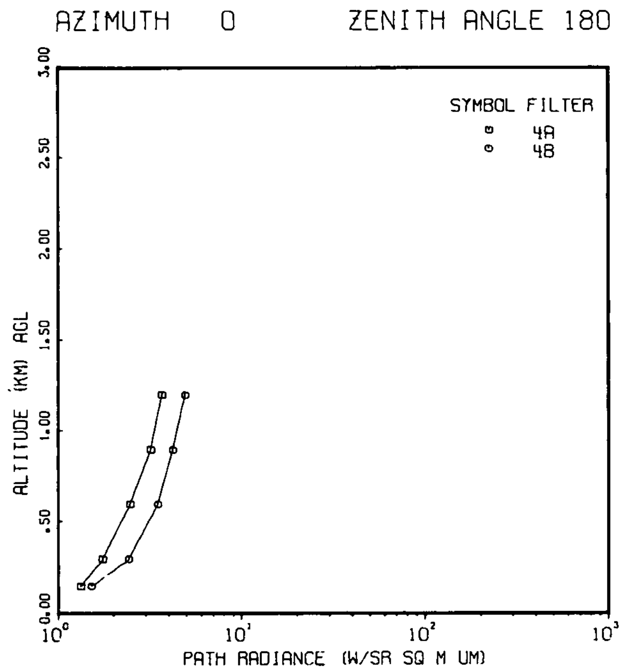

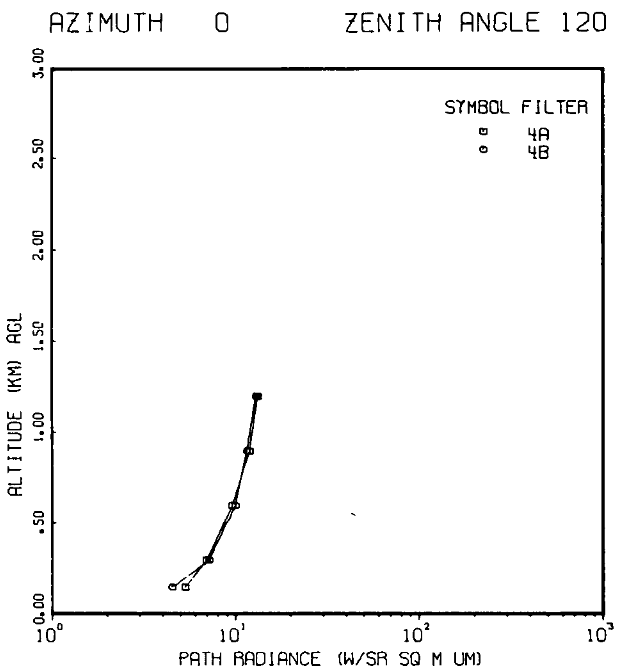

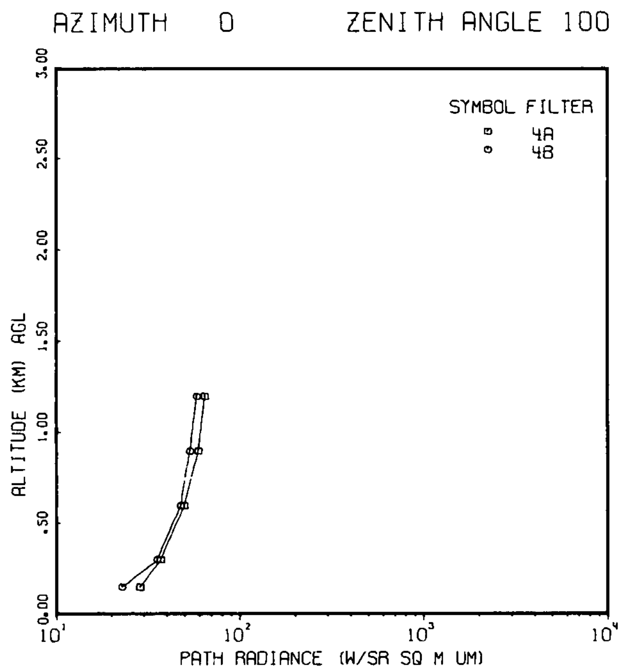

FLIGHT NO. C-360A

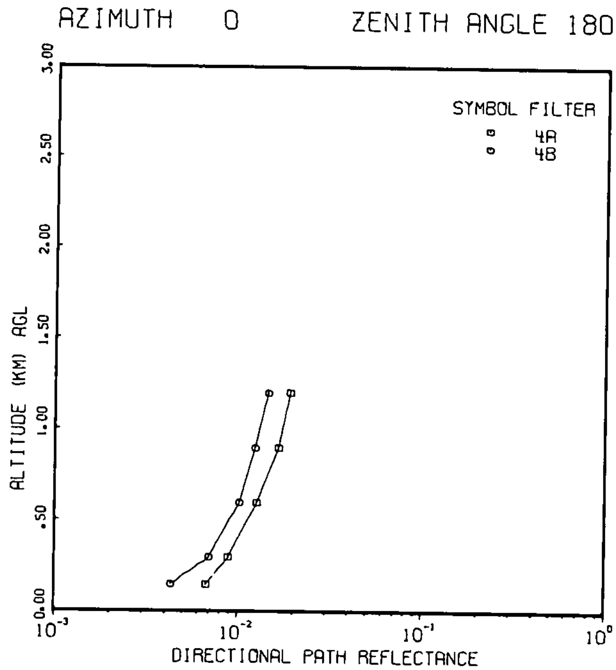

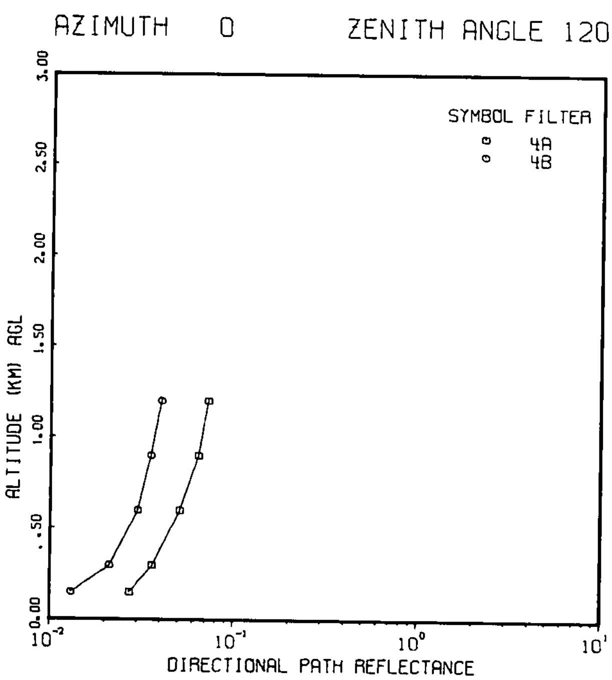

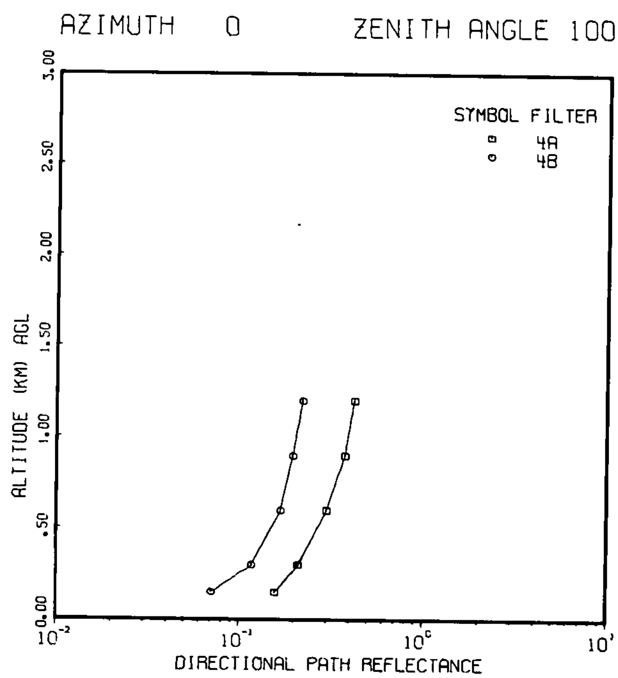

FLIGHT NO. C-360A
IRRADIANCE

(JOB 5990 DATE 05/21/75)

FLIGHT NO.C-360A FILTER NO. 4A SUN ZENITH ANGLE 68.7

IRRADIANCE (W/SQ M UM)

ALTITUDE (METERS)	DOWN-WELLING	UP-WELLING	ALBEDO	SCALAR SUN	SCALAR SKY	SCALAR UPWELLING	SCALAR TOTAL	SCALAR ALBEDO
320	6.31E 02	3.81E 01	.060	1.08E 03	6.13E 02	9.16E 01	1.78E 03	.054
923	6.15E 02	3.59E 01	.058	1.13E 03	4.65E 02	1.10E 02	1.70E 03	.069

FLIGHT NO.C-360A FILTER NO. 4B SUN ZENITH ANGLE 51.1

IRRADIANCE (W/SQ M UM)

ALTITUDE (METERS)	DOWN-WELLING	UP-WELLING	ALBEDO	SCALAR SUN	SCALAR SKY	SCALAR UPWELLING	SCALAR TOTAL	SCALAR ALBEDO
296	1.12E 03	8.01E 01	.071	1.35E 03	6.15E 02	1.98E 02	2.16E 03	.101
880	1.13E 03	7.46E 01	.066	1.38E 03	6.45E 02	2.00E 02	2.23E 03	.099

FLIGHT NO. C-360A
DIRECTIONAL REFLECTANCE OF TERRAIN

(JOB 5990 DATE 05/21/75)

FLIGHT NO. C-360A
AZIMUTH OF PATH OF SIGHT = 0
DIRECTIONAL REFLECTANCE OF TERRAIN

ZENITH ANGLE	FILTERS 4A	4B
95	.1427	.3086
100	.0921	.1158
105	.0708	.0923
120	.0482	.0938
150	.0629	.0514
180	.0326	.0383

FLIGHT NO. C-360A
AZIMUTH OF PATH OF SIGHT = 90
DIRECTIONAL REFLECTANCE OF TERRAIN

ZENITH ANGLE	FILTERS 4A	4B
95	.1444	.1208
100	.0711	.0783
105	.0531	.0730
120	.0347	.0657
150	.0626	.0469
180	.0326	.0383

FLIGHT NO. C-360A
AZIMUTH OF PATH OF SIGHT = 180
DIRECTIONAL REFLECTANCE OF TERRAIN

ZENITH ANGLE	FILTERS 4A	4B
95	.1765	.1402
100	.1469	.1374
105	.1422	.1595
120	.1155	.1205
150	.0796	.0872
180	.0326	.0383

FLIGHT NO. C-360A
AZIMUTH OF PATH OF SIGHT = 270
DIRECTIONAL REFLECTANCE OF TERRAIN

ZENITH ANGLE	FILTERS 4A	4B
95	.1241	.1116
100	.0710	.0656
105	.0554	.0529
120	.0348	.0740
150	.0582	.0635
180	.0326	.0383

FLIGHT NO. C-360A
TOTAL VOLUME SCATTERING COEFFICIENT

(JOB 5990 DATE 05/21/75)
DATE 72874 FLIGHT NO. C-360A GROUND LEVEL ALTITUDE (M)= 158

ALTITUDE (M)	TOTAL VOLUME SCATTERING COEFFICIENT (PER M) FILTERS 4A	4B
0	1.94E-04	2,15E-04
30	1.63E-04	1,70E-04
60	1.32E-04	1,24E-04
90	1.02E-04	7,86E-05
120	7.08E-05	7,96E-05
150	4.00E-05	6,92E-05
180	3.80E-05	7,44E-05
210	3.78E-05	7,57E-05
240	3.66E-05	8,21E-05
270	3.53E-05	6,69E-05
300	3.52E-05	5,17E-05
330	3.46E-05	4,64E-05
360	3.45E-05	4,27E-05
390	3.30E-05	4,69E-05
420	2.77E-05	4,33E-05
450	3.28E-05	4,08E-05
480	3.39E-05	3,69E-05
510	3.42E-05	3,61E-05
540	2.16E-05	2,61E-05
570	2.41E-05	2,27E-05
600	3.40E-05	2,25E-05
630	4.17E-05	2,19E-05
660	3.78E-05	2,15E-05
690	3.75E-05	2,04E-05
720	3.38E-05	2,06E-05
750	3.13E-05	2,06E-05
780	2.08E-05	2,02E-05
810	2.02E-05	1,82E-05
840	2.04E-05	1,83E-05
870	1.95E-05	1,84E-05
900	1.85E-05	1,83E-05
930	1.82E-05	1,83E-05
960	1.84E-05	1,82E-05
990	1.84E-05	1,82E-05
1020	1.83E-05	1,81E-05
1050	1.83E-05	1,81E-05
1080	1.82E-05	1,80E-05
1110	1.81E-05	1,80E-05
1140	1.81E-05	1,79E-05
1170	1.80E-05	1,78E-05
1200	1.80E-05	1,78E-05
FIRST DATA ALT	0	0
LAST DATA ALT	960	870

FLIGHT NO. C-360A
BEAM TRANSMITTANCE FROM GROUND TO ALTITUDE

(JOB 5990 DATE 05/21/75)

FLIGHT NO. C-360A FILTER NO. 4A
BEAM TRANSMITTANCE FROM GROUND TO ALTITUDE

ALTITUDE	ZENITH ANGLE OF PATH OF SIGHT (DEG)					
M	95	100	105	120	150	180
150	8.17E-01	9.04E-01	9.34E-01	9.66E-01	9,80E-01	9,83E-01
300	7.66E-01	8.75E-01	9.15E-01	9.55E-01	9,74E-01	9,77E-01
600	6.87E-01	8.30E-01	8.82E-01	9.37E-01	9,63E-01	9,68E-01
900	6.21E-01	7.89E-01	8.53E-01	9.21E-01	9,54E-01	9,60E-01
1200	5.81E-01	7.65E-01	8.35E-01	9.11E-01	9,48E-01	9,54E-01

FLIGHT NO. C-360A FILTER NO. 4B
BEAM TRANSMITTANCE FROM GROUND TO ALTITUDE

ALTITUDE	ZENITH ANGLE OF PATH OF SIGHT (DEG)					
M	95	100	105	120	150	180
150	8.15E-01	9.02E-01	9.33E-01	9.65E-01	9,80E-01	9,82E-01
300	7.19E-01	8.48E-01	8.95E-01	9.44E-01	9,68E-01	9,72E-01
600	6.30E-01	7.94E-01	8.57E-01	9.23E-01	9,55E-01	9,61F-01
900	5.86F-01	7.67E-01	8.37E-01	9.12E-01	9,48E-01	9,55E-01
1200	5.49E-01	7.44E-01	8.20E-01	9.02E-01	9,42E-01	9,50E-01

FLIGHT NO. C-360A
PATH RADIANCE FROM GROUND TO ALTITUDE
AZIMUTH OF PATH OF SIGHT = 0

(JOB 5990 DATE 5/21/75)
AZIMUTH OF PATH OF SIGHT = 0

FLIGHT NO. C-360A FILTER NO. 4A
PATH RADIANCE FROM GROUND TO ALTITUDE (W/SR SQ M UM)

ALTITUDE	ZENITH ANGLE OF PATH OF SIGHT (DEG)					
M	95	100	105	120	150	180
150	6.58E 01	2.86E 01	1.64E 01	5.31E 00	1.65E 00	1.33E 00
300	8.59E 01	3.71E 01	2.13E 01	6.96E 00	2.16E 00	1.75E 00
600	1.10E 02	4.99E 01	2.90E 01	9.62E 00	3.04E 00	2.47E 00
900	1.26E 02	5.96E 01	3.52E 01	1.19E 01	3.87E 00	3.20E 00
1200	1.34E 02	6.48E 01	3.87E 01	1.33E 01	4.41E 00	3.68E 00

FLIGHT NO. C-360A FILTER NO. 4B
PATH RADIANCE FROM GROUND TO ALTITUDE (W/SR SQ M UM)

ALTITUDE	ZENITH ANGLE OF PATH OF SIGHT (DEG)					
M	95	100	105	120	150	180
150	5.29E 01	2.28E 01	1.34E 01	4.51E 00	1.67E 00	1.52E 00
300	7.98E 01	3.54E 01	2.11E 01	7.16E 00	2.67E 00	2.42E 00
600	1.04E 02	4.77E 01	2.87E 01	9.97E 00	3.81E 00	3.50E 00
900	1.14E 02	5.35E 01	3.25E 01	1.15E 01	4.53E 00	4.22E 00
1200	1.21E 02	5.84E 01	3.58E 01	1.30E 01	5.22E 00	4.93E 00

FLIGHT NO. C-360A
PATH RADIANCE FROM GROUND TO ALTITUDE
AZIMUTH OF PATH OF SIGHT = 90

(JOB 5990 DATE 05/21/75)
AZIMUTH OF PATH OF SIGHT = 90

FLIGHT NO. C-360A FILTER NO. 4A
PATH RADIANCE FROM GROUND TO ALTITUDE (W/SR SQ M UM)

ALTITUDE	ZENITH ANGLE OF PATH OF SIGHT (DEG)					
M	95	100	105	120	150	180
150	1.72E 01	8.65E 00	5.73E 00	2.79E 00	1.53E 00	1.33E 00
300	2.20E 01	1.12E 01	7.46E 00	3.65E 00	2.00E 00	1.75E 00
600	2.94E 01	1.54E 01	1.03E 01	5.13E 00	2.83E 00	2.47E 00
900	3.57E 01	1.92E 01	1.31E 01	6.56E 00	3.66E 00	3.20E 00
1200	3.94E 01	2.16E 01	1.48E 01	7.50E 00	4.21E 00	3.68E 00

FLIGHT NO. C-360A FILTER NO. 4B
PATH RADIANCE FROM GROUND TO ALTITUDE (W/SR SQ M UM)

ALTITUDE	ZENITH ANGLE OF PATH OF SIGHT (DEG)					
M	95	100	105	120	150	180
150	1.90E 01	9.51E 0	6.26E 00	3.08E 00	1.73E 00	1.52E 00
300	2.87E 01	1.48E 01	9.85E 00	4.89E 00	2.76E 00	2.42E 00
600	3.84E 01	2.[illegible]5E 01	1.38E 01	6.94E 00	3.96E 00	3.50E 00
900	4.40E 01	2.38E 01	1.62E 01	6.24E 00	4.76E 00	4.22E 00
1200	4.96E 01	2.70E 01	1.84E 01	9.50E 00	5.54E 00	4.93E 00

FLIGHT NO. C-360A
PATH RADIANCE FROM GROUND TO ALTITUDE
AZIMUTH OF PATH OF SIGHT = 180

(JOB 5990 DATE 05/21/75)
AZIMUTH OF PATH OF SIGHT = 180

FLIGHT NO. C-360A FILTER NO. 4A
PATH RADIANCE FROM GROUND TO ALTITUDE (W/SR SQ M UM)

ALTITUDE	ZENITH ANGLE OF PATH OF SIGHT (DEG)					
M	95	100	105	120	150	180
150	2.40E 01	1.27E 01	8.79E 00	4.47E 00	1.95E 00	1.33E 00
300	3.06E 01	1.65E 01	1.15E 01	5.86E 00	2.56E 00	1.75E 00
600	4.20E 01	2.33E 01	1.63E 01	8.44E 00	3.65E 00	2.47E 00
900	5.41E 01	3.08E 01	2.19E 01	1.14E 01	4.83E 00	3.20E 00
1200	6.23E 01	3.60E 01	2.57E 01	1.35E 01	5.65E 00	3.68E 00

FLIGHT NO. C-360A FILTER NO. 4B
PATH RADIANCE FROM GROUND TO ALTITUDE (W/SR SQ M UM)

ALTITUDE	ZENITH ANGLE OF PATH OF SIGHT (DEG)					
M	95	100	105	120	150	180
150	2.19E 01	1.15E 01	8.02E 00	4.44E 00	2.26E 00	1.52E 00
300	3.31E 01	1.80E 01	1.26E 01	7.06E 00	3.60E 00	2.42E 00
600	4.58E 01	2.57E 01	1.83E 01	1.05E 01	5.34E 00	3.50E 00
900	5.48E 01	3.14E 01	2.26E 01	1.32E 01	6.65E 00	4.22E 00
1200	6.35E 01	3.70E 01	2.69E 01	1.59E 01	8.00E 00	4.93E 00

FLIGHT NO. C-360A
PATH RADIANCE FROM GROUND TO ALTITUDE
AZIMUTH OF PATH OF SIGHT = 270

(JOB 5990 DATE 05/21/75)
AZIMUTH OF PATH OF SIGHT = 270

FLIGHT NO. C-360A FILTER NO. 4A
PATH RADIANCE FROM GROUND TO ALTITUDE (W/SR SQ M UM)

ALTITUDE	ZENITH ANGLE OF PATH OF SIGHT (DEG)					
M	95	100	105	120	150	180
150	1.66E 01	8.42E 00	5.62E 00	2.79E 00	1.55E 00	1.33E 00
300	2.12E 01	1.09E 01	7.32E 00	3.66E 00	2.04E 00	1.75E 00
600	2.84E 01	1.50E 01	1.02E 01	5.14E 00	2.88E 00	2.47E 00
900	3.47E 01	1.88E 01	1.29E 01	6.58E 00	3.71E 00	3.20E 00
1200	3.85E 01	2.12E 01	1.46E 01	7.53E 00	4.27E 00	3.68E 00

FLIGHT NO. C-360A FILTER NO. 4B
PATH RADIANCE FROM GROUND TO ALTITUDE (W/SR SQ M UM)

ALTITUDE	ZENITH ANGLE OF PATH OF SIGHT (DEG)					
M	95	100	105	120	150	180
150	1.88E 01	9.42E 00	6.23E 00	3.09E 00	1.74E 00	1.52E 00
300	2.83E 01	1.47E 01	9.79E 00	4.91E 00	2.78E 00	2.42E 00
600	3.79E 01	2.03E 01	1.37E 01	6.97E 00	4.00E 00	3.50E 00
900	4.34E 01	2.36E 01	1.61E 01	8.26E 00	4.80E 00	4.22E 00
1200	4.84E 01	2.67E 01	1.83E 01	9.51E 00	5.58E 00	4.93E 00

FLIGHT NO. C-360A
DIRECTIONAL PATH REFLECTANCE FROM GROUND TO ALTITUDE
AZIMUTH OF PATH OF SIGHT = 0

(JOB 5990 DATE 05/21/75)
AZIMUTH OF PATH OF SIGHT = 0

FLIGHT NO. C-360A FILTER NO. 4A
DIRECTIONAL PATH REFLECTANCE FROM GROUND TO ALTITUDE

ALTITUDE	ZENITH ANGLE OF PATH OF SIGHT (DEG)					
M	95	100	105	120	150	180
150	4.01E-01	1.57E-01	8.72E-02	2.74E-02	8.37E-03	6.74E-03
300	5.45E-01	2.11E-01	1.16E-01	3.63E-02	1.11E-02	8.90E-03
600	7.93E-01	3.00E-01	1.64E-01	5.11E-02	1.57E-02	1.27E-02
900	1.01E 00	3.76E-01	2.06E-01	6.44E-02	2.02E-02	1.66E-02
1200	1.15E 00	4.22E-01	2.30E-01	7.25E-02	2.31E-02	1.92E-02

FLIGHT NO. C-360A FILTER NO. 4B
DIRECTIONAL PATH REFLECTANCE FROM GROUND TO ALTITUDE

ALTITUDE	ZENITH ANGLE OF PATH OF SIGHT (DEG)					
M	95	100	105	120	150	180
150	1.82E-01	7.06E-02	4.01E-02	1.31E-02	4.78E-03	4.33E-03
300	3.10E-01	1.17E-01	6.58E-02	2.12E-02	7.73E-03	6.98E-03
600	4.60E-01	1.68E-01	9.37E-02	3.02E-02	1.12E-02	1.02E-02
900	5.42E-01	1.95E-01	1.09E-01	3.54E-02	1.34E-02	1.24E-02
1200	6.19E-01	2.20E-01	1.22E-01	4.02E-02	1.55E-02	1.45E-02

FLIGHT NO. C-360A
DIRECTIONAL PATH REFLECTANCE FROM GROUND TO ALTITUDE
AZIMUTH OF PATH OF SIGHT = 90

(JOB 5990 DATE 05/21/75)
AZIMUTH OF PATH OF SIGHT = 90

FLIGHT NO. C-360A FILTER NO. 4A
DIRECTIONAL PATH REFLECTANCE FROM GROUND TO ALTITUDE

ALTITUDE	ZENITH ANGLE OF PATH OF SIGHT (DEG)					
M	95	100	105	120	150	180
150	1.05E-01	4.76E-02	3.05E-02	1.44E-02	7.75E-03	6.74E-03
300	1.43E-01	6.38E-02	4.06E-02	1.90E-02	1.02E-02	8.90E-03
600	2.13E-01	9.24E-02	5.84E-02	2.72E-02	1.46E-02	1.27E-02
900	2.86E-01	1.21E-01	7.62E-02	3.55E-02	1.91E-02	1.66E-02
1200	3.38E-01	1.41E-01	8.80E-02	4.10E-02	2.21E-02	1.92E-02

FLIGHT NO. C-360A FILTER NO. 4B
DIRECTIONAL PATH REFLECTANCE FROM GROUND TO ALTITUDE

ALTITUDE	ZENITH ANGLE OF PATH OF SIGHT (DEG)					
M	95	100	105	120	150	180
150	6.53E-02	2.95E-02	1.88E-02	8.92E-03	4.94E-03	4.33E-03
300	1.12E-01	4.89E-02	3.08E-02	1.45E-02	7.97E-03	6.98E-03
600	1.71E-01	7.21E-02	4.50E-02	2.10E-02	1.16E-02	1.02E-02
900	2.10E-01	8.71E-02	5.41E-02	2.53E-02	1.40E-02	1.24E-02
1200	2.50E-01	1.02E-01	6.29E-02	2.95E-02	1.64E-02	1.45E-02

FLIGHT NO. C-360A
DIRECTIONAL PATH REFLECTANCE FROM GROUND TO ALTITUDE
AZIMUTH OF PATH OF SIGHT = 180

(JOB 5990 DATE 05/21/75)
AZIMUTH OF PATH OF SIGHT = 180

FLIGHT NO. C-360A FILTER NO. 4A
DIRECTIONAL PATH REFLECTANCE FROM GROUND TO ALTITUDE

ALTITUDE	ZENITH ANGLE OF PATH OF SIGHT (DEG)					
M	95	100	105	120	150	180
150	1.46E-01	7.00E-02	4.68E-02	2.31E-02	9.90E-03	6.74E-03
300	1.99E-01	9.37E-02	6.23E-02	3.05E-02	1.31E-02	8.90E-03
600	3.04E-01	1.40E-01	9.22E-02	4.48E-02	1.89E-02	1.27E-02
900	4.34E-01	1.94E-01	1.27E-01	6.17E-02	2.52E-02	1.66E-02
1200	5.34E-01	2.34E-01	1.53E-01	7.39E-02	2.97E-02	1.92E-02

FLIGHT NO. C-360A FILTER NO. 4B
DIRECTIONAL PATH REFLECTANCE FROM GROUND TO ALTITUDE

ALTITUDE	ZENITH ANGLE OF PATH OF SIGHT (DEG)					
M	95	100	105	120	150	180
150	7.53E-02	3.58E-02	2.40E-02	1.29E-02	6.45E-03	4.33E-03
300	1.29E-01	5.93E-02	3.94E-02	2.09E-02	1.04E-02	6.98E-03
600	2.03E-01	9.07E-02	5.99E-02	3.18E-02	1.56E-02	1.02E-02
900	2.61E-01	1.14E-01	7.56E-02	4.04E-02	1.96E-02	1.24E-02
1200	3.23E-01	1.39E-01	9.19E-02	4.93E-02	2.37E-02	1.45E-02

FLIGHT NO. C-360A

DIRECTIONAL PATH REFLECTANCE FROM GROUND TO ALTITUDE

AZIMUTH OF PATH OF SIGHT = 270

(JOB 5990 DATE 05/21/75)
AZIMUTH OF PATH OF SIGHT = 270

FLIGHT NO. C-360A FILTER NO. 4A
DIRECTIONAL PATH REFLECTANCE FROM GROUND TO ALTITUDE

ALTITUDE	ZENITH ANGLE OF PATH OF SIGHT (DEG)					
M	95	100	105	120	150	180
150	1.01E-01	4.64E-02	2.99E-02	1.44E-02	7.88E-03	6.74E-03
300	1.38E-01	6.20E-02	3.98E-02	1.91E-02	1.04E-02	8.90E-03
600	2.06E-01	9.01E-02	5.74E-02	2.73E-02	1.49E-02	1.27E-02
900	2.78E-01	1.19E-01	7.51E-02	3.56E-02	1.94E-02	1.66E-02
1200	3.29E-01	1.38E-01	8.70E-02	4.11E-02	2.24E-02	1.92E-02

FLIGHT NO. C-360A FILTER NO. 4B
DIRECTIONAL PATH REFLECTANCE FROM GROUND TO ALTITUDE

ALTITUDE	ZENITH ANGLE OF PATH OF SIGHT (DEG)					
M	95	100	105	120	150	180
150	6.45E-02	2.92E-02	1.87E-02	8.96E-03	4.98E-03	4.33E-03
300	1.10E-01	4.84E-02	3.06E-02	1.45E-02	8.05E-03	6.98E-03
600	1.69E-01	7.14E-02	4.47E-02	2.11E-02	1.17E-02	1.02E-02
900	2.07E-01	8.62E-02	5.37E-02	2.54E-02	1.42E-02	1.24E-02
1200	2.47E-01	1.01E-01	6.25E-02	2.95E-02	1.66E-02	1.45E-02

FLIGHT C-360B – 28 JULY 1974 – DESCRIPTION OF FLIGHT AND WEATHER CHARACTERISTICS

It was a sunlit morning. There were scattered clouds on the horizon during the first flight profile, and it was clear during the second profile. The flight was conducted over flat grassy prairie surrounded by thick pine woods. The data-taking for the first profile, Filter 4A, started at 1704 GMT and continued until 1725 GMT. The data-taking for the second profile, Filter 4B, started at 1818 GMT and continued until 1833 GMT. The sun zenith angle during sky radiance data-taking for Filter 4A was 48.2 degrees at the beginning and 46.5 degrees at the end, and for Filter 4B it was 37.0 degrees at the beginning and 35.4 degrees at the end. The maximum altitude for the Filter 4A profile was 926 meters, and for the Filter 4B profile it was 990 meters. The average elevation of the terrain was 158 meters.

> The ground station reported clear, few cirrus on the horizon, and unlimited visibility.
>
> At the beginning of Flight C-360A, McChord Air Force Base was reporting 0.3 scattered cirrocumulus clouds at 25000 feet (7500 meters) and 15-mile (24-kilometer) visibility. At the same time, Gray Army Air Field was reporting scattered clouds at 15000 feet (4500 meters) and thin scattered clouds at 20000 feet (6000 meters) with 35-mile (56-kilometer) visibility. At the end of Flight C-360B, McChord Air Force Base was reporting 0.1 cirrocumulus at 20000 feet (6000 meters) and 15-mile (24-kilometer) visibility. Gray Army Air Field reported scattered clouds at 20000 feet (6000 meters) and 35-mile (56-kilometer) visibility.
>
> The flight log read light to moderate haze, with no significant clouds.

The surface charts showed a weak gradient with weak ridging in northwestern Washington. At 500 millibars there was a high in Utah with ridging to British Columbia. The winds were moderate westsouthwesterly. The airmass was continental polar.

These data were taken from the 3-hourly surface facsimile charts issued by the National Meteorological Center and obtained from the Lindbergh Field NOAA office. The 500-millibar charts were for 0000 GMT and 1200 GMT, and were obtained from the same source.

FLIGHT NO. C-360B

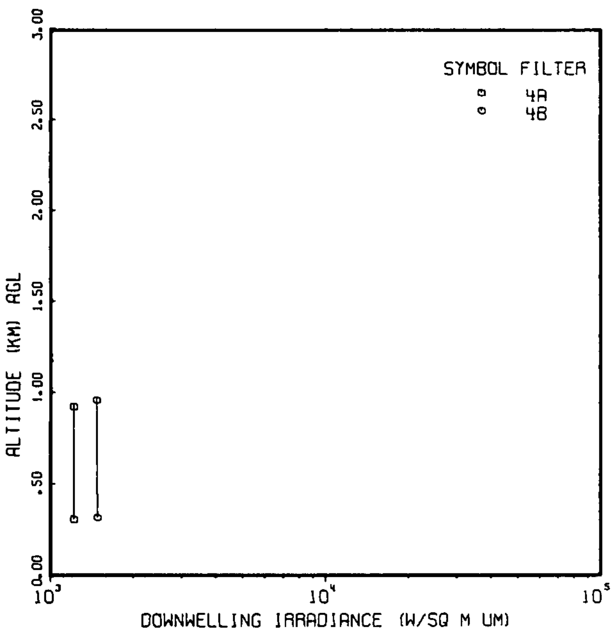

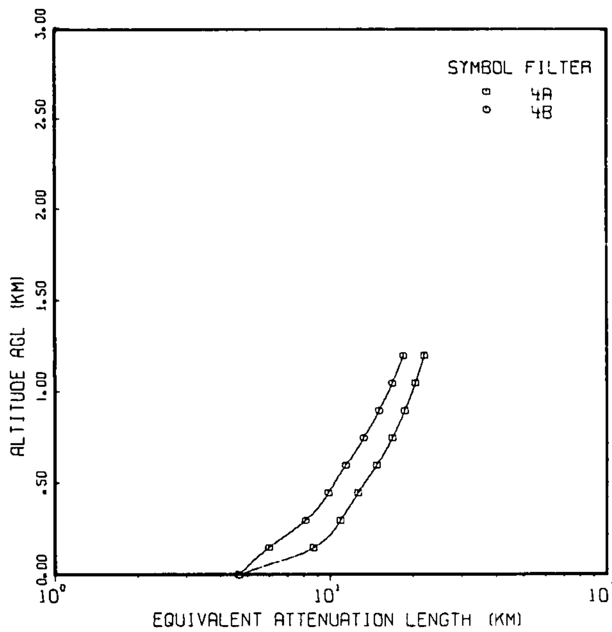

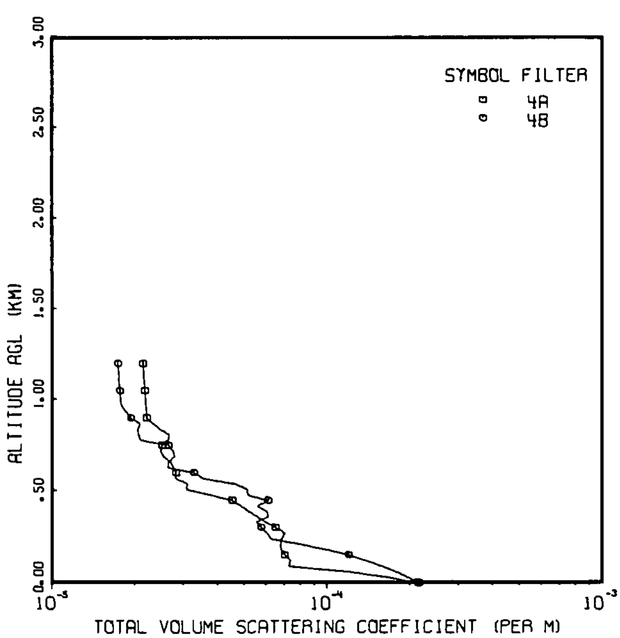

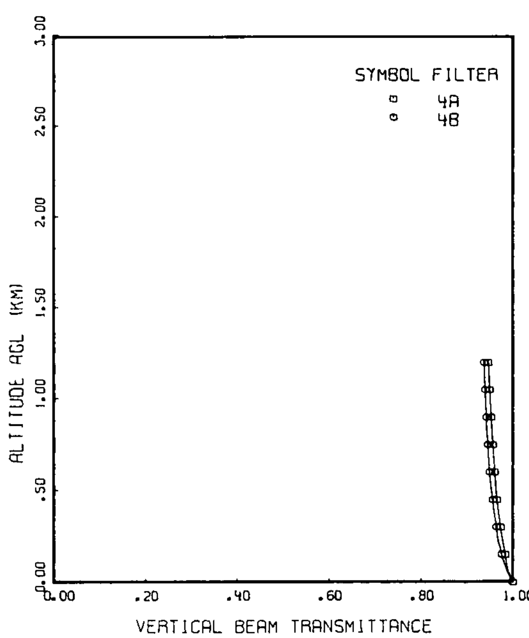

FLIGHT NO. C-360B

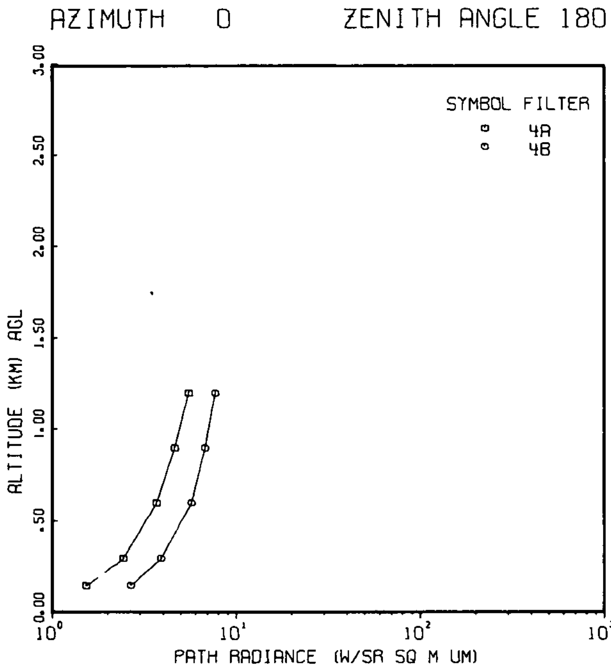

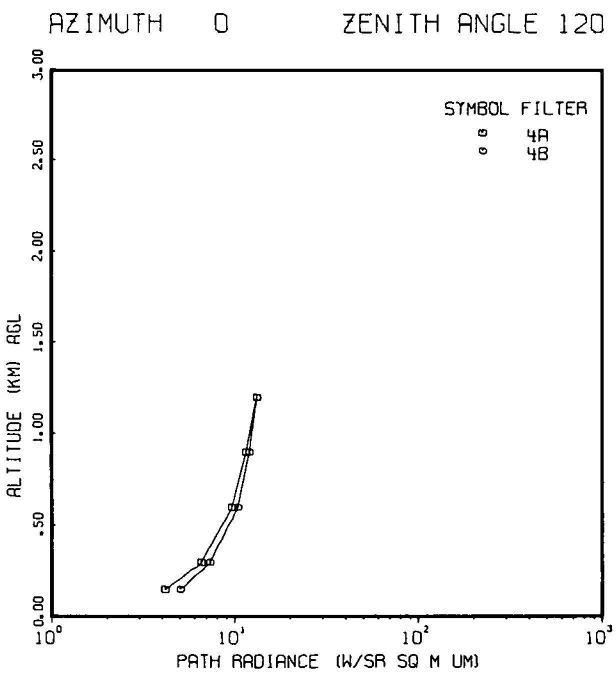

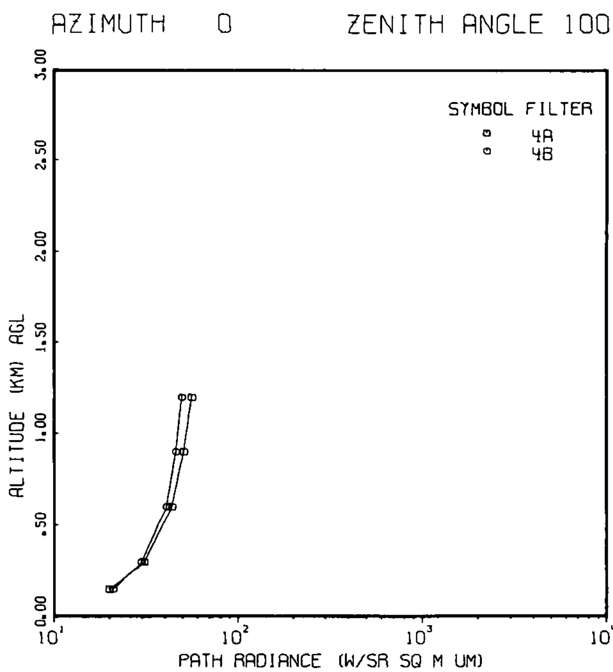

FLIGHT NO. C-360B

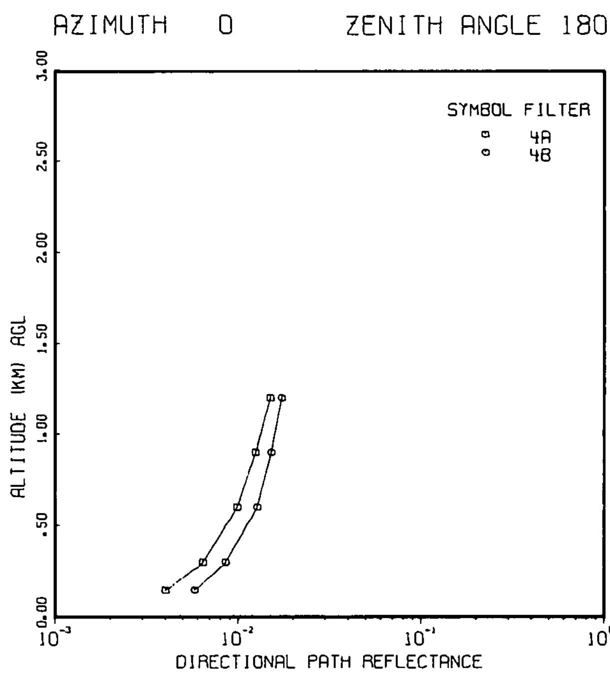

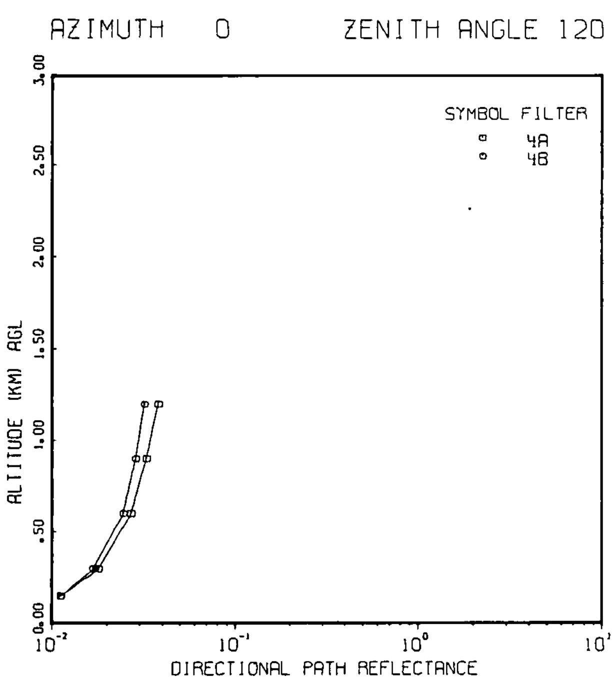

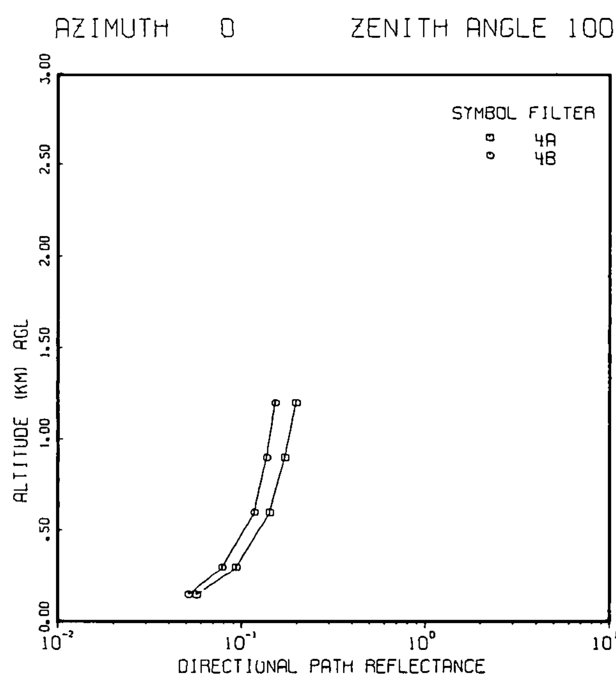

FLIGHT NO. C-360B
IRRADIANCE

(JOB 5691 DATE 05/15/75)

FLIGHT NO.C-360B FILTER NO. 4A SUN ZENITH ANGLE 47.3

IRRADIANCE (W/SQ M UM)

ALTITUDE (METERS)	DOWN-WELLING	UP-WELLING	ALBEDO	SCALAR SUN	SCALAR SKY	SCALAR UPWELLING	SCALAR TOTAL	SCALAR ALBEDO
311	1.22E 03	6.87E 01	.056	1.37E 03	6.17E 02	1.90E 02	2.18E 03	.096
926	1.21E 03	7.54E 01	.062	1.41E 03	6.19E 02	2.16E 02	2.25E 03	.106

FLIGHT NO.C-360B FILTER NO. 4B SUN ZENITH ANGLE 36.2

IRRADIANCE (W/SQ M UM)

ALTITUDE (METERS)	DOWN-WELLING	UP-WELLING	ALBEDO	SCALAR SUN	SCALAR SKY	SCALAR UPWELLING	SCALAR TOTAL	SCALAR ALBEDO
320	1.48E 03	8.[illegible]E 01	.054	1.44E 03	6.05E 02	1.72E 02	2.22E 03	.084
963	1.47E 03	8.69E 01	.059	1.48E 03	5.91E 02	2.10E 02	2.28E 03	.101

FLIGHT NO. C-360B
DIRECTIONAL REFLECTANCE OF TERRAIN

(JOB 5691 DATE 05/15/75)

FLIGHT NO. C-360B
AZIMUTH OF PATH OF SIGHT = 0
DIRECTIONAL REFLECTANCE OF TERRAIN

ZENITH ANGLE	FILTERS 4A	4B
95	.2965	.1377
100	.1740	.0683
105	.1281	.0553
120	.0627	.0261
150	.0329	.0593
180	.0340	.0343

FLIGHT NO. C-360B
AZIMUTH OF PATH OF SIGHT = 90
DIRECTIONAL REFLECTANCE OF TERRAIN

ZENITH ANGLE	FILTERS 4A	4B
95	.0967	.1476
100	.0710	.0644
105	.0773	.0405
120	.0420	.0290
150	.0367	.0537
180	.0340	.0343

FLIGHT NO. C-360B
AZIMUTH OF PATH OF SIGHT = 180
DIRECTIONAL REFLECTANCE OF TERRAIN

ZENITH ANGLE	FILTERS 4A	4B
95	.1180	.1655
100	.0859	.0614
105	.0829	.0606
120	.1[illegible]00	.0683
150	.0639	.1082
180	.0340	.0343

FLIGHT NO. C-360B
AZIMUTH OF PATH OF SIGHT = 270
DIRECTIONAL REFLECTANCE OF TERRAIN

ZENITH ANGLE	FILTERS 4A	4B
95	.1615	.1087
100	.0876	.0453
105	.0843	.038[illegible]
120	.0792	.0276
150	.0395	.1103
180	.0340	.0343

FLIGHT NO. C-360B
TOTAL VOLUME SCATTERING COEFFICIENT

(JOB 5691 DATE 5/15/75)
DATE 72874 FLIGHT NO. C-360B GROUND LEVEL ALTITUDE (M)= 158

ALTITUDE (M)	TOTAL VOLUME SCATTERING COEFFICIENT (PER M) FILTERS 4A	4B
0	2.15E-04	2,15E-04
30	1.67E-04	1,96E-04
60	1.26E-04	1,77E-04
90	7.25E-05	1,58E-04
120	7.36E-05	1,39E-04
150	7.01E-05	1,20E-04
180	6.79E-05	1,01E-04
210	6.79E-05	8,16E-05
240	6.84E-05	6,26E-05
270	7.06E-05	6,04E-05
300	6.49E-05	5,76E-05
330	5.98E-05	5,52E-05
360	5.57E-05	6,10E-05
390	5.18E-05	6,05E-05
420	4.86E-05	5,57E-05
450	4.52E-05	6,12E-05
480	3.80E-05	5,16E-05
510	3.09E-05	5,10E-05
540	3.16E-05	4,62E-05
570	2.81E-05	3,54E-05
600	2.83E-05	3,28E-05
630	2.76E-05	2,63E-05
660	2.69E-05	2,64E-05
690	2.54E-05	2,79E-05
720	2.48E-05	2,74E-05
750	2.51E-05	2,64E-05
780	2.64E-05	2,10E-05
810	2.66E-05	2,06E-05
840	2.46E-05	2,05E-05
870	2.33E-05	2,09E-05
900	2.21E-05	1,93E-05
930	2.20E-05	1,86E-05
960	2.20E-05	1,80E-05
990	2.19E-05	1,77E-05
1020	2.18E-05	1,77E-05
1050	2.18E-05	1,76E-05
1080	2.17E-05	1,76E-05
1110	2.16E-05	1,75E-05
1140	2.16E-05	1,75E-05
1170	2.15E-05	1,74E-05
1200	2.14E-05	1,74E-05
FIRST DATA ALT	0	0
LAST DATA ALT	900	990

FLIGHT NO. C-360B
BEAM TRANSMITTANCE FROM GROUND TO ALTITUDE

(JOB 5691 DATE 05/15/75)

FLIGHT NO. C-360B FILTER NO. 4A
BEAM TRANSMITTANCE FROM GROUND TO ALTITUDE

ALTITUDE M	ZENITH ANGLE OF PATH OF SIGHT (DEG) 95	100	105	120	150	180
150	8.20E-01	9.05E-01	9.35E-01	9.66E-01	9.80E-01	9.83E-01
300	7.28E-01	8.53E-01	8.99E-01	9.46E-01	9.69E-01	9.73E-01
600	6.25E-01	7.91E-01	8.55E-01	9.22E-01	9.54E-01	9.60E-01
900	5.71E-01	7.57E-01	8.30E-01	9.08E-01	9.46E-01	9.53E-01
1200	5.28E-01	7.29E-01	8.09E-01	8.96E-01	9.39E-01	9.47E-01

FLIGHT NO. C-360B FILTER NO. 4B
BEAM TRANSMITTANCE FROM GROUND TO ALTITUDE

ALTITUDE M	ZENITH ANGLE OF PATH OF SIGHT (DEG) 95	100	105	120	150	180
150	7.49E-01	8.65E-01	9.08E-01	9.51E-01	9.71E-01	9.75E-01
300	6.54E-01	8.08E-01	8.67E-01	9.29E-01	9.58E-01	9.64E-01
600	5.44E-01	7.39E-01	8.16E-01	9.00E-01	9.41E-01	9.49E-01
900	4.99E-01	7.08E-01	7.93E-01	8.87E-01	9.33E-01	9.42E-01
1200	4.67E-01	6.87E-01	7.77E-01	8.78E-01	9.27E-01	9.37E-01

FLIGHT NO. C-360B
PATH RADIANCE FROM GROUND TO ALTITUDE
AZIMUTH OF PATH OF SIGHT = 0

(JOB 5691 DATE 5/15/75)
AZIMUTH OF PATH OF SIGHT = 0

FLIGHT NO. C-360B FILTER NO. 4A
PATH RADIANCE FROM GROUND TO ALTITUDE (W/SR SQ M UM)

ALTITUDE	ZENITH ANGLE OF PATH OF SIGHT (DEG)					
M	95	100	105	120	150	180
150	4.49E 01	2.[illegible]E 01	1.17E 01	4.17E 00	1.64E 00	1.53E 00
300	6.75E 01	3.10E 01	1.83E 01	6.58E 00	2.60E 00	2.42E 00
600	9.19E 01	4.38E 01	2.63E 01	9.65E 00	3.90E 00	3.68E 00
900	1.04E 02	5.[illegible]7E 01	3.08E 01	1.16E 01	4.81E 00	4.62E 00
1200	1.12E 02	5.61E 01	3.45E 01	1.32E 01	5.65E 00	5.51E 00

FLIGHT NO. C-360B FILTER NO. 4B
PATH RADIANCE FROM GROUND TO ALTITUDE (W/SR SQ M UM)

ALTITUDE	ZENITH ANGLE OF PATH OF SIGHT (DEG)					
M	95	100	105	120	150	180
150	4.45E 01	2.10E 01	1.26E 01	5.03E 00	2.51E 00	2.66E 00
300	6.16E 01	2.99E 01	1.81E 01	7.32E 00	3.66E 00	3.89E 00
600	8.1[illegible]E 01	4.10E 01	2.52E 01	1.04E 01	5.30E 00	5.70E 00
900	8.91E 01	4.59E 01	2.86E 01	1.20E 01	6.21E 00	6.77E 00
1200	9.47E 01	4.95E 01	3.11E 01	1.33E 01	6.96E 00	7.67E 00

FLIGHT NO. C-360B
PATH RADIANCE FROM GROUND TO ALTITUDE
AZIMUTH OF PATH OF SIGHT = 90

(JOB 5691 DATE 5/15/75)
AZIMUTH OF PATH OF SIGHT = 90

FLIGHT NO. C-360B FILTER NO. 4A
PATH RADIANCE FROM GROUND TO ALTITUDE (W/SR SQ M UM)

ALTITUDE	ZENITH ANGLE OF PATH OF SIGHT (DEG)					
M	95	100	105	120	150	180
150	1.94E 01	9.68E 00	6.36E 00	3.09E 00	1.73E 00	1.53E 00
300	2.92E 01	1.50E 01	9.94E 00	4.88E 00	2.74E 00	2.42E 00
600	4.07E 01	2.17E 01	1.46E 01	7.27E 00	4.14E 00	3.68E 00
900	4.76E 01	2.59E 01	1.76E 01	8.92E 00	5.16E 00	4.62E 00
1200	5.35E 01	2.97E 01	2.03E 01	1.04E 01	6.12E 00	5.51E 00

FLIGHT NO. C-360B FILTER NO. 4B
PATH RADIANCE FROM GROUND TO ALTITUDE (W/SR SQ M UM)

ALTITUDE	ZENITH ANGLE OF PATH OF SIGHT (DEG)					
M	95	100	105	120	150	180
150	2.70E 01	1.37E 01	9.11E 00	4.54E 00	2.81E 00	2.66E 00
300	3.72E 01	1.95E 01	1.31E 01	6.59E 00	4.10E 00	3.89E 00
600	4.94E 01	2.71E 01	1.85E 01	9.48E 00	5.97E 00	5.70E 00
900	5.53E 01	3.09E 01	2.13E 01	1.11E 01	7.05E 00	6.77E 00
1200	5.98E 01	3.39E 01	2.35E 01	1.23E 01	7.95E 00	7.67E 00

FLIGHT NO. C-360B
PATH RADIANCE FROM GROUND TO ALTITUDE
AZIMUTH OF PATH OF SIGHT = 180

(JOB 5691 DATE 5/15/75)
AZIMUTH OF PATH OF SIGHT = 180

FLIGHT NO. C-360B FILTER NO. 4A
PATH RADIANCE FROM GROUND TO ALTITUDE (W/SR SQ M UM)

ALTITUDE	ZENITH ANGLE OF PATH OF SIGHT (DEG)					
M	95	100	105	120	150	180
150	2.15E 01	1.14E 01	7.95E 00	4.64E 00	2.45E 00	1.53E 00
300	3.24E 01	1.76E 01	1.24E 01	7.32E 00	3.88E 00	2.42E 00
600	4.63E 01	2.62E 01	1.88E 01	1.13E 01	5.99E 00	3.68E 00
900	5.65E 01	3.28E 01	2.38E 01	1.45E 01	7.73E 00	4.62E 00
1200	6.60E 01	3.91E 01	2.87E 01	1.77E 01	9.43E 00	5.51E 00

FLIGHT NO. C-360B FILTER NO. 4B
PATH RADIANCE FROM GROUND TO ALTITUDE (W/SR SQ M UM)

ALTITUDE	ZENITH ANGLE OF PATH OF SIGHT (DEG)					
M	95	100	105	120	150	180
150	2.68E 01	1.46E 01	1.03E 01	6.06E 00	4.06E 00	2.66E 00
300	3.70E 01	2.[illegible]8E 01	1.48E 01	8.80E 00	5.94E 00	3.89E 00
600	5.02E 01	2.94E 01	2.13E 01	1.30E 01	8.80E 00	5.70E 00
90	5.76E 01	3.43E 01	2.51E 01	1.56E 01	1.06E 01	6.77E 00
1200	6.38E 01	3.85E 01	2.84E 01	1.79E 01	1.22E 01	7.67E 00

FLIGHT NO. C-360B
PATH RADIANCE FROM GROUND TO ALTITUDE
AZIMUTH OF PATH OF SIGHT = 270

(JOB 5691 DATE 05/15/75)
AZIMUTH OF PATH OF SIGHT = 270

FLIGHT NO. C-360B FILTER NO. 4A
PATH RADIANCE FROM GROUND TO ALTITUDE (W/SR SQ M UM)

ALTITUDE	ZENITH ANGLE OF PATH OF SIGHT (DEG)					
M	95	100	105	120	150	180
150	1.91E 01	9.57E 00	6.32E 00	3.11E 00	1.74E 00	1.53E 00
300	2.87E 01	1.48E 01	9.88E 00	4.90E 00	2.75E 00	2.42E 00
600	4.00E 01	2.14E 01	1.45E 01	7.30E 00	4.16E 00	3.68E 00
900	4.69E 01	2.57E 01	1.75E 01	8.97E 00	5.19E 00	4.62E 00
1200	5.28E 01	2.94E 01	2.02E 01	1.05E 01	6.16E 00	5.51E 00

FLIGHT NO. C-360B FILTER NO. 4B
PATH RADIANCE FROM GROUND TO ALTITUDE (W/SR SQ M UM)

ALTITUDE	ZENITH ANGLE OF PATH OF SIGHT (DEG)					
M	95	100	105	120	150	180
150	2.59E 01	1.32E 01	8.84E 00	4.48E 00	2.85E 00	2.66E 00
300	3.57E 01	1.88E 01	1.27E 01	6.52E 00	4.16E 00	3.89E 00
600	4.77E 01	2.62E 01	1.80E 01	9.39E 00	6.06E 00	5.70E 00
900	5.36E 01	3.30E 01	2.07E 01	1.10E 01	7.15E 00	6.77E 00
1200	5.81E 01	3.31E 01	2.36E 01	1.23E 01	8.06E 00	7.67E 00

FLIGHT NO. C-360B
DIRECTIONAL PATH REFLECTANCE FROM GROUND TO ALTITUDE
AZIMUTH OF PATH OF SIGHT = 0

(JOB 5691 DATE 5/15/75)
AZIMUTH OF PATH OF SIGHT = 0

FLIGHT NO. C-360B FILTER NO. 4A
DIRECTIONAL PATH REFLECTANCE FROM GROUND TO ALTITUDE

ALTITUDE	ZENITH ANGLE OF PATH OF SIGHT (DEG)					
M	95	100	105	120	150	180
150	1.41E-01	5.70E-02	3.23E-02	1.11E-02	4.33E-03	4.02E-03
300	2.39E-01	9.37E-02	5.25E-02	1.80E-02	6.94E-03	6.44E-03
600	3.80E-01	1.43E-01	7.94E-02	2.70E-02	1.06E-02	9.90E-03
900	4.69E-01	1.73E-01	9.59E-02	3.29E-02	1.31E-02	1.25E-02
1200	5.50E-01	1.99E-01	1.1 E-01	3.81E-02	1.56E-02	1.50E-02

FLIGHT NO. C-360B FILTER NO. 4B
DIRECTIONAL PATH REFLECTANCE FROM GROUND TO ALTITUDE

ALTITUDE	ZENITH ANGLE OF PATH OF SIGHT (DEG)					
M	95	100	105	120	150	180
150	1.26E-01	5.16E-02	2.94E-02	1.12E-02	5.47E-03	5.78E-03
300	[illegible]	7.85E-02	4.43E-02	1.67E-02	8.11E-03	8.56E-03
600	3.16E-01	1.18E-01	6.55E-02	2.46E-02	1.20E-02	1.27E-02
900	[illegible]	1.38E-01	7.64E-02	2.87E-02	1.41E-02	1.52E-02
120	[illegible]	1.53E-01	8.48E-02	3.20E-02	1.59E-02	1.74E-02

FLIGHT NO. C-360B
DIRECTIONAL PATH REFLECTANCE FROM GROUND TO ALTITUDE
AZIMUTH OF PATH OF SIGHT = 90

(JOB 5691 DATE 05/15/75)
AZIMUTH OF PATH OF SIGHT = 90

FLIGHT NO. C-360B FILTER NO. 4A
DIRECTIONAL PATH REFLECTANCE FROM GROUND TO ALTITUDE

ALTITUDE	ZENITH ANGLE OF PATH OF SIGHT (DEG)					
M	95	100	105	120	150	180
150	6.12E-02	2.76E-02	1.76E-02	8.27E-03	4.55E-03	4.02E-03
300	1.04E-01	4.54E-02	2.85E-02	1.33E-02	7.30E-03	6.44E-03
600	1.68E-01	7.07E-02	4.40E-02	2.04E-02	1.12E-02	9.90E-03
900	2.15E-01	8.85E-02	5.48E-02	2.54E-02	1.41E-02	1.25E-02
1200	2.62E-01	1.05E-01	6.48E-02	3.01E-02	1.68E-02	1.50E-02

FLIGHT NO. C-360B FILTER NO. 4B
DIRECTIONAL PATH REFLECTANCE FROM GROUND TO ALTITUDE

ALTITUDE	ZENITH ANGLE OF PATH OF SIGHT (DEG)					
M	95	100	105	120	150	180
150	7.64E-02	3.36E-02	2.13E-02	1.01E-02	6.13E-03	5.78E-03
300	1.21E-01	5.12E-02	3.21E-02	1.51E-02	9.07E-03	8.56E-03
600	1.93E-01	7.78E-02	4.80E-02	2.23E-02	1.35E-02	1.27E-02
900	2.35E-01	9.27E-02	5.69E-02	2.65E-02	1.60E-02	1.52E-02
1200	2.72E-01	1.05E-01	6.41E-02	2.98E-02	1.82E-02	1.74E-02

FLIGHT NO. C-360B
DIRECTIONAL PATH REFLECTANCE FROM GROUND TO ALTITUDE
AZIMUTH OF PATH OF SIGHT = 180

(JOB 5691 DATE 05/15/75)
AZIMUTH OF PATH OF SIGHT = 180

FLIGHT NO. C-360B FILTER NO. 4A
DIRECTIONAL PATH REFLECTANCE FROM GROUND TO ALTITUDE

ALTITUDE	ZENITH ANGLE OF PATH OF SIGHT (DEG)					
M	95	100	105	120	150	180
150	6.78E-02	3.25E-02	2.20E-02	1.24E-02	6.45E-03	4.02E-03
300	1.15E-01	5.34E-02	3.57E-02	2.00E-02	1.03E-02	6.44E-03
600	1.91E-01	8.55E-02	5.68E-02	3.16E-02	1.62E-02	9.90E-03
900	2.56E-01	1.12E-01	7.41E-02	4.13E-02	2.11E-02	1.25E-02
1200	3.23E-01	1.38E-01	9.15E-02	5.11E-02	2.60E-02	1.50E-02

FLIGHT NO. C-360B FILTER NO. 4B
DIRECTIONAL PATH REFLECTANCE FROM GROUND TO ALTITUDE

ALTITUDE	ZENITH ANGLE OF PATH OF SIGHT (DEG)					
M	95	100	105	120	150	180
150	7.60E-02	3.58E-02	2.41E-02	1.35E-02	8.88E-03	5.78E-03
300	1.20E-01	5.45E-02	3.63E-02	2.01E-02	1.31E-02	8.56E-03
600	1.96E-01	8.44E-02	5.54E-02	3.06E-02	1.98E-02	1.27E-02
900	2.45E-01	1.03E-01	6.72E-02	3.73E-02	2.41E-02	1.52E-02
1200	2.90E-01	1.19E-01	7.75E-02	4.32E-02	2.79E-02	1.74E-02

FLIGHT NO. C-360B
DIRECTIONAL PATH REFLECTANCE FROM GROUND TO ALTITUDE
AZIMUTH OF PATH OF SIGHT = 270

(JOB 5691 DATE [illegible]8/15/75)
AZIMUTH OF PATH OF SIGHT = 270

FLIGHT NO. C-360B FILTER NO. 4A
DIRECTIONAL PATH REFLECTANCE FROM GROUND TO ALTITUDE

ALTITUDE	ZENITH ANGLE OF PATH OF SIGHT (DEG)					
M	95	100	105	120	150	180
150	6.01E-02	2.73E-02	1.75E-02	8.30E-03	4.57E-03	4.02E-03
300	1.02E-01	4.49E-02	2.84E-02	1.34E-02	7.33E-03	6.44E-03
600	1.65E-01	7.[illegible]E-02	4.38E-02	2.05E-02	1.13E-02	9.90E-03
900	2.12E-01	8.76E-02	5.45E-02	2.55E-02	1.42E-02	1.25E-02
1200	2.58E-01	1.04E-01	6.46E-02	3.02E-02	1.69E-02	1.50E-02

FLIGHT NO. C-360B FILTER NO. 4B
DIRECTIONAL PATH REFLECTANCE FROM GROUND TO ALTITUDE

ALTITUDE	ZENITH ANGLE OF PATH OF SIGHT (DEG)					
M	95	100	105	120	150	180
150	7.34E-02	3.24E-02	2.07E-02	1.00E-02	6.22E-03	5.78E-03
300	1.16E-01	4.94E-02	3.11E-02	1.49E-02	9.21E-03	8.56E-03
600	1.86E-01	7.53E-02	4.67E-02	2.21E-02	1.37E-02	1.27E-02
900	2.28E-01	9.00E-02	5.55E-02	2.62E-02	1.63E-02	1.52E-02
1200	2.64E-01	1.02E-01	6.27E-02	2.97E-02	1.84E-02	1.74E-02

8. DATA INTERPRETATION AND EVALUATION

8.1 METEOROLOGICAL DATA

The basic discussion of meteorological conditions, as presented in Section 6 and summarized with each flight description, is based upon meteorological data reported for McChord Air Force Base and Gray Army Air Field. It should be remembered that the test site was 20 miles from McChord Air Force Base and 13 miles from Gray Army Air Field, so that the reports of visibility or cloud conditions may vary slightly from the conditions encountered along the flight tracks.

CLOUD CONDITIONS

The airborne pictures which documented the cloud conditions during each flight were examined, and their general features are summarized in Table 8-1. The descriptions are divided into five categories. Since all lower sky pictures were free of clouds, the lower hemisphere characteristics are not included in that table.

The sky and sun radiance and downwelling irradiance data for the flight profiles in categories 1 and 2 are quite consistent, thus the path radiances and path reflectances for these flights were readily derivable. The sun component for categories 3 through 5, however, showed more variability. Consequently, the derived path radiance and path reflectance values in these three categories are for an average illumination condition, between those encountered at the low and high altitude, for each profile.

TEMPERATURE

The temperature measurements were made using the AN/AMQ-17 aerograph set. Unfortunately, it is one of the instruments that appears to have had an offset in its recorded millivolt signal. As a result, the temperatures reported in Section 6 may be about 2 degrees Celsius low. The cause of the offset is currently being investigated in order to measure and eliminate the error. Comparison of temperatures measured at low altitudes with values reported on the ground at McChord Air Force Base and Gray Army Air Field at comparable times indicates the low altitude temperatures to be averaging 3 degrees Celsius lower. On the basis of the standard temperature lapse rate for the 45° N. July Standard Atmosphere Supplement, only 1.5 degrees lower would have been predicted.

Table 8-1

Airborne Hemispherical Picture Summary

Category	Upper Sky Description	Flight Profiles
1	Clear	C-351 4A and 4B C-352 4B C-360B 4B
2	Scattered clouds; sun unobscured	C-352 4A C-357 4A and 4B C-360A 4A and 4B C-360B 4A
3	Broken clouds; sun partially obscured	C-359 4A and 4B
4	Overcast; sun partially obscured	C-358 4A and 4B
5	Overcast; sun fully obscured	C-354 4A and 4B

There were seven project flights, yielding the 16 flight profiles listed in Table 8-1, accomplished during July 1974 at 46.9°N. latitude. Temperature data measured during these flights can be profitably compared to equivalent data from the U. S. Standard Atmosphere Supplements. To facilitate this comparison, the average temperature profile measured during each of the seven flights has been superimposed on a graph of the temperatures anticipated for July in Fig. 8-1. The anticipated temperature profiles are for 45° and 60°N latitude in July, and 45°N. latitude in spring/fall as specified in the U. S. Standard Atmosphere Supplements (1966). The altitude scale in Fig. 8-1 is kilometers above mean sea level (MSL), and the ground elevation at the test site was 158 meters.

The temperatures for all the flights but C-360 tend to lie below the curve for 45°N. July and above the curves for 60°N. July and 45°N. spring/fall. On Flight C-360 the temperature indicates the base of an inversion at about 0.45 kilometer. Above 0.50 kilometer the temperature for C-360 remains nearly constant or increases to the highest altitude rather than decreasing with altitude at the normal lapse rate. Since the curve for July 45°N. is not an upper limit but an average for July, the measured temperatures appear to be reasonable, although possibly 2 degrees low as noted above.

As reported in Duntley *et al.* (1973 and 1974), the temperature profile shape does not appear to correlate with the presence or absence of clouds.

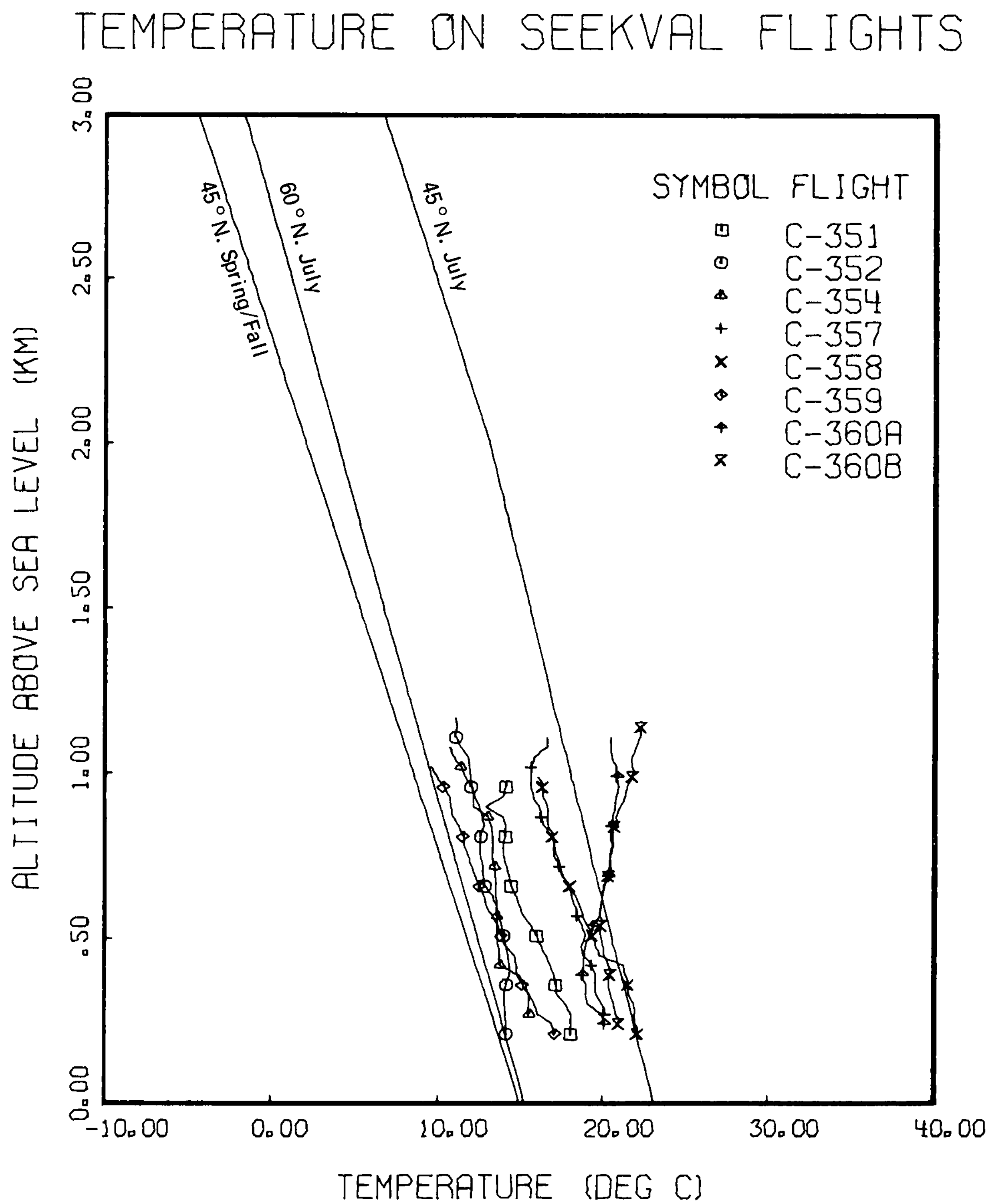

Fig. 8-1. Temperature for SEEKVAL Flights Compared to 45° N. July, 60° N. July, and 45° N. Spring/Fall Temperatures from the U. S. Standard Atmosphere Supplements.

RELATIVE HUMIDITY

Relative humidity was computed from the measured values of ambient temperature and dewpoint temperature. The dewpoint temperatures were measured using the modified Cambridge hygrometer system [Duntley, *et al.* (1972c)] and are the first data reported since the modification was completed. The dewpoint temperatures measured at low altitudes compare well with the values reported by McChord Air Force Base and Gray Army Air Field.

The computed relative humidities reported in Section 6 are probably slightly high because of the previously mentioned error of approximately −2 degrees Celsius in the measured ambient temperature. Comparison of the relative humidities computed for low altitudes with the ground-level values reported at McChord and Gray at comparable times indicated the computed relative humidities to be slightly higher in most cases.

The average relative humidity profile for each of the double profiles listed in Table 8-1 is depicted in Fig. 8-2. Note that the altitude scale is above ground level (AGL), rather than above mean sea level (MSL).

The relative humidity varied more between flights at high altitudes than at low altitudes. At the two extremes are Flights C-359 and C-360B. C-359 started at low altitude with a relatively high humidity of around 70 and increased to humidities around 90 at the higher altitudes. C-360B had humidities of around 60 at the lower altitudes and decreased to values in the twenties and thirties at the higher altitudes.

8.2 AIRBORNE RADIOMETRIC DATA

TOTAL VOLUME SCATTERING COEFFICIENT

During much of the Project SEEKVAL deployment, the integrating nephelometer projector system was optically contaminated, resulting in a severe loss of data. Consequently, valid measurements of total volume scattering coefficient are not available for flights preceding C-359. Therefore, in order to derive the atmospheric optical properties for these flights, it was necessary to determine the equivalent values of volume attenuation coefficient using Eq. 8.1. The general procedure, which is basically a two-stage approximation for the most probable value of equilibrium radiance coupled with the best available measurement of path function, is described in the following paragraphs.

Derivation from Measured Data. When valid measurements of total volume scattering coefficient $s(z)$ are not available, the volume attenuation coefficient $\alpha(z)$, which is equal to $s(z)$ in the absence of absorption, can be readily derived if one has measurements of path function $N_*(z,\theta,\phi)$ and equilibrium radiance $N_q(z,\theta,\phi)$. The defining relationship is

$$\alpha(z) = N_*(z,\theta,\phi)/N_q(z,\theta,\phi) \quad . \tag{8.1}$$

The measured data from the airborne variable path function meter filled the requirements for the first property, but the necessary values for equilibrium radiance were not as readily available.

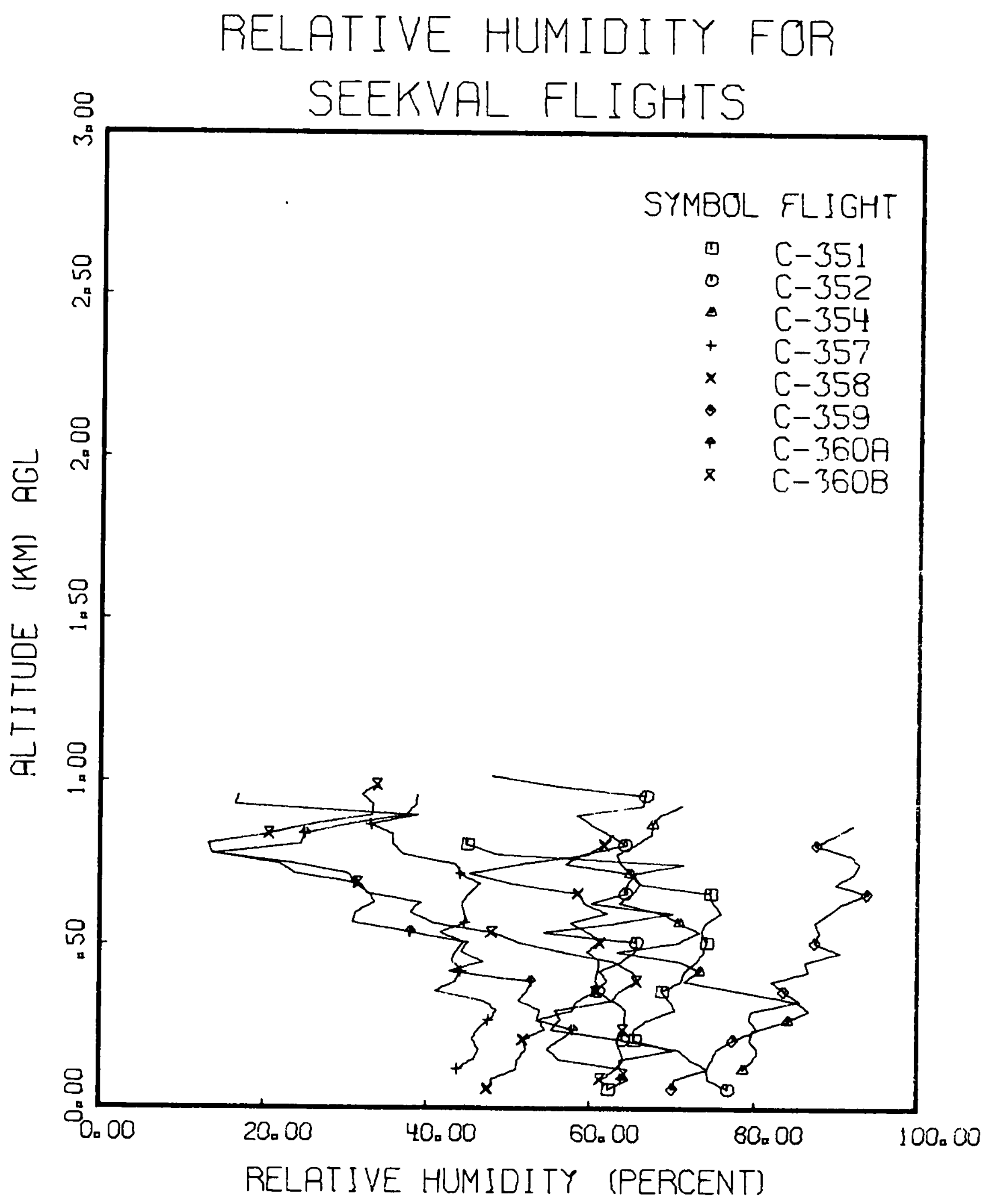

Fig. 8-2. Relative Humidity for SEEKVAL Flights.

Since valid measurements of equilibrium radiance were not always accomplished on each SEEKVAL flight, the equilibrium radiances required for use with Eq. 8.1 were computed. There are several general advantages gained from using computed values of equilibrium radiance rather than measured values. First among them, a computed value can be determined for any path of sight, whereas a measured value can be determined only for horizontal paths. Second and most important, considering the SEEKVAL weather conditions, computed values are valid for all real radiance arrays representing clear, hazy, or cloudy skies, whereas measurements of horizontal equilibrium radiance can be made only when the horizon is completely cloud-free and uncluttered.

All equilibrium radiance computations were restricted to the use of the sky radiance measurements made only during the straight and level flight elements for several reasons. The two most significant were related to ensuring the quality of the path function measurement which would subsequently be used with the equilibrium radiance in Eq. 8.1: First, during the ST & LV flight elements the lighting distribution, i.e., the sun, sky, and terrain radiances, was measured simultaneously with the path function measurements, thus eliminating errors that might be introduced by a nonsimultaneity of measurement. Second, during the ST & LV flight elements, the path function meter (VPFM) was visually verified as being in the correct horizontal orientation. Thus, errors in the VPFM orientation readout channel were readily corrected. During the ascent and descent (V-PRO) flight elements, however, the position of the path function meter was variable, and inclined. To use these data in Eq. 8.1 required a measurement of the VPFM orientation analog which was beyond the precision and accuracy capability of the system.

The two-stage approximation for each flight profile's most probable value of equilibrium radiance was accomplished in the following manner.

The first approximation of equilibrium radiance was computed from scalar irradiances and an approximate volume scattering function as in Gordon (1969), Eq. 21, which is repeated here as Eq. 8.2:

$$N_q(z,\theta,\phi) \;=\; {}_sh(z)\,\sigma(z,\beta)\,/\,s(z) + [\,{}_kh(z,d) + h(z,u)]\,/\,4\pi \;. \tag{8.2}$$

For this computation, the scalar sun irradiance ${}_sh(z)$, the scalar sky irradiance ${}_kh(z,d)$, and the scalar upwelling irradiance $h(z,u)$ were calculated from the measured upper and lower hemisphere radiances determined during each straight and level (ST & LV) flight segment. The Barteneva (1960) class 4 values for the proportional volume scattering function were used as a reasonable first estimate, since the class 4 values are applicable to photopic attenuation coefficients throughout the range of $3.0E{-}5\,m^{-1}$ to $1.5E{-}4\,m^{-1}$.

A first approximation of attenuation coefficient $\alpha(z)$ was then calculated using the results from Eq. 8.2, an appropriate measurement of path function, and Eq. 8.1. This value of attenuation coefficient was then used to select the most probable Barteneva scattering function appropriate for the sample aerosol. The relationship of the Barteneva catalog of directional volume scattering functions to the total volume scattering coefficient (or attenuation coefficient in the absence of absorption) is described in Section 2.1.

The second approximation of equilibrium radiance utilized Eq. 2.22, repeated here as Eq. 8.3:

$$N_q(z,\theta,\phi) = {}_s h(z) \frac{\sigma(z,\beta)}{s(z)} + \int_{4\pi} N(z,\theta',\phi') \frac{\sigma(z,\beta')}{s(z)} \, d\Omega \ . \tag{8.3}$$

For this computation, the upper and lower hemisphere radiance arrays were edited as discussed in Sections 2 and 5 to yield the most realistic representation of the actual radiance distribution as possible. The directional volume scattering function $\sigma(z,\beta)/s(z)$ was selected on the basis of the Barteneva catalog and the initial approximation of attenuation coefficient. The evaluation of Eq. 8.3 was accomplished by means of the computer program AVIZC130 which is capable of utilizing all of the equations and methods described in Section 2.1.

A second approximation of attenuation coefficient $\alpha(z)$ was then determinable using the results from Eq. 8.3, an appropriate measurement of path function, and Eq. 8.1. Comparisons between the first and second approximations of attenuation coefficient indicated the differences to be small. Thus, no further iterations of the procedure were deemed necessary.

In order to utilize the path function data taken during ascent or descent to obtain the attenuation coefficient as a function of altitude, it was necessary to establish a value of equilibrium radiance $N_q(z,\theta'',\phi'')$ appropriate for that time/space interval and path function orientation. This equilibrium radiance was computed using the second approximation of attenuation coefficient $\alpha(z)$ and the path function $N_*(z,\theta'',\phi'')$ measured during the vertical profile flight element connecting each pair of straight and level flight elements, at the time the aircraft passed through each straight and level altitude z:

$$N_q(z,\theta'',\phi'') = N_*(z,\theta'',\phi'')/\alpha(z) \ . \tag{8.4}$$

After equilibrium radiance was computed for each of the two endpoint straight and level altitudes, these values were averaged. This average equilibrium radiance value was then used in Eq. 8.1 for computing the volume attenuation coefficient as a function of altitude from the path function data measured during the vertical profile.

This indirect method for obtaining the volume attenuation coefficient during the vertical profile flight element can be used only if the lighting distribution is relatively constant during that time/space interval because it is essential that the variation in measured path function be dependent solely upon variations in aerosol characteristics. Downwelling irradiance measured during the vertical profile flight element was used as an indicator of the constancy or variability of the lighting distribution.

Of the 10 flights completed during the SEEKVAL deployment, three were unusable due to their highly variable lighting conditions. Flight C-359, although possessing highly variable lighting, yielded valid nephelometer data and was therefore suitable for inclusion in this report. The remaining six flights, listed in Table 7-2, all had relatively stable lighting conditions during their vertical profile elements and thus their data were appropriate for use with the indirect method.

Validation of Method. On two of the double profiles, C-360A and C-360B, there was both stability of lighting, which permitted using the indirect method for determining $\alpha(z)$, and valid nephelometer data. This fortuitous situation was therefore used as a test case to validate the indirect procedure.

Using Eq. 8.1, the attenuation coefficient at each straight and level altitude was determined first from the straight and level path function measurements and the computed values of equilibrium radiance and second from the ascent and descent path function measurements and the averaged value of computed equilibrium radiance. These values of attenuation coefficient were then divided by the total scattering coefficient measured by the nephelometer at the comparable time and altitude. These ratios are depicted in Fig. 8-3 as a function of the measured total scattering coefficient.

Fortunately, Flight C-360 contained a wide range of values for total scattering coefficient even though the overall altitude interval was relatively short. In the total scattering coefficient range from 3.2E-5 to 8.4E-5, the ratios were all relatively close to 1, i.e., small error in the attenuation coefficient, but the ratios were large for all of the very low scattering coefficients encountered at the higher altitudes.

When the ratio, or potential error, is graphed as a function of the derived attenuation coefficient, the relationship is not as clear-cut, but values of attenuation coefficient above 5 E-5 are all still in the low error range. All the attenuation coefficients for Flights C-351 and C-358 are in the low error range. For the other three flights, C-352, C-354, and C-357, values of attenuation coefficient are also in the low error range, if one makes an assumption about data consistency within the flights. The necessary assumption is the following: If one attenuation coefficient is in the low error range for a given flight at a given altitude and time, the coefficient for the same altitude but different time is more likely to be of similar value than radically lower.

The error in path function measurement at low total scattering coefficients (very clear air), indicated by Fig. 8-3, should be eliminated to a large degree by modifications to the variable path function meter which were devised and implemented subsequent to the SEEKVAL deployment.

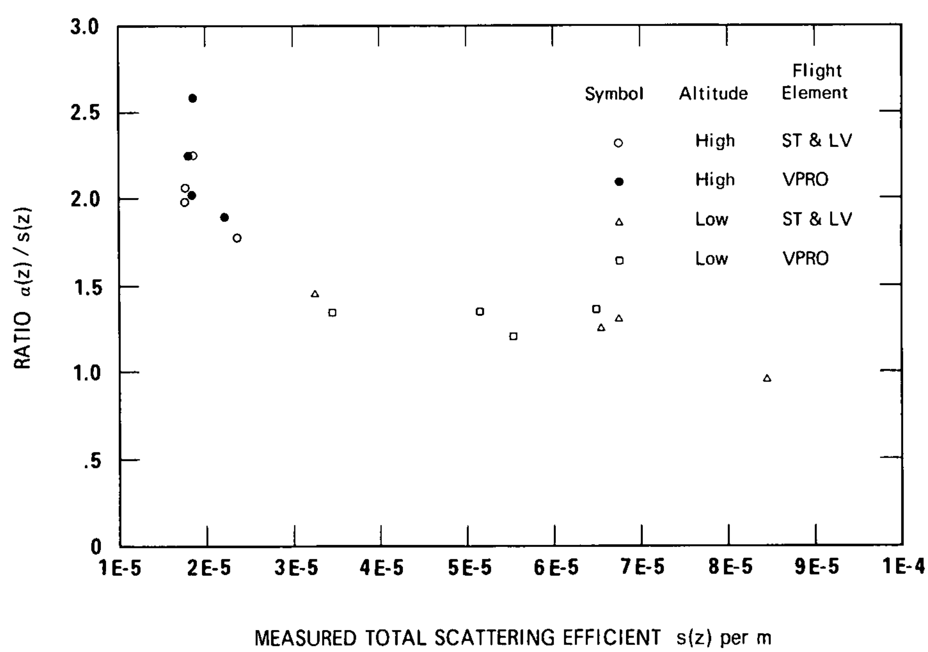

Fig. 8-3. Ratio of Derived Attenuation Coefficient to Measured Total Scattering Coefficient as a Function of the Measured Value for Flights C-360A and C-360B.

General Evaluation. In 13 of the profiles in this report, the vertical profile data were taken in the normal sequence between the low and high altitude straight and level elements. For the remaining three profiles, C-354 Filter 4B, C-360A Filter 4B, and C-360B Filter 4A, the vertical profile data were taken following the two straight and level flight elements. The average elapsed time between the start of the first element and the end of the final element in each profile was 19 minutes.

Generally, it was possible to take airborne data down to 360 meters and occasionally as low as 60 meters. To extend the profile data to ground level, the ground-based nephelometer data are normally used for the interpolation. During SEEKVAL, these ground-based values were always significantly greater than the low altitude values so that the linear interpolation from the lowest altitude airborne datum to the ground-based value is readily apparent on the graphs of total scattering coefficient as a function of altitude.

Airborne data were generally taken up to 870 meters. (The highest altitude during the vertical profile elements varied between 660 and 1020 meters as indicated at the bottom of the tabulations of total scattering coefficient in Section 7.3.) The extrapolation upward to 1200 meters is based on the density ratios of the U.S. Standard Atmosphere (45°N. spring/fall), and it appears on the graphs of total scattering coefficient as a slightly slanting straight line ending at 1200 meters. The extrapolating line follows the general trend of the data for Flights C-352, C-354, C-357, C-358, and C-359. For C-351, the upper altitude data indicate the edge of a haze layer, but because it is not certain that the top of the haze layer was reached at the highest altitude of measurement, the extrapolated values are possibly high. For C-360, three of the profiles reach a common value at the higher altitudes so the top of the haze may indeed have been reached, but the upward extrapolation for C-360B Filter 4A is also probably high.

To more easily compare the scattering characteristics of the seven flights, the Filter 4A (pseudo-photopic) total scattering coefficient profiles for each flight have been graphed in Fig. 8-4. (The curve for C-357, however, is for Filter 4B.) There is considerable variability in the eight profiles but all indicate haze near ground level. Similar composite graphs of total scattering coefficient data for the pseudo-photopic filter were given in Section 7.3 of Duntley, *et al.* (1972c) for three previous field trips: HAVEN VIEW (southern Germany), ATOM (central New Mexico), and METRO (southern Illinois). The SEEKVAL total scattering coefficient data are generally the same as the HAVEN VIEW data at ground level, but SEEKVAL airborne values are smaller (clearer air) than the HAVEN VIEW air borne values except for C-359. In comparison with the ATOM data, the SEEKVAL ground-based and airborne values for C-359 are larger (hazier air), whereas the remaining SEEKVAL airborne values are lower (clearer air) except for C-351, C-358, and C-359. METRO had no ground-based values for the flight tracks. The airborne SEEKVAL total scattering coefficients are higher (clearer) than the METRO values at the same altitudes except for C-351 and C-359.

The wide range of total scattering coefficients encountered on SEEKVAL was more similar to the range of values encountered on the SHEDLIGHT (nighttime, Thailand) field trips reported in Duntley, *et al.* (1970). The SHEDLIGHT measurements did not include a pseudo-photopic filter but did use a broad band Filter 5 with a mean wavelength of 532 nanometers and a response area of 184 nanometers. The SHEDLIGHT Filter 5 total scattering coefficients can probably be reasonably compared to the pseudo-photopic filter total scattering values. The total volume scattering coefficients for SHEDLIGHT Filter 5 for seven wet-season flights and the first dry-season flight are presented in Fig. 8-5.

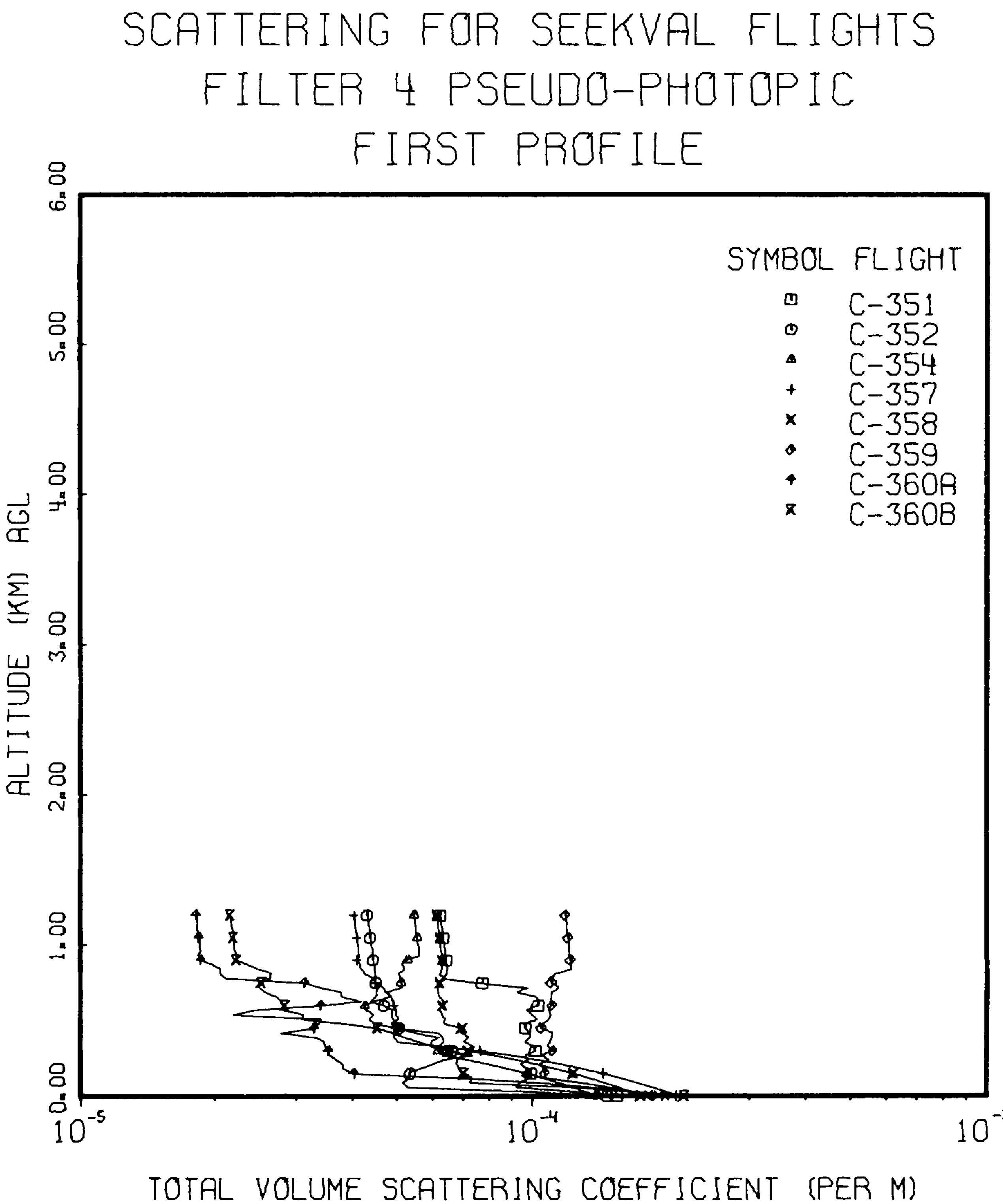

Fig. 8-4. Total Volume Scattering Coefficient for Filter 4A (Pseudo-Photopic) for Seven SEEKVAL Flights.

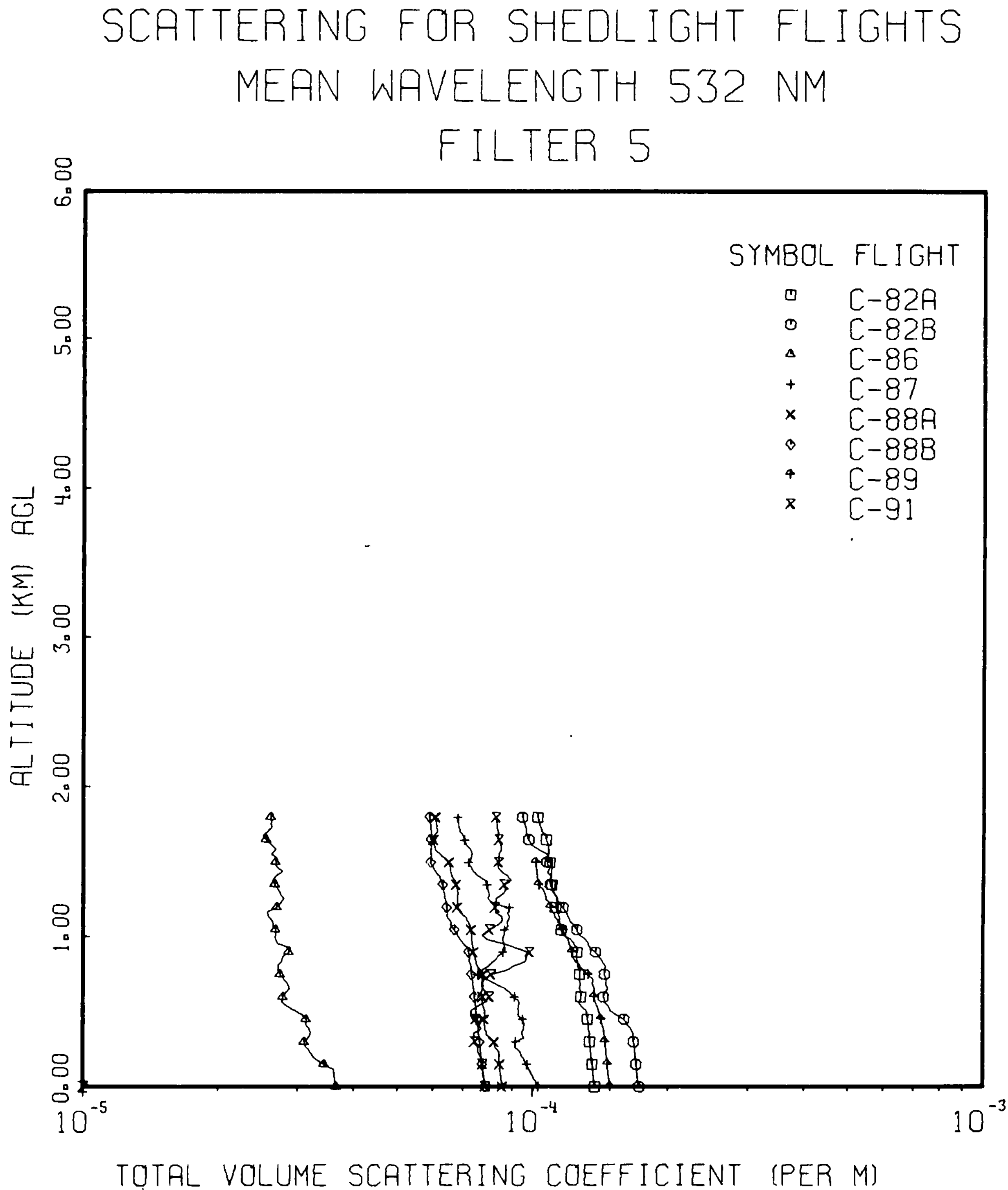

Fig. 8-5. Total Volume Scattering Coefficient for SHEDLIGHT Filter 5 for Seven Wet-Season Flights and One Dry-Season Flight.

A similar graph for the remaining nine dry-season SHEDLIGHT flights is presented as Fig. 8-6. The values of total scattering coefficient were corrected from the values reported in Duntley, *et al.* (1970) with an improved calibration factor before being graphed. The correction factor which depended on scattering function shape had a range of 0.86 to 0.93.

All the SEEKVAL total scattering coefficient data lie in the range of the SHEDLIGHT values except for C-360 at the higher altitudes. Both the HAVEN VIEW and METRO data indicate heavier hazes between ground and a 2-kilometer altitude than were encountered during either SHEDLIGHT or SEEKVAL.

Comparison of Visibility Estimates. The meteorological estimates of horizontal visibility VV have been related to the attenuation coefficient α by Douglas and Young (1945), and hence are related to the scattering coefficient in the absence of absorption by

$$VV = \ln 18/\alpha \approx 3/s \quad . \qquad (8.5)$$

Visibility values appropriate to the times of the SEEKVAL flights are presented in Table 8-2. Columns 3 and 4 contain the evaluation of visibility by the weather observers at McChord Air Force Base and Gray Army Air Field. Column 5 contains the visual estimates made by Visibility Laboratory personnel at the ground site beneath the flight track. Column 6 is comprised of the values of visibility computed from the ground-based nephelometer measurements. In column 7, values for the first five flights are based upon the attenuation coefficient derived from the low altitude path function measurements, and the values for the last two flights are from the low altitude nephelometer measurements of total scattering coefficient.

Table 8-2

Visibility Based on Visual Estimates, Measurements of Total Scattering Coefficient, and Calculations of Attenuation Coefficient

Date (1974)	Flight	Visibility (Statute Miles)				
		Meteorological Estimates			Computed From	
		McChord AFB	Gray AAF	SEEKVAL Ground Station	Ground Nephelometer	Airborne Path Function Meter or Nephelometer
13 July	C-351	30	35	45	12	19–24
14 July	C-352	15–30	10–35	35	12	28–37
16 July	C-354	7–15	7–10	–	13	29–49
20 July	C-357	20–40	35	–	9–12	36–37
21 July	C-358	15	35	20	11–12	22–30
23 July	C-359	10–15	10	–	10	13–18
28 July	C-360A & B	15	35	40	9–10	27–57

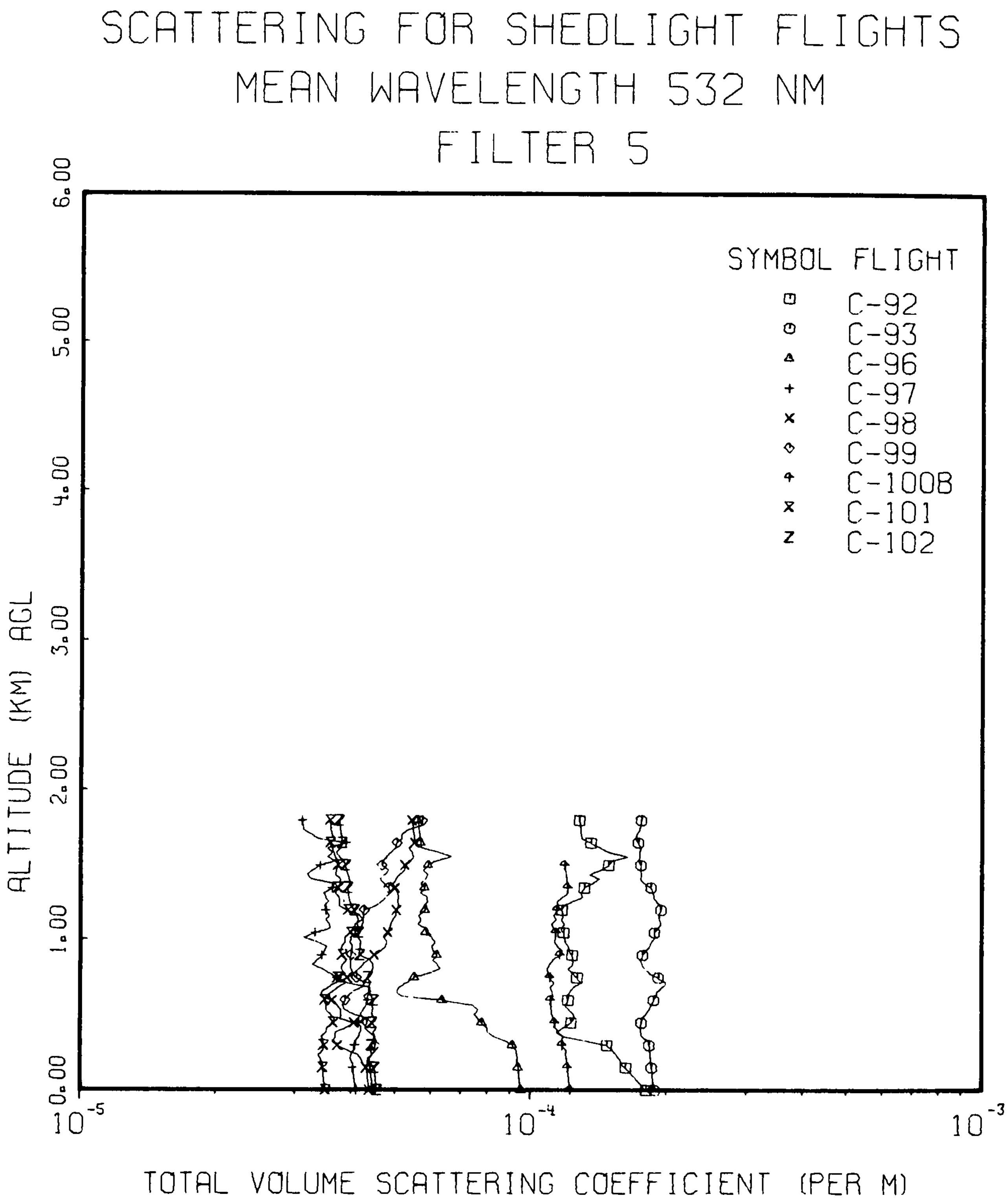

Fig. 8-6. Total Volume Scattering Coefficient for SHEDLIGHT Filter 5 for Nine Dry-Season Flights.

The visibility values based on the ground-based nephelometer are lower than the ground-site estimations in all four cases and lower than both the McChord Air Force Base and Gray Army Air Field observations in four out of the seven cases. Generally speaking, the ground-based nephelometer values were relatively invariant over the period of the seven flights, whereas the reported visibilities indicate a larger variability for the horizontal visual range. Also, during the field trip fairly large shifts were noted in the readings of the internal reference source for the ground-based nephelometer. For both of these reasons, the ground-based values of total scattering coefficient should be used with some caution.

The visibility values derived from the low altitude airborne data lie generally within the visibility estimate range for five out of the seven flights. They are lower than the visibility estimates for Flight C-351 and higher for C-354. The Douglas and Young (1945) data on visual range compared to measured beam transmittance also show a fair variability in the visibility range above 10 kilometers (6.2 statute miles).

Correlation with Relative Humidity. Early attempts to correlate optical measurements of scattering with the moisture content of the atmosphere indicated the need for simultaneous measurement by instruments with relatively short time constants. This was first achieved by the Visibility Laboratory when a B-29 aircraft with an attenuation meter (consisting of a combined horizontal path function meter and equilibrium radiance meter) was flown in tandem with a C-131 carrying a refractometer during 1956 as reported by Duntley, *et al.* (1957). Profiles of path function and dewpoint temperature versus altitude showed the close correlation of path function and humidity. Results from a similar flight in 1957 were reported by Boileau (1959). He subtracted the Rayleigh path function from the measured value to obtain a path function value due to liquid water and particulate matter only. He presented a linear graph of the normalized value of the resultant path function versus relative humidity which showed a clearly exponentially increasing function with relative humidity.

The modifications to the Cambridge hygrometer system [AFCRL-72-0593, Duntley, *et al.* 1972c)] clearly decreased the time constant of the instrument to the point where it produced valid measurements during ascent and descent flight elements. Thus we were again able to make simultaneous measurements of optical scattering and relative humidity. The total scattering coefficient measured by the integrating nephelometer for three flights during Project SEEKVAL is graphed on a semi-log plot as a function of the relative humidity in Fig. 8-7. The relationship between log scattering coefficient and relative humidity for these three flights is apparently roughly linear. Since all the data were taken at relatively low altitudes, the Rayleigh scattering coefficient appropriate to each datum lies within the range from 9.6E-6 to 1.09E-5, where 1.0E-5 is very nearly midrange. Thus the graph also represents the approximate relationship of relative humidity to the ratio of total scattering to Rayleigh scattering $s(z)/{}_{R}s(z)$, and the right-hand scale is so marked. The line drawn is the best fit to the data for the equation $y = mx$, where $y = \log s(z)/{}_{R}s(z)$ and $x = RH/100$ where RH is the relative humidity. The slope $m = 1.28$ was found by the relationship

$$m = \frac{\Sigma y}{\Sigma x} = \frac{\Sigma s(z)/{}_{R}s(z)}{\Sigma RH/100} \tag{8.6}$$

The above relationship which indicates Rayleigh scattering at zero relative humidity is perhaps not unreasonable for the site. The flight track was over forest near an agricultural area, removed from major sources of industrial pollution and auto emissions.

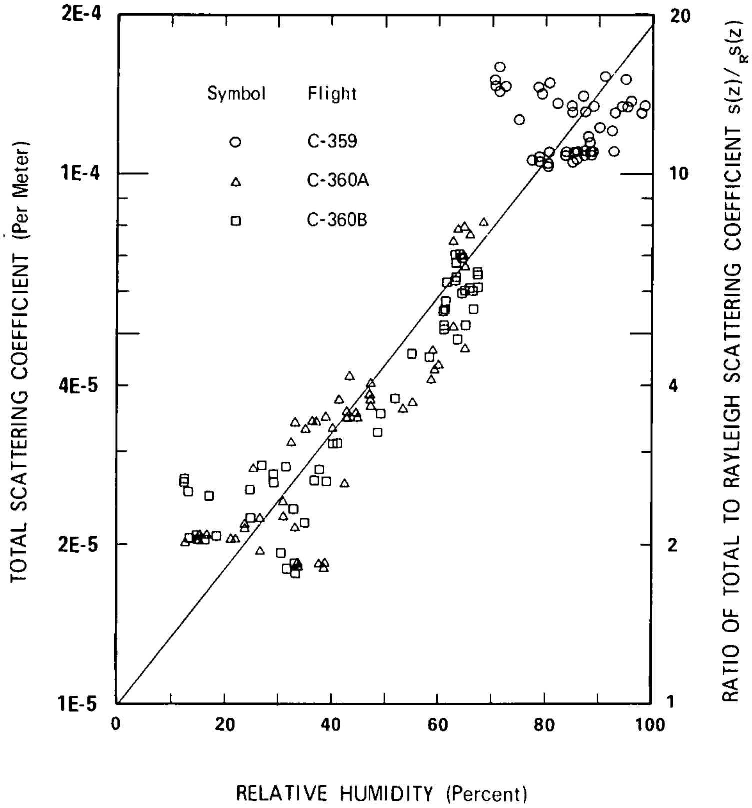

Fig. 8-7. Total Scattering Coefficient as a Function of Relative Humidity.

The attenuation coefficients derived from the path function measurements and computed equilibrium radiance are plotted on a semi-log graph as a function of the relative humidity in Fig. 8-8. The best-fit line from Fig. 8-7 is superimposed in order to compare the two sets of data more easily. The Rayleigh scattering coefficients for these data lie in the range from 9.8E-6 to 1.10E-5, so 1E-5 is still in the range. Thus this graph also represents the approximate relationship of the relative humidity to the ratio of attenuation coefficient to Rayleigh scattering $\alpha(z)/_R s(z)$, and the right-hand scale is so marked.

The data for C-351 and C-358 fit the curve fairly well. These are the two flights for which the attenuation coefficient should be low in error. The data for the other three flights, C-352, C-354, and C-357, show increasingly more scatter. All three of these flights had at least some attenuation coefficient values lying in the range of data with potentially high error.

It should be remembered that the ambient temperature measurements are probably in error by about −2 degrees Celsius and that, therefore, the relative humidities are probably too large. The relative humidity error would be small at the lower humidities and large at the higher humidities. However, the relationship as indicated by Fig. 8-7 is nonetheless provocative. The relationship between scattering coefficient and relative humidity should be further explored when data become available from other field trips.

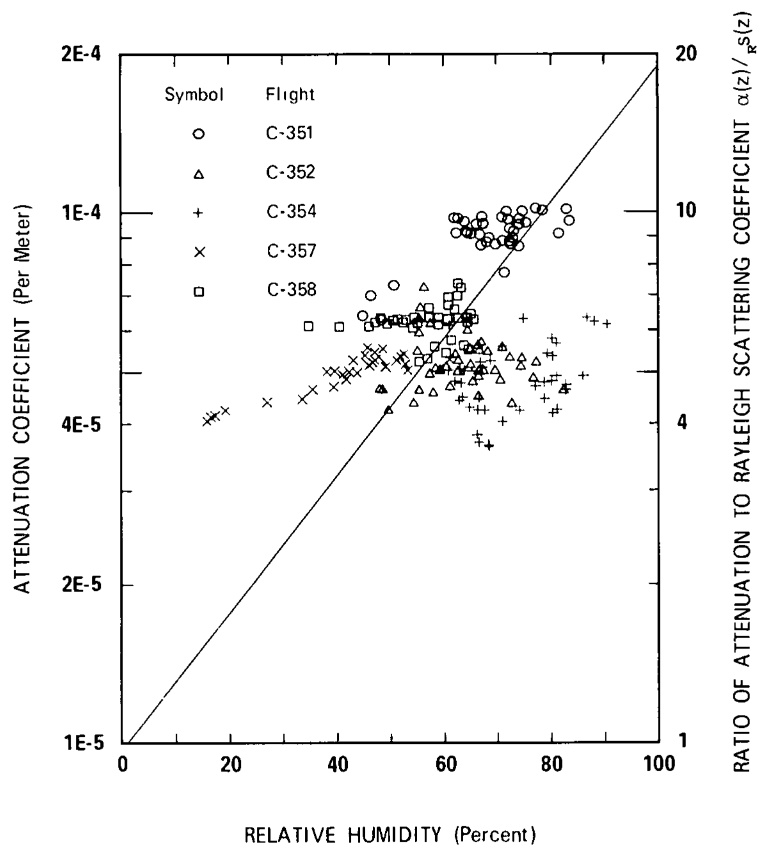

Fig. 8-8. Attenuation Coefficient as a Function of Relative Humidity.

EQUIVALENT ATTENUATION LENGTH AND BEAM TRANSMITTANCE

At ground level the equivalent attenuation length is the reciprocal of the total scattering coefficient s(z). As altitude increases, the equivalent attenuation length shows the cumulative effect of summing s(z) from ground level to altitude z. Large increases in equivalent attenuation length at low altitude occur for those profiles where airborne data were measured down to relatively low altitude. This emphasized the difference between the airborne total scattering coefficient and the larger ground-based total scattering coefficient.

The vertical beam transmittance starts at 1.0 at ground level and shows the cumulative effect of the summation of the total scattering coefficient with altitude.

IRRADIANCE

The downwelling irradiance at the lowest straight and level altitude is used as the irradiance for computing the directional reflectance of the terrain and the directional path reflectance. The low-altitude downwelling irradiance values for photopic Filter 4 for all the SEEKVAL profiles are graphed in Fig. 8-9.

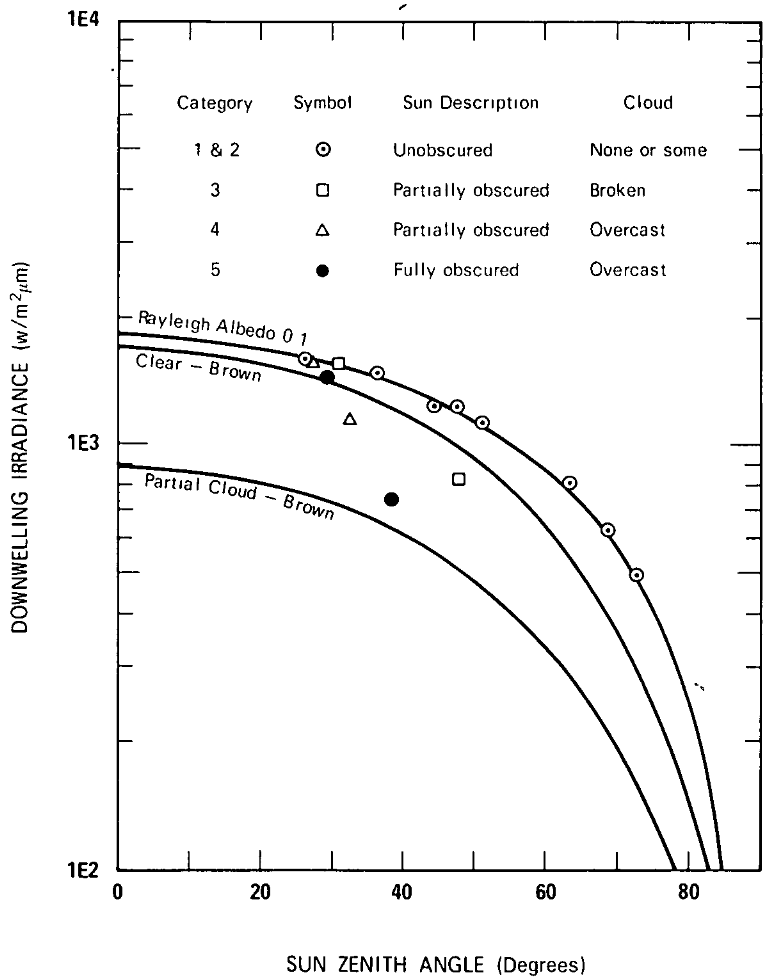

Fig. 8-9. Project SEEKVAL Low Altitude Downwelling Irradiance for Filter 4 (Pseudo-Photopic) Compared to Brown (1952) and a Rayleigh Atmosphere.

The symbols indicate the cloud categories described in Table 8-1. Since the altitudes for the lowest straight and level sequences ranged between 151 and 375 meters above ground level, they can be compared to the ground-level values of Brown (1952). The illuminance values of Brown for unobscured sun and partial cloud have been converted to irradiance units and depicted as solid curves in Fig. 8-9. Also superimposed on Fig. 8-9 is a curve for the photopic Rayleigh atmosphere at sea level with a scalar albedo of 0.10. (The range of the low-altitude scalar albedo for the SEEKVAL flights is 0.044 to 0.10.) The Rayleigh values, which may represent an upper limit for a clear cloudless sky, were computed using the model atmosphere equations of Gordon (1969).

The category 1 and 2 (unobscured sun) values of downwelling irradiance tend to be above the Brown clear-day curve and to cluster about the Rayleigh curve for 0.10 albedo. The category 1 and 2 flights are C-351, C-352, C-357, C-360A, and C-360B. The low-altitude-to-space transmittance values ranged from 0.82 to 0.84 for these flights, whereas the Brown curve is most likely appropriate to the average clear-day photopic transmittance of 0.7. Therefore it is reasonable for the category 1 and 2 irradiances to be above the Brown clear-day values but not to equal or exceed the Rayleigh atmosphere values appropriate for a transmittance of 0.907. Thus the downwelling irradiances for the cloud categories 1 and 2 are probably slightly high although the presence of clouds for the category 2 profiles can conceivably raise the total irradiance due to high reflectance from the clouds.

The broken cloud and overcast data, categories 3, 4, and 5, flights C-354, C-358, and C-359, have three values above and three below the Brown clear-day curve. The low-altitude-to-space transmittances used were all less than 0.7; however, the presence of highly reflective clouds evidently raised some of the irradiances above that of the average clear day.

The graphs of downwelling irradiance versus altitude for the SEEKVAL flights in cloud categories 1 and 2 are very regular. The graphs of downwelling irradiance versus altitude for the flights in categories 3, 4, and 5 are slightly less regular because the lighting conditions for those three flights (C-354, C-358, and C-359) were more variable during the straight and level sequences. The irradiance irregularities in Flights C-358 and C-359 result from averaging the transmittance appropriate to the high and low straight and level sequences for each profile. The irregularity of C-354 results from the variability of the sky radiance map since the sun was fully obscured.

In general, the SEEKVAL downwelling irradiances, as a function of altitude, are similar in regularity to the METRO downwelling irradiances [Duntley, *et al.* (1973 and 1974)] and more regular than the irradiances for HAVEN VIEW [Duntley, *et al.* 1972a)] and ATOM [Duntley, *et al.* 1972b)].

DIRECTIONAL REFLECTANCE OF TERRAIN

The tables of directional reflectance of terrain presented with each flight are derived from data obtained with the lower hemisphere scanner at the lowest flight altitude. This instrument is a telephotometer with a 5-degree field of view. The tabular values of reflectance therefore relate to an average radiance throughout that field of view, and it is completely possible that no specific part of the terrain has that exact value of reflectance. In addition, objects of interest will almost certainly be located on a background having a different reflectance than that tabulated for the terrain. That is why ground-based measurements of directional reflectance of backgrounds are also made during the flight interval – to help provide appropriate values for generating contrast transmittance for a given problem. The affect of background reflectance on the contrast transmittance is not a trivial one. Care should be used in selecting the appropriate value for application to a specific problem.

Table 8-3 summarizes all the SEEKVAL airborne data on terrain reflectance for the nadir path of sight. This summary presents the data in order by cloud category and by increasing sun zenith angle. For the nadir path of sight at the lowest altitude of all the flights, 151 meters, a 5-degree field would cover a circle 13 meters in diameter, whereas at the highest minimum altitude of all the flights, 375 meters, a 5-degree field would cover a circle 33 meters in diameter. The nadir value is the average of the values obtained during one azimuthal revolution of the scanner (10 seconds). At flight speeds of 142 to 151 knots, the average distance covered in 10 seconds is 750 meters. Thus the tabulated nadir reflectances relate to an average radiance in areas 13 by 763 meters, to 33 by 783 meters in size.

Table 8-3

SEEKVAL Nadir Terrain Reflectances Based Upon Airborne Scanner Radiances for Filter 4, Pseudo-Photopic

Cloud Category	Sun Zenith Angle (degrees)	Flight	Filter	Altitude (meters AGL)	Nadir Reflectance
1 or 2	26.0	C-351	4A	318	0.068
	26.0	C-351	4B	266	0.038
	36.2	C-360B	4B	320	0.034
	44.4	C-352	4B	272	0.030
	47.3	C-357	4A	154	0.070
	47.3	C-360B	4A	311	0.034
	51.1	C-360A	4B	296	0.038
	63.2	C-352	4A	303	0.035
	68.7	C-360A	4A	320	0.033
	72.6	C-357	4B	284	0.024
3	31.0	C-359	4A	151	0.016
	47.8	C-359	4B	264	0.057
4	26.5	C-358	4B	318	0.060
	32.3	C-358	4A	297	0.039
5	29.3	C-354	4B	375	0.026
	38.3	C-354	4A	369	0.053
Meadows*	40.4 to 45				0.035 to 0.10
Crops*	45				0.057 to 0.14
Forests*	33.5 to 45				0.032 to 0.038

* See Table 8-2, Duntley, *et al.* (1973).

The seeming inconsistency of the reflectances flight to flight is a function of the patchiness of the terrain as illustrated in Fig. 7-1 and 7-2. The description in Table 7-1 of each terrain picture does not necessarily coincide with the reflectance since the time the picture was taken does not directly coincide with the time of the scanner nadir measurement.

The reflectances can be compared to the nadir reflectances of meadows, crops, and forests from the literature which were presented in Table 8-2 of Duntley, *et al.* (1973). The range of those reflectances is indicated in the last three rows of data in Table 8-3 of this report. Four of the measured reflectances are less than the literature range of values. The two for cloud categories 1 and 2 may be reasonable. The first, for C-352 Filter 4B, is only slightly below the range of values from the literature. The second, for C-357 Filter 4B, is for a sun zenith angle of 72.6 degrees, whereas none of the values in the literature was measured for such a large zenith angle. Also, for the SEEKVAL data in cloud categories 1 and 2, there appears to be a slight tendency for the terrain reflectance to decrease with increasing sun zenith angle for sun angles 51 degrees and greater.

The two low reflectances in cloud categories 3 and 5 are the result of computations using downwelling irradiances which are above the Brown clear-day values. Hence these two reflectances, for C-359 Filter 4A and C-354 Filter 4B, should probably be used with caution.

EQUILIBRIUM RADIANCE

Equilibrium radiance (Eq. 2.22) is obtained by using an integrative method. An advantage of this method is the ability to handle highly variable data, variable in the sense of changing flux levels due to real changes occurring in space and/or time during the flight. For instance, specific features of the terrain vary in position relative to the aircraft as it flies the track. Anomalies in the sky-lighting distribution occur due to subtle changes in the weather. Also, the sun zenith angle increases or decreases in varying degrees due to changes in procedural elapsed times. These local occurrences contribute to the variability of the overall sky radiance flux level and directional radiance pattern, and these two properties plus the apparent sun radiance define the equilibrium radiance. The values of equilibrium radiance derived using the integrative method are directly descriptive of the real conditions encountered and measured during a flight, except for the average sun zenith angle used for obtaining the apparent sun radiances and the assumption that beam transmittance from space to the highest altitude remains constant throughout the profile. Thus clouds, when present, contribute only to the variability of the sky irradiance at each altitude. The assumption of an unobscured sun for the cloud category 2 profiles is consistent with the real-world case when checked against the scanner data arrays for the six profiles containing scattered clouds in the upper sky.

Under comparatively stable clear-day conditions, equilibrium radiance tends to be relatively invariant with altitude. Several atmospheric models are based upon this tendency [Duntley (1948) and Gordon (1969)]. The first model assumes an invariant particle-size distribution which decreases with increased altitude. The second model assumes both a clear day with no clouds and no absorption, and an invariant equilibrium radiance with altitude.

In contrast to these models, the 16 SEEKVAL flight profiles have equilibrium radiance functions which vary with altitude. The standard deviation of the equilibrium radiance from the average values varied from less than 1 to 47 percent, with the nadir path of sight often having standard deviations in the upper portion of that range. To illustrate this, the nadir equilibrium radiance for Flight C-360B photopic response Filter 4B has been graphed in Fig. 8-10. Flight C-360B was one of the more optically stable flights in terms of consistency of irradiance with altitude, but the Filter 4B standard deviation for the

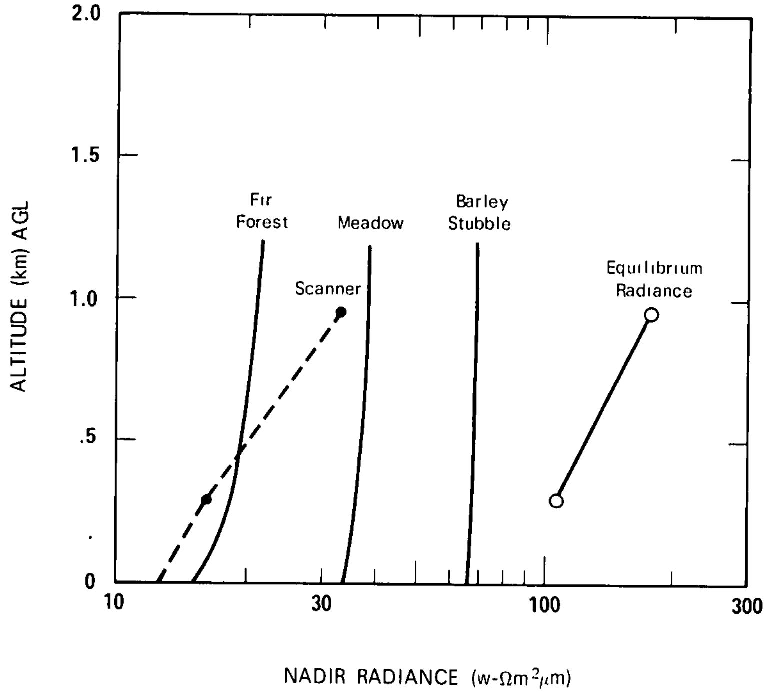

Fig. 8-10. Comparison of Equilibrium Nadir Radiance with Several Computed Apparent Nadir Terrain Radiances and the Measured Scanner Nadir Radiance from Flight C-360B Filter 4B.

equilibrium radiance varied from less than 1 to 43 percent for the various paths of sight (standard deviation for the nadir path of sight was 35 percent). Thus, the atmospheric models cited above appear inapplicable to the SEEKVAL flights.

There is a certain amount of consistency, however, in the equilibrium reflectance for the lowest altitude of the nadir path of sight. Equilibrium reflectance R_q is derived from the equilibrium radiance and the downwelling irradiance:

$$R_q(z,\theta,\phi) = N_q(z,\theta,\phi)\,\pi/H(z,d) \quad . \tag{8.7}$$

Since the apparent radiance of a terrain, background, or object tends to approach the equilibrium radiance, a look at the equilibrium reflectance at the lowest altitude will tell us whether a terrain will increase or decrease in radiance with altitude, at least initially. The nadir equilibrium reflectance for the 16 flight profiles are given in Table 8-4 in the same groupings as for Table 8-3. As can be seen, there is a rough overall consistency among the reflectances for zenith angles 52 degrees or less, the reflectances falling within the range from 0.17 to 0.29 with most of the values between 0.22 and 0.24. There also seems to be a general increase of equilibrium reflectance at the larger sun zenith angles from 63 degrees to 73 degrees for the cloud category 1 and 2 data. However, all the nadir terrain reflectances (Table 8-3) are lower than the equilibrium reflectances for the same day, and, therefore, the apparent terrain radiance will increase with altitude, at least at the lower altitudes.

Table 8-4

SEEKVAL Nadir Equilibrium Reflectance at Lowest Altitude for Filter 4 Pseudo-Photopic

Category	Sun Zenith Angle (degrees)	Flight	Filter	Altitude (meters AGL)	Nadir Equilibrium Reflectance
1 or 2	26.0	C-351	4A	318	0.22
	26.0	C-351	4B	266	0.22
	36.2	C-360B	4B	320	0.23
	44.4	C-352	4B	272	0.24
	47.3	C-357	4A	154	0.26
	47.3	C-360B	4A	311	0.23
	51.1	C-360A	4B	296	0.24
	63.2	C-352	4A	303	0.33
	68.7	C-360A	4A	320	0.38
	72.6	C-357	4B	284	0.41
3	31.0	C-359	4A	151	0.17
	47.8	C-359	4B	264	0.22
4	26.5	C-358	4B	318	0.24
	32.3	C-358	4A	297	0.24
5	29.3	C-354	4B	375	0.29
	38.3	C-354	4A	369	0.25

PATH RADIANCE

Path radiance is calculated from the values of equilibrium radiance for a given path of sight by means of Eq. 2.18 and 2.21. In this way, the path radiance combines the values of equilibrium radiance from each of several altitudes. The required path radiance is essentially a scattered radiance in a given path at any one instant. The derived value, however, represents an averaging of the light conditions present during the entire flight (the use of integral Eq. 2.18 effectively combines the variable path into an unrefined average of the prevalent condition). The averaging, though is progressive. The lowest altitude value is derived solely from the low-altitude data, whereas the highest altitude value is an average of all the data. Thus, the path radiances represent neither the clearest nor the cloudiest portion of a flight, but a combination of the various segments.

The derived path radiance profiles are relatively smooth as a function of altitude, partially due to the averaging process of the integration of Eq. 2.18. The path radiances for both the METRO and SEEKVAL field trips are more regular than those for the HAVEN VIEW and ATOM trips. This change indicates an overall improvement in data quality.

The path radiance and other related parameters are routinely evaluated using a variety of diagnostic tests. For example, one important diagnostic is that for the same downward looking path of sight, the path radiance should be less than the apparent terrain radiance. In all cases, the internal diagnostics indicate that the data quality has improved substantially since Project METRO. This improvement is a direct result of the current method of measuring the sky radiance near the sun, and the method for obtaining apparent sun radiance using the best of five independently determined values of space-to-high altitude beam transmittance.

Path Radiance Applications. The path radiance enters into the equation for contrast transmittance, Eq. 2.2, into the equation for directional path reflectance, Eq. 2.4, and into the equation for computing apparent radiance, Eq. 7.2. By rearranging Eq. 7.2, we obtain an equation for predicting the inherent radiance of the terrain at ground level $N_o(0,\theta,\phi)$ from the apparent radiance, the beam transmittance, and the path radiance:

$$N_o(0,\theta,\phi) = [N_r(z,\theta,\phi) - N_r^*(z,\theta,\phi)] / T_r(z,\theta) \ . \tag{8.8}$$

For example, the resultant inherent radiance for the nadir path of sight for Flight C-360B, Filter 4B (pseudo-photopic) is 12.6 $w/\Omega m^2 \mu m$. Then using Eq. 2.5, we obtain a reflectance of 0.027. This reflectance is indicative of the forested area underlying much of the flight track. The measured scanner radiances and the extrapolated ground value have been graphed in Fig. 8-10 and labeled as "scanner."

For conceptual purposes, we have computed the apparent nadir radiances for three types of terrains appropriate to Flight C-360B, Filter 4B using Eq. 7.2. The three terrains chosen were: lush meadow in autumn having a reflectance of 0.071, a fir forest in late summer having a reflectance of 0.032, and barley stubble with a reflectance of 0.14. The latter two photopic reflectances are the minimum and maximum from the last three rows in Table 8-3 and illustrate high and low values from the literature for woods interspersed with meadows and cultivated fields. The computed radiances for these three terrains are graphed in Fig. 8-10.

The measured scanner radiance is closest to the computed fir forest radiance at low altitude and closest to the computed meadow radiance at high altitude. This variability of the scanner radiance with altitude is indicative of the patchiness of the terrain beneath the flight track. Pictures taken simultaneously with the nadir measurement would be necessary before appropriate descriptions of the terrain could be made for the nadir measurement.

Note how all the computed terrain radiances increase, tending to approach the equilibrium radiance. All the computed radiances increase with altitude since they are all less than the equilibrium radiance and thus tend to approach it.

CONTRAST TRANSMITTANCE

Contrast transmittance can be expressed as the beam transmittance times the ratio of the inherent to apparent background radiance:

$$_b\tau_r(z,\theta,\phi) = T_r(z,\theta)\ _bN_o(0,\theta,\phi)/_bN_r(z,\theta,\phi) \ . \tag{8.9}$$

Thus, the contrast transmittance is a direct function of the background and the manner in which the background radiance changes with altitude. The contrast transmittance for items displayed against a background lower in reflectance than the equilibrium reflectance will always be less than the beam transmittance. This is true because the ratio of inherent to apparent background radiance is always less than 1, since apparent radiance increases with altitude as shown in Fig. 8-10. This characteristic is illustrated in Fig. 8-11. On the other hand, the contrast transmittance for a background higher in reflectance than the equilibrium reflectance will be greater than the beam transmittance.

The discussion above emphasizes the importance of selecting the appropriate terrain reflectance for use as background reflectance when computing valid contrast transmittance values. Photopic reflectances of many backgrounds are available for clear days with moderately high suns in Gordon (1964) and Gordon and Church (1966a), for low suns in Boileau and Gordon (1966), and for overcast skies in Gordon and Church (1966b).

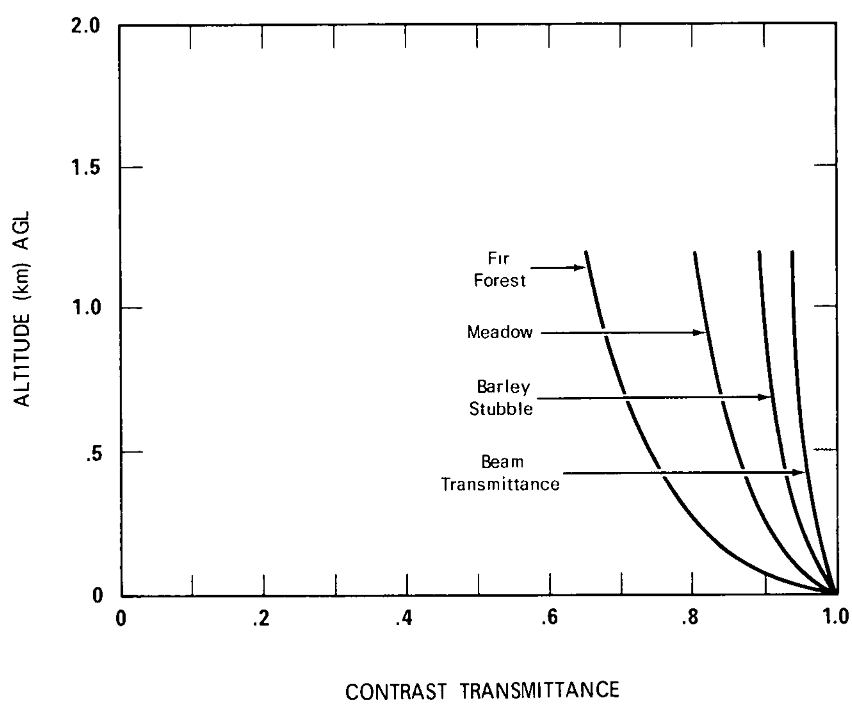

Fig. 8-11. Contrast Transmittance for Several Different Backgrounds and Beam Transmittance for Flight C-360B Filter 4B (Pseudo-Photopic) Nadir Path of Sight.

DIRECTIONAL PATH REFLECTANCE

Using data from the two scanners to obtain both the path radiance $N_r^*(z,\theta,\phi)$ and the downwelling irradiance H(z,d) adds to the reliability of the path reflectance $R_r^*(z,\theta,\phi)$ since these two quantities are ratioed in Eq. 2.4 to obtain path reflectance. In this manner, any absolute error in the calibration of the scanners or in the estimate of space-to-altitude transmittance is effectively minimized. Also, since both the path radiance and the downwelling irradiance are obtained by integration of a large number of radiance measurements, precision errors tend to cancel or average out.

The path reflectances for both the METRO and SEEKVAL field trips were more regular than those for the earlier HAVEN VIEW and ATOM trips. The continuing improvement within these four data sets is another indication of the improving quality of the path radiance and beam transmittance determinations.

8.3 SUMMARY

The derived optical properties for the SEEKVAL flights are similar to those for the METRO flights, in terms of consistency as a function of altitude. The optical properties are more consistent than the equivalent values for HAVEN VIEW and ATOM. In addition, the internal diagnostics which cross-compare the various computed properties as well as the measured properties indicate a significant improvement in data quality since Project METRO. This is the direct result of utilizing advanced methods for measuring, evaluating, and handling the radiance distribution for the upper hemisphere.

The first major improvement was implementing a measuring technique which allowed measurement of the solar aureole data. This resulted in a measured radiance array for the complete upper hemisphere including the near sun regions. The second major improvement was in the technique for determining the apparent sun radiance from the altitude to space beam transmittance. Five independent determinations of beam transmittance were evaluated prior to selecting the final value. The most important technique for this application was the computation of the transmittance from sky radiance ratios. The implementation of these two major improvements and their related corollaries, has resulted in computed optical properties which are internally self-consistent and compare well with redundant or related measurements by the other instruments.

Recent improvements to the instruments for measuring path function and determining relative humidity have greatly enhanced both our ability to obtain key optical properties by more than one method of measurement, and our ability to examine the correlations between the meteorological and optical properties of the atmosphere. We are confident that our developing techniques are producing consistently more reliable and higher fidelity representations of the real world.

9. ACKNOWLEDGEMENTS

To be conducted successfully, Project SEEKVAL required the active support of many organizations and individuals. To all of those who so willingly contributed their skills, talents, and inspiration, the authors gratefully acknowledge their debt.

Dr. Robert W. Fenn, Chief, Atmospheric Optics Branch, AFCRL,
Scientific Counsel and Technical Monitor
Major Robert W. Endlich, USAF, Project Organization and Coordination
Mr. Raymond S. Silva, Operational Services Division, Field Requirements Section
AFCRL, for continuing logistical support and advice

4900 Test Group (FTOT), Kirtland AFB, for all aircrew assignments:
Capt. Mathew Earl, Aircraft Commander
1st Lt. Ralph Brands, Pilot
T/Sgt. Edward J. Duraczynski, Flight Engineer
S/Sgt. Mike G. Barcome, Crew Chief
S/Sgt. Clark B. Butler, Maintenance
A1C Ronald T. Nore, Maintenance

AFTEC/JT SEEKVAL, Kirtland AFB:
Col. J. R. Douglas, USAF, Joint Test Director
Cdr. J. J. Moynihan, USN, Project Manager
Mr. D. R. Power, Deputy for Technical Support
Maj. A. Barr, USAF, Staff Meteorologist

Visibility Laboratory, Technical Field Team:
Mr. Gerald D. Edwards, Ground Station Crew
Mr. George F. Simas, Ground Station Crew
Mr. Robert L. Stapleford, Technical Flight Crew

Visibility Laboratory Data Processing and Analysis Team:
Mr. Nils R. Persson, Jr.
Ms. Janet E. Shields
Ms. Catharine F. Edgerton
Mr. Steven J. Bettinger

Visibility Laboratory, Editorial and Reproduction Team:

Ms. Sally L. Poor

Mr. John C. Brown

Ms. Arlene C. Streed

Mr. James Rodriguez

Ms. Alicia G. Enriquez

9. ACKNOWLEDGEMENTS

To be conducted successfully, Project SEEKVAL required the active support of many organizations and individuals. To all of those who so willingly contributed their skills, talents, and inspiration, the authors gratefully acknowledge their debt.

Dr. Robert W. Fenn, Chief, Atmospheric Optics Branch, AFCRL,
Scientific Counsel and Technical Monitor
Major Robert W. Endlich, USAF, Project Organization and Coordination
Mr. Raymond S. Silva, Operational Services Division, Field Requirements Section
AFCRL, for continuing logistical support and advice

4900 Test Group (FTOT), Kirtland AFB, for all aircrew assignments:
Capt. Mathew Earl, Aircraft Commander
1st Lt. Ralph Brands, Pilot
T/Sgt. Edward J. Duraczynski, Flight Engineer
S/Sgt. Mike G. Barcome, Crew Chief
S/Sgt. Clark B. Butler, Maintenance
A1C Ronald T. Nore, Maintenance

AFTEC/JT SEEKVAL, Kirtland AFB·
Col. J. R. Douglas, USAF, Joint Test Director
Cdr. J. J. Moynihan, USN, Project Manager
Mr. D. R. Power, Deputy for Technical Support
Maj. A. Barr, USAF, Staff Meteorologist

Visibility Laboratory, Technical Field Team:
Mr. Gerald D. Edwards, Ground Station Crew
Mr. George F. Simas, Ground Station Crew
Mr. Robert L. Stapleford, Technical Flight Crew

Visibility Laboratory Data Processing and Analysis Team:
Mr. Nils R. Persson, Jr.
Ms. Janet E. Shields
Ms. Catharine F. Edgerton
Mr. Steven J. Bettinger

10. REFERENCES

Barteneva, O. D. (1960), "Scattering Functions of Light in the Atmospheric Boundary Layer," Bull. Acad. Sci. U.S.S.R., Geophysics Series, 1237 – 1244.

Boileau, A. R. (1959), "Correlation Between Measured Path Function and Relative Humidity," University of California at San Diego, Scripps Institution of Oceanography, Visibility Laboratory, SIO Ref. 59-5.

Boileau, A. R. (1964), "VI. Atmospheric Properties," Appl. Opt. **3**, 570 – 581.

Boileau, A. R. and J. I. Gordon (1966), "Atmospheric Properties and Reflectances of Ocean Water and Other Surfaces for a Low Sun," Appl. Opt. **5**, 803 – 813.

Brown, D. R. E. (1952), Natural Illumination Charts, Report 374-1, Project Ns-714-100, Department of the Navy, Bureau of Ships, Washington, D. C.

Douglas, C. A. and L. L. Young (1945), "Development of Transmissometer for Determining Visual Range," U. S. Dept. of Commerce, Civil Aeronautics Administration, Washington, D. C., Technical Development Report No. 47.

Duntley, S. Q. (1948), "Reduction of Apparent Contrast by the Atmosphere," J. Opt. Soc. Am. **38**, 179 – 191.

Duntley, S. Q., A. R. Boileau, and R. W. Preisendorfer (1957), "Image Transmission by the Troposphere I," J. Opt. Soc. Am. **47**, 499 – 506.

Duntley, S. Q. (1964), "Visibility, I. Introduction and II. Summary," Appl. Opt. **3**, 550 – 556.

Duntley, S. Q. (1969), "Directional Reflectance of Atmospheric Paths of Sight," Duntley Rep. No. 69-1.

Duntley, S. Q., R. W. Johnson, J. I. Gordon, and A. R. Boileau (1970), "Airborne Measurements of Optical Atmospheric Properties at Night," University of California, San Diego, Scripps Institution of Oceanography, Visibility Laboratory, SIO Ref. 70-7, AFCRL-70-0137.

Duntley, S. Q., R. W. Johnson, and J. I. Gordon (1972a), "Airborne Measurements of Optical Atmospheric Properties in Southern Germany," University of California, San Diego, Scripps Institution of Oceanography, Visibility Laboratory, SIO Ref. 72-64, AFCRL-72-0255.

Duntley, S. Q., R. W. Johnson, and J. I. Gordon (1972b), "Airborne and Ground-Based Measurements of Optical Atmospheric Properties in Central New Mexico," University of California, San Diego, Scripps Institution of Oceanography, Visibility Laboratory, SIO Ref. 72-71, AFCRL-72-0461.

Duntley, S. Q., R. W. Johnson, and J. I. Gordon (1972c), "Airborne Measurements of Optical Atmospheric Properties, Summary and Review," University of California, San Diego, Scripps Institution of Oceanography, Visibility Laboratory, SIO Ref. 72-82, AFCRL-72-0593.

Duntley, S. Q., R. W. Johnson, and J. I. Gordon (1973), "Airborne Measurements of Optical Atmospheric Properties in Southern Illinois," University of California, San Diego, Scripps Institution of Oceanography, Visibility Laboratory, SIO Ref. 73-24, AFCRL-TR-73-0422.

Duntley, S. Q., R. W. Johnson, and J. I. Gordon (1974), "Airborne and Ground-Based Measurements of Atmospheric Optical Properties in Southern Illinois," University of California, San Diego, Scripps Institution of Oceanography, Visibility Laboratory, SIO Ref. 74-25, AFCRL-TR-74-0298.

Gordon, J. I., J. L. Harris, and S. Q. Duntley (1963), "Earth-to-Space Contrast Transmittance Measurements from Ground Stations," University of California, San Diego, Scripps Institution of Oceanography, Visibility Laboratory, SIO Ref. 63-2.

Gordon, J. I. (1964), "III. Optical Properties of Objects and Backgrounds," Appl. Opt. **3**, 556 – 562.

Gordon, J. I. and P. V. Church (1966a), "Sky Luminances and Directional Luminous Reflectances of Objects and Backgrounds for a Moderately High Sun," Appl. Opt. **5**, 793 – 801.

Gordon, J. I. and P. V. Church (1966b), "Overcast Sky Luminances and Directional Luminous Reflectances of Objects and Backgrounds Under Overcast Skies," Appl. Opt. **5**, 919 – 923.

Gordon, J. I. (1969), "Model for a Clear Atmosphere," J. Opt. Soc. Am. **59**, 14 – 18.

Gordon, J. I., J. L. Harris, Sr., and S. Q. Duntley (1973), "Measuring Earth-to-Space Contrast Transmittance from Ground Stations," Appl. Opt. **12**, 1317 – 1323.

Johnson, F. S. (1954), "The Solar Constant," J. Meteorol. **11**, 431 – 439.

Kasten, F. (1965), "A New Table and Approximation Formula for the Relative Optical Airmass," Arch. Met. Geophys. Bioklim. **B14**, 206 – 233.

Kushpil', V. I. and L. F. Petrova (1971), "Determination of the Atmospheric Transmittance from Sky Brightness Distribution," Optical Technology **38**, No. 4, 191 – 193.

Penndorf, R. (1957), "Tables for the Refractive Index for Standard Air and the Rayleigh Scattering Coefficient for the Spectral Region Between 0.2 and 20.0μ and Their Application to Atmospheric Optics," J. Opt. Soc. Am. **47**, 176 – 182.

Preisendorfer, R. W. (1958), "Theory of Attenuation Measurements in Planetary Atmospheres," University of California, San Diego, Scripps Institution of Oceanography, Visibility Laboratory, SIO Ref. 58-81.

Tousey, R. and E. O. Hulburt (1947), "Brightness and Polarization of the Daylight Sky at Various Altitudes Above Sea Level," J. Opt. Soc. Am. **37**, 88.

Tyler, J. E. and R. W. Preisendorfer (1962), "Light," Chap. 8 in *The Sea*, M. N. Hill, Ed. (Interscience Publishers, Inc., N. Y.), Vol. 1, pp. 397 – 451.

USNAF TP-133, U. S. Naval Avionics Facility (1962), "Handbook, Operation and Service Instructions Aerograph Sets AN/AMQ-17 and AN/AMQ-18," Indianapolis 18, Indiana.

U. S. Standard Atmosphere (1962), U. S. Government Printing Office, Washington, D. C. 20402.

U. S. Standard Atmosphere Supplements (1966), U. S. Government Printing Office, Washington, D. C. 20402.